AD_____

Award Number: DAMD17-00-1-0077

TITLE: Signal Transduction in Prostate Cancer

PRINCIPAL INVESTIGATOR: Charles L. Sawyers, M.D.
Michael Carey, Ph.D.
Pinchas Cohen, M.D.
Hong Wu, Ph.D.

CONTRACTING ORGANIZATION: The University of California, Los Angeles
Los Angeles, California 90095-1406

REPORT DATE: April 2002

TYPE OF REPORT: Annual

PREPARED FOR: U.S. Army Medical Research and Materiel Command
Fort Detrick, Maryland 21702-5012

REPORT DOCUMENTATION PAGE

Form Approved
OMB No. 074-0188

1. AGENCY USE ONLY (Leave blank)	2. REPORT DATE	3. REPORT TYPE AND DATES COVERED
	April 2002	Annual (1 Apr 01 - 31 Mar 02)

4. TITLE AND SUBTITLE
Signal Transduction in Prostate Cancer

5. FUNDING NUMBERS
DAMD17-00-1-0077

6. AUTHOR(S)
Charles L. Sawyers, M.D., Michael Carey, Ph.D., Pinchas Cohen, M.D., Hong Wu, Ph.D.

7. PERFORMING ORGANIZATION NAME(S) AND ADDRESS(ES)
The University of California, Los Angeles
Los Angeles, California 90095-1406

E-Mail: csawyers@mednet.ucla.edu

8. PERFORMING ORGANIZATION REPORT NUMBER

9. SPONSORING / MONITORING AGENCY NAME(S) AND ADDRESS(ES)
U.S. Army Medical Research and Materiel Command
Fort Detrick, Maryland 21702-5012

10. SPONSORING / MONITORING AGENCY REPORT NUMBER

11. SUPPLEMENTARY NOTES

12a. DISTRIBUTION / AVAILABILITY STATEMENT
Approved for Public Release; Distribution Unlimited

12b. DISTRIBUTION CODE

13. Abstract ***(Maximum 200 Words)*** *(abstract should contain no proprietary or confidential information)*
The goal of this Prostate Cancer Center Initiation Award is to examine signal transduction pathways involved in prostate cancer progression, with an eye toward translational research applications. The program has two Projects and a Core Animal Facility. The first project (Dr. Carey) is focused on crosstalk between receptor tyrosine kinases and the androgen receptor (AR), using the Her2/neu kinase as a model system. Progress in the second year includes the completion of preclinical studies with an EGFR/Her2-neu kinase inhibitor with new, unexpected insights about the clinical application of these drugs. During year 3, we anticipate further progress toward a better understanding of AR crosstalk and developing imaging technologies to follow disease progression in mouse models. The second project (Dr. Cohen) examines the role of IGF binding protein 3 (IGFBP-3) in the context of crosstalk with the retinoic acid co-receptor RXRα. Progress to date confirms that IGFBP-3 induces apoptosis in synergistic fashion with RXR ligands in multiple prostate models. Year 3 will focus on in vivo studies of IGFBP-3 protein therapy alone and in combination with RXRα ligands in mouse models, using the Core facility. Both projects have led to the conception of clinical translational projects that are components of the UCLA Prostate SPORE application scheduled for funding in late 2002.

14. SUBJECT TERMS	15. NUMBER OF PAGES
tyrosine kinase, androgen receptor, insulin-like growth factor, IGFBP-3, prostate cancer	146
	16. PRICE CODE

17. SECURITY CLASSIFICATION OF REPORT	18. SECURITY CLASSIFICATION OF THIS PAGE	19. SECURITY CLASSIFICATION OF ABSTRACT	20. LIMITATION OF ABSTRACT
Unclassified	Unclassified	Unclassified	Unlimited

Table of Contents

Introduction

Overview

The goal of this Prostate Cancer Center Initiation Award is to examine signal transduction pathways involved in prostate cancer progression, with an eye toward translational research applications. The current funded program has two Projects and a Core Animal Facility. The first project, directed by Dr. Carey, is focused on crosstalk between receptor tyrosine kinases and the androgen receptor (AR), using the Her2/neu kinase as a model system. The second project, directed by Dr. Cohen, examines the role of IGF binding protein 3 (IGFBP-3) in the context of crosstalk with the retinoic acid co-receptor RXRα. The Core facility, directed by Dr. Sawyers, provides xenograft tissue and mouse models for preclinical therapeutic studies for both projects. Dr. Sawyers is also a collaborator for both projects.

Project 1 (Carey)

In the early phases of androgen-independence, genes traditionally regulated by androgen receptor are activated. The thesis underlying this project is that receptor tyrosine kinase (RTK) signaling pathways lead to modifications of AR or its co-activators, which in turn permit AR to function in a ligand-deprived environment. We and others have previously shown that tyrosine kinases such as Her-2/neu/Erb-B2 (Craft et al., 1999a). This project examines the hypothesis that there is a common theme in ligand-independent activation of AR using the receptor tyrosine kinases Her-2 and IGF-1R as models to pursue the mechanism. The study is a multidisciplinary collaboration with Dr. Charles Sawyers (Her-2) and Dr. Pinchas Cohen (IGF-I/IGF-1R). Our proposal articulated a plan to systematically test predictions of the RTK signaling hypothesis. First, the signaling should be blocked by interfering directly with RTK function and this should in principle revert tumors to ligand-dependence. During year 2 of the project Dr. Sawyers' group successfully tested this hypothesis using an EGFR/Her-2 kinase inhibitor. This work will be published shortly, and a preprint is appended (Mellinghoff et al., 2002). One outcome of this study is the recognition that Erk kinase activation (also called MAP kinase) is associated with evolution to androgen independence. Therefore, new efforts have been undertaken to development imaging technologies that will allow the transition to androgen independence to be visualized in mouse models. Our first paper describing this two-step transcriptional activation system was published in year 2 (Zhang et al., 2002). Second, because AR is the proposed endpoint of the pathway, its biochemical alteration represents an important step in cancer progression. A direct effect of this pathway on association of co-activators with AR was proposed. Intensive efforts to address this question using a proteomics approach were made in year 2, but the results have been disappointing, largely for technical reasons. Recognizing the shortcomings of this strategy, we have modified our approach and have significant new data using chromatin immunoprecipitation of AR bound to the promoter of AR response genes. We are confident that this new methodology will allow us to address our underlying hypothesis.

Project 2 (Cohen)

The goals of this project are to identify and characterize the role of IGFBP-3 in androgen receptor-signaling in androgen-dependent and -independent prostate cancer models. We are examining if IGFBP-3 is essential for apoptosis in response to androgen withdrawal. We are testing the effects of androgen deprivation on IGFBP-3 induction, IGF/IGF-R suppression, and prostatic apoptosis, in the AI and AD LAPC-4 and -9 cell lines and xenograft models of prostate cancer and in genetically altered mouse models. We are attempting to induce prostate cell death by treating these mice with systemic IGFBP-3. We are also trying to examine the role of RXR-α in IGFBP-3 actions in the prostate. We have begun to

generate prostatic RXR-α conditional (cre-lox) knockout models in order to evaluate the prostates of these mice before and after castration or IGFBP-3 treatment. These experiments will determine if RXR is required for apoptosis in response to androgen deprivation. We are also studying IGFBP-3 synergism with ligands of RXR-alpha and related receptors both *in vivo* in the AD and AI LAPC models and *in vitro* in prostate cancer cell line models.

Body

Project 1 (Carey)

Changes in the IGF pathway during progression to androgen independence

In the year 1 progress report, we reported our initial findings on the expression of insulin-like growth factors (IGFs), IGF binding proteins and the IGF receptor during the progression of prostate cancer xenografts to androgen independence (AI). We used three *in vivo* models of androgen-dependent human prostate cancer to study this issue, in collaboration with Dr. Michael Pollack's lab in Canada. Progression to AI growth was associated with a 60-fold increase in expression of IGF-I mRNA in LAPC-9 xenografts and a 28-fold increase in IGF-I expression in LNCAP xenografts, relative to the initial AD neoplasms. *IGF-IR* mRNA levels were ~2.5-fold and ~5-fold higher respectively in AI LAPC-9 and LNCaP tumors compared to the original AD neoplasms (fig 1). AI growth of these xenografts was also associated with significant reductions in IGFBP-3 expression. LAPC-4 xenografts, which previously have been shown to exhibit molecular pathology related to HER2-neu expression with progression to AI, showed relatively minor changes in expression of the genes investigated, but we nevertheless found evidence of increased IGF-IR phosphorylation with progression to AI in this model. Taken together with prior observations, our results suggest that deregulation of expression of genes related to any one of several critical receptor tyrosine kinase regulatory systems, including cellular IGF signaling, may confer androgen independence (Nickerson et al., 2001).

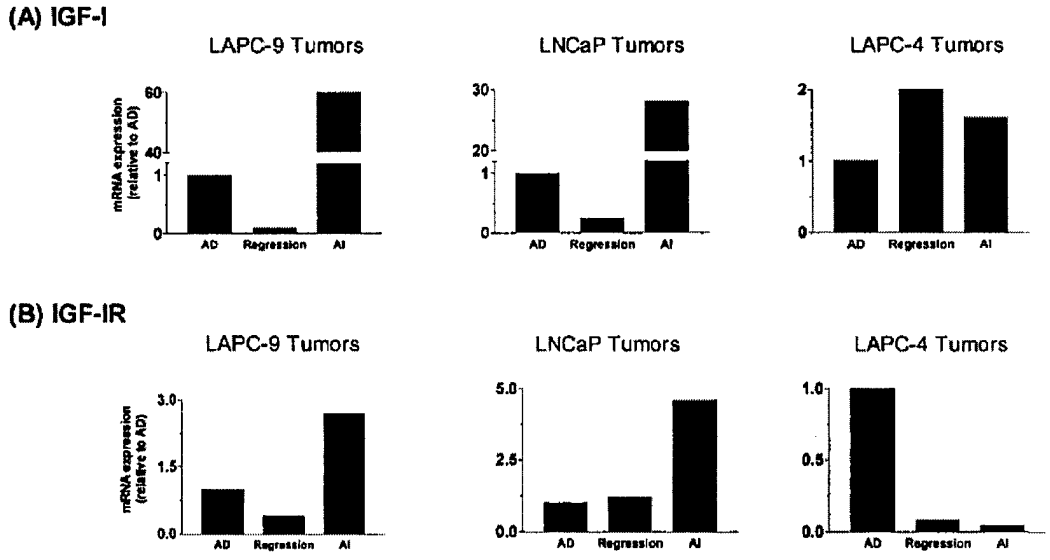

Figure 1. Expression of IGF-1 and IGFR by quantitative RT-PCR in prostate cancer xenografts after castration.

Evidence for selective requirement of the EGFR/Her2 pathway in androgen-independent prostate cancer

We previously showed that signaling through the epidermal growth factor (EGF) receptor family can affect androgen receptor activity and growth in human prostate cancer (Craft et al., 1999a). Here we asked whether interruption of ErbB-1 receptor signaling by an ErbB-1 receptor kinase specific inhibitor affects growth of human prostate cancer xenografts in our *scid* mice model (Klein et al., 1997). PKI-166 (Novartis) is an orally administered, ATP-site specific, reversible inhibitor of the ErbB-1 receptor kinase domain. In year 2 we completed a comprehensive series of preclinical studies of PKI-166 using our prostate cancer models which are now in press at **Cancer Research**. The major findings are summarized below.

1) PKI-166 blocks ErbB1/ErbB2 activity in prostate cancer cells.

We first examined the effects of PKI-166 on EGF-induced signal transduction through ErbB1 and ErbB2 RTKs in the human prostate cancer cell lines LAPC4 and LNCaP, both of which express the androgen receptor. The human vulvar carcinoma cell line A431, which expresses high levels of ErbB1 due to amplification of the erbB1 locus, was used as a positive control. In A431 cells treated with EGF, immunoblotting with a phosphotyrosine antibody showed a dominant band of about 170 kD representing the phosphorylated ErbB1 receptor (Fig. 2A). In EGF-treated LAPC-4 cells, which express considerably less ErbB1 than A431 cells but more ErbB2 *(data not shown)*, tyrosine phosphorylation of a 170 kD and a 185 kD band was observed representing phosphorylated ErbB1 and ErbB2, respectively. Dose-dependent inhibition of receptor autophosphorylation was noted following pretreatment with PKI-166, with estimated IC50 values of 0.5 μM for ErbB1 and 5 μM for ErbB2. Similar doses of PKI-166 have been reported to inhibit phosphorylation of ErbB1 and ErbB2 RTKs, but not other tyrosine or serine/threonine kinases, in non-prostatic human cancer cell lines (Bruns et al., 2000) (Brandt et al., 2001) (Scheving et al., 2002) . We also noted that PKI-166 treatment resulted in a dose-dependent increase in the level of ErbB1 protein in A431 cells and ErbB2 protein in LAPC4-cells. The increase in ErbB2 expression in LAPC4-cells was apparent at 0.5 μM PKI-166, a concentration that predominantly inhibits phosphorylation of ErbB1.

Previous work has indicated that ErbB1 protein is degraded following receptor activation by ligand, raising the possibility that the increased levels of ErbB1 and ErbB2 in PKI-166 treated cells are a reflection of kinase inhibition. To determine if pharmacologic inhibition of receptor tyrosine kinase activity delays receptor degradation, we measured the effect of PKI-166 on immunoprecipitated, ^{35}S-methionine/cysteine radiolabeled ErbB1 receptors in A431 cells (Fig. 2B, left panel). In the absence of PKI-166 and EGF, the receptor half-life of ErbB1 was between 6 and 12 hours, consistent with the previously published half-life of about 9 hours (Stoscheck and Carpenter, 1984). Stimulation of A431 cells with EGF resulted in phosphorylation of ErbB1, as evidenced by retarded electrophoretic mobility compared to the unphosphorylated receptor, and shortening of the receptor half-life to less than 6 hours. PKI-166 impaired the degradation of ErbB-1 receptor protein in both presence and absence of EGF. This data supports the concept that kinase activity is required for receptor degradation, consistent with prior work showing increased receptor half-life in ErbB1 alleles containing point mutations within the ErbB1 ATP-binding site (Honegger et al., 1987) (Chen et al., 1987). We also noted accumulation of a lower molecular weight protein in the ErbB1 immunoprecipitates from PKI-166 treated cells. This 145 kDa protein was immunoprecipitated by an ErbB1 antibody directed against a cell surface epitope, but not by an antibody directed against a C-terminal epitope (Figure 2B, right panel), indicating that it is likely to be a C-terminal truncation of the receptor. Similarly sized bands have previously been observed after

treatment of A431 cells with the lysosomal inhibitor methylamine (Stoscheck and Carpenter, 1984), and presumably represent an intermediate step in receptor degradation.

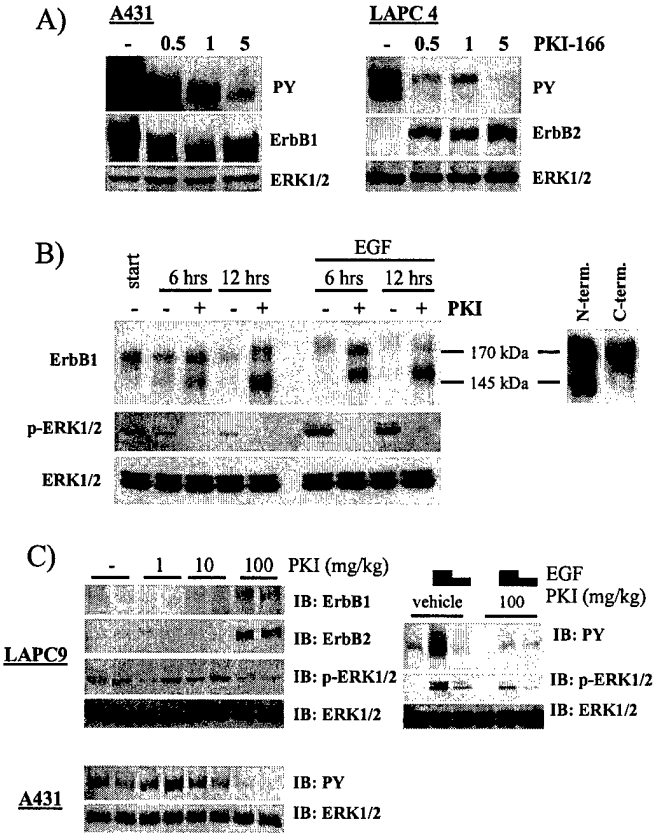

Figure 2. PKI-166 inhibits ErbB1 and ErbB2 receptor signaling and degradation A.) Immunoblots of A431 (*left panel*) and LAPC4 (*right panel*) cells treated for 12 hours with PKI-166 prior to stimulation with EGF (100 ng/ml) for 10 minutes B.) *left panel*: Autoradiograph of immunoprecipitated ErbB1 (upper row) and Immunoblots (middle and lower row) of lysates from A431 cells metabolically labeled for 12 hours with [^{35}S]-methionine and chased in the presence of PKI-166 (5μM) and/or EGF (100 ng/ml). PKI-166 was added 10 minutes prior to EGF where indicated. *right panel*: Immunoblot of A431 cells treated with PKI-166 for 12 hours using a ErbB1 antibodies directed against N-terminal and C-terminal epitopes C.) Immunoblots of lysates from LAPC9 (*left upper panel and right panel*) or A431 (*left lower panel*) xenograft tumors harvested one hour after the fifth daily dose of PKI-166 (2 tumors per condition). The right panel shows lysates of LAPC9 tumors from mice injected intraperitoneally with PBS, 0.1 mg EGF, or 0.01 mg EGF one hour following the fifth daily dose of PKI-166. Tumors were harvested five minutes after EGF injection.

Since many growth factor signals are transmitted to the nucleus through extracellular signal-regulated kinases (ERK) (Yarden and Sliwkowski, 2001), we also measured the effect of PKI-166 on ERK1/2 activation. At a dose which inhibits ErbB1 phosphorylation, PKI-166 completely blocked basal and EGF-induced ERK1/2 activation in A431 cells (Fig. 2B). Similar results were obtained in LAPC4 and LNCaP prostate cancer cells *(data not shown)*. These data establish the biochemical activity of PKI-166 against ErbB1/ErbB2 RTKs in vitro, including effects on receptor autophosphorylation, receptor degradation, and further signal transduction.

2) PKI-166 blocks ErbB1/ErbB2 signal transduction in tumors in mice.

We next examined the effects of PKI-166 treatment on ErbB1/ErbB2 mediated signaling in vivo. *SCID*-mice bearing tumors from the human prostate cancer xenografts LAPC4 (Klein et al., 1997) and LAPC9 (Craft et al., 1999a) or from the A431 cell line were treated for five days with 0, 1, 10, and 100 mg/kg of

PKI-166 and tumor tissue was harvested one hour after the last dose was administered. Lysates from A431-tumors displayed constitutive phosphorylation of ErbB-1 that was inhibited by treatment of mice with 100 mg/kg PKI-166. Similar analysis of ErbB phosphorylation in prostate cancer xenografts was not informative because of low basal levels of phosphotyrosine *(data not shown)*. However, we did observe decreased ERK1/2 activation and increased levels of total ErbB1 and ErbB2 protein in the prostate cancer xenografts from mice treated with 100 mg/kg of PKI-166, providing indirect evidence for ErbB1/ErbB2 RTK inhibition at this dose (Figure 2C, left panel). To obtain direct evidence of ErbB1/ErbB2 blockade in PKI-166 treated mice, we induced receptor activation by systemic administration of EGF (Donaldson and Cohen, 1992). Two different doses of EGF were injected intraperitoneally and resulted in dose-dependent receptor phosphorylation and ERK1/2 activation in LAPC9 tumors (Fig 2C, right panel). PKI-166 given orally at a dose of 100 mg/kg markedly blunted this activation (Figure 2C, right panel). Similar results were obtained in mice bearing LAPC4 or A431 xenografts *(data not shown)*.

3) PKI-166 blocks the growth of prostate cancers in mice in an androgen-dependent fashion.

Having defined the dose of PKI-166 required to inhibit ErbB1/ErbB2 RTKs in vivo, we were now able to examine the role of these RTKs in the growth of human prostate cancer. We chose the LAPC xenograft model to address this question, because of its similarity to clinical prostate cancer (Klein et al., 1997) and the convenience of monitoring drug effects on subcutaneous tumor volumes. Tumors derived from the A431 cell line were used as a positive control and were completely growth arrested by PKI-166 *(data not shown)*. Androgen-independent sublines of the prostate cancer xenografts grown in castrated host mice were consistently more sensitive to growth-inhibition by PKI-166 than androgen-dependent sublines of the same xenograft growing in intact male mice. This observation was confirmed in multiple experiments and noted in both LAPC4 and LAPC9 xenografts (Figure 3A).

The trend toward enhanced activity of PKI-166 in the absence of androgen was reminiscent of our previous data showing more dramatic effects of forced ErbB2 overexpression on prostate cancer growth in castrate versus intact male mice (Craft et al., 1999b). At that time we postulated that the major effects of ErbB1/ ErbB2 pathway activation might be mediated through AR, but that these effects were most relevant in the setting of low (castrate) levels of androgen. To examine this hypothesis, we asked if the suppression of growth by PKI-166 in castrated male mice could be rescued by androgen supplementation, which was administered by subcutaneous implantation of slow release Testosterone pellets. In both LAPC4 and LAPC9 xenografts, androgen add-back partially rescued the growth inhibitory effects of PKI-166 (Figure 3B, upper panel). One potential explanation for this result is that androgen impairs the ability of PKI-166 to inhibit ErbB1/ErbB2 RTKs. To examine this possibility, we treated eight castrated male mice bearing LAPC tumors with PKI-166 in the presence or absence of supplemental Testosterone and measured ErbB receptor and ERK1 activation in tumor lysates following systemic administration of EGF. Androgen supplementation did not impair the ability of PKI-166 to inhibit EGF-induced signal transduction (Figure 3B, middle panel) nor did androgen affect the bioavailablitiy of PKI-166 as shown by similar mean plasma and tumor drug levels in castrate and androgen-supplemented mice (Figure 3B, lower panel). These data indicate that the rescue of PKI-166 – induced growth suppression by androgen supplementation cannot be explained by a failure of PKI-166 to inhibit its target. Rather, our findings suggest that ErbB1/ ErbB2 signaling is not required for prostate cancer growth when androgen is present at high levels.

If a threshold level of circulating androgen exists below which ErbB1/ ErbB2 RTKs are required for prostate cancer growth, acute androgen withdrawal by surgical castration should increase the growth-inhibitory effects of PKI-166. To test this hypothesis, we randomized intact male SCID mice bearing the

LAPC4 xenograft to four treatment groups. Compared to vehicle-treated mice, androgen withdrawal (AW) by surgical castration slowed the growth of LAPC4 tumors, as expected (Klein et al., 1997). Growth inhibition by PKI-166 given at 100 mg/kg daily did not reach statistical significance. However, the combination of PKI-166 with androgen withdrawal resulted in nearly complete growth suppression. The difference between the combined treatment group and any of the other three treatment groups was highly statistically significant (Fig. 3C).

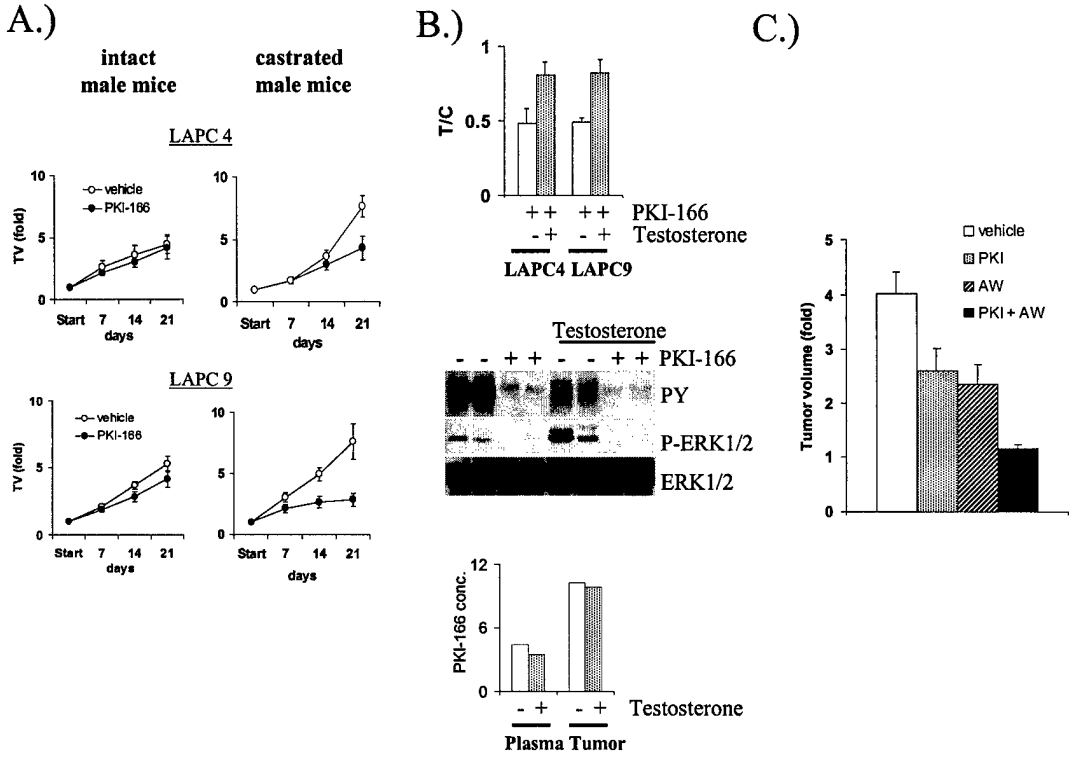

Figure 3. Androgen modifies the growth response to PKI-166 A.) PKI-166 inhibits the growth of human prostate cancer xenografts growing in castrated mice. Mice bearing LAPC4 or LAPC9 xenograft tumors were treated daily for three weeks with 100 mg/kg PKI-166 versus vehicle. B.) *upper panel*: Testosterone rescues growth inhibition by PKI-166 in castrated animals. Castrated male mice bearing androgen-independent xenografts were randomized to four treatment groups (vehicle, PKI-166, vehicle plus testosterone, and PKI plus testosterone). Data is expressed as ratio between the fold increase in tumor volume for PKI-166 treated mice and the fold increase of tumor volume for vehicle treated mice (T/C). *middle panel*: Testosterone does not impair the ability of PKI-166 to inhibit ErbB1/ErbB2 signaling. Castrated male mice bearing LAPC9 xenograft tumors were treated with PKI-166 +/- testosterone for 21 days and EGF (0.1 mg) was administered intraperitoneally 1 hour after the last PKI-166 dose. Tumors were harvested 5 minutes later. Displayed are immunoblots for PY, ERK1/2, and total ERK1/2. *lower panel*: Testosterone does not affect PKI-166 bioavailability in mice. PKI-166 levels in plasma [μM] and LAPC9 tumors [nmol/g] were determined by reversed-phase HPLC in castrated mice after 21 days of treatment with PKI-166 (100 mg/kg) +/- testosterone. Displayed are mean values. C.) Androgen withdrawal augments inhibitory effect of PKI-166 on LAPC4 xenografts in intact male mice. Surgical castration was performed on the same day as PKI-166 treatment was started. Data is expressed as fold tumor volume compared to day 1 (mean + SEM).

4) Sensitivity to growth inhibition by PKI-166 is correlated with ERK activation

The LAPC-4 and LAPC-9 xenografts have been passaged in mice over multiple generations and various AD and AI subclones derived from the original parental lines have been maintained independently. In the

course of these studies we noted that subclones derived from the same parental line occasionally displayed differences in their sensitivity to PKI-166. These sublines provide an opportunity, within an isogenic system, to examine variables in the ErbB1/ErbB2 signaling pathway that might determine response to ErbB1/ErbB2 inhibition. To address this question, we performed biochemical analysis on six LAPC xenograft clones, of which four were grown in intact male mice (clones 1 and 2 for both LAPC 4 and LAPC 9) and two in castrated male mice (clones # 3 for both LAPC 4 and LAPC 9). We examined not only the expression levels of the direct PKI-166 targets ErbB1 and ErbB2, but also the activation state of the Ras/MAPK and PI-3 kinase/Akt-pathways. Both pathways are considered central effectors of the ErbB signaling network (Yarden and Sliwkowski, 2001) and have been implicated in the progression of human prostate cancer (Yeh et al., 1999) (Gioeli et al., 2001) (Wen et al., 2000) (Malik et al., 2002). Expression of the ErbB-1 ligand TGF-α was included in the analysis due to its suggested role as an autocrine growth factor in androgen-independent prostate cancer (Scher et al., 1995). In order to be able to correlate for each subline the expression of these biochemical parameters with the growth response to PKI-166, we quantified the relevant immunoblot bands (Figure 3A) by densitometry. Despite differences in the magnitude of ERK1/2-activation between the LAPC4 and LAPC9 xenograft models, we found within each model a positive correlation between the degree of growth-inhibition by PKI-166 and the level of ERK1/2-activation (Fig. 4B). No such correlation was found for expression levels of ErbB1, ErbB2, TGF-α, or activation level of Akt. While the number of available sublines for each xenograft was not sufficient to perform a multivariate analysis, our results in an isogenic system suggest that expression levels of ErbB-1 or ErbB-2 are not sufficient to determine sensitivity to PKI-166 and is consistent with studies using the ErbB-1 inhibitor ZD1839 (Moasser et al., 2001) or the anti-ErbB-2 monoclonal antibody Mab 4D5 (Lane et al., 2000). Compared to tumors grown in intact male mice (clones#1 and #2), androgen-independent tumors (clones #3) showed increased activation of ERK1/2 (Figure 4A). This observation was confirmed in a new androgen-independent subclone derived from androgen-dependent LAPC4 xenografts (Figure 4B). This data is consistent with results of immunohistochemical analyses of human prostate cancer specimens using phospho-specific antibodies to ERK1/2 (Gioeli et al., 1999).

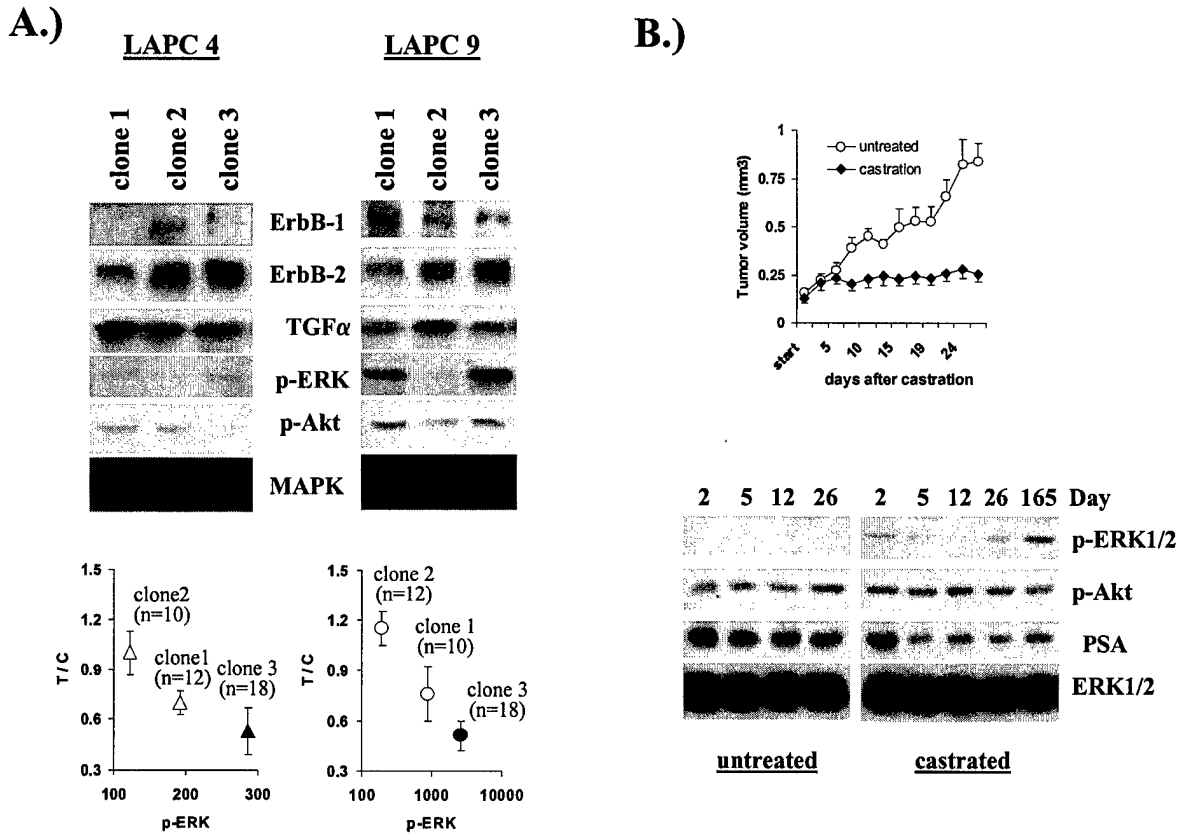

Figure 4. Activity of p-ERK correlates with growth-inhibition by PKI-166 in vivo and is increased in androgen-independent tumors. A.) *upper panel*: Immunoblot of tumor lysates from six different LAPC sublines; *lower panel*: Correlation between growth inhibition by PKI-166 and levels of activated ERK for six LAPC clones. Immunoblot bands were scanned by densitometry and the absolute value under the peak was plotted on the x-axis. The y-axis shows the ratio between the fold increase in tumor volume for PKI-166 treated mice and the fold increase of tumor volume for vehicle treated mice (T/C). Open symbols represent xenograft clones grown in intact mice, closed symbols represent xenograft clones growing in castrated animals B.) Effect of castration on p-ERK levels in LAPC4 xenograft tumors.

In summary, our preclinical findings with PKI-166 support the hypothesis that EGFR/Her2 pathway signaling plays a functional role in androgen-independent prostate cancer growth, and we begin to define molecular correlates of response.

Developing novel systems to monitor androgen independent progression

Based on the success of the preclinical studies with the EGFR/Her-2 kinase inhibitor and the potential importance of Erk kinase activation as a biomarker, we have begun working to develop an imaging system in which the transition to the hormone refractory stage can be visualized in a living mouse. This will serve as a tool for further evaluation of the transition to hormone independence and for evaluation of novel therapeutics. First, we developed enhancers from the prostate specific antigen gene (PSA) that express the highly active chimeric transcription factor GAL4-VP16. Within the same construct we engineered expression of the reporter gene firefly luciferase from 5 GAL4 sites (which respond specifically to the GAL4-VP16 fusion protein). We have recently shown that this approach, known as the two-step transcriptional activation system (TSTA), works extremely well in mouse prostate cancer models (Zhang et al, Molecular Therapy, manuscript appended). We have built this system (AdTSTALuc) into adenovirus vectors and shown that it detects tumors in LAPC9 AD and AI mice using charge coupled device imaging (Fig. 5). The figure demonstrates that the system demonstrates tight specificity for prostate tumors in contrast to Ad based CMV vectors, which express in the liver. Based on our data showing that Erk kinase activation is tightly correlated with evolution to androgen independence in the LAPC models, we are adapting the system to express GAL4-Elk1, a chimeric transcription factor that will respond to the Erk kinase. We have demonstrated a robust response of the PSA-GAL4-Elk-1 system to activators of Erk kinase in LNCaP cells. The goal in year 3 is to generate viral vectors and transgenic animals that express this TSTA-MAPK sensing system for examining levels of Erk activity in androgen independent prostate cancer. In parallel we will examine the utility of the prostate stem cell

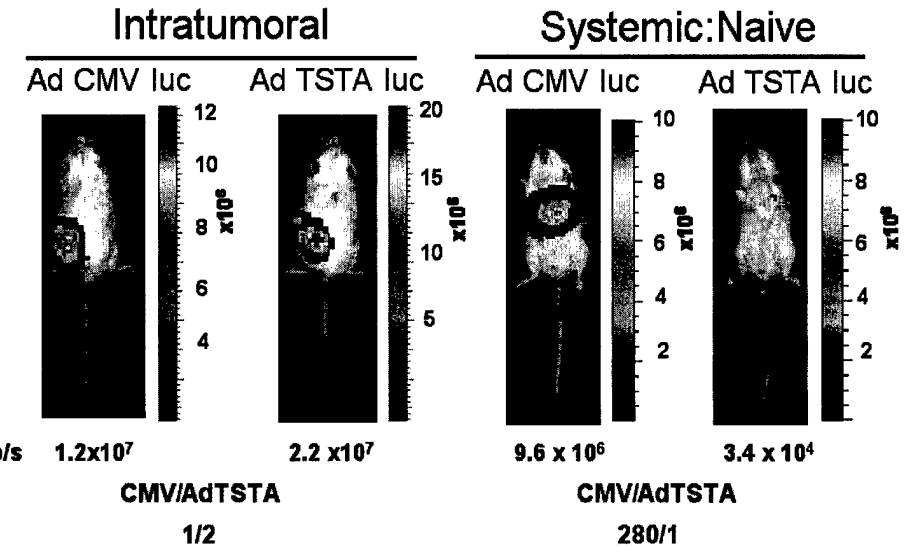

Figure 5. Intratumoral injection of 10^7 AdCMV-luc and AdTSTA-luc into LAPC9 (left set of panels) and naïve mice (right panels). After injection mice were injected with D-luciferin and imaged using a CCD optical imaging system. The TSTA system exhibited twice the activity of CMV in the tumor but was hundreds of fold more specific when analyzing the background signals in liver.

antigen promoter (PSCA) as an reporter for androgen receptor activity (in place of PSA). The rationale is that PSCA is more highly expressed in advanced stage prostate cancer and may serve as a useful marker. Our major progress toward this goal is the mapping of a 0.3 kb enhancer between 2.7 and 3 Kb upstream of the gene that controls androgen dependent and independent transcription in prostate and bladder (Jain et al, Molecular Endo, 2002, manuscript appended). Our goal will be to build this into viral TSTA vectors and examine the activity of the imaging system in LAPC4 and 9 Ad and AI sublines.

Identification of androgen receptor alterations that occur during progression to androgen independence

The focus of this part of the project is to probe the molecular alterations of AR when androgen signaling is replaced by RTKs. The ability to complete this aim is predicated on the development of techniques for efficiently analyzing AR, its modifications and its associated factors from cell lines and tumors. Our hypothesis is that signal transduction pathways regulate association of AR and its co-factors during the AD-AI transition. The goal of our proposal is to develop a methodology for identifying the AR-associated proteins participating in this transition. To develop this methodology, we initiated a collaboration in year 1 between with Drs. Michael Weber and Don Hunt at University of Virginia. Unfortunately, we have been stymied by technical issues that have limited our ability to make rapid progress toward these goals. Although we have accumulated evidence for associated proteins none of these are conventional AR co-activators. Although we continue to probe methods that will trap bona-fide co-activators (like the SRC family), we have shifted our emphasis to the use of chromatin immunoprecipitation technology to analyze the AR complexes present on genes like PSA in androgen-dependent versus androgen-independent disease. This technology has already been shown to work for AR by others (Shang et al., 2002) and is working very well in our hands (see below).

1. Results from the AR proteomics studies:

Our initial model for testing the technology was a HeLa cell line expressing fAR (epitope-tagged with FLAG) from an amphotropic retrovirus (Huang et al., 1999). We employed HeLa cells because they can be grown in spinner culture in 32-liter scale and yield 500 pmol of fAR. Although we began at this scale for practical reasons, the sensitivity of the procedure is in the 50-attomole range. FLAG-tagged AR is precipitated along with any associated proteins using FLAG antibody affinity resin. The advantage of this approach was that the fAR and associated proteins can be eluted from the resin with FLAG-peptide. The methodological details of the approach were described in last years' progress report and will not be repeated here.

Last year we reported that we had already identified key AR-associated proteins from this analysis in HeLa, such as AR, glucocorticoid receptor, mineralcorticoid receptor, several heat shock proteins, several DEAD box proteins, a nuclear matrix associated protein and others. However, we found few co-activator candidates of the type that were reported to interact with steroid receptors. We were concerned that HeLa cells might represent an artificial system, therefore we focused our efforts in year 2 on applying the technology to LNCaP cells and LAPC9 xenograft tumors where endogenous AR is known to be active. Unfortunately, we have run into serious technical issues that complicate the application of this approach. We were able to precipitate AR from LNCaP and LAPC tumor extracts with numerous antibodies against the FLAG-tag, the N and C terminus and internally. However, we analyzed our peptides against known AR co-activators by both MS/MS and immunoblotting and found no matches. Since one possible explanation is excess noise in the system, we performed double immunoprecipitations of AR from extracts of LNCaP and HeLa and subjected the samples to mass spectrometry analysis. However, no

additional proteins were found attached to AR, indicating that this double immunoprecipitation approach is too harsh. This work will continue, but we are diverting our focus to a newer technology.

2. Initial results from chromatin immunoprecipitation analysis of AR:

Rather than continue to troubleshoot these technical barriers, we have changed our strategy and adapted the technique of chromatin immunoprecipitation analysis of AR and pol II in LNCaP and LAPC cell lines and xenografts. This technique allows the composition of transcription complexes bound to endogenous chromatin templates to be discerned in living cells. In our case, we immunoprecipitate AR from formaldehyde treated cells under varying conditions of androgen stimulation and determine if AR is

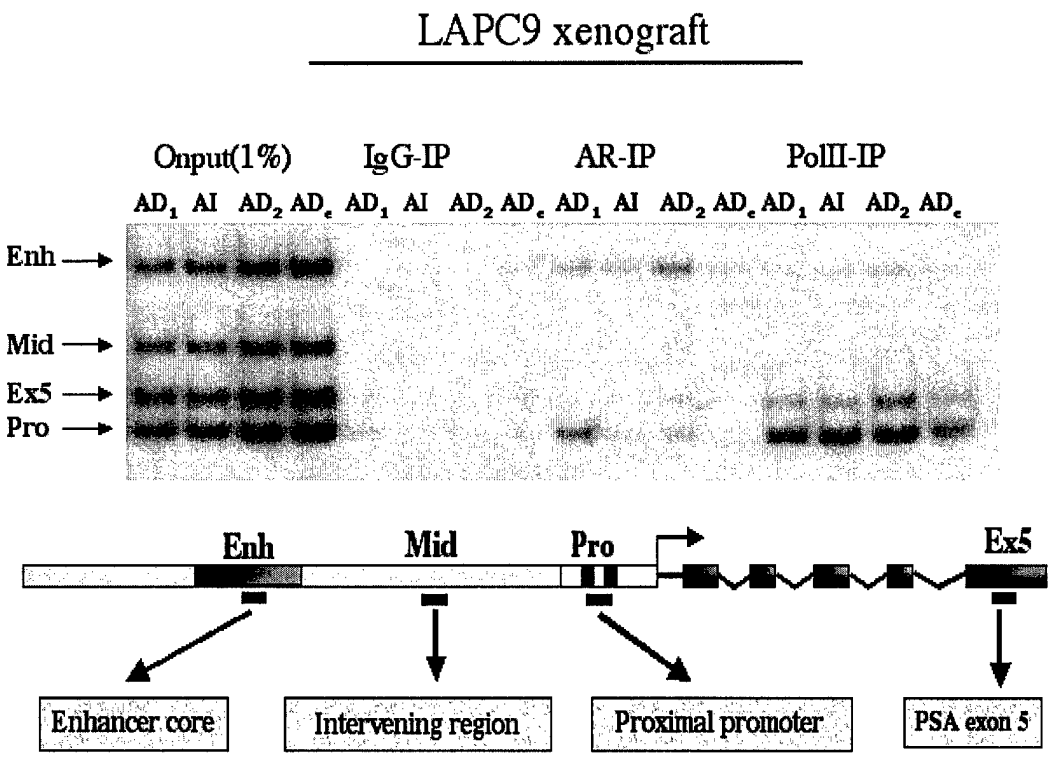

Figure. 6. Binding of AR and Pol II to the PSA Gene in Tumors. The results are in groups of 4. LAPC9 tumors were subcutaneously grown on the dorsal flank of intact (for AD_1 and $_2$) or castrated (for AI) SCID mice. In case of ADc, an AD tumor bearing mouse was castrated and the tumor was extracted 5 days later. Serum PSA levels were measured to assure efficient androgen ablation in ADc. The extracted tumors were washed in PBS, quickly minced and incubated in 1% formaldehyde, while further minced and homogenized with a tissue homogenizer. Cross-linked and homogenized tumors were washed with high salt and LiCl buffer and sonicated. Sonicated samples were immunoprecipitated with AR, pol II or control (IgG) antibodies and analyzed by PCR using the primer sets against the enhancer (Enh), middle or intervening region (Mid), the promoter (Pro), or downstream exon 5 (Ex5).

bound to the endogenous PSA promoter using specific PCR primers. The presence or absence of coactivators and corepressors present in the complex can be discerned using appropriate antibodies. We have been able to demonstrate AR binding the PSA enhancer in LNCaP cells and in AI and AD tumors. The experiment of Figure 6 shows an autoradiograph of a polyacrylamide gel of the fractionated PCR products. The onput of this multiplex PCR experiment represents the starting DNA isolated from LAPC9 AD, AD castrated (ADc) and AI tumor samples. There are two separate AD experiments (AD_1 and $_2$). We

have been able to demonstrate AR binding consistently to the AR-responsive enhancer (Enh) of the PSA gene in AD and AI tumors but the signal is greatly diminished in AD tumors from castrated animals. The binding of AR to the PSA enhancer in AI cells was predicted by the studies of Craft et al., 1999, which showed that RTKs can signal directly with AR in AI cancer. The binding of AR to the promoter (Pro) is less discernible but evident in one AD tumor and in many experiments performed on LNCaP cells in culture (not shown). RNA pol II binds to the promoter and a downstream exon 5 as expected, and shows some very weak binding to the enhancer. Weak binding to the enhancer was predicted based on the results of Brown and colleagues who have provided evidence for higher order interactions between the enhancer and promoter in vivo. Pol II is diminished but not absent in ADc. We do not fully understand this phenomenon since PSA levels returned to baseline after castration. The goal for year 3 is to determine if differences exist between AI and AD cells with respect to known AR co-activators like SRC-1, -2 and -3 and p300.

Summary

During years 1 and 2, Project 1 has clearly established the role of RTKs such as EGFR/Her2 in modulating AR function and provide insight into potential clinical applications of EGFR pathway inhibitors. We have also developed in vivo imaging technologies to measure gene expression in mouse models, and we will adapt this technology in year 3 to study progression to androgen independence by making Erk-responsive luciferase reporter constructs. During year 3 we will also use chromatin immunoprecipitation to eludicate the mechanism of crosstalk between EGFR/Her2 and AR, as this assay is likely to be important in evaluating the clinical use of signaling pathway inhibitors.

Project 2 (Cohen)

The goals of this project are to identify and characterize the role of IGFBP-3 in androgen receptor-signaling in androgen-dependent and -independent prostate cancer models. We are examining if IGFBP-3 is essential for apoptosis in response to androgen withdrawal. We are testing the effects of androgen deprivation on IGFBP-3 induction, IGF/IGF-R suppression, and prostatic apoptosis, in the AI and AD LAPC-4 and -9 cell lines and xenograft models of prostate cancer and in genetically altered mouse models. We are attempting to induce prostate cell death by treating these mice with systemic IGFBP-3. We are also trying to examine the role of RXR-α in IGFBP-3 actions in the prostate. We have begun to generate prostatic RXR-α conditional (cre-lox) knockout models in order to evaluate the prostates of these mice before and after castration or IGFBP-3 treatment. These experiments will determine if RXR is required for apoptosis in response to androgen deprivation. We are also studying IGFBP-3 synergism with ligands of RXR-alpha and related receptors both *in vivo* in the AD and AI LAPC models and *in vitro* in prostate cancer cell line models.

IGFBP-3 and RXR synergism *in vitro*

We also showed (Fig. 5) that IGFBP-3 and a specific rexinoid (from Allergan Inc.) had additive effects in inhibiting LAPC-4 cells. This is an important observation as it suggests that IGFBP-3 and RXR ligands co-operate on inducing gene transcription that leads to apoptosis. Furthermore, these data suggest that these agents will have a synergistic effect on CaP tumors *in vivo* and thus may be useful as co-adjuvant therapy in prostate cancer.

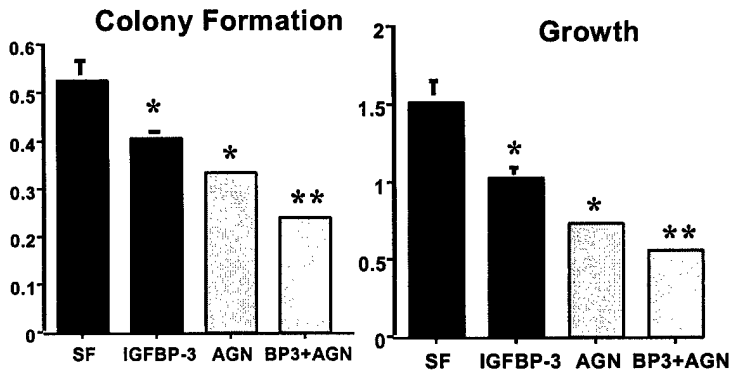

Figure 5 Synergistic effects of IGFBP-3 and RXR agonists on the growth of LAPC-4 prostate cancer cells. This experiments illustrates the potential utility of IGFBP-3 as a adjuvant therapy for prostate cancer.

IGFBP-3 and RXR synergism *in vivo*

On going experiments are evaluating the effect of infusing IGFBP-3 alone or in combination with RXR ligands on the growth of LAPC-4 and LAPC-9 xenografts in SCID mice. Preliminary data shows combination therapy with IGFBP-3 and an RXR ligand from Allergan results in suppression of tumor growth (data presented in the 2002 AACR meetings and shown below).

Creation of prostatic RXR knockout mice

We are proceeding in the generation of these mice by crossing Flox RXR mice with transgenic mice expressing Cre under the control of the probasin promoter to achieve prostate-specific excision of RXR. We will begin to examine homozygous mice histologically before and after castration and will treat mice with IGFBP-3 and rexinoids and study prostates looking for apoptotic effects. These experiments are scheduled for year 3.

Mechanism of action of IGFBP-3

We have enhanced our understanding of the mechanism of interaction between RXR and IGFBP-3 in terms of mediating apoptosis in CaP cells. This appears to involve IGFBP-3 induced dissociation of the RXR-TR3 complex and translocation of TR3/Nur77 to the mitochondria. Our xenograft studies are allowing us to refine the in vivo dosing strategy for IGFBP-3 and RXR-ligands. Protigen and Allergan are companies that supply us with appropriate reagents for this development. IGFBP-3 as well as several nuclear receptor systems are critical regulators of CaP death/survival signaling pathways, and RXR-α is an IGFBP-3 association protein which is critical to IGFBP-3 signal transduction (and vice versa). Our investigation into the interactions between IGFBP-3/RXR/TR3, has confirmed that IGFBP-3 does translocate the nuclear receptor TR3 leading to cellular apoptosis in vitro. We are currently testing if this phenomenon also occurs in vivo. Our preliminary studies also indicate that co-overexpression of IGFBP-3 and TR3 are synergistic in their apoptotic effects on prostate cancer cells (Figure 7).

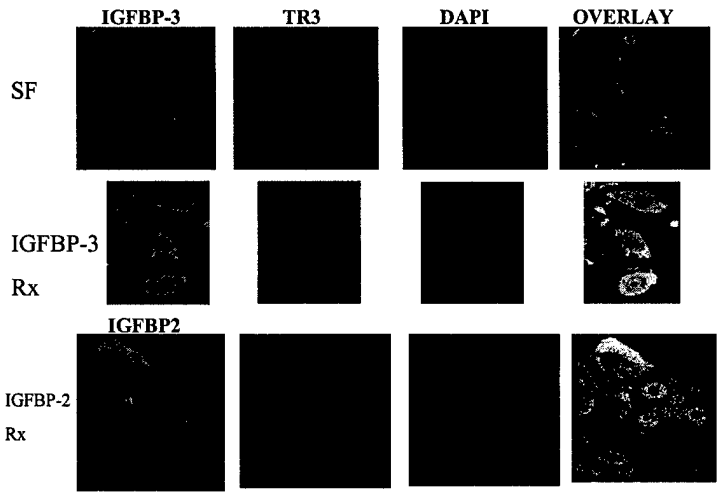

Figure 6 IGFBP-3 Translocates TR3 in Primary Prostate Cancer Culture Row Headings are treatments, column headings are staining. Note absence of nuclear TR3 after IGFBP-3 treatment.

TR3 translocation by IGFBP-3 is specific to cancerous cells

In preliminary work with Dr. Donna Peehl at Stanford University, we obtained prostate cancer primary cultures with matched adjacent normal prostate epithelium at the time of surgery. These primary cells were cultured and treated with IGFBP-3 and then immunostained for TR3 using confocal microscopy. Treatment with IGFBP-3 completes leaves the nucleus devoid of TR3. This is a specific action of IGFBP-3 as IGFBP-2 does not translocate TR3 (Figure 6). Treatment of matched primary non-malignant epithelial cells from the same donor fails to show translocation (data not shown). This TR3 translocation specificity to malignant cells by IGFBP-3 mirrors effects on apoptosis that we observe in cell lines.

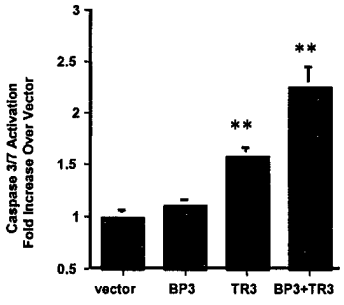

Figure 7 IGFBP-3 and TR3 synergize in killing prostate cancer cells Note that co-transfection of IGFBP-3 and TR3 has additive effects.

The present work clearly demonstrates that IGFBP-3 is *a unique* signal molecule in its ability to both a) modulate traditional nuclear receptor roles as DNA transcription factors and b) modulate novel nuclear receptor roles as extra-nuclear mediators of cellular biologic processes. The specificity of IGFBP-

3 induced TR3 translocation to cancerous cells makes it an attractive target in the therapy of prostatic malignancy. Thus, IGFBP-3 protein therapy, a molecule downstream of the AR, is of potential value in the treatment of AI CaP. By using a SCID mouse LAPC-4 xenograft model, we have very early data that these observations are confirmed *in vivo*. We utilized LAPC-4 xenografts in SCID mice that were treated with daily IP injections of either saline, IGFBP-3, an RXR ligand produced by Allergan, or IGFBP-3/RXR ligand combination. The individual treatments showed little or no effect in terms of tumor size, but the combination showed a dramatic reduction in growth. The PSA levels demonstrated a similar trend and a gene array analysis in response to these treatments also demonstrated a coordinated pattern of gene induction (data not shown).

Summary:

Collectively, our recently obtained data indicate, that IGFBP-3 as well as IGF-I are critical regulators of androgen-dependent as well as androgen-independent CaP death/survival signalling pathways, and that RXR-α and TR3 are IGFBP-3 association protein which are critical to IGFBP-3 signal transduction. We have demonstrated, this year, that androgen withdrawal induces IGFBP-3 in a variety of systems. Our experiments show that both exogenous addition of IGFBP-3 protein or transfection of IGFBP-3 kills CaP cells and enhances the effects of other chemo-therapeutic agents such as Taxol and RXR-ligands. Most importantly, we can reproduce these effects in the absence of androgens, indicating that IGFBP-3 can kill androgen-independent CaP cells.

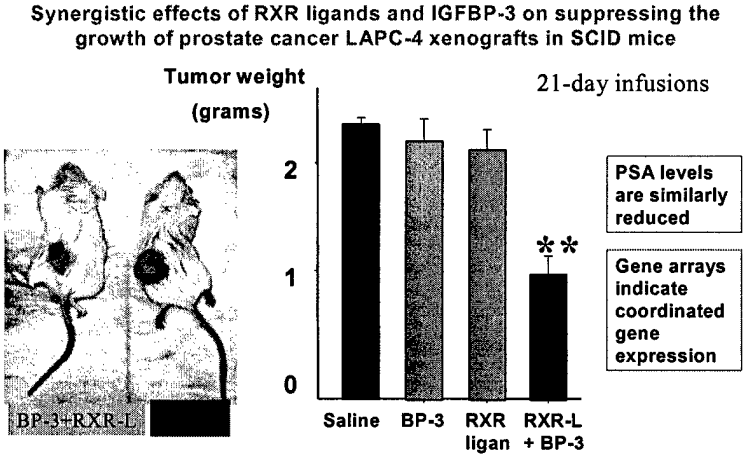

Figure 8 IGFBP-3 and RXR ligands synergize in killing prostate cancer cells *in vivo* Note that a 21-day infusion of either agent alone has minimal effects, but a combination arm resulted in a dramatic suppression of tumor growth.

Conclusions

Project 2 has used innovative approaches to characterize prostate cancer pathophysiology as it relates to nuclear receptors and their interactions with IGFBP-3. The data show that IGFBP-3 is an important regulator of apoptosis in prostate cells, particularly in conjunction with RXR agonists. The novel observation linking TR3 to IGFBP-3 actions opens new avenues of addressing CaP. Since pharmacological modulation of this pathway is clinically feasible, we anticipate that this project will also lead to clinical trials.

Core Facility (Sawyers)

Under Dr. Sawyers' direction, the core facility has continues to provide human prostate cancer xenograft material for study of signaling pathways in Projects 1 and 2. In addition the core facility has set up the tumor models for preclinical studies and assisted investigators in the conduct of these studies by measuring tumor volume and serum PSA levels. The core facility also assists in genotype analysis RXRα knockout mice for Project 2 and in crossing the mice to probasin-Cre strains. Finally, the core handles tissue fixation, H&E staining and immunohistochemical analysis of xenograft and mouse tissues (Dr. Said, Pathology).

Key Research Accomplishments

Project 1

1. We have shown that IGF-I and IGF-IR expression and activity are altered in some xenografts during the transition to androgen independence and published the findings.
2. We shown shown specific activity of the EGFR/Her-2 tyrosine kinase inhibitor PKI-166 against androgen independent prostate cancer xenografts and published the findings.
3. We identified the phosphorylation status of Erk kinase as the best determinant of sensitivity to EGFR/Her-2 inhibition in prostate cancer and published the findings.
4. We have constructed a 2-step luciferace reporter gene imaging system to measure Erk kinase activation in mouse prostate cancer models.
5. We have defined the promoter region of the prostate stem cell antigen gene.
6. We have developed chromatin immunoprecipitation as a tool to monitor AR transcriptional function in living cells on endogenous gene templates.

Project 2

7. We have identified a clear effect of IGFBP-3 on the induction of prostate cell apoptosis which is mediated by interactions with RXR
8. We have identified a synergistic effect of IGFBP-3 and RXR ligands on the killing of prostate cancer cells.
9. We discovered a novel mechanism for the actions of IGFBP-3 involving TR3 translocation from the nucleus

Reportable Outcomes

Publications

Project 1

Mellinghoff, I. K., Tran, C., and Sawyers, C. L. (2002). Growth inhibitory effects of the dual ErbB1/ErbB2 tyrosine kinase inhibitor PKI-166 on human prostate cancer xenografts. Cancer Research *In press*.

Nickerson, T., Chang, F., Lorimer, D., Smeekens, S. P., Sawyers, C. L., and Pollak, M. (2001). In vivo progression of LAPC-9 and LNCaP prostate cancer models to androgen independence is associated with increased expression of insulin-like growth factor I (IGF-I) and IGF-I receptor (IGF-IR). Cancer Res *61*, 6276-6280.

Zhang, L., Adams, J. Y., Billick, E., Ilagan, R., Iyer, M., Le, K., Smallwood, A., Gambhir, S. S., Carey, M., and Wu, L. (2002). Molecular engineering of a two-step transcription amplification (TSTA) system for transgene delivery in prostate cancer. Mol Ther *5*, 223-232.

Jain, A., Lam, A., Carey, M., and Reiter, R. (2002). Identification of an Androgen-Dependent Enhancer Within the Prostate Stem Cell Antigen Gene. Molecular Endocrinology *In press*.

Wu, L., Matherly, J., Smallwood, A., Adams, J. Y., Billick, E., Belldegrun, A., and Carey, M. (2001). Chimeric PSA enhancers exhibit augmented activity in prostate cancer gene therapy vectors. Gene Ther *8*, 1416-1426.

Adams, J. A., Johnson, M., Sato, M., Berger, F., Gambhir, S. S., Carey, M., Iruela-Arispe, L., and Wu, L. (2002). Visualization of Advanced Human Prostate Cancer Lesions in Living Mice by a Targeted Gene Transfer Vector and Optical Imaging. Nature Medicine *In press*.

Project 2

Publications

Boyle, B. J., Zhao, X. Y., Cohen, P., and Feldman, D. (2001). Insulin-like growth factor binding protein-3 mediates 1 alpha,25-dihydroxyvitamin d(3) growth inhibition in the LNCaP prostate cancer cell line through p21/WAF1. J Urol *165*, 1319-1324.

Weinzimer, S. A., Gibson, T. B., Collett-Solberg, P. F., Khare, A., Liu, B., and Cohen, P. (2001). Transferrin is an insulin-like growth factor-binding protein-3 binding protein. J Clin Endocrinol Metab *86*, 1806-1813.

Cohen, P. (2001). Clinical implications of the IGF-cancer connection. Growth Horm IGF Res *11*, 336-338.

Rajah, R., Lee, K. W., and Cohen, P. (2002). Insulin-like Growth Factor Binding Protein-3 Mediates Tumor Necrosis Factor-alpha-induced Apoptosis: Role of Bcl-2 Phosphorylation. Cell Growth Differ *13*, 163-171.

Grimberg, A., Liu, B., Bannerman, P., El-Deiry, W. S., and Cohen, P. (2002). IGFBP-3 mediates p53-induced apoptosis during serum starvation. Int J Oncol *21*, 327-335.

Lee, H. Y., Chun, K. H., Liu, B., Wiehle, S. A., Cristiano, R. J., Hong, W. K., Cohen, P., and Kurie, J. M. (2002). Insulin-like growth factor binding protein-3 inhibits the growth of non-small cell lung cancer. Cancer Res *62*, 3530-3537.

Major Presentations:

Project 1

Mar	2001	American Association of Cancer Research Education Session, New Orleans, Louisiana. Lecture: "Signal Transduction by P13K/PTEN/Akt"
Sept	2001	CaP CURE Annual Retreat, Lake Tahoe, Nevada. Lecture: "Interrogating AR Signaling In Vitro and In Vivo"
Nov	2001	Society for Basic Urologic Research, Tucson, Arizona. Lecture: "Kinase Signaling in Prostate Tumorigenesis"
Feb	2002	UCSF Urology Department in San Francisco, CA Lecture: "Interrogating AR Signaling In Vitro and In Vivo"
Apr	2002	American Association for Cancer Research (AACR) Annual Meeting, Symposium on Targeted Therapy, San Francisco, California. Lecture: "PTEN Pathway in Prostate Cancer"
Apr	2002	CaP CURE, Los Angeles, California. Lecture: "Signal Transduction Inhibitor Therapy in Prostate Cancer"

Project 2

Aug	2001	Annual Japanese Growth Study meeting, Tokyo, Japan. Lecture: "IGFBP-3 and its biological functions"
Jan	2002	Cal Tech Research Symposium, Pasadena CA. "Nuclear interactions of IGFBPs".
Feb	2002	International Aging Male Symposium, Berlin, Germany. "The IGFs axis in prostate cancer".
Apr	2002	International Growth Hormone Symposium, Budapest, Hungary. "IGFBPs, what do they do and why should we monitor them".
May	2002	ACVIM Annual meeting, Dallas TX. "Interactions between the IGF axis and retinoid receptors".

Translational research:

Both projects formed the basis for two projects that were recommended for funding within the UCLA Prostate Cancer SPORE grant, which is scheduled to become active in the latter half of 2002. Project 1 laid the groundwork for a translational clinical trial with monoclonal antibody therapy directed against Her2/neu using the antibody 2C4 (Genetech, David Agus, PI) and a separate study of the small molecule EGFR kinase inhibitor Iressa (AstraZeneca). Project 2 had led to further translational studies to define the mechanism of IGFBP3/ RXR syngergy using expression profiling technlogy, which is expected to lead to a clinical trial within 3 years.

Conclusions

This Prostate Cancer Center Initiation Award continues to examine signal transduction pathways involved in prostate cancer progression, with an eye toward translational research applications. Project 1 has

shown the potential role of the EGFR/Her-2 pathway in androgen independence, with a clear path toward testing kinase inhibitors of this pathway in patients. Importantly, this work identified a candidate biomarker for signaling prostate cancer progression to androgen independence, which will also be useful for molecular imaging studies. In the final year we will gain a better mechanistic understanding of the role of RTKs in AI cancer from both a clinical and biochemical perspective. Project 2 has used innovative approaches to characterize prostate cancer pathophysiology as it relates to nuclear receptors and their interactions with IGFBP-3. The data show that IGFBP-3 is an important regulator of apoptosis in prostate cells, particularly in conjunction with RXR agonists. Since pharmacological modulation of this pathway is clinically feasible, we anticipate that this project will also lead to clinical trials within 3 years in the context of the UCLA Prostate Cancer SPORE.

References

Brandt, R., Wong, A. M., and Hynes, N. E. (2001). Mammary glands reconstituted with Neu/ErbB2 transformed HC11 cells provide a novel orthotopic tumor model for testing anti-cancer agents. Oncogene *20*, 5459-5465.

Bruns, C. J., Solorzano, C. C., Harbison, M. T., Ozawa, S., Tsan, R., Fan, D., Abbruzzese, J., Traxler, P., Buchdunger, E., Radinsky, R., and Fidler, I. J. (2000). Blockade of the epidermal growth factor receptor signaling by a novel tyrosine kinase inhibitor leads to apoptosis of endothelial cells and therapy of human pancreatic carcinoma. Cancer Res *60*, 2926-2935.

Chen, W. S., Lazar, C. S., Poenie, M., Tsien, R. Y., Gill, G. N., and Rosenfeld, M. G. (1987). Requirement for intrinsic protein tyrosine kinase in the immediate and late actions of the EGF receptor. Nature *328*, 820-823.

Craft, N., Chhor, C., Tran, C., Belldegrun, A., DeKernion, J., Witte, O. N., Said, J., Reiter, R. E., and Sawyers, C. L. (1999a). Evidence for clonal outgrowth of androgen-independent prostate cancer cells from androgen-dependent tumors through a two-step process. Cancer Res *59*, 5030-5036.

Craft, N., Shostak, Y., Carey, M., and Sawyers, C. L. (1999b). A mechanism for hormone-independent prostate cancer through modulation of androgen receptor signaling by the HER-2/neu tyrosine kinase. Nat Med *5*, 280-285.

Donaldson, R. W., and Cohen, S. (1992). Epidermal growth factor stimulates tyrosine phosphorylation in the neonatal mouse: association of a M(r) 55,000 substrate with the receptor. Proc Natl Acad Sci U S A *89*, 8477-8481.

Gioeli, D., Mandell, J. W., Petroni, G. R., Frierson, H. F., Jr., and Weber, M. J. (1999). Activation of mitogen-activated protein kinase associated with prostate cancer progression. Cancer Res *59*, 279-284.

Gioeli, D., Zecevic, M., and Weber, M. J. (2001). Immunostaining for activated extracellular signal-regulated kinases in cells and tissues. Methods Enzymol *332*, 343-353.

Honegger, A. M., Dull, T. J., Felder, S., Van Obberghen, E., Bellot, F., Szapary, D., Schmidt, A., Ullrich, A., and Schlessinger, J. (1987). Point mutation at the ATP binding site of EGF receptor abolishes protein-tyrosine kinase activity and alters cellular routing. Cell *51*, 199-209.

Klein, K. A., Reiter, R. E., Redula, J., Moradi, H., Zhu, X. L., Brothman, A. R., Lamb, D. J., Marcelli, M., Belldegrun, A., Witte, O. N., and Sawyers, C. L. (1997). Progression of metastatic human prostate cancer to androgen independence in immunodeficient SCID mice. Nat Med *3*, 402-408.

Lane, H. A., Beuvink, I., Motoyama, A. B., Daly, J. M., Neve, R. M., and Hynes, N. E. (2000). ErbB2 potentiates breast tumor proliferation through modulation of p27(Kip1)-Cdk2 complex formation: receptor overexpression does not determine growth dependency. Mol Cell Biol *20*, 3210-3223.

Malik, S. N., Brattain, M., Ghosh, P. M., Troyer, D. A., Prihoda, T., Bedolla, R., and Kreisberg, J. I. (2002). Immunohistochemical demonstration of phospho-akt in high Gleason grade prostate cancer. Clin Cancer Res *8*, 1168-1171.

Mellinghoff, I. K., Tran, C., and Sawyers, C. L. (2002). Growth inhibitory effects of the dual ErbB1/ErbB2 tyrosine kinase inhibitor PKI-166 on human prostate cancer xenografts. Cancer Research *In press*.

Moasser, M. M., Basso, A., Averbuch, S. D., and Rosen, N. (2001). The tyrosine kinase inhibitor ZD1839 ("Iressa") inhibits HER2-driven signaling and suppresses the growth of HER2-overexpressing tumor cells. Cancer Res *61*, 7184-7188.

Nickerson, T., Chang, F., Lorimer, D., Smeekens, S. P., Sawyers, C. L., and Pollak, M. (2001). In vivo progression of LAPC-9 and LNCaP prostate cancer models to androgen independence is associated with increased expression of insulin-like growth factor I (IGF-I) and IGF-I receptor (IGF-IR). Cancer Res *61*, 6276-6280.

Scher, H. I., Sarkis, A., Reuter, V., Cohen, D., Netto, G., Petrylak, D., Lianes, P., Fuks, Z., Mendelsohn, J., and Cordon-Cardo, C. (1995). Changing pattern of expression of the epidermal growth factor receptor and transforming growth factor alpha in the progression of prostatic neoplasms. Clin Cancer Res *1*, 545-550.

Scheving, L. A., Stevenson, M. C., Taylormoore, J. M., Traxler, P., and Russell, W. E. (2002). Integral role of the EGF receptor in HGF-mediated hepatocyte proliferation. Biochem Biophys Res Commun *290*, 197-203.

Shang, Y., Myers, M., and Brown, M. (2002). Formation of the androgen receptor transcription complex. Mol Cell *9*, 601-610.

Stoscheck, C. M., and Carpenter, G. (1984). Down regulation of epidermal growth factor receptors: direct demonstration of receptor degradation in human fibroblasts. J Cell Biol *98*, 1048-1053.

Wen, Y., Hu, M. C., Makino, K., Spohn, B., Bartholomeusz, G., Yan, D. H., and Hung, M. C. (2000). HER-2/neu promotes androgen-independent survival and growth of prostate cancer cells through the Akt pathway. Cancer Res *60*, 6841-6845.

Yarden, Y., and Sliwkowski, M. X. (2001). Untangling the ErbB signalling network. Nat Rev Mol Cell Biol *2*, 127-137.

Yeh, S., Lin, H. K., Kang, H. Y., Thin, T. H., Lin, M. F., and Chang, C. (1999). From HER2/Neu signal cascade to androgen receptor and its coactivators: a novel pathway by induction of androgen target genes through MAP kinase in prostate cancer cells. Proc Natl Acad Sci U S A *96*, 5458-5463.

Zhang, L., Adams, J. Y., Billick, E., Ilagan, R., Iyer, M., Le, K., Smallwood, A., Gambhir, S. S., Carey, M., and Wu, L. (2002). Molecular engineering of a two-step transcription amplification (TSTA) system for transgene delivery in prostate cancer. Mol Ther *5*, 223-232.

Growth inhibitory effects of the dual ErbB1/ErbB2 tyrosine kinase inhibitor PKI-166 on human prostate cancer xenografts

Ingo K. Mellinghoff[1], Chris Tran[1], and Charles L Sawyers[1,2]

Departments of Medicine[1] and Molecular Biology Institute[2]; UCLA School of Medicine; Los Angeles, CA

Address correspondence to: Charles L. Sawyers; 11-934 Factor Building; UCLA-Hematology-Oncology; 10833 Le Conte Avenue; Los Angeles, CA 90095-1678

310-206-5585 (tel); 310-206-8502 (fax); email: csawyers@mednet.ucla.edu

Key words include: EGFR, Her-2/neu, androgen-independent, targeted therapy, small molecule kinase inhibitor.

Abstract

Experiments with human prostate cancer cell lines have shown that forced overexpression of the ErbB2-receptor tyrosine kinase (RTK) promotes androgen-independent growth and increases androgen receptor (AR) transcriptional activity in a ligand independent fashion. To investigate the relationship between ErbB-RTK signaling and androgen in genetically unmanipulated human prostate cancer, we performed biochemical and biologic studies with the dual ErbB1/ErbB2 RTK inhibitor PKI-166 using human prostate cancer xenograft models with isogenic sublines reflecting the transition from androgen dependent to androgen independent growth. In the presence of low androgen concentrations, PKI-166 showed profound growth-inhibitory effects on tumor growth, which could be partially reversed by androgen add-back. At physiologic androgen concentrations, androgen withdrawal greatly enhanced the ability of PKI-166 to retard tumor growth. The level of extracellular signal regulated kinase (ERK) activation correlated with the response to PKI-166 treatment, whereas the expression levels of ErbB1 and ErbB2 did not. These results suggest that ErbB1/ErbB2 RTKs play an important role in the biology of androgen-independent prostate cancer and provide a rationale for clinical evaluation of inhibitors targeted to this pathway.

Introduction

Carcinoma of the prostate is the most common malignancy affecting males and causes enormous morbidity and mortality in the U.S. and Western Europe. About one third of men relapse after radical prostatectomy surgery due to previously undetected metastatic disease. Metastatic prostate cancer responds for a variable period of time to androgen-deprivation therapy, but eventually resumes growth despite castrate levels of androgen. This state of disease,

termed "androgen-independent" prostate cancer, is characterized by expression of the androgen-receptor (AR) and AR-regulated genes, suggesting that the AR pathway is reactivated in a "ligand-independent" fashion. Several mechanisms have been proposed to explain the phenomenon of AR reactivation in the setting of castrate levels of ligand. These include mutations in AR that alter its ligand-binding affinity, overexpression of AR due to gene amplification, and / or increased recruitment of intracellular signal transduction pathways which activate AR through ligand-independent mechanisms (1).

ErbB receptor tyrosine kinases (RTKs) have been implicated as one such pathway that may play a role in androgen-independent prostate cancer progression. Experimental support for this concept comes from the observation that i.) activation of ErbB1 and / or ErbB2 RTKs by epidermal growth factor (EGF) or forced overexpression of ErbB2, respectively, results in androgen-independent activation of AR transcriptional activity in prostate cancer cell lines (2) (3) (4), ii.) forced overexpression of ErbB2 promotes androgen-independent growth of prostate cancer cells (2) (3), and iii.) androgen-independent prostate cancers express increased levels of ErbB2 receptor protein (2) (5) (6) (7). It is still uncertain, however, whether ErbB1- and ErbB2-mediated signals contribute to the progression of human prostate cancer, which – unlike breast cancer (8) – rarely shows amplification of ErbB-gene loci. Using xenograft models of human prostate cancer, we here show a striking interplay of AR and ErbB signaling pathways. Growth inhibition by the ATP-site specific ErbB1/ErbB2 RTK inhibitor PKI-166 was greatest in androgen-independent tumors, significantly augmented by simultaneous androgen withdrawal, and partially rescued by androgen supplementation. Growth inhibition by PKI-166 was positively correlated with the basal activation state of the extracellular signal regulated kinases

ERK1/2. Our findings suggest that ErbB1/ErbB2 RTKs play an important role in the biology of human prostate cancer and may be a viable therapeutic target for novel kinase inhibitors (9).

Materials and Methods

Reagents. The LAPC4 cell line was established from the LAPC4 human prostate cancer xenograft (10), A431 cells were kindly provided by Dr. Harvey Hershman (UCLA), and LNCaP cells were purchased from ATCC. PKI-166 was obtained from Novartis Pharma AG, Basel, Switzerland. Epidermal growth factor and standard chemical reagents were obtained from Sigma. Antibodies against ErbB1 (*sc-101*, *sc-03*), ERK1/2 (*sc-94*), TGF-alpha (*sc-9043*), and PSA (*sc-7638*) were obtained from Santa Cruz Biotechnology, against ErbB2 from Oncogene Sciences (*OP-15*), against Phosphotyrosine from Upstate (*4G10*), against activated ErbB1 from Chemicon (*MAb3052*), against phospho-ERK (Thr183/Tyr185) from Promega (*V8031*), and against phospho-Akt (Ser473) from Cell Signaling Technology (*Ab9271*).

Pulse-chase experiments and immunoblotting. A431 cells were labeled for 12 hours in methionine-free DMEM with 0.2 mCi ^{35}S-Methionine/Cysteine (Translabel, ICN Biomedicals) per 10 cm plate. Cells were subsequently washed three times in serum-free DMEM. Serum-free DMEM with 15 mg/l unlabeled Methionine ("chase-media") was added to each plate in the presence or absence of 5 μM PKI-166. Ten minutes later 100 ng/ml EGF was added where indicated in Figure 1B. Cells were lysed immediately after the third wash in serum-free DMEM (baseline sample) and at various intervals following the addition of chase-media. Cell lysis, immunoprecitation, SDS-PAGE-electropheresis, autoradiography, and immunoblotting was performed following standard protocols (11). Protein concentration was determined in all lysates

by Biorad and equal amounts of protein were loaded per lane. Quantification of immunoblot bands was performed using ImageQuant software.

Animal Experiments. Severe combined immunodeficient (C.B.-17 *Scid/Scid)* mice were bred and maintained in a laminar flow tower in a defined flora colony as described previously (12). All manipulations with the animals were performed in a laminar flow hood with sterile techniques following the guidelines of the UCLA Animal Research Committee. For preparation of single cell suspensions, LAPC4 (10) and LAPC9 (13) tumors continuously passaged in *SCID* mice were minced in serum-free Iscove's medium (Life Technologies, Grand Island, NY), washed, digested with 0.1% Pronase E (EM Science, Gibbstown, NJ), washed again, and filtered through a 200 micron nylon mesh (BioDesign Inc. of New York, Carmel, NY). The cells were plated overnight, resuspended in PrEGM, and injected with Matrigel into the right flank of *SCID* mice. Tumor size was determined with calipers and mice were randomized to treatment groups when tumor size reached about 100 mm^3. Mean tumor volumes (in mm^3) at treatment begin was equal between groups. PKI-166 was administered daily by gavage with a 18 gauge animal feeding needle (VWR, San Dimas, CA). Testosterone pellets (Innovative Research of America) were implanted subcutaneously. Tumor growth data is expressed as fold tumor volume compared to day 1 (Figures 2A and 2C) or as ratio between the fold increases in tumor volume for PKI-166 and vehicle treated mice ("T/C"; Figures 2B and 3B). Statistical analyses comparing fold-increases between groups were performed on the natural logarithms of the tumor volumes corrected for baseline volumes. Student's t-Test was used for comparison of two groups. Analysis of variance using the Tukey Studentized range method was used for multigroup comparisons.

Results

PKI-166 blocks ErbB1/ErbB2 activity in prostate cancer cells.

We first examined the effects of PKI-166 on EGF-induced signal transduction through ErbB1 and ErbB2 RTKs in the human prostate cancer cell lines LAPC4 and LNCaP, both of which express the androgen receptor. The human vulvar carcinoma cell line A431, which expresses high levels of ErbB1 due to amplification of the erbB1 locus, was used as a positive control. In A431 cells treated with EGF, immunoblotting with a phosphotyrosine antibody showed a dominant band of about 170 kD representing the phosphorylated ErbB1 receptor (Fig. 1A). In EGF-treated LAPC-4 cells, which express considerably less ErbB1 than A431 cells but more ErbB2 *(data not shown)*, tyrosine phosphorylation of a 170 kD and a 185 kD band was observed representing phosphorylated ErbB1 and ErbB2, respectively. Dose-dependent inhibition of receptor autophosphorylation was noted following pretreatment with PKI-166, with estimated IC50 values of 0.5 μM for ErbB1 and 5 μM for ErbB2. Similar doses of PKI-166 have been reported to inhibit phosphorylation of ErbB1 and ErbB2 RTKs, but not other tyrosine or serine/threonine kinases, in non-prostatic human cancer cell lines (14) (15) (16) . We also noted that PKI-166 treatment resulted in a dose-dependent increase in the level of ErbB1 protein in A431 cells and ErbB2 protein in LAPC4-cells. The increase in ErbB2 expression in LAPC4-cells was apparent at 0.5 μM PKI-166, a concentration that predominantly inhibits phosphorylation of ErbB1.

Previous work has indicated that ErbB1 protein is degraded following receptor activation by ligand, raising the possibility that the increased levels of ErbB1 and ErbB2 in PKI-166 treated cells are a reflection of kinase inhibition. To determine if pharmacologic inhibition of receptor tyrosine kinase activity delays receptor degradation, we measured the effect of PKI-166 on

immunoprecipitated, ^{35}S-methionine/cysteine radiolabeled ErbB1 receptors in A431 cells (Fig. 1B, left panel). In the absence of PKI-166 and EGF, the receptor half-life of ErbB1 was between 6 and 12 hours, consistent with the previously published half-life of about 9 hours (17). Stimulation of A431 cells with EGF resulted in phosphorylation of ErbB1, as evidenced by retarded electrophoretic mobility compared to the unphosphorylated receptor, and shortening of the receptor half-life to less than 6 hours. PKI-166 impaired the degradation of ErbB-1 receptor protein in both presence and absence of EGF. This data supports the concept that kinase activity is required for receptor degradation, consistent with prior work showing increased receptor half-life in ErbB1 alleles containing point mutations within the ErbB1 ATP-binding site (18) (19). We also noted accumulation of a lower molecular weight protein in the ErbB1 immunoprecipitates from PKI-166 treated cells. This 145 kDa protein was immunoprecipitated by an ErbB1 antibody directed against a cell surface epitope, but not by an antibody directed against a C-terminal epitope (Figure 1B, right panel), indicating that it is likely to be a C-terminal truncation of the receptor. Similarly sized bands have previously been observed after treatment of A431 cells with the lysosomal inhibitor methylamine (17), and presumably represent an intermediate step in receptor degradation.

Since many growth factor signals are transmitted to the nucleus through extracellular signal-regulated kinases (ERK) (20), we also measured the effect of PKI-166 on ERK1/2 activation. At a dose that inhibits ErbB1 phosphorylation, PKI-166 completely blocked basal and EGF-induced ERK1/2 activation in A431 cells (Fig. 1B). Similar results were obtained in LAPC4 and LNCaP prostate cancer cells *(data not shown).* These data establish the biochemical activity of PKI-166 against ErbB1/ErbB2 RTKs in vitro, including effects on receptor autophosphorylation, receptor degradation, and further signal transduction.

PKI-166 blocks ErbB1/ErbB2 signal transduction in tumors in mice

We next examined the effects of PKI-166 treatment on ErbB1/ErbB2 mediated signaling in vivo. *SCID*-mice bearing tumors from the human prostate cancer xenografts LAPC4 (10) and LAPC9 (13) or from the A431 cell line were treated for five days with 0, 1, 10, and 100 mg/kg of PKI-166 and tumor tissue was harvested one hour after the last dose was administered. Lysates from A431-tumors displayed constitutive phosphorylation of ErbB-1 that was inhibited by treatment of mice with 100 mg/kg PKI-166. Similar analysis of ErbB phosphorylation in prostate cancer xenografts was not informative because of low basal levels of phosphotyrosine *(data not shown)*. However, we did observe decreased ERK1/2 activation and increased levels of total ErbB1 and ErbB2 protein in the prostate cancer xenografts from mice treated with 100 mg/kg of PKI-166, providing indirect evidence for ErbB1/ErbB2 RTK inhibition at this dose (Figure 1C, left panel). To obtain direct evidence of ErbB1/ErbB2 blockade in PKI-166 treated mice, we induced receptor activation by systemic administration of EGF (21). Two different doses of EGF were injected intraperitoneally and resulted in dose-dependent receptor phosphorylation and ERK1/2 activation in LAPC9 tumors (Fig 1C, right panel). PKI-166 given orally at a dose of 100 mg/kg markedly blunted this activation (Figure 1C, right panel). Similar results were obtained in mice bearing LAPC4 or A431 xenografts *(data not shown)*.

PKI-166 blocks the growth of prostate cancers in mice in an androgen-dependent fashion.

Having defined the dose of PKI-166 required to inhibit ErbB1/ErbB2 RTKs in vivo, we were now able to examine the role of these RTKs in the growth of human prostate cancer. We chose the LAPC xenograft model to address this question, because of its similarity to clinical prostate cancer (10) and the convenience of monitoring drug effects on subcutaneous tumor volumes. Tumors derived from the A431 cell line were used as a positive control and were

completely growth arrested by PKI-166 *(data not shown)*. Androgen-independent sublines of the prostate cancer xenografts grown in castrated host mice were consistently more sensitive to growth-inhibition by PKI-166 than androgen-dependent sublines of the same xenograft growing in intact male

($p< 0.005$). This observation was confirmed in multiple experiments and noted in both LAPC4 and LAPC9 xenografts (Figure 2A).

The trend toward enhanced activity of PKI-166 in the absence of androgen was reminiscent of our previous data showing more dramatic effects of forced ErbB2 overexpression on prostate cancer growth in castrate versus intact male mice (2). At that time we postulated that the major effects of ErbB1/ ErbB2 pathway activation might be mediated through AR, but that these effects were most relevant in the setting of low (castrate) levels of androgen. To examine this hypothesis, we asked if the suppression of growth by PKI-166 in castrated male mice could be rescued by androgen supplementation, which was administered by subcutaneous implantation of slow release Testosterone pellets. In both LAPC4 and LAPC9 xenografts (Figure 2B, upper panel), androgen add-back partially rescued the growth inhibitory effects of PKI-166 ($p< 0.05$). One potential explanation for this result is that androgen impairs the ability of PKI-166 to inhibit ErbB1/ErbB2 RTKs. To examine this possibility, we treated eight castrated male mice bearing LAPC tumors with PKI-166 in the presence or absence of supplemental Testosterone and measured ErbB receptor and ERK1 activation in tumor lysates following systemic administration of EGF. Androgen supplementation did not impair the ability of PKI-166 to inhibit EGF-induced signal transduction (Figure 2B, middle panel) nor did androgen affect the bioavailablitiy of PKI-166 as shown by similar mean plasma and tumor drug levels in castrate and androgen-supplemented mice (Figure 2B, lower panel). These data indicate that the rescue of PKI-166 –

induced growth suppression by androgen supplementation cannot be explained by a failure of PKI-166 to inhibit its target. Rather, our findings suggest that ErbB1/ ErbB2 signaling is not required for prostate cancer growth when androgen is present at high levels.

If a threshold level of circulating androgen exists below which ErbB1/ ErbB2 RTKs are required for prostate cancer growth, acute androgen withdrawal by surgical castration should increase the growth-inhibitory effects of PKI-166. To test this hypothesis, we randomized intact male SCID mice bearing the LAPC4 xenograft to four treatment groups. Compared to vehicle-treated mice, androgen withdrawal (AW) by surgical castration slowed the growth of LAPC4 tumors ($p< 0.05$), as expected (10). Growth inhibition by PKI-166 given at 100 mg/kg daily did not reach statistical significance. However, the combination of PKI-166 with androgen withdrawal resulted in nearly complete growth suppression (Fig. 2C). The difference between the combined treatment group and any of the other three treatment groups was highly statistically significant ($p< 0.001$).

Sensitivity to growth inhibition by PKI-166 is correlated with ERK activation

The LAPC-4 and LAPC-9 xenografts have been passaged in mice over multiple generations and various AD and AI subclones derived from the original parental lines have been maintained independently. In the course of these studies we noted that subclones derived from the same parental line occasionally displayed differences in their sensitivity to PKI-166. These sublines provide an opportunity, within an isogenic system, to examine variables in the ErbB1/ErbB2 signaling pathway that might determine response to ErbB1/ErbB2 inhibition. To address this question, we performed biochemical analysis on six LAPC xenograft clones, of which four were grown in intact male mice (clones 1 and 2 for both LAPC 4 and LAPC 9) and two in castrated male mice (clones 3 for both LAPC 4 and LAPC 9). We examined not only the

expression levels of the direct PKI-166 targets ErbB1 and ErbB2, but also the activation state of the Ras/MAPK and PI-3 kinase/Akt-pathways. Both pathways are considered central effectors of the ErbB signaling network (20) and have been implicated in the progression of human prostate cancer (3) (22) (23) (24). Expression of the ErbB-1 ligand TGF-α was included in the analysis due to its suggested role as an autocrine growth factor in androgen-independent prostate cancer (25). In order to be able to correlate for each subline the expression of these biochemical parameters with the growth response to PKI-166, we quantified the relevant immunoblot bands (Figure 3A) by densitometry. Despite differences in the magnitude of ERK1/2-activation between the LAPC4 and LAPC9 xenograft models, we found within each model a positive correlation between the degree of growth-inhibition by PKI-166 and the level of ERK1/2-activation (Fig. 3B). No such correlation was found for expression levels of ErbB1, ErbB2, TGF-α, or activation level of Akt. While the number of available sublines for each xenograft was not sufficient to perform a multivariate analysis, our results in an isogenic system suggest that expression levels of ErbB-1 or ErbB-2 are not sufficient to determine sensitivity to PKI-166 and is consistent with studies using the ErbB-1 inhibitor ZD1839 (26) or the anti-ErbB-2 monoclonal antibody Mab 4D5 (27).

We also noted that androgen-independent tumors (clones 3) showed increased activation of ERK1/2 when compared to tumors grown in intact male mice (Figure 3A). This observation was confirmed by serial analysis of androgen-dependent LAPC4 xenografts at various times post-castration during the evolution to androgen independence (Figure 3B). This data is consistent with results of immunohistochemical analyses of human prostate cancer specimens using phospho-specific antibodies to ERK1/2 (28).

Discussion

In conclusion, our study shows that ErbB1/ErbB2 RTKs contribute to the growth of human prostate cancer and that this contribution is greatest when levels of androgen are limiting. The nature of the interaction between androgen receptor pathway and ErbB1/ErbB2 receptor tyrosine kinases remains to be defined. It is conceivable that ErbB-RTKs provide growth and survival signals for prostate cancer cells which are completely independent of AR and only biologically relevant under the selective pressure of androgen deprivation. Alternatively, ErbB-RTKs might promote prostate cancer growth through ligand-independent activation of AR (2, 3). MAP kinases, the primary effectors of the ErbB/Ras/Raf signaling pathway, have been suggested to link growth factor receptors and steroid hormone receptors, possibly by direct phosphorylation of the latter (29). In that context, our observation that increased ERK1/2 activation is positively correlated with response to ErbB1/ErbB2 pathway inhibition is particularly intriguing and warrants further investigation.

A growing number of small molecule inhibitors of ErbB1 and /or ErbB2 are making their way into clinical trials and show slightly different potencies in relative inhibition of ErbB1 versus ErbB2 RTKs (9). Since these compounds appear to have therapeutic effects in subsets of patients, the question of which kinase is important for targeting – ErbB1 or ErbB2 – is frequently raised. The dose of PKI-166 (100 mg/kg) used in most of our experiments inhibited both ErbB1 and ErbB2 RTKs, as evidenced by biochemical studies on tumor lysates, comparison of drug levels in mice with in vitro drug concentrations, and recent data from other mouse models of cancer treated with PKI-166 (15). Interestingly, the ErbB-2 RTK monoclonal antibody Herceptin failed to inhibit the growth of androgen-independent sublines of the CWR22 human prostate cancer xenograft model (30). While this difference may reflect the use of different cell lines, it

raises the possibility that inhibition of the ErbB-1 RTK is required to halt androgen-independent growth.

Despite the difficulty in dissecting the relative contribution of individual ErbB-receptor family members in naturally arising tumors, our data provides rationale for testing ErbB1/2-RTK inhibitors in clinical trials of human prostate cancer. It may also offer some guidance for the design of such studies. While most current trials study the effects of ErbB-inhibitors in patients who failed hormonal therapy, our data suggests a role for combining ErbB-RTK inhibition with androgen withdrawal for patients with early-stage disease. Our findings also raise the possibility that the activation state of the Ras/MAPK pathway in clinical specimens might serve as a biomarker to identify tumors which "depend" on this pathway and may be more likely to respond to treatment with ErbB1/ErbB2 inhibitors.

Acknowledgements

We thank Dr. Elisabeth Buchdunger and Dr. Peter Traxler (Novartis Pharma AG) for providing PKI-166, Dr. Josef Brueggen and Dr. Robert Cozens (Novartis Pharma AG) for determination of PKI-166 concentrations, Dr. Elliot Landaw (UCLA) for statistical analyses, Randy Chen for technical assistance, and Phuong Huynh for assistance in preparation of the manuscript. This work was supported by grants from the NCI, DOD, and CaPCure. CLS is a Doris Duke Distinguished Clinical Scientist.

References

1. Grossmann, M. E., Huang, H., and Tindall, D. J. Androgen receptor signaling in androgen-refractory prostate cancer. J Natl Cancer Inst, *93:* 1687-1697., 2001.

2. Craft, N., Shostak, Y., Carey, M., and Sawyers, C. L. A mechanism for hormone-independent prostate cancer through modulation of androgen receptor signaling by the HER-2/neu tyrosine kinase. Nat Med, *5:* 280-285., 1999.

3. Yeh, S., Lin, H. K., Kang, H. Y., Thin, T. H., Lin, M. F., and Chang, C. From HER2/Neu signal cascade to androgen receptor and its coactivators: a novel pathway by induction of androgen target genes through MAP kinase in prostate cancer cells. Proc Natl Acad Sci U S A, *96:* 5458-5463., 1999.

4. Culig, Z., Hobisch, A., Cronauer, M. V., Radmayr, C., Trapman, J., Hittmair, A., Bartsch, G., and Klocker, H. Androgen receptor activation in prostatic tumor cell lines by insulin-like growth factor-I, keratinocyte growth factor, and epidermal growth factor. Cancer Res, *54:* 5474-5478., 1994.

5. Signoretti, S., Montironi, R., Manola, J., Altimari, A., Tam, C., Bubley, G., Balk, S., Thomas, G., Kaplan, I., Hlatky, L., Hahnfeldt, P., Kantoff, P., and Loda, M. Her-2-neu expression and progression toward androgen independence in human prostate cancer. J Natl Cancer Inst, *92:* 1918-1925., 2000.

6. Osman, I., Scher, H. I., Drobnjak, M., Verbel, D., Morris, M., Agus, D., Ross, J. S., and Cordon-Cardo, C. HER-2/neu (p185neu) protein expression in the natural or treated history of prostate cancer. Clin Cancer Res, *7:* 2643-2647., 2001.

7. Shi, Y., Brands, F. H., Chatterjee, S., Feng, A. C., Groshen, S., Schewe, J., Lieskovsky, G., and Cote, R. J. Her-2/neu expression in prostate cancer: high level of expression associated with exposure to hormone therapy and androgen independent disease. J Urol, *166:* 1514-1519., 2001.

8. Slamon, D. J., Clark, G. M., Wong, S. G., Levin, W. J., Ullrich, A., and McGuire, W. L. Human breast cancer: correlation of relapse and survival with amplification of the HER-2/neu oncogene. Science, *235:* 177-182., 1987.

9. Mendelsohn, J. The epidermal growth factor receptor as a target for cancer therapy. Endocr Relat Cancer, *8:* 3-9., 2001.

10. Klein, K. A., Reiter, R. E., Redula, J., Moradi, H., Zhu, X. L., Brothman, A. R., Lamb, D. J., Marcelli, M., Belldegrun, A., Witte, O. N., and Sawyers, C. L. Progression of metastatic human prostate cancer to androgen independence in immunodeficient SCID mice. Nat Med, *3:* 402-408., 1997.

11. Daub, H., Wallasch, C., Lankenau, A., Herrlich, A., and Ullrich, A. Signal characteristics of G protein-transactivated EGF receptor. Embo J, *16:* 7032-7044., 1997.

12. Chackal-Roy, M., Niemeyer, C., Moore, M., and Zetter, B. R. Stimulation of human prostatic carcinoma cell growth by factors present in human bone marrow. J Clin Invest, *84:* 43-50., 1989.

13. Craft, N., Chhor, C., Tran, C., Belldegrun, A., DeKernion, J., Witte, O. N., Said, J., Reiter, R. E., and Sawyers, C. L. Evidence for clonal outgrowth of androgen-independent prostate cancer cells from androgen-dependent tumors through a two-step process. Cancer Res, *59:* 5030-5036., 1999.

14. Bruns, C. J., Solorzano, C. C., Harbison, M. T., Ozawa, S., Tsan, R., Fan, D., Abbruzzese, J., Traxler, P., Buchdunger, E., Radinsky, R., and Fidler, I. J. Blockade of the epidermal growth factor receptor signaling by a novel tyrosine kinase inhibitor leads to apoptosis of endothelial cells and therapy of human pancreatic carcinoma. Cancer Res, *60:* 2926-2935., 2000.

15. Brandt, R., Wong, A. M., and Hynes, N. E. Mammary glands reconstituted with Neu/ErbB2 transformed HC11 cells provide a novel orthotopic tumor model for testing anti-cancer agents. Oncogene, *20:* 5459-5465., 2001.

16. Scheving, L. A., Stevenson, M. C., Taylormoore, J. M., Traxler, P., and Russell, W. E. Integral role of the EGF receptor in HGF-mediated hepatocyte proliferation. Biochem Biophys Res Commun, *290:* 197-203., 2002.

17. Stoscheck, C. M. and Carpenter, G. Down regulation of epidermal growth factor receptors: direct demonstration of receptor degradation in human fibroblasts. J Cell Biol, *98:* 1048-1053., 1984.

18. Honegger, A. M., Dull, T. J., Felder, S., Van Obberghen, E., Bellot, F., Szapary, D., Schmidt, A., Ullrich, A., and Schlessinger, J. Point mutation at the ATP binding site of

EGF receptor abolishes protein-tyrosine kinase activity and alters cellular routing. Cell, *51:* 199-209., 1987.

19. Chen, W. S., Lazar, C. S., Poenie, M., Tsien, R. Y., Gill, G. N., and Rosenfeld, M. G. Requirement for intrinsic protein tyrosine kinase in the immediate and late actions of the EGF receptor. Nature, *328:* 820-823., 1987.

20. Yarden, Y. and Sliwkowski, M. X. Untangling the ErbB signalling network. Nat Rev Mol Cell Biol, *2:* 127-137., 2001.

21. Donaldson, R. W. and Cohen, S. Epidermal growth factor stimulates tyrosine phosphorylation in the neonatal mouse: association of a M(r) 55,000 substrate with the receptor. Proc Natl Acad Sci U S A, *89:* 8477-8481., 1992.

22. Gioeli, D., Zecevic, M., and Weber, M. J. Immunostaining for activated extracellular signal-regulated kinases in cells and tissues. Methods Enzymol, *332:* 343-353, 2001.

23. Wen, Y., Hu, M. C., Makino, K., Spohn, B., Bartholomeusz, G., Yan, D. H., and Hung, M. C. HER-2/neu promotes androgen-independent survival and growth of prostate cancer cells through the Akt pathway. Cancer Res, *60:* 6841-6845., 2000.

24. Malik, S. N., Brattain, M., Ghosh, P. M., Troyer, D. A., Prihoda, T., Bedolla, R., and Kreisberg, J. I. Immunohistochemical demonstration of phospho-akt in high Gleason grade prostate cancer. Clin Cancer Res, *8:* 1168-1171., 2002.

25. Scher, H. I., Sarkis, A., Reuter, V., Cohen, D., Netto, G., Petrylak, D., Lianes, P., Fuks, Z., Mendelsohn, J., and Cordon-Cardo, C. Changing pattern of expression of the epidermal growth factor receptor and transforming growth factor alpha in the progression of prostatic neoplasms. Clin Cancer Res, *1:* 545-550., 1995.

26. Moasser, M. M., Basso, A., Averbuch, S. D., and Rosen, N. The tyrosine kinase inhibitor ZD1839 ("Iressa") inhibits HER2-driven signaling and suppresses the growth of HER2-overexpressing tumor cells. Cancer Res, *61:* 7184-7188., 2001.

27. Lane, H. A., Beuvink, I., Motoyama, A. B., Daly, J. M., Neve, R. M., and Hynes, N. E. ErbB2 potentiates breast tumor proliferation through modulation of p27(Kip1)-Cdk2 complex formation: receptor overexpression does not determine growth dependency. Mol Cell Biol, *20:* 3210-3223., 2000.

28. Gioeli, D., Mandell, J. W., Petroni, G. R., Frierson, H. F., Jr., and Weber, M. J. Activation of mitogen-activated protein kinase associated with prostate cancer progression. Cancer Res, *59:* 279-284., 1999.

29. Kato, S., Endoh, H., Masuhiro, Y., Kitamoto, T., Uchiyama, S., Sasaki, H., Masushige, S., Gotoh, Y., Nishida, E., Kawashima, H., and et al. Activation of the estrogen receptor through phosphorylation by mitogen- activated protein kinase. Science, *270:* 1491-1494., 1995.

30. Agus, D. B., Scher, H. I., Higgins, B., Fox, W. D., Heller, G., Fazzari, M., Cordon-Cardo, C., and Golde, D. W. Response of prostate cancer to anti-Her-2/neu antibody in androgen- dependent and -independent human xenograft models. Cancer Res, *59:* 4761-4764., 1999.

Figures

Figure 1. PKI-166 inhibits ErbB1 and ErbB2 receptor signaling and degradation.

A.) Immunoblots of A431 (*left panel*) and LAPC4 (*right panel*) cells treated for 12 hours with various concentrations of PKI-166 (in μM) prior to stimulation with EGF (100 ng/ml) for 10 minutes B.) *left panel*: Autoradiograph of immunoprecipitated ErbB1 (upper row) and Immunoblots (middle and lower row) of lysates from A431 cells metabolically labeled for 12 hours with [^{35}S]-methionine and chased in the presence of PKI-166 (5μM) and/or EGF (100 ng/ml). PKI-166 was added 10 minutes prior to EGF where indicated. *right panel*: Immunoblot of A431 cells treated with PKI-166 for 12 hours using a ErbB1 antibodies directed against N-terminal and C-terminal epitopes C.) Immunoblots of lysates from LAPC9 (*left upper panel and right panel*) or A431 (*left lower panel*) xenograft tumors harvested one hour after the fifth daily dose of PKI-166 (2 tumors per condition). The right panel shows lysates of LAPC9 tumors from mice injected intraperitoneally with PBS, 0.1 mg EGF, or 0.01 mg EGF one hour following the fifth daily dose of PKI-166. Tumors were harvested five minutes after EGF injection.

Figure 2. Androgen modifies the growth response to PKI-166

A.) PKI-166 inhibits the growth of human prostate cancer xenografts growing in castrated mice. Mice bearing LAPC4 or LAPC9 xenograft tumors were treated daily for three weeks with 100 mg/kg PKI-166 versus vehicle (n = 6-9 per group). Data is expressed as fold tumor volume compared to day 1 (mean + SEM). B.) *upper panel*: Testosterone rescues growth inhibition by PKI-166 in castrated animals. Castrated male mice bearing androgen-independent xenografts were randomized to four treatment groups (vehicle, PKI-166, vehicle plus testosterone, and PKI plus testosterone). Data is expressed as ratio between the fold increase in tumor volume for PKI-

166 treated mice and the fold increase in tumor volume for vehicle treated mice (T/C). Each treatment group consisted of 8-9 mice. *middle panel*: Testosterone does not impair the ability of PKI-166 to inhibit ErbB1/ErbB2 signaling. Castrated male mice bearing LAPC9 xenograft tumors were treated with PKI-166 +/- testosterone for 21 days and EGF (0.1 mg) was administered intraperitoneally 1 hour after the last PKI-166 dose. Tumors (n=2 per treatment condition) were harvested 5 minutes later. Displayed are immunoblots for PY, ERK1/2, and total ERK1/2. *lower panel*: Testosterone does not affect PKI-166 bioavailability in mice. PKI-166 levels in plasma [μM] and LAPC9 tumors [nmol/g] were determined by reversed-phase HPLC in castrated mice after 21 days of treatment with PKI-166 (100 mg/kg) +/- testosterone. Blood and tumors were collected one hour after the last dose of PKI-166 and displayed as mean values (n=3 per group) C.) Androgen withdrawal augments inhibitory effect of PKI-166 on LAPC4 xenografts in intact male mice. Surgical castration was performed on the same day as PKI-166 treatment was started. Data is expressed as fold tumor volume compared to day 1 (mean + SEM). Six mice were treated per group.

Figure 3. Activity of p-ERK correlates with growth-inhibition by PKI-166 in vivo and is increased in androgen-independent tumors

A.) *upper panel*: Immunoblot of tumor lysates from six different LAPC sublines; *lower panel*: Correlation between growth inhibition by PKI-166 and levels of activated ERK for six LAPC clones. Immunoblot bands were quantified by densitometry and the absolute value under the peak was plotted on the x-axis. The y-axis shows the ratio between the fold increase in tumor volume for PKI-166 treated mice and the fold increase in tumor volume for vehicle treated mice (T/C). Open symbols represent xenograft clones grown in intact mice, closed symbols represent

xenograft clones growing in castrated animals B.) Effect of castration on p-ERK levels in LAPC4 xenograft tumors harvested at various time points after castration.

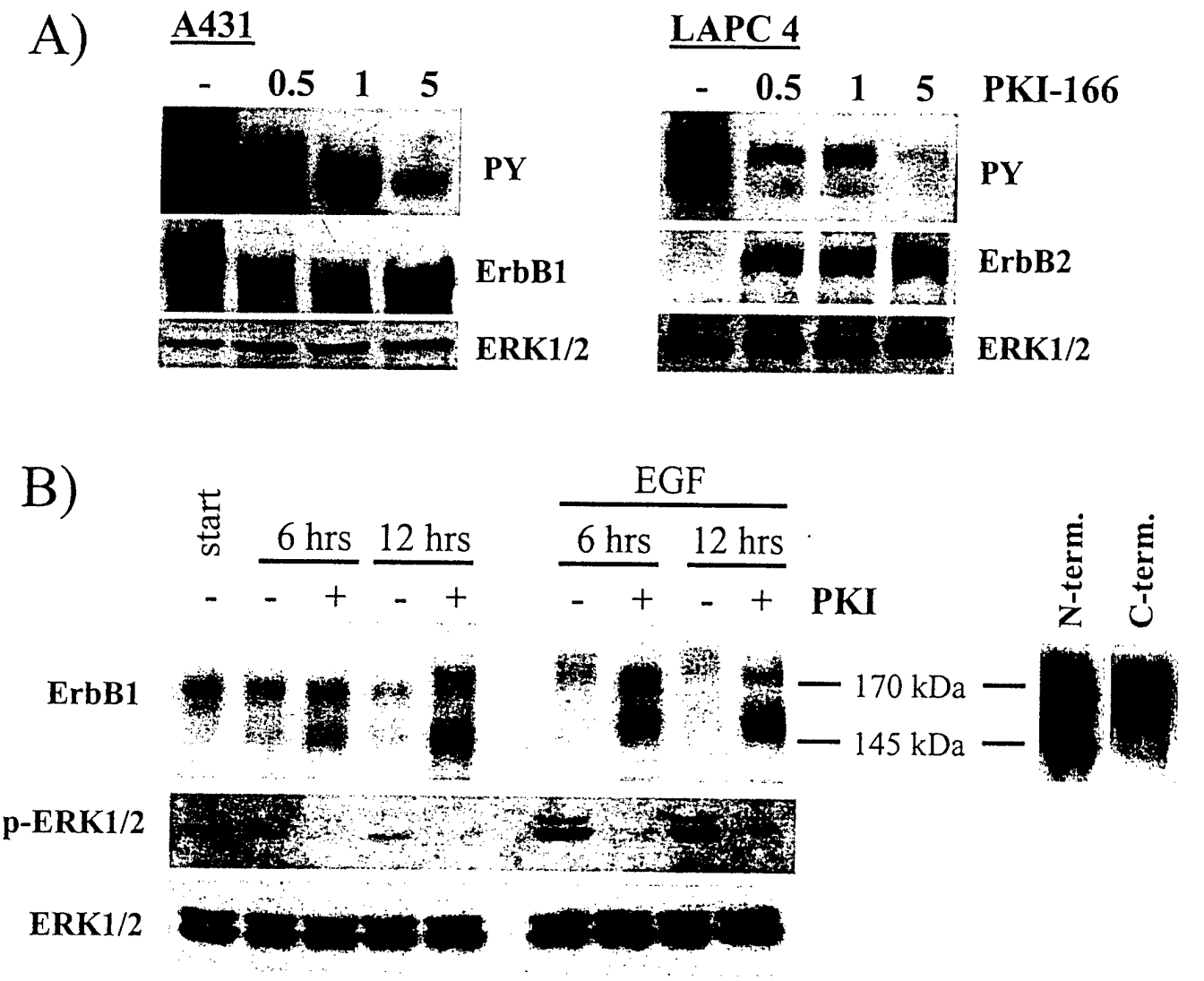
A)
A431
- 0.5 1 5
PY
ErbB1
ERK1/2
LAPC 4
- 0.5 1 5 PKI-166
PY
ErbB2
ERK1/2
B)
start
6 hrs 12 hrs
EGF
6 hrs 12 hrs
- - + - + - + - + PKI
N-term.
C-term.
ErbB1
170 kDa
145 kDa
p-ERK1/2
ERK1/2
C)
- 1 10 100 PKI (mg/kg)
IB: ErbB1
IB: ErbB2
IB: p-ERK1/2
IB: ERK1/2
LAPC9
vehicle 100 EGF PKI (mg/kg)
IB: PY
IB: p-ERK1/2
IB: ERK1/2
A431
IB: PY
IB: ERK1/2

A.)

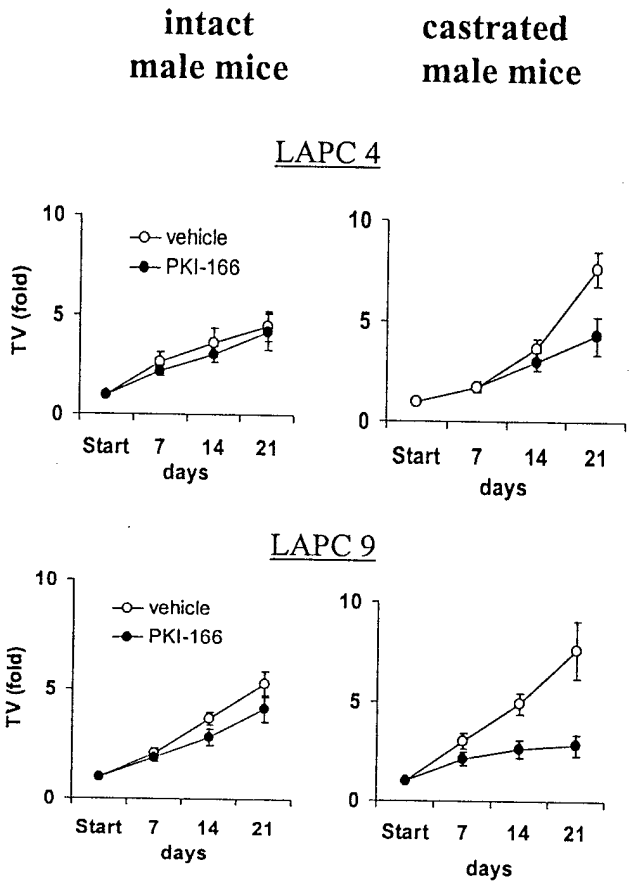
intact male mice
castrated male mice
LAPC 4
LAPC 9
vehicle
PKI-166
TV (fold)
Start 7 14 21
days

B.)

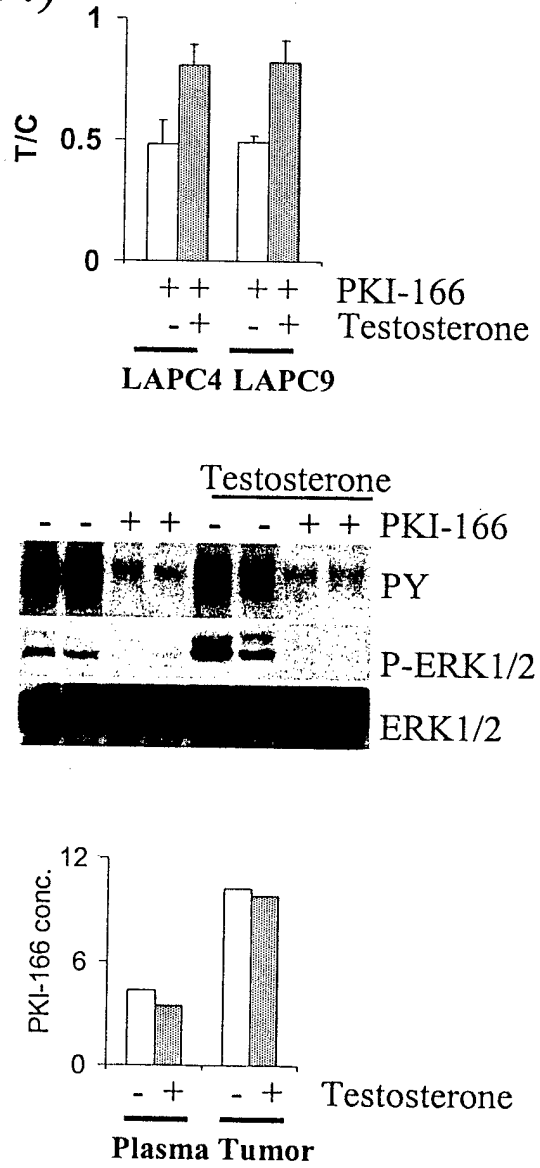
T/C
PKI-166
Testosterone
LAPC4 LAPC9
Testosterone
PY
P-ERK1/2
ERK1/2
PKI-166 conc.
Plasma Tumor

C.)

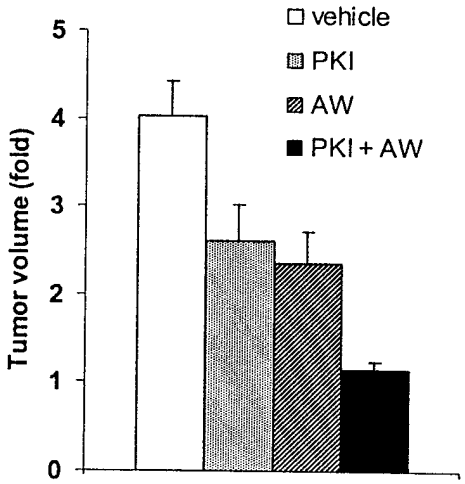
vehicle
PKI
AW
PKI + AW
Tumor volume (fold)

A.)

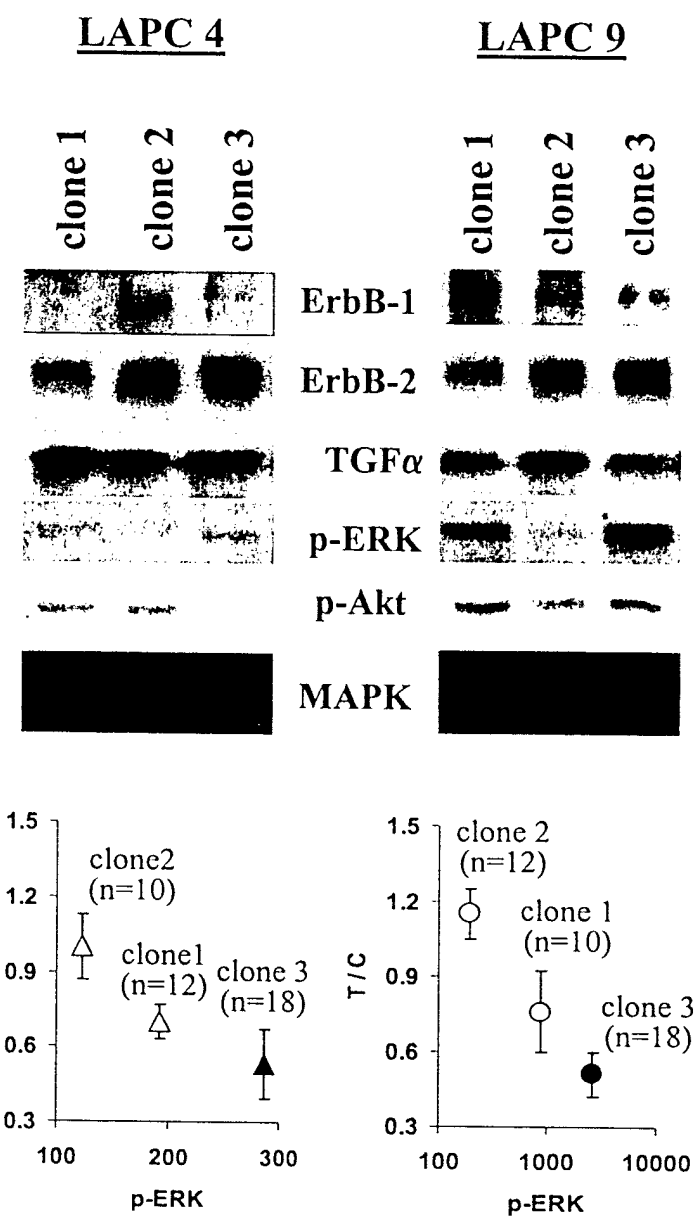
LAPC 4
LAPC 9
clone 1
clone 2
clone 3
clone 1
clone 2
clone 3
ErbB-1
ErbB-2
TGFα
p-ERK
p-Akt
MAPK
T / C
1.5
1.2
0.9
0.6
0.3
clone2 (n=10)
clone1 (n=12)
clone 3 (n=18)
100
200
300
p-ERK
T / C
1.5
1.2
0.9
0.6
0.3
clone 2 (n=12)
clone 1 (n=10)
clone 3 (n=18)
100
1000
10000
p-ERK

B.)

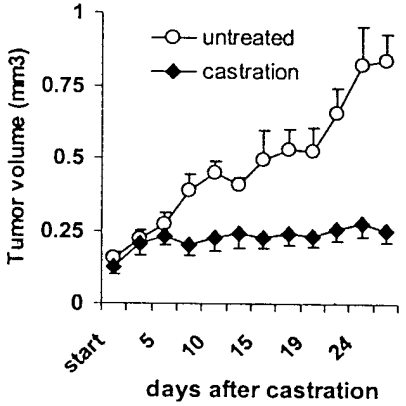
Tumor volume (mm3)
1
0.75
0.5
0.25
0
untreated
castration
start
5
10
15
19
24
days after castration

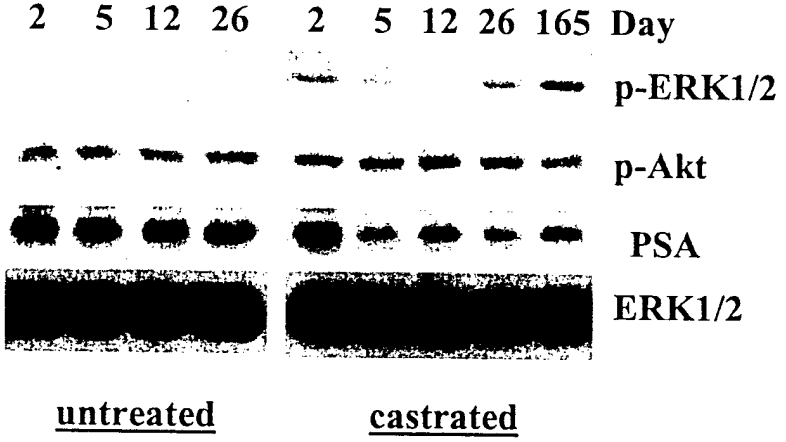
2
5
12
26
2
5
12
26
165
Day
p-ERK1/2
p-Akt
PSA
ERK1/2
untreated
castrated

[CANCER RESEARCH 61, 6276–6280, August 15, 2001]

In Vivo Progression of LAPC-9 and LNCaP Prostate Cancer Models to Androgen Independence Is Associated with Increased Expression of *Insulin-like Growth Factor I (IGF-I)* and *IGF-I Receptor (IGF-IR)*[1]

Tara Nickerson, Francis Chang, Donald Lorimer, Steven P. Smeekens, Charles L. Sawyers, and Michael Pollak[2]

Cancer Prevention Research Unit of the Jewish General Hospital and McGill University, Montreal, Quebec, H3T 1E2 Canada [T. N., M. P.]; Department of Hematology-Oncology, UCLA School of Medicine, Los Angeles, California, 90095-1678 [F. C., C. L. S.]; and Axys Pharmaceuticals, Inc., San Francisco, California 94080 [S. P. S., D. L.]

ABSTRACT

Androgen deprivation therapies for metastatic prostate cancer are useful initially, but progression to androgen independence usually results in relapse within 2 years. The molecular mechanisms underlying the clinically important transition from androgen dependence to androgen independence are poorly described. Several lines of investigation have suggested that insulin-like growth factors (IGFs) are involved in the biology of prostate cancer, but little is known about their relevance to progression to androgen independence. We used three *in vivo* models of androgen-dependent (AD) human prostate cancer to study this issue. Progression to androgen-independent (AI) growth was associated with a 60-fold increase in expression of IGF-I mRNA in LAPC-9 xenografts and a 28-fold increase in IGF-I expression in LNCAP xenografts, relative to the initial AD neoplasms. *IGF type I receptor (IGF-IR)* mRNA levels were ~2.5-fold and ~5-fold higher, respectively, in AI LAPC-9 and LNCaP tumors compared with the original AD neoplasms. AI growth of these xenografts was also associated with significant reductions in IGF binding protein-3 expression. LAPC-4 xenografts, which previously have been shown to exhibit molecular pathology related to HER-2/neu expression with progression to AI, showed relatively minor changes in expression of the genes investigated, but we nevertheless found evidence of increased IGF-IR phosphorylation with progression to androgen independence in this model. Taken together with prior observations, our results suggest that deregulation of expression of genes related to any one of several critical receptor tyrosine kinase regulatory systems, including IGF signaling, may confer androgen independence.

INTRODUCTION

AD[3] prostate cancer can be treated with androgen deprivation strategies such as castration or antiandrogens, but progression to AI cancer, for which there are no satisfactory treatments, usually occurs. There is a clear need to identify molecular targets for novel therapeutic approaches to either prevent the progression of prostate cancer to androgen independence or to treat AI cancers.

Study of the molecular mechanisms associated with progression to androgen independence has been limited by the availability of suitable models. The work we report here is based on three human prostate cancer models of *in vivo* progression to androgen independence, LAPC-9, LNCaP, and LAPC-4. The recently described LAPC-9 model is a human prostate cancer xenograft that requires androgens for growth in SCID mice, secretes PSA, and expresses a normal androgen receptor. LAPC-9 tumor cells enter a dormant state in response to castration of the host, and a subset of tumors resumes growth with an AI phenotype after prolonged androgen deprivation (1). The LNCaP model is an androgen-sensitive, PSA-secreting, immortalized prostate cancer cell line (2). A mutation in the hormone-binding domain of the androgen receptor has been demonstrated in LNCaP cells (3). LNCaP cells readily form tumors in SCID mice when co-injected with Matrigel and are associated with serum PSA levels that are directly proportional to tumor volume in intact hosts (4). After castration, the growth of LNCaP tumors is arrested, and serum PSA levels decrease significantly. Although this aspect of the model has been studied in some detail, less attention has been given to the finding that prolonged androgen deprivation leads to AI growth of LNCaP tumors, which is accompanied by PSA production similar to precastrate levels (5). The LAPC-4 human prostate cancer xenograft model has been used previously to study molecular changes associated with transition from AD to AI growth (6, 7).

IGF-I has well-characterized mitogenic and antiapoptotic effects that are mediated through the IGF-IR (8, 9). Ligand-receptor interactions are modulated by a family of high-affinity IGFBPs (reviewed in Ref. 10). There is considerable evidence from both laboratory and population studies that IGF physiology is relevant to prostate cancer. For example, it has been shown that both normal prostate epithelial cells and prostate cancer cells exhibit IGF responsiveness *in vitro* (11, 12), that IGF-IR inhibition inhibits prostate cancer cell proliferation (13), and that overexpression of IGF-I in prostate epithelial cells in a transgenic model leads to transformation (14). We (15) and others (16, 17) have demonstrated in prospective studies that a positive correlation exists between circulating IGF-I concentration in healthy men and risk of subsequent prostate cancer. This finding is consistent with results from many (but not all) case-control studies (reviewed in Refs. 18, 19).

A precedent for the importance of peptide growth factors in progression of prostate cancer to androgen independence is provided by the association of androgen independence in LAPC-4 human tumor xenografts with overexpression of HER-2/neu, a tyrosine kinase receptor activated by ligands in the epidermal growth factor family (6, 7). The evidence that both epidermal growth factor and IGF-I can directly activate the androgen receptor in the absence of androgens (20, 21) raises the possibility that IGF receptor signaling may also be involved in progression of prostate cancer to androgen independence. We undertook experiments to determine whether progression to AI growth *in vivo* is related to changes in expression of genes encoding key molecules involved in IGF signaling.

MATERIALS AND METHODS

Tumor Xenografts. The LAPC-4 and LAPC-9 xenografts were derived as described (1, 6). The clinical material was minced into 2-mm chunks and implanted with 200 μl of Matrigel (Collaborative Research, Bedford, MA) s.c. into male SCID mice. After initial tumor formation, tumors were harvested, minced, and reimplanted into SCID mice. The LNCaP xenograft was derived from the LNCAP cell line obtained from American Type Culture Collection,

Received 8/13/00; accepted 6/15/01.

The costs of publication of this article were defrayed in part by the payment of page charges. This article must therefore be hereby marked *advertisement* in accordance with 18 U.S.C. Section 1734 solely to indicate this fact.

[1] Supported by grants from the National Cancer Institute of Canada (to M. P.) and from the National Cancer Institute, Department of Defense, and CapCURE (to C. L. S.). C. L. S. is a Leukemia Society of America scholar.

[2] To whom requests for reprints should be addressed, at Lady Davis Institute for Medical Research, 3755 Cote Ste Catherine Road, Montreal, Quebec, H3T 1E2 Canada. Phone: (514) 340-8222, extension 5527; Fax: (514) 340-8302; E-mail: michael.pollak@mcgill.ca.

[3] The abbreviations used are: AD, androgen dependent; AI, androgen independent; PSA, prostate-specific antigen; SCID, severe combined immunodeficient; IGFBP, IGF binding protein; IGF-I, insulin-like growth factor type I; IGF-IR, IGF-I receptor; RT-PCR, reverse transcription-PCR.

which was injected (1×10^6 cells) with Matrigel into flanks of male SCID mice. Once tumors formed, the tumors were serially passaged into male mice as described for the LAPC-9 xenograft.

AD xenografts were removed from mice either before or after castration or after acquiring an AI phenotype, and mRNA was extracted for quantification of mRNA abundance by quantitative RT-PCR and Northern blotting as described previously (22).

Quantitative RT-PCR. Quantitative RT-PCR was performed using TaqMan technology. First-strand cDNA was synthesized from 5 μg of total RNA. PCR reactions (50 μl) were performed in a buffer containing 50 mM KCl, 10 mM Tris-HCl, 10 mM EDTA, 5 mM $MgCl_2$, 200 μM each of dATP, dCTP and dGTP, 400 μM dUTP, 300 μM each of forward and reverse primers, 200 μM probe, 1.25 units of AmpliTaq Gold, 0.5 unit of uracil-*N*-glycosylase and ~150 ng of cDNA. Primers and probes were designed using Primer Express (ABI-Perkin-Elmer) and are listed in Table 1. Thermal cycling was performed using an ABI-7700 under the following reaction conditions: 50°C for 2 min, 95°C for 10 min, followed by 40 cycles of 95°C for 15 s and 60°C for 60 s. Data were normalized to rRNA and calculated as described (23). Changes in gene expression patterns were confirmed by Northern blot analysis. Control studies were carried out to demonstrate assay reproducibility by showing similar results from multiple RNA samples derived from a single tissue sample.

Western Blotting. Cell culture and tumor lysates were prepared with 1% Triton buffer [12.5 mM EDTA (pH 8.0), 25 mM HEPES (pH 7.5), 150 mM NaCl, 1% Triton X-100, and 1% glycerol) with protease and phosphatase inhibitors. The antibodies used were rabbit anti-IGF-IR (1:1000; Santa Cruz Biotechnology, Inc. Santa Cruz, CA), rabbit anti-IRS-1 (1:100; Santa Cruz Biotechnology), and mouse anti-β-actin (1:2000; Promega Corp., Madison, WI). Phosphotyrosine was detected with mouse antibody 4G10 (1:2000; Upstate Biotechnologies, Inc., Lake Placid, NY). RIG cells (Rat-1 fibroblasts overexpressing IGF-IR) were a kind gift of Michael Weber (University of Virginia Health Sciences Center, Charlottesville, VA).

RESULTS

***In Vivo* Progression to Androgen Independence.** We confirmed that LAPC-9 tumor xenografts (1) grow readily in intact SCID mice, remain static after castration, and in some cases eventually develop an AI phenotype associated with growth in castrated mice (Fig. 1). Similar observations have been reported for the LAPC-4 and LNCaP models (5–7).

Changes in Expression of IGF-I, IGF-II, and IGF-IR Associated with Progression to Androgen Independence. Castration resulted in decreased *IGF-I* gene expression in AD LAPC-9 tumors, with mRNA levels dropping to ~10% of control (Fig. 2*A*). Emergence of AI growth of LAPC-9 tumors was associated with a dramatic increase in *IGF-I* gene expression. *IGF-I* mRNA in AI LAPC-9 tumors is ~60-fold higher than the level in AD tumors, as determined by quantitative RT-PCR (Fig. 2*A*). Northern blot analysis of the same RNA confirmed a significant increase in *IGF-I* mRNA abundance. Progression to androgen independence in LAPC-9 tumors was also accompanied by a ~2.5-fold increase in *IGF-IR* mRNA abundance relative to that in AI tumors (Fig. 2*B*).

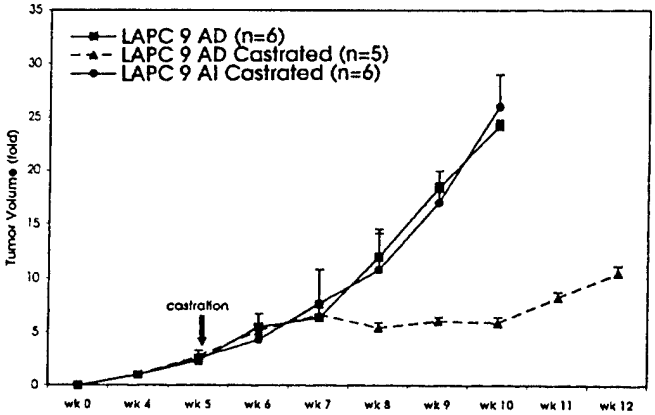

Fig. 1. Growth of AD and AI LAPC-9 tumor xenografts. LAPC-9 xenografts were established as described in "Materials and Methods." The growth of AD LAPC-9 tumors in intact mice is shown plotted as means; *bars*, SE. Some animals were castrated 5 weeks after tumor implantation (*arrow*), and the growth of AD and AI tumors after castration is shown.

The effects of castration on expression of *IGF-I* and its receptor in LNCaP tumor xenografts were remarkably similar to those observed in the LAPC-9 model. *IGF-I* mRNA decreased to <40% of control values in LNCaP tumors within 2 weeks after castration, whereas AI LNCaP tumors were found to have ~28-fold higher *IGF-I* mRNA levels than AD control tumors (Fig. 2*A*). *IGF-IR* gene expression increased ~5-fold in AI LNCaP tumors compared with AD tumors (Fig. 2*B*).

In contrast, progression to androgen independence in the LAPC-4 model was not associated with major increases in expression of *IGF-I* (Fig. 2*A*). *IGF-IR* mRNA levels decreased to ~15% of control after castration and remained low in AI tumors (Fig. 2*B*).

IGF-II mRNA levels in LAPC-9, LNCaP, and LAPC-4 xenografts were also quantitated by RT-PCR. AI growth of LNCaP tumors was associated with up-regulation of *IGF-II* mRNA, with levels ~5-fold higher than control. No difference in *IGF-II* mRNA level was observed between AD and AI tumors in the LAPC-9 or LAPC-4 models (data not shown).

Fig. 3*A* shows that the ~5-fold increase in *IGF-IR* mRNA abundance associated with acquisition of AI in the LNCaP model is associated with an increase in IGF-IR expression at the protein level. Neither the ~2.5-fold increase in *IGF-IR* mRNA abundance in the LAPC-9 model nor the decrease in *IGF-IR* mRNA in the LAPC-4 model were associated with a detectable change in IGF-IR protein level, as estimated by Western blot (Fig. 3*A*). Interestingly, however, phosphotyrosine immunoblots of LAPC-4 AI xenografts showed an increase in tyrosine phosphorylation of IGF-IR relative to AD LAPC-4 (Fig. 3*B*). Lysates immunoprecipitated with IGF-IR and blotted with anti-phosphotyrosine 4G10 antibody confirm this observation. Upon ligand binding and activation, IGF-IR autophosphorylates cytoplasmic tyrosine residues. The observation that LAPC-4 AI tumors have increased phosphorylation but decreased expression of IGF-IR suggests that IGF signaling pathway may be up-regulated in LAPC-4 AI tumors relative to the AD LAPC-4 tumors.

One of the main signaling effectors of IGF-IR is IRS-1. LNCaP has been shown recently to lack IRS-1 expression along with lack of PTEN expression (24). Surprisingly, IRS-1 could not be detected in

Table 1 *Sequences of primers/probes used for quantitative RT-PCR*

The primers and probes were designed with Primer Express (ABI-Perkin-Elmer) using the Genbank Accession number, which appears in parentheses.

Gene		Oligonucleotide sequence
IGF-I (M27544)	Forward	5′-AAGTCAGCTCGCTCTGTCCG-3′
	Reverse	5′-TTCCTGCACTCCCTCTACTTGC-3′
	Probe	5′-TCTGGGTCTTGGGCATGTCGGTGT-3′
IGF-IR (X04434)	Forward	5′-GTGAAAGTGACGTCCTGCATTTC-3′
	Reverse	5′-CCTTGTAGTAAACGGTGAAGCTGA-3′
	Probe	5′-CACCACCACGTCGAAGAATCGCATC-3′
IGFBP-3 (X64875)	Forward	5′-CGCCAGCTCCAGGAAATG-3′
	Reverse	5′-GCATGCCCTTTCTTGATGATG-3′
	Probe	5′-CAGCACGCACCGGGTGTCTGATC-3′
IGFBP-5 (M62782)	Forward	5′-AAAGAGCTACCGCGAGCAAG-3′
	Reverse	5′-GGAGATGCGGGTGTGTTTG-3′
	Probe	5′-ACGAGGAGCCCACCACCTCTGAGA-3′
rRNA (M10098)	Forward	5′-CGGCTACCACATCCAAGGAA-3′
	Reverse	5′-GCTGGAATTACCGCGGCT-3′
	Probe	5′-TGCTGGCACCAGACTTGCCCTC-3′

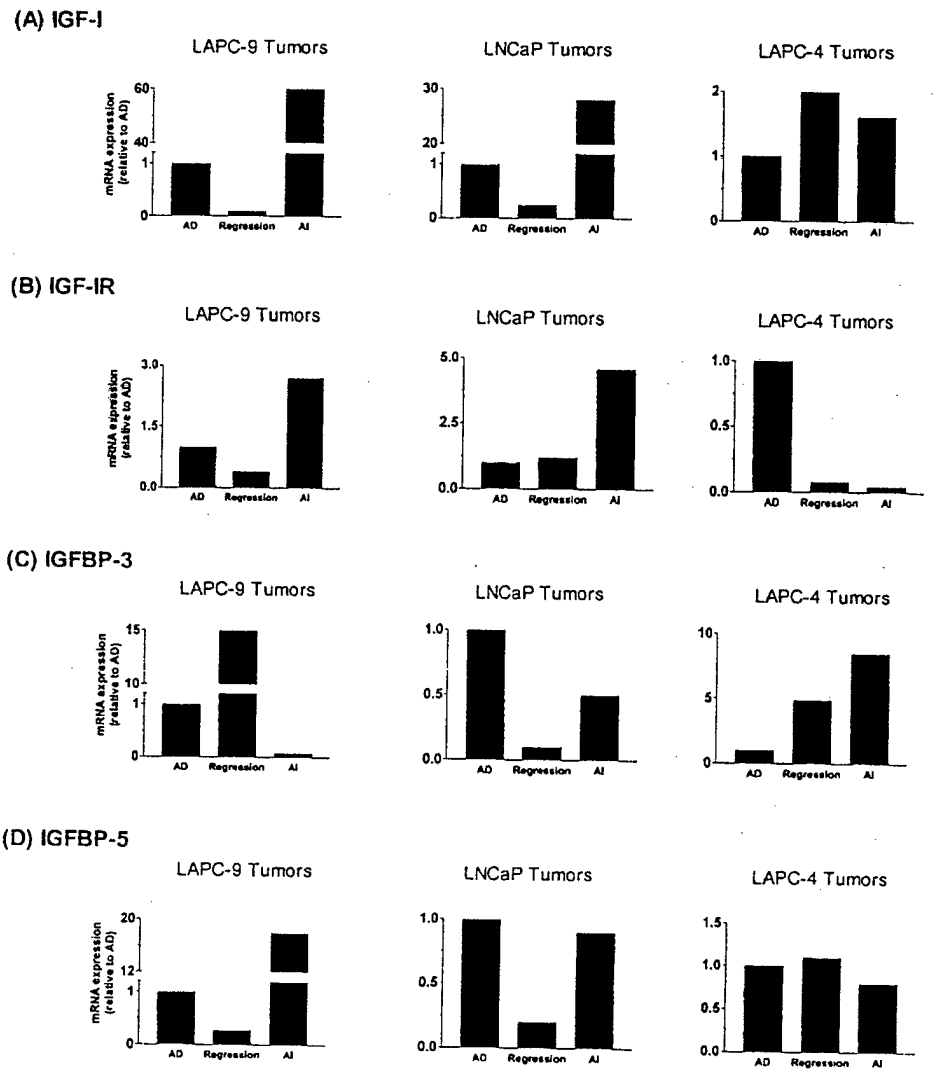

Fig. 2. Expression of IGF-I (*A*), IGF-IR (*B*), IGFBP-3 (*C*), and IGFBP-5 (*D*) in prostate tumor xenografts after castration. Quantitative RT-PCR was used to measure mRNA levels in tumors at various times after castration. Gene expression was calculated as described in "Materials and Methods." For each time point, mRNA levels are normalized to levels of rRNA and are shown expressed relative to expression in AD tumors at day 0. Quantitation of gene expression was repeated on at least three separate tumors derived from independent experiments and yielded similar results. *Regression*, AD tumors 14 days after castration.

LAPC-4 and LAPC-9 xenografts either (Fig. 3*C*). In addition, IRS-1 mRNA was undetectable in these xenografts by oligonucleotide microarray analysis (data not shown). This suggests that IGF-IR substrates other than IRS-1 may be important in prostate cancer.

Changes in Expression of IGFBPs Associated with Progression to Androgen Independence. *IGFBP-3* mRNA levels in LAPC-9 tumors increased ~15-fold by 14 days after castration, consistent with our prior results (22, 25). With emergence of androgen independence, however, *IGFBP-3* mRNA abundance decreased to <20% of levels present in AD tumors (Fig. 2*C*). In contrast, AI LAPC-9 tumors expressed ~18-fold higher *IGFBP-5* mRNA than AD tumors (Fig. 2*D*).

The findings concerning IGFBP expression in the LNCaP model were different in some respects to those seen in the LAPC-9 system. In the LNCaP model, *IGFBP-3* mRNA was relatively abundant in AD tumors and decreased to ~15% of control by 14 days after castration (Fig. 2*C*). At the time of progression to an AI phenotype, a reduction in IGFBP-3 expression compared with control was seen (as in the LAPC-9 model). Relatively minor changes in *IGFBP-5* gene expression with progression to AI were observed in the LNCaP model (Fig. 2*D*).

In contrast to the decrease in *IGFBP-3* expression observed during progression to androgen independence in the LAPC-9 and LNCaP models, AI LAPC-4 tumors expressed ~8-fold higher levels of *IGFBP-3* mRNA than AD tumors (Fig. 2*C*). Androgen independence in the LAPC-4 model was not associated with significant changes in *IGFBP-5* expression (Fig. 2*D*).

IGFBP-2 mRNA levels were ~10-fold higher in AI LNCaP tumors compared with AD LNCaP tumors, and no changes in *IGFBP-2* were observed in either the LAPC-9 or LAPC-4 model (data not shown). We also measured mRNA levels of IGFBPs 1, 4, and 6 in AI LAPC-9, LNCaP, and LAPC-4 xenografts but found no significant differences in gene expression compared with AD tumors (data not shown).

DISCUSSION

Our major finding is that progression of both LAPC-9 and LNCaP tumors to AI growth after castration is associated with a major increase in *IGF-I* gene expression in the neoplastic tissue. AI growth in these tumor models is also associated with up-regulation of *IGF-IR* gene expression and decreased expression of IGFBP-3. These changes could contribute to increased IGF bioactivity in the tumor microenvironment. This in turn could contribute to androgen independence by androgen receptor-independent changes related to hyperstimulation of the signaling pathways distal to the IGF-IR and/or by mechanisms related to IGF-mediated activation of the androgen receptor (20).

It seems plausible that increased IGF signaling, which is associated with mitogenic and antiapoptotic effects in most experimental systems (8, 9), could be a mechanism that would enable prostate cells to

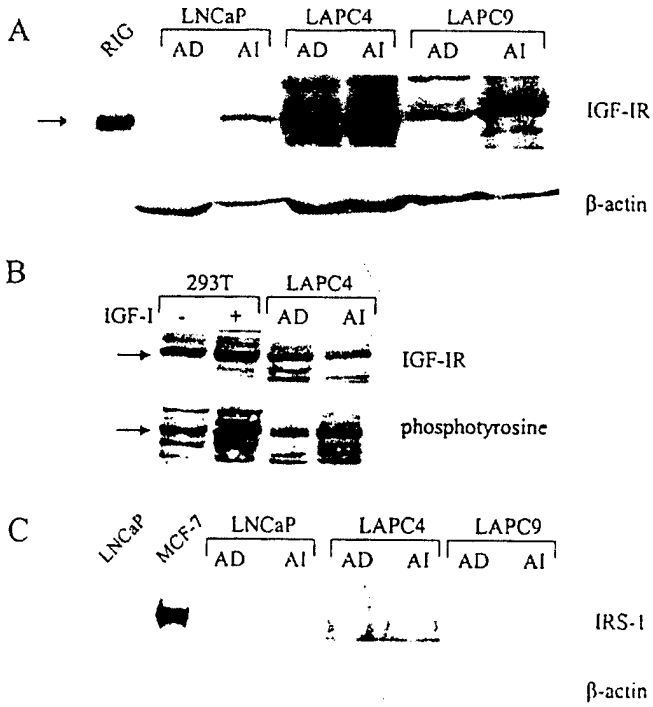

Fig. 3. Western blots for IGF-IR and IRS-1 expression in human prostate xenografts. *A*, IGF-IR Western blots for positive control RIG cells (Rat-1 fibroblasts engineered to overexpress IGF-IR) and lysates from different xenografts. β-actin staining of each lane was used as loading control. *B*, IGF-IR and phosphotyrosine Western blots for LAPC-4 xenografts. 293T cell cultures were serum starved and then exposed to vehicle or to 500 ng/ml IGF-I and served as negative and positive controls, respectively. *C*, IRS-1 Western blots for xenografts. LNCaP and MCF-7 cell cultures were used as negative and positive controls, respectively. β-actin staining of each lane was used as loading control. Lysates and immunoblots were prepared as detailed in "Materials and Methods."

survive and proliferate in an androgen-deficient environment. Our data from the LnCaP and LAPC-9 *in vivo* neoplastic progression models of human prostate cancer suggest that up-regulation of expression of *IGF-I* and to a lesser extent *IGF-IR* are indeed associated with progression to androgen independence. It has been shown recently (24) that AI proliferation of LnCaP cells is increased after transfection with IGF-IR together with the IGF-IR substrate IRS-1.

In experimental systems based on SV40-transformed human prostate epithelial cells, paradoxical down-regulation of IGF-IR expression has been found to be associated with transformation (26–29), raising the possibility that IGF-IR exerts a negative influence on tumor progression, which is overcome by reduced expression. Our results showing up-regulation of IGF-IR are distinct from these reports in that our models compare AD human prostate cancer xenografts and spontaneously arising AI cancers, while prior work compared IGF-IR expression in normal prostate epithelial cells with that in prostate epithelial cells transformed by SV40 transfection. SV40 expression in prostate epithelial cells clearly leads to transformation, but it is not certain that the molecular mechanisms underlying SV40 transformation reflect the molecular pathology of all human prostate cancers. Clearly, prostate neoplasia may involve more than one type of IGF receptor dysregulation mechanism. Taken together, the data encourage additional studies of IGF signal transduction in primary AD and AI human prostate cancer tissue.

Several molecular mechanisms have been proposed to account for the ability of prostate cancer cells to overcome the growth-inhibitory effects of androgen withdrawal and develop a more aggressive neoplastic phenotype characterized by rapid proliferation in the absence of androgenic stimulation. For example, overexpression of Her-2/neu (7) and overexpression of Bcl-2 (30) have been linked to progression of prostate cancer to androgen independence. It is possible that molecular changes in any one of several critical regulatory pathways would be sufficient to confer AI growth. Our demonstration that progression to androgen independence is associated with changes in expression of IGF-I, IGF-IR, and IGFBP-3 provides evidence that IGF signaling pathways are relevant to neoplastic progression of prostate cancer. In the LAPC-4 model, although AI was associated with no major changes in expression of IGF ligands and an decrease in *IGF-IR* expression, we obtained evidence for increased phosphorylation of the IGF-I receptor. The basis for this observation requires further investigation, but one possibility involves deficiency of a phosphotyrosine phosphatase activity that normally reduces the half-life of activated receptors. There is a precedent for this type of mechanism in other systems (31, 32). Furthermore, there is prior evidence that in the LAPC-4 model a separate regulatory abnormality (up-regulation of Her-2/neu) is involved in progression to androgen independence (7), and this could affect IGF-IR phosphorylation through cross-talk receptor tyrosine kinases.

It is unclear whether critical changes in gene expression that occur during prostate cancer progression arise from epigenetic mechanisms resulting from adaptation of dormant AD cells to growth after androgen depletion or whether AI cancers represent the outgrowth by clonal selection of a subset of cells within the tumor population with a preexisting pattern of gene expression that confers a growth advantage in the absence of androgens (33). Previous evidence that androgen independence in the LAPC-9 model arises from clonal expansion (1) suggests that the observed deregulation of IGF signaling in AI LAPC-9 tumors existed in a fraction of the cells present in the AD tumor prior to castration.

IGFBP-3 has been associated with direct and indirect growth-inhibitory actions (34–37). We reported previously that increases in IGFBP-3 expression are associated with apoptotic regression of the normal rat ventral prostate induced by either castration (22) or the antiandrogen bicalutamide (25). The data demonstrating increased IGFBP-3 expression in the LAPC-9 system after castration extend these findings to certain human prostate cancer models and are consistent with the possibility of a functional role of IGFBP-3 expression in mediating the apoptosis that follows castration. In view of the growth-inhibitory actions of IGFBP-3, it is not surprising that expression of this gene is greatly reduced when LAPC-9 tumors achieve AI growth.

Less is known about the role of IGFBP-5 in prostate cancer. Castration-induced apoptotic regression of AD Shionogi tumors is associated with up-regulation of IGFBP-5 (38). In the Shionogi model, both induction of IGFBP-5 and apoptosis can be inhibited by treating mice with calcium channel blockers prior to castration. Although this suggests the possibility that IGFBP-5 may be involved in mediating castration-induced apoptosis, recent reports demonstrating that IGFBP-5 actually confers protection from apoptosis (39, 40) suggest the possibility that up-regulation of expression of IGFBP-5 may represent an attempt to survive despite the presence of other signals favoring apoptosis. Our observation that IGFBP-5 is up-regulated during AI growth of LAPC-9 also suggests the possibility that in certain physiological contexts, IGFBP-5 expression enhances cell survival.

The hypothesis that any one of several sets of molecular derangements is sufficient to confer an AI phenotype is consistent with the clinical observation that progression to androgen independence is a common rather than a rare event. Our data provide evidence that changes in expression of genes in the IGF regulatory system within prostate cancers are associated with acquisition of androgen independence. The results are in keeping with the general hypothesis (41) that

receptor kinases are important determinants of neoplastic behavior and provide a rationale for studies concerning molecular pathology of IGF signaling in paired clinical AD and AI prostate cancer specimens. Finally, the data raise the possibility that novel pharmacological approaches that target IGF signaling may be of therapeutic value for at least a subset of AI prostate cancers.

ACKNOWLEDGMENTS

We thank M. J. Blouin for assistance in preparation of the manuscript.

REFERENCES

1. Craft, N., Chhor, C., Tran, C., Belldegrun, A., DeKernion, J., Witte, O. N., Said, J., Reiter, R. E., and Sawyers, C. L. Evidence for clonal outgrowth of androgen-independent prostate cancer cells from androgen-dependent tumors through a two-step process. Cancer Res., *59:* 5030–5036, 1999.
2. Horoszewicz, J. S., Leong, S. S., Kawinski, E., Karr, J. P., Rosenthal, Chu, T. M., Mirand, E. A., and Murphy, G. P. LNCaP model of human prostatic carcinoma. Cancer Res., *43:* 1809–1818, 1983.
3. Veldscholte, J., Berrevoets, C. A., Ris-Stalpers, C., Kuiper, G. G., Jenster, G., Trapman, J., Brinkmann, A. O., and Mulder, E. The androgen receptor in LNCaP cells contains a mutation in the ligand binding domain which affects steroid binding characteristics and response to antiandrogens. J. Steroid Biochem. Mol. Biol., *41:* 665–669, 1992.
4. Sato, N., Gleave, M. E., Bruchovsky, N., Rennie, P. S., Beraldi, E., and Sullivan, L. D. A metastatic and androgen-sensitive human prostate cancer model using intraprostatic inoculation of LNCaP cells in SCID mice. Cancer Res., *57:* 1584–1589, 1997.
5. Gleave, M. E., Hsieh, J. T., Wu, H-C., and Chung, L. W. K. Serum PSA levels in mice bearing human prostate LNCaP tumor are determined by tumor volume and endocrine and growth factors. Cancer Res., *52:* 1598–1605, 1992.
6. Klein, K. A., Reiter, R. E., Redula, J., Moradi, H., Zhu, X. L., Brothman, A. R., Lamb, D. J., Marcelli, M., Belldegrun, A., Witte, O. N., and Sawyers, C. L. Progression of metastatic human prostate cancer to androgen independence in immunodeficient SCID mice. Nat. Med., *3:* 402–408, 1997.
7. Craft, N., Shostak, Y., Carey, M., and Sawyers, C. L. A mechanism for hormone-independent prostate cancer through modulation of androgen receptor signaling by the HER-2/neu tyrosine kinase. Nat. Med., *5:* 280–285, 1999.
8. Baserga, R. The insulin-like growth factor I receptor: a key to tumor growth? Cancer Res., *55:* 249–252, 1995.
9. Peruzzi, F., Prisco, M., Dews, M., Salomoni, P., Grassilli, G., Romano, G., Calabretta, B., and Baserga, R. Multiple signaling pathways of the insulin-like growth factor I receptor in protection from apoptosis. Mol. Cell. Biol., *19:* 7203–7215, 1999.
10. Clemmons, D. R. Insulin-like growth factor binding proteins and their role in controlling IGF actions. Cytokine Growth Factor Rev., *8:* 45–62, 1997.
11. Cohen, P., Pechl, D. M., Lamson, G., and Rosenfeld, R. G. Insulin-like growth factors (IGFs), IGF receptors, and IGF-binding proteins in primary cultures of prostate epithelial cells. J. Clin. Endocrinol. Metab., *73:* 401–407, 1991.
12. Pechl, D. M., Cohen, P., and Rosenfeld, R. G. Role of insulin-like growth factors in prostate biology. J. Androl., *17:* 2–4, 1996.
13. Burfeind, P., Chernicky, C. L., Rininsland, F., and Ilan, J. Antisense RNA to the type I insulin-like growth factor receptor suppresses tumor growth and prevents invasion by rat prostate cancer cells *in vivo*. Proc. Natl. Acad. Sci. USA, *93:* 7263–7268, 1996.
14. DiGiovanni, J., Kiguchi, K., Frijhoff, A., Wilker, E., Bol, D. K., Beltran, L., Moats, S., Ramirez, A., Jorcano, J., and Conti, C. Deregulated expression of insulin-like growth factor 1 in prostate epithelium leads to neoplasia in transgenic mice. Proc. Natl. Acad. Sci. USA, *97:* 3455–3460, 2000.
15. Chan, J. M., Stampfer, M. K., Giovannucci, E., Gann, P. H., Ma, J., Wilkinson, P., Hennekens, C. H., and Pollak, M. Plasma insulin-like growth factor-I and prostate cancer risk: a prospective study. Science (Wash. DC), *279:* 563–566, 1998.
16. Stattin, P., Bylund, A., Rinaldi, S., Biessy, C., Dechaud, H., Stenman, U. H., Egevad, L., Riboli, E., Hallmans, G., and Kaaks, R. Plasma insulin-like growth factor-I, insulin-like growth factor-binding proteins, and prostate cancer risk: a prospective study. J. Natl. Cancer Inst. (Bethesda), *92:* 1910–1917, 2000.
17. Harman, S. M., Metter, E. J., Blackman, M. R., Landis, P. K., and Carter, H. B. Serum levels of insulin-like growth factor I (IGF-I), IGF-II, IGF-binding protein-3, and prostate-specific antigen as predictors of clinical prostate cancer. J. Clin. Endocrinol. Metab., *85:* 4258–4265, 2000.
18. Shaneyfelt, T., Husein, R., Bubley, G. J., and Mantzoros, C. S. Hormonal predictors of prostate cancer: a meta-analysis. J. Clin. Oncol., *18:* 847–853, 2000.
19. Pollak, M. Insulin-like growth factors (IGFs) and prostate cancer. Epidemiol. Rev., in press, 2001.
20. Culig, Z., Hobisch, A., Cronauer, M. V., Radmayr, C., Trapman, J., Hittmair, A., Bartsch, G., and Klocker, H. Androgen receptor activation in prostatic tumor cell lines by insulin-like growth factor-I, keratinocyte growth factor, and epidermal growth factor. Cancer Res., *54:* 5474–5478, 1994.
21. Putz, T., Culig, Z., Eder, I. E., Nessler-Menardi, C., Bartsch, G., Grunicke, H., Uberall, F., and Klocker, H. Epidermal growth factor (EGF) receptor blockade inhibits the action of EGF, insulin-like growth factor I, and a protein kinase A activator on the mitogen-activated protein kinase pathway in prostate cancer cell lines. Cancer Res., *59:* 227–233, 1999.
22. Nickerson, T., Pollak, M., and Huynh, H. Castration-induced apoptosis in the rat ventral prostate is associated with increased expression of genes encoding insulin-like growth factor binding proteins 2, 3, 4 and 5. Endocrinology, *139:* 807–810, 1998.
23. Winer, J., Jung, C. K., and Williams, P. M. Development and validation of real-time quantitative reverse transcriptase-polymerase chain reaction for monitoring gene expression in cardiac myocytes *in vitro*. Anal. Biochem., *270:* 41–49, 1999.
24. Reiss, K., Wang, J. Y., Romano, G., Furnari, F. B., Cavenee, W. K., Morrione, A., Tu, X., and Baserga, R. IGF-I receptor signaling in a prostatic cancer cell line with a PTEN mutation. Oncogene, *19:* 2687–2694, 2000.
25. Nickerson, T., and Pollak, M. Bicalutamide (Casodex)-induced prostate regression involves increased expression of genes encoding insulin-like growth factor binding proteins. Urology, *54:* 1120–1125, 1999.
26. Plymate, S. R., Bae, V. L., Maddison, L., Quinn, L. S., and Ware, J. L. Type-1 insulin-like growth factor receptor reexpression in the malignant phenotype of SV40-T-immortalized human prostate epithelial cells enhances apoptosis. Endocrine, *7:* 119–124, 1997.
27. Plymate, S. R., Bae, V. L., Maddison, L., Quinn, L. S., and Ware, J. L. Reexpression of the type 1 insulin-like growth factor receptor inhibits the malignant phenotype of simian virus 40 T antigen immortalized human prostate epithelial cells. Endocrinology, *138:* 1728–1735, 1997.
28. Damon, S. E., Plymate, S. R., Carroll, J. M., Sprenger, C. C., Dechsukhum, C., Ware, J. L., and Roberts, C. T., Jr. Transcriptional regulation of insulin-like growth factor-I receptor gene expression in prostate cancer cells. Endocrinology, *142:* 21–27, 2001.
29. Plymate, S. R., Tennant, M., Birnbaum, R. S., Thrasher, J. B., Chatta, G., and Ware, J. L. The effect of the insulin-like growth factor system in human prostate epithelial cells of immortalization and transformation by simian virus-40 T antigen. J. Clin. Endocrinol. Metab., *81:* 3709–3716, 1996.
30. Miyake, H., Tolcher, A., and Gleave, M. E. Antisense Bcl-2 oligodeoxynucleotides inhibit progression to androgen-independence after castration in the Shionogi tumor model. Cancer Res., *59:* 4030–4034, 1999.
31. Wu, X., Senechal, K., Neshat, M. S., Whang, Y. E., and Sawyers, C. L. The PTEN/MMAC1 tumor suppressor phosphatase functions as a negative regulator of the phosphoinositide 3-kinase/Akt pathway. Proc. Natl. Acad. Sci. USA, *95:* 15587–15591, 1998.
32. Whang, Y. E., Wu, X., Suzuki, H., Reiter, R. E., Tran, C., Vessella, R. L., Said, J. W., Isaacs, W. B., and Sawyers, C. L. Inactivation of the tumor suppressor PTEN/MMAC1 in advanced human prostate cancer through loss of expression. Proc. Natl. Acad. Sci. USA, *95:* 5246–5250, 1998.
33. Rennie, P. S., and Nelson, C. C. Epigenetic mechanisms for progression of prostate cancer. Cancer Metastasis Rev., *17:* 401–409, 1998.
34. Oh, Y., Muller, H. L., Lamson, G., and Rosenfeld, R. G. Insulin-like growth factor (IGF)-independent action of IGF-binding protein-3 in Hs578T human breast cancer cells. J. Biol. Chem., *268:* 14964–14971, 1993.
35. Rajah, R., Valentinis, B., and Cohen, P. Insulin-like growth factor binding protein-3 induces apoptosis and mediates the effects of transforming growth factor-β1 on programmed cell death through a p53- and IGF-independent mechanism. J. Biol. Chem., *272:* 12181–12188, 1997.
36. Nickerson, T., Huynh, H., and Pollak, M. Insulin-like growth factor binding protein-3 induces apoptosis in MCF7 breast cancer cells. Biochem. Biophys. Res. Commun., *237:* 690–693, 1997.
37. Hwa, V., Oh, Y., and Rosenfeld, R. G. The insulin-like growth factor-binding protein (IGFBP) superfamily. Endocr. Rev., *20:* 761–787, 1999.
38. Nickerson, T., Miyake, H., Gleave, M. E., and Pollak, M. Castration-induced apoptosis of androgen-dependent Shionogi carcinoma is associated with increased expression of genes encoding IGF-binding proteins. Cancer Res., *59:* 3392–3395, 1999.
39. Perks, C. M., Bowen, S., Gill, Z., Newcomb, P., and Holly, J. Differential IGF-independent effects of insulin-like growth factor binding proteins (1–6) on apoptosis of breast epithelial cells. J. Cell. Biochem., *75:* 652–664, 1999.
40. Miyake, H., Pollak, M., and Gleave, M. E. Castration-induced up-regulation of insulin-like growth factor binding protein-5 potentiates insulin-like growth factor-I activity and accelerates progression to androgen independence in prostate cancer models. Cancer Res., *60:* 3058–3064, 2000.
41. Blume-Jensen, P., and Hunter, T. Oncogenic kinase signalling. Nature (Lond.), *411:* 355–365, 2001.

Molecular Endocrinology. First published July 18, 2002 as doi:10.1210/me.2002-0004

Identification of an Androgen-Dependent Enhancer Within the Prostate Stem Cell Antigen Gene

Anjali Jain[1], Amanda Lam[2], Igor Vivanco[3], Michael F. Carey[2,4*] and Robert E. Reiter[1,4]

Departments of Urology[1], Biological Chemistry[2], Medicine[3] and Molecular Biology Institute[4]

UCLA School of Medicine

Los Angeles CA 90095

***Corresponding author**

Box 951737, Phone: 310-206-7859, Fax: 310-206-9598, Email:mcarey@mednet.ucla.edu

Address requests for reprints to: Dr. Michael F. Carey, Department of Biological Chemistry, UCLA School of Medicine, Box 951737, Los Angeles, CA 90095.

Abbreviated title: Androgen-dependent PSCA enhancer

Keywords: prostate stem cell antigen, enhancer, prostate cancer, androgen-responsive

This work was supported in part by the CaP CURE grant to M.C., a DOD project grant to C. Sawyers, M. Carey and P. Cohen (DAMD17-00-1-0077) and NCI grants to R.E.R. (NCI K08 CA74169 & NCI RFA CA-98-013). A.J. was supported by California Cancer Research Program (2PD0109).

ABSTRACT

Prostate stem cell antigen (PSCA) is emerging as an important diagnostic marker and therapeutic target in prostate cancer. Previous studies indicated that prostate stem cell antigen was directly regulated by androgens but the mechanism has not been elucidated. Here we describe the identification of a compact cell-specific and androgen-responsive enhancer between 2.7 and 3 kb upstream of the transcription start site. The enhancer functions autonomously when positioned immediately adjacent to a minimal promoter. DNase I footprinting analysis with recombinant androgen receptor (AR) reveals that the enhancer contains two androgen receptor binding sites at one end. Mutational analysis of the androgen receptor binding sites revealed the importance of the higher affinity one. The dissociation constant (K_d) of the high affinity binding site (AREI) was determined to be ~87 nM. The remainder of the enhancer contains elements that function synergistically with the androgen receptor. We discuss the structural organization of the PSCA enhancer and compare it to that found in other AR-regulated genes.

INTRODUCTION

Prostate cancer begins as an androgen-dependent (AD)[5] tumor but progresses to an androgen-independent (AI)[5] phenotype upon androgen deprivation (1-3). Serum levels of the prostate specific antigen (PSA)[5] are used clinically as a marker for diagnosis and management of prostate cancer. Analysis of PSA gene regulation has provided considerable insight into the mechanisms of prostate cancer progression and the role that the androgen receptor (AR)[5] plays in this transition (4-10). However, PSA is not an ideal marker for prostate cancer progression (11-13) and considerable effort has been expended to identify new markers and understand their regulation.

One such marker is prostate stem cell antigen (PSCA)[5] (14), a cell surface protein related to the Ly-6/Thy-1 family of glycosylphosphatidyl-inositol (GPI)[5]-anchored antigens. PSCA is expressed in normal prostate and bladder and is upregulated in a large proportion of localized and metastatic prostate cancers (15). Overexpression of PSCA correlates with increasing tumor stage, grade and metastasis to bone. A murine homologue of PSCA (mPSCA[5]) has been isolated and has a similar tissue distribution to human PSCA (16, 17). Like human PSCA, expression of mPSCA is upregulated in multiple mouse models of prostate cancer, such as TRAMP[5] (transgenic adenocarcinoma of the mouse prostate) and PTEN[5] (phosphatase and tensin homologue) heterozygous mice. PSCA is also overexpressed in a large percentage of bladder and pancreatic cancers (18, 19). Although the precise role of PSCA in cancer progression is not known, its homologues (Thy-1 and Ly-6) have defined roles in cell signaling (20, 21) and have been implicated in cancer progression. A role for PSCA in cancer progression is suggested by

studies showing that monoclonal antibodies targeting PSCA can block prostate cancer growth and metastasis in xenograft models of human prostate cancer (22). Together, these studies suggest that PSCA expression is both linked to and may play a biological role in carcinogenesis.

The mechanism(s) by which PSCA expression is regulated in normal tissue and cancer is not known. In order to study PSCA gene regulation, we recently isolated a 9-kb genomic fragment containing the human PSCA promoter/enhancer region (23). Consistent with the normal tissue distribution of PSCA, the 9-kb promoter/enhancer region was active in cell lines derived from normal and malignant prostate and bladder cells. This region was also androgen responsive in the LNCaP prostate cancer cell line, consistent with *in vivo* studies of mPSCA showing downregulation of PSCA after castration (16). These initial studies suggest that the PSCA promoter is tissue-specific and may be regulated by both AD (LNCaP) and AI (normal androgen receptor negative prostate epithelial cells and bladder cells) pathways.

Transgenic mice bearing the human PSCA promoter region fused to green fluorescent protein (GFP)[5] express GFP in mid-gestation following the appearance of prostatic buds from the urogenital sinus (23). In adult mice, GFP expression was restricted to a subset of cells located in the distal tips of the glands, which are hypothesized to be progenitors for the terminally differentiated secretory cells. GFP expression increased and expanded during periods of active ductal growth, such as puberty and after administration of testosterone to castrate mice, but was barely detectable after castration-induced prostate

regression. Prostate carcinogenesis driven by T antigen in the TRAMP model resulted in an increased percentage and intensity level for PSCA promoter-driven GFP positive cells. These results indicate that PSCA expression *in vivo* is related to growth, regeneration and tumorigenesis of the prostate and that PSCA is regulated at the transcriptional level.

A critical observation is that PSCA and its regulatory regions are androgen regulated. It is not known whether androgen regulates the PSCA promoter directly or indirectly. It is possible, for example, that androgen induction of the PSCA promoter is related to the positive proliferative effect of androgen on LNCaP or to the expansion of GFP-positive progenitor cells during prostatic growth. To address this specific question, we have now carried out a detailed analysis of the PSCA regulatory region. Our major findings are (1) that androgen regulates PSCA directly and (2) that the bulk of PSCA androgen responsiveness can be mapped to one of two androgen receptor binding sites within a 300-bp enhancer region located 2.7 kb upstream of its transcription start site. Mutation of the high affinity binding site results in loss of binding to an androgen receptor DNA binding domain (ARDBD)[5] *in vitro* and to a significant loss of androgen responsiveness *in vivo*. These studies demonstrate that the PSCA promoter/enhancer has an androgen responsive region with structure and function reminiscent of other prostate-specific and androgen-dependent genes. The relationship of this region to PSCA overexpression in cancer remains to be determined.

RESULTS

Transcription Start Site Mapping

As a preliminary step in characterizing the DNA elements involved in androgen regulation of PSCA it was necessary to identify the transcriptional start site. Total RNA from the LAPC9-AD and AI prostate cancer xenografts (24) was subjected to Cap-dependent RACE[5] (Rapid Amplification of cDNA Ends), which accurately identifies transcription initiation sites because it is dependent upon the presence of a 7meGTP Cap at the 5'end of the mRNA. Out of 19 clones sequenced, 10 indicated that the major transcription start site was an adenine, 18 bp upstream from the initiating AUG (Genbank accession # AF176678; this sequence represents the antisense strand of the genomic clone where nucleotide # 65248 represents the initiating ATG) and 23 bp downstream of the putative TATA box. A minor startsite was located 2 bp downstream of the adenine.

Promoter Activity in Cell Line Transfections Correlates with Endogenous PSCA Expression

To determine whether the cell specificity of the PSCA promoter constructs match that of the endogenous gene, a PSCA promoter-luciferase construct bearing 6 kb of upstream sequence was transfected into a panel of prostate and non-prostate cell lines and normalized to CMV luciferase activity (Fig. 1). Previous studies had shown that the 6-kb construct elicited a transcriptional activity similar to that of the 9-kb construct employed in the transgenic study (23). Transfections were performed in the presence and absence of the synthetic androgen R1881.

The promoter was found to be active and androgen-inducible in the AR-positive, prostate cancer LNCaP cell line (25) and in a cell line derived from the LAPC4 xenograft. It was also active but not inducible in the bladder carcinoma cell line HT1376 (26), which lacks AR but still expresses PSCA, and in the LAPC9 xenograft, which contains AR and expresses PSCA. The transfected gene was active but not androgen inducible in AR-negative, PrEC[5] populations, which express PSCA. In contrast, the promoter was relatively inactive in a panel of cell lines derived from tissues that do not express PSCA, such as primary PrSCs[5] (Fig. 1), HeLa cells expressing FLAG-AR (cervical carcinoma) (27), 293T (human kidney) (not shown), BHK (baby hamster kidney) cells (not shown), MCF7 (breast carcinoma) and NIH3T3 fibroblasts (23). The data indicate a selectivity of PSCA expression in cell culture that parallels the *in vivo* pattern.

Authentic Regulation is Achieved with Stably Integrated Reporter Constructs in LNCaP Cells

LNCaP cells were employed as an experimental system for promoter mapping because these cells support a robust androgen response analogous to that observed in the transgenic models (23). To validate the system for detailed expression studies, a 6kb PSCA-GFP fusion was stably integrated into LNCaP cells and androgen inducible GFP expression was assessed by fluorescence microscopy and fluorescence activated cell sorting (FACS[5]). In the absence of androgen, the PSCA 6-kb GFP cells displayed low but measurable levels of expression versus the GFP control by both microscopy and FACS analysis (Fig. 2, panels c vs a). However, with the addition of androgen a 2-fold increase in the number of cells expressing GFP (panels c vs d) was observed along with a 10-fold

increase in the fluorescence intensity (Fig. 2, panels c vs d). These data demonstrated that authentic PSCA gene regulation could be recreated in the LNCaP cell line and that it maintained its binary mode of regulation in the context of a chromatin environment. This is an important observation since it has been established that appropriate assessment of endogenous transcriptional responses to hormones requires a chromatin environment (28, 29).

Identification of the PSCA Enhancer and Promoter

LNCaP cells were employed to systematically map the promoter using a collection of 5' promoter deletions between –38 bp and – 6 kb (Fig. 3A). We performed the analysis in a stepwise fashion by gradually homing in on the androgen responsive enhancer using two sets of deletions. The first set comprised 500-bp to 1-kb deletions (Fig. 3B) and the second set comprised 200 to 300-bp deletions (Fig. 3C). Each set provided data that allowed us to assign functional borders to the regions conferring androgen-independent and androgen-dependent promoter activity. The PSA basic promoter-enhancer construct (PSA-2.4; (30)), a classic AR-responsive regulatory region, and two other constructs, ARE4 (30) and EnhE4 (27), were used as positive controls for androgen induction. All three positive controls lacked androgen-independent activity but displayed a robust androgen response in the presence of 10 nM R1881 (Fig. 3B).

The PSCA-0.038 construct or $PSCA_T$, bearing the putative TATA box, does not contribute significantly to the reporter activity in either the presence or absence of R1881 (Fig. 3B). The androgen-independent promoter activity is first detected in PSCA-0.5 and

continues to increase gradually (~67 fold) up to PSCA-6.0. The androgen-inducible transcription is first measurable in PSCA-0.5. The most dramatic increase occurs between PSCA-2.0 and PSCA–3.0 (Fig. 3B). No additional fold increases in androgen responsiveness are observed between PSCA-3.0 and PSCA-6.0. To delineate the DNA region conferring the steep increase in androgen responsiveness further, we analyzed a second set of deletions between PSCA-2.0 and PSCA-3.0 (Fig. 3C). The R1881-induced luciferase activity of PSCA-3.0 is significantly higher than that of PSCA-2.7. The androgen responsiveness of PSCA-3.0 is 19-fold, as compared to 5-fold for PSCA-2.7. The results indicated the sharp increase in androgen responsiveness was conferred by DNA elements located within a 300-bp region between 2.7-3 kb.

Sufficiency of the PSCA Enhancer

The deletion data suggested the possibility that the 300-bp region contained an enhancer. One definition of an enhancer is its ability to function autonomously when tethered to a heterologous promoter (i.e., a sufficiency clone). The enhancer was positioned upstream of both the heterologous adenovirus E4 minimal promoter from –38 to +40, and its own minimal promoter from -38 to +12, each bearing the natural TATA box, startsite and 5' untranslated region. The two sufficiency constructs, $E4_T$+2.7-3 and $PSCA_T$+2.7-3, were transfected into LNCaP cells (Fig. 4A) to measure androgen inducibility and into HT1376 (Fig. 4B), 293T and fAR-Hela (data not shown) to determine whether the enhancer maintained the proper cell specificity (see Fig. 1). In LNCaP, both constructs exhibited increased basal expression above the minimal promoter controls and responded to androgen 12.4 and 18.0 fold, respectively. The constructs were active in HT1376 but

not induced by androgen (Fig. 4B), indicating that the enhancer maintains a level of androgen independent activity. Finally, the constructs were inactive in 293T cells and fAR-HeLa cells, indicating that the enhancer maintains tissue selectivity (data not shown). Remarkably, the constructs were as active and specific as PSCA-3.0, indicating that they retained the stimulatory activity and specificity of the parental construct. The strong androgen responsiveness of the constructs indicated that the 0.3kb PSCA enhancer might plausibly contain AREs[5] (androgen response elements), the binding sites for AR.

Identification of AREs within the PSCA Enhancer

To determine if AR was acting directly we mapped binding sites for AR within the 300-bp androgen-responsive PSCA enhancer by DNase I footprinting using recombinant ARDBD (27). The PSA enhancer was included as a positive control because it contains AREs that have been validated by footprinting and detailed mutational analysis (27). Two DNase I footprints, each encompassing a region of 23-bp and separated from each other by a distance of 25-bp, were detected on the PSCA enhancer (Fig. 5, right panel). Both these sites were present between -2.7 kb to -2.8 kb. We term these sites 'high affinity' and 'low affinity'. The high affinity site appeared at ~14.8 nM of recombinant ARDBD (active protein) whereas the low affinity site did not appear until ~133.3 nM of ARDBD. As shown in the left panel of Fig. 5, AREIII of the PSA enhancer (31) and PSCA high affinity site seem to display comparable affinities for ARDBD. The sequence of the high affinity site is GGAACTttcCGTCCT and the sequence of the low affinity site is CGCACAagaCGTTTT. Both sites display ~67% homology to the ARE consensus sequence (GGTACAnnnTGTTCT) (32).

Determination of the Relative Affinity of ARDBD to PSCA AR Binding Sites

To evaluate the binding affinities of the two AR binding sites within the PSCA enhancer, their dissociation constants or K_d[5] values were determined and compared to several known naturally occurring ARE sequences (summarized in Table I). The active protein concentration of ARDBD was first shown to be ~$4X10^{-7}$ M. This preparation was used to determine the dissociation constants in electrophoretic mobility shift assays (EMSAs[5]) (see Materials and Methods and Fig. 6A). The PSCA low affinity site sequence did not display a detectable DNA-protein complex in a gel shift assay. The apparent dissociation constant of the PSCA high affinity binding site was determined to be ~87 nM, which was about twice that for PSA AREIII sequence (~46 nM). The affinity of PSA AREIII was almost half of that reported for the PSA AREI sequence (~26 nM), which agrees with the PSA ARE affinity order as determined by Huang et al. ((27).

Both PSCA AR Binding Site Mutants Abolish ARDBD Binding while Only the High Affinity Site Mutation Abolishes Function

To determine whether PSCA AR binding site sequences are functional, we mutated the sites at positions important for AR binding (33-35). The mutations (Table II) were tested in an EMSA (Fig. 6A) and a DNase I footprinting assay (Fig. 6B). They were also introduced in the context of the PSCA-6.0 construct or the $PSCA_T$+2.7-3 construct and subjected to transfection analyses (Fig. 7).

The gel shift assay indicated that the ARDBD binding was abolished in the high affinity site mutant (compare PSCA-high to PSCA high-mut; Fig. 6A). As stated earlier, we could not detect a stable DNA-protein complex using the PSCA low affinity binding site in this assay. The consensus ARE sequence, its mutant and the PSA AREIII sequence were used for comparisons (Fig. 6A). The footprinting analysis indicated that ARDBD binding was also abrogated in both the high affinity (high mut) and low affinity (low mut) site mutants compared to the wild-type probe (Fig. 6B).

The transfection analyses into LNCaP and LAPC4 cells revealed that mutations in the high affinity site (PSCA-6.0 high-mut) cause a significant reduction in androgen-responsive activity (Figs. 7A and 7B). In contrast, mutations in the low affinity site (PSCA-6.0 low-mut) had only a marginal effect (Fig. 7A). Note that in some cases the basal activity is reduced with the mutation. We have found via casodex inhibition with the PSA enhancer that there are still residual androgens in our depleted medium. Based on these results, it was clear that the high affinity binding site was an authentic androgen response element and we termed it PSCA AREI. The low affinity site did not seem to play an essential role in the androgen responsiveness of the PSCA enhancer. The effect of the AREI mutant was restricted to LNCaP and LAPC4 cells because the mutations failed to affect the androgen-independent activity of PSCA-6.0 in HT1376 cells (not shown).

To solidify our conclusion that the reduction in androgen responsiveness was due to mutation of the high affinity AREI, the same mutations were tested in the context of the

minimal construct, $PSCA_T$+2.7-3. As expected, the AREI mutant ($PSCA_T$+2.7-3.0 AREImut) caused a decrease in androgen inducibility (Fig. 7C).

PSCA AREI Sequence has a Low Affinity in Isolation but can, nevertheless, Function as a Genuine Androgen Response Element

A bona fide ARE should be able to function by itself and from a heterologous gene promoter, i.e., respond to androgens *in vivo*. To test these definitions for PSCA AREI, we multimerized the AREI sequence and cloned it next to a TATA box from the adenovirus E4 gene. The constructs were subjected to transient transfection analyses in the presence of the androgen analogue R1881 in LNCaP cells. While a duplicated version of the ARE displayed a low level of androgen responsiveness (data not shown), a robust response (~18 fold induction) was observed with a quadruplicated version of the ARE ($E4_T$+PSCA ARE4; Fig. 8). This androgen response was lowered to 3.6 fold when the quadruplicated sequence contained the AREI mutation ($E4_T$+PSCA ARE4mut). As a control, we compared the PSCA ARE4 construct to the PSA ARE4 construct (quadruplicated PSA AREI sequence upstream of an E4 TATA box). The androgen induction of the PSA ARE4 construct was ~137 fold. The higher responsiveness of this construct is in agreement with the higher affinity of PSA AREI (Table I). These data demonstrate that the PSCA AREI sequence, albeit of a lower affinity, has the ability to direct androgen response from a heterologous promoter.

Sequences Flanking AREI are Required for the Androgen Dependent Activity of the PSCA Enhancer

The functional AREI sequence is located between 2.7 and 2.8 kb upstream of the gene and constitutes the downstream end of the enhancer. To determine if the enhancer could be further delineated we analyzed it in greater detail by creating additional 100-bp deletions within the 300-bp region (Fig. 9, PSCA-2.8 and PSCA-2.9). Surprisingly, deletions outside of the ARE between 2.8 and 3.0 kb severely reduced enhancer activity. To rule out the possibility of additional AR binding sites between 2.8 and 3.0 kb, we carried out DNase I footprinting assays and gel shift assays (data not shown) with the 300-bp enhancer region. The major binding site was that of AREI, which was abolished upon mutation. We saw very low affinity non-specific complexes of varying mobilities within the 2.8-3.0 region, but only at very high concentrations of ARDBD. We also analyzed two additional clones, $PSCA_T$+2.8-3.0 and $PSCA_T$+2.7-2.8 in transient transfection assays (data not shown). Neither of the two clones displayed any androgen responsiveness above that of the $PSCA_T$ construct, however, they interacted synergistically to provide robust levels of androgen responsiveness in $PSCA_T$+2.7-3.0. The data suggest that the PSCA enhancer comprises an androgen responsive component in combination with other elements important for synergizing with the ARE and possibly for conferring the cell specificity of the enhancer.

DISCUSSION

We have focused our efforts on the identification and characterization of androgen-responsive enhancers that function during prostate cancer progression from the AD to the AI state (27, 30, 36). PSCA is an ideal gene to pursue this problem because of its natural expression patterns and response to androgens only in certain epithelial cells of the

prostate and in prostate cancer. Our study indicates that PSCA contains a proximal promoter located within the 500-bp region upstream from the TATA box and an enhancer located between -2.7 and –3.0 kb. The promoter is weakly responsive to androgens and contains a putative sequence that binds to ARDBD in *in vitro* DNA binding assays. However, this sequence element is not responsible for the androgen responsiveness as determined by mutagenesis (data not shown). A deletion analysis of the promoter narrowed the androgen responsive region to another sequence element which does not bind ARDBD. The androgen responsive mechanism of the promoter region is not fully understood, but it is possible that this may be an indirect effect, i.e., another androgen dependent protein may bind to and regulate this region. Analysis of PSCA upstream sequences (-3.0 to –6.0 kb) failed to identify any additional androgen responsive activity in transient transfection assays (data not shown). The enhancer, however, is localized to a 300-bp region and confers strong androgen responsiveness.

The enhancer functions autonomously in the context of a heterologous promoter and contains cell-type specific elements that allow PSCA to be expressed in both AI cell lines such as the bladder cancer line HT1376, and in the AD prostate cancer lines such as LNCaP and LAPC4. It does not function in human kidney (293T) or cervical carcinoma (HeLa) cells that do not support the expression of PSCA. The absolute promoter activity and androgen responsiveness of this "mini-enhancer" is equal to that of the entire 3-kb PSCA regulatory sequence. The data imply that the "tissue-specific" and "androgen-independent" elements overlap at the PSCA enhancer, making it an important target for detailed genetic analysis. Intriguingly, the enhancer also responds to dexamethasone (data

not shown) but only at much higher concentrations than its K_d for a wild-type GR[5] (glucocorticoid receptor) (37). It would be interesting to analyze the effect of GR on the endogenous PSCA gene. We have identified the key enhancer ARE through DNA binding and transfection studies and have validated its relevance by mutagenesis and multimerization studies. The K_d of PSCA AREI is higher than that of PSA AREI which is also reflected on multimerizing the two ARE sequences.

It is remarkable that PSCA promoter is not androgen-responsive in the LAPC9 cells, which express AR and PSA. LAPC9 cells express the highest levels of PSCA that we have detected. It is plausible that expression in these cells has plateaued, muting the effect of added androgens. It is also plausible that PSCA expression in this cell population has evolved to become independent of androgen as in PrEC cells and bladder carcinomas. The physiological role of androgens in expression of PSCA is not known and the other signaling pathways that influence PSCA expression *in vivo* need to be examined.

The promoter-enhancer of PSCA conforms to the general organizational principles observed in other androgen-regulated, prostate-specific genes like PSA, Slp[5] (sex limited protein), probasin and hK2 (31, 38-40). The PSA regulatory region comprises a 541-bp core promoter bearing two AREs with an enhancer element at -4.2 kb. The enhancer contains multiple AREs that function with nearby cell-specific elements to activate transcription (27, 31, 41-43). Slp and probasin regulatory regions have identified *androgen responsive regions* (ARR)[5] where single or multiple AR binding sequences

function in conjunction with neighboring sequences (44-46). The principle of coupling an ARR to a strong ARE was initially elucidated for the enhancer within the first intron of the C3(1) gene (47-49). The PSCA enhancer follows a similar scheme of an ARR in that the adjoining sequences in combination with AREI are necessary for providing androgen responsiveness. DNA-binding studies failed to identify additional AR binding sites within –2.8 to –3.0 kb (data not shown), however, this region was necessary to provide androgen responsiveness from the enhancer. The sequence between –2.8 to –3.0 kb was also scanned for potential transcription factor binding sites. We did not find sites for any prostate-specific transcription factors, such as the Ets family member PDEF (50). However, some interesting observations were: AML-1a (85% homology), Arnt (aryl hydrocarbon receptor nuclear receptor; 86% homology), GATA-1 (89% homology), and AP-1 (87% homology). An AML family member has been shown to be functionally required for hormonal induction of the Slp enhancer (51). Likewise, six GATA sites have been shown flanking an androgen-response element located in the far-upstream enhancer of the PSA gene and the study suggested the involvement of prostatic GATA factors in androgen regulation of the gene (52).

A key issue that we and others have faced is what DNA sequences constitute an authentic ARE. It is becoming apparent that the answer to this question involves several complexities. Subtle amino acid differences in the ARDBD coupled with subtle differences in the steroid receptor responsive elements play a role in simple recognition by AR and allow it to be utilized in place of related steroid receptors (33-35, 53).

However, cooperativity of AR both with itself and nearby proteins also probably contributes to the stringency of the receptor response (27, 43).

The optimized ARE is an imperfect palindrome, GGTACAnnnTGTTCT (32, 33) comprising four highly conserved guanines on the sense and antisense strands (Table III). Modeling of the crystal structure of the related GR (54, 55), suggests that these guanines directly contact the recognition helix (CGSCKVFFKRAAE) of the protein. Functional AREs apparently display a minimal requirement for three out of the four guanine contacts. PSCA AREI (AGGACGgaaAGTTCC) and PSCA low affinity site (AAAACGtctTGTGCG) maintain this requirement. However, PSCA low affinity site displays a poor match with other bases in the optimal site (32, 56). This observation is reinforced by comparison to the ARE consensus determined in a $CAAB^5$ assay (competitive amplification and binding), where AR was forced to select a binding site in the presence of a competing steroid receptor. Based on this assay, Nelson and colleagues (33) determined the androgen receptor specific ARE sequence as: (G/A)G(T/A)AC(A/G) (C/t)(g/a)(G/c) TGTTCT. This site contains a bias away from the optimized steroid response element at positions -2, -5 and -7 (Table III). The middle base of the 3-base pair spacer is considered as position 0 for nomenclature purposes. The authors noticed a bias against cytosines except at position –3 in the left half-site (Table III). Both PSCA AR binding sequences adhere to this restriction. The weaker binding of AR at the low affinity binding site may inhibit association with specific coactivators making the site non-functional (57, 58).

Although binding site selection studies have assumed that AR typically recognizes an imperfect inverted repeat (32), an argument has been made that structural determinants in AR may allow it to bind direct repeats of the consensus half site. It was proposed that this is one mechanism for conferring AR-specificity (35, 56). The PSCA ARE sequences match to a certain extent both the putative inverted repeat and the direct repeat. More work will have to be done to resolve this issue.

Claessens and colleagues (59, 60) have defined an HRE^5 (hormone response element) as a sequence which responds to multiple steroid receptors. Various sequence changes in these HREs cause them to favor one steroid receptor over another. An AR-specific consensus HRE sequence (called AR-specific ARE; see Table III) was determined by mutagenesis of AR-specific AREs from the SC^5 (secretory component) and Slp enhancers and the probasin promoter. An 'A' at position +2 (relative to the central nucleotide in the three nucleotide spacer) and a 'T' at position -4 are critical to these AR-specific AREs and are never found in sequences recognized by $GRDBD^5$ (glucocorticoid receptor DNA binding domain) (59). In contrast, a 'C' at position -3 and an 'A' at position -4 will favor binding of GR^5 (glucocorticoid receptor) and response to dexamethasone (61). PSCA AREI has an 'A' at position +2, suggesting that this ARE may be AR-selective (Table III). However, it has a 'C' and an 'A' at positions -3 and -4, respectively. Not surprisingly, the 300-bp PSCA enhancer responds to dexamethasone but only at very high concentrations (data not shown). In conclusion, it seems that PSCA AREI is largely AR-selective but less than the AR-specific AREs. Further experiments would be needed to address this issue in detail.

Androgen response elements have been further classified as class I and class II elements (62) determined by the nucleotide sequences that function to mediate cooperative binding, hormone sensitivity and transcriptional activity. It has been suggested that the two classes function cooperatively to achieve a robust hormone response. PSCA AREI seems to conform as a class I element in terms of its guanine contacts and androgen sensitivity (Table III). This is also apparent by comparing the sequence to other class I elements identified in naturally occurring ARE sequences (see Table III). PSCA low affinity site matches well with the class I sequences only in one half-site. It does not match very well with the suggested class II consensus sequence and the ARDBD binding at the two sites is not cooperative.

The PSCA promoter sequence is well conserved across species. DNA sequencing analysis of the first 3-kb of the mouse PSCA promoter revealed a 49.3% identity with the human sequence. The mouse promoter sequence has several gaps in it as 2930 bp of the mouse sequence aligns up with 3513 bp of the human sequence. More importantly, however, comparison of the 300-bp human PSCA enhancer with the corresponding mouse sequence revealed a high homology (~60%) (Fig. 10). Interestingly, the sequence corresponding to the PSCA AREI displayed a higher identity than the low affinity binding site sequence and contained base pair changes that would still maintain the site as an AR binding site. Further, the 5' sequence flanking the AREI was identical (~80% identity within the first 50 bp 5' to AREI) to the human sequence. This sequence was shown to be important for androgen responsiveness from the human PSCA enhancer.

With the identification of a dual regulatory pathway within the PSCA promoter, we have demonstrated that the nature of the PSCA-expressing cells is mirrored within the promoter itself. The natural AI and AD response patterns of the promoter will provide an important tool to generate models that can be utilized to address basic questions in prostate cancer progression and the role of PSCA in that process.

MATERIALS AND METHODS

Transcription Startsite Mapping

The PSCA transcription start site was mapped using the GeneRacer™ Kit (Invitrogen), which employs the Cap-dependent RACE method to detect transcripts containing authentic 5'ends. 5 μg of total RNA from LAPC9 AD and AI tumors was decapped and ligated to an RNA oligonucleotide. PCR was performed using a 3' PSCA-specific primer with the 5' GeneRacer™ primer complementary to the RNA oligonucleotide. The sequence and the T_m of the primer were 5' CTGGCTGCAGGGCCAAGCCT 3' and 76 C, respectively. The PCR product, a slightly diffuse single band of ~100-bp, was cloned into the pCR4Blunt-TOPO vector using the Zero Blunt TOPO PCR cloning kit (Invitrogen, CA). Plasmid DNA was extracted from 19 colonies and sequenced (Laragen, Inc.; Santa Monica, CA) using the flanking T7 promoter primer. The DNA sequences were aligned to the human PSCA genomic sequence to determine the transcription start site.

PSCA Deletions

The PSCA promoter-luciferase reporter constructs (PSCA-1.0, PSCA-3.0 and PSCA-6.0) are as described (23). Briefly, PSCA-1.0, PSCA-3.0 and PSCA-6.0 contain 1 kb, 3 kb and 6 kb of sequence upstream of the PSCA transcription start site. The ATG of the PSCA coding sequence was changed to CTG so that the ATG of luciferase gene could be utilized in the transient transfection experiments. All the subsequent promoter deletion constructs were constructed from the PSCA-6.0 clone. The promoter deletion constructs PSCA-0.038 or $PSCA_T$ (10-bp upstream to the TATA box) and PSCA-0.5 were constructed by subcloning the appropriate PCR promoter fragments into KpnI/HindIII cleaved pGL3basic vector (Promega). Likewise, PSCA-2.0 was generated by subcloning the appropriate PCR promoter fragment into BglII/HindIII sites of the pGL3basic vector (Promega). The constructs PSCA-1.5, PSCA-2.2, PSCA-2.5, PSCA-2.7, PSCA-2.8 and PSCA-2.9 were generated by subcloning the appropriate PCR promoter fragments into the KpnI site of the PSCA-1.0 construct. The integrity of all the constructs was confirmed by automated sequencing reactions (Laragen Inc., Santa Monica, CA).

PSCA Sufficiency Clones

The $E4_T$ construct contains the adenovirus E4 TATA, startsite and 5'untranslated sequences (-38 to +40) cloned into pGL3basic vector (Promega) at the SacI and XhoI restriction enzyme sites. $PSCA_T$+2.7-3.0 and $E4_T$+2.7-3.0 were constructed by PCR-amplifying the 300-bp enhancer and subcloning it into the KpnI site of the $PSCA_T$ and $E4_T$ constructs. Multimerized PSCA AREI clones were constructed by phosphorylation followed by self-ligation of the following oligonucleotides: For $E4_T$+PSCA ARE4 (5'

CGGAACTTTCCGTCCTCCTTGAACACGGAACTTTCCGTCCTGGTAC 3') and for $E4_T$+PSCA ARE4mut (5' CGCGGGTTTCCGTCCTCCTTGAACACGCGGGTTTCCGTCCTCCTAC 3'). The *underlined* sequences represent the PSCA AREI sequence. The ligated oligonucleotides were cloned into KpnI site of $E4_T$ construct. All constructs were confirmed by automated sequencing (Laragen Inc., Santa Monica, CA).

PSCA ARE Mutations

PSCA ARE mutations were generated using a site-directed mutagenesis technique based on the Quick Change procedure described by Stratagene. Briefly, complementary oligonucleotides containing the desired high affinity AR binding site mutation (5'-CAAGGTGCCAGCCTGCGGGTTTCCGTCCTCAAATATTTATA-3') and the low affinity AR binding site mutation (5'-ACTCTGGCCACTCCCCGGGAAGACGTTTTCTTATCTGTCTC-3') (the mutant bases are *underlined*) were synthesized and used as primers with wild-type PSCA-6.0 or the sufficiency clone $PSCA_T$+2.7-3.0 as template in a standard amplification reaction. The resulting product was cleaved with DpnI to remove the wild-type template and the products were transformed into competent DH5α E.coli. The clones were sequenced by automated sequencing (Laragen Inc., Santa Monica, CA) to confirm the position of the mutation and integrity of the clone.

Cell Culture and Transfections

LNCaP cells were grown in RPMI 1640 (Life Technologies, Inc.) supplemented with 10% FBS, L-glutamine, and antibiotics (penicillin/streptomycin). 24 h prior to transfections, 2.5 X 10^5 cells per well were seeded into 6-well plates in phenol red-free RPMI 1640 (Mediatech) supplemented with 10% charcoal/dextran-treated FBS (Omega Scientific), L-glutamine, and antibiotics (penicillin/streptomycin). LNCaP cells were transfected with 1.5 μg of plasmid DNA containing 400 ng of reporter plasmid using Tfx-50 reagent (Promega). Androgen-responsive expression was induced with 10 nM R1881. After 48 h, reporter gene expression was measured using a luciferase assay kit (Promega). Each experiment was repeated three times or more and in each experiment the transfection assays were carried out in triplicate to determine the standard deviations. Relative luciferase activity is maintained in different experiments but due to cell density and other experimental variations, absolute luciferase units vary.

fAR-HeLa cells stably express FLAG-tagged androgen receptor. These were maintained as described previously (27). HT1376, human bladder carcinoma cells, were maintained in DMEM medium (Gibco-BRL) supplemented with 10% FBS, 1% non-essential amino acids (Gibco-BRL), 1% sodium pyruvate (Gibco-BRL) and antibiotics (penicillin/streptomycin). LAPC4 (cell line derived from a human prostate xenograft) were cultured in Iscove's modified Dulbecco's medium (Gibco-BRL) with 10% FBS and antibiotics. fAR-HeLa, HT1376 and LAPC4 were transfected with 1.5 μg of plasmid DNA containing 400 ng of reporter plasmid using Tfx-20 reagent (Promega). Prostate epithelial cells (PrECs) were maintained in serum free Prostate Epithelial Cell Growth

Medium BulletKit (PrEGM~BulletKit$_{TM}$, Clonetics) according to manufacturer's instructions. Prostate stromal cells (PrSC) were maintained in RPMI1640 with 10% FBS. Both the primary cell populations were transfected with similar amounts of plasmid DNA as described above using Tfx50 reagent (Promega). LAPC9 tumor explants were maintained as a disaggregated single-cell suspension in short-term culture in PrEGM and were transfected with Tfx50 reagent. The disaggregated single-cell suspensions were prepared from ~1g of LAPC9-AD tumor (~1.3-1.5 cm^3) using a standard protocol (63). Briefly, under sterile conditions, the tumor was washed and cut into small pieces of ~1-2mm^3. These pieces were resuspended in Iscove's modified Dulbecco's medium (Gibco-BRL) and the tissue was disintegrated with 1% pronase for 20 min at room temperature. The cells were washed with Iscove's medium and then resuspended in 25 ml of PrEGM media with 1X fungizone and 10nM R1881 and seeded in 10 cm cell culture dishes. Next day, the cells were filtered through a sterile 40 μm mesh to get rid of the cellular aggregates and they were plated back again in 10 cm petri dishes. Approximately 3 x10^7 cells were obtained from 1g tumor.

DNase I Footprinting

The binding reactions for DNase I footprinting were as described previously (27). Radiolabeled probes were prepared by PCR, where the PSCA-6.0 plasmid (or the respective binding site mutant plasmids) was employed as a template. Two primers, 3kb-fp1 (5'-GTGTGTTGCCCCCTCCTTGGCC-3') and 2.7kb-fp1 (5'-CCGCCCCAGCTCGCCCGGACTC-3'), flanking the 300-bp enhancer region were used for the PCR amplification of the probe. One of the primers, 2.7kb-fp1 was ^{32}P-end-

labeled with polynucleotide kinase and [γ^{32}P]ATP. The probes were purified on a 4% polyacrylamide gel before they were used in DNase I footprinting reactions. The amounts of recombinant ARDBD (27) used were as indicated in the figure legends.

Electrophoretic Mobility Shift Assay (EMSA)

10 pmoles of ARE containing double-stranded oligonucleotides were ^{32}P-end-labeled with polynucleotide kinase and [γ^{32}P]ATP. The oligonucleotides used were as follows: Consensus ARE (5' CCCCCCCGGTACATGATGTTCTCCCCC 3'), Consensus ARE mutant (5' CCCCCCCGGTACATGAACAAGACCCCC 3'), PSA AREIII (5' CTCTGGAGGAACATATTGTATTGATTG 3'), PSCA high (5' CCTGGAACTTTCCGTCCTCAAATA 3') and PSCA high-mut (5' CCTGTAATTTTCCGTCCTCAAATA 3'). Indicated amounts of recombinant ARDBD was incubated in a 10 µl reaction volume containing 5 fmoles of the radiolabeled probe, 20 mM HEPES, pH 7.9, 25% glycerol, 1.5 mM $MgCl_2$, 0.2 mM EDTA, 100 mM KCl, 0.5 mg/ml bovine serum albumin, 0.01% NP-40, and 400 ng of poly(dI-dC). When carrying out a cold competition assay, the required amount of the cold competitor was added to the reaction mixture along with the labeled oligonucleotide. After 20 min at room temperature, the complexes were separated at 4 C on a 4% polyacrylamide gel containing 1% glycerol and 0.5X TBE.

Calculation of the Dissociation Constant

To determine the K_d of ARDBD, we first calculated the active protein concentration. This was determined by an oligonucleotide competition assay in an EMSA. The ARDBD

concentration was raised 50- to 100-fold above the concentration required to generate 50% occupancy of the probe or the K_d. At this stage, the amount of cold competitor was gradually raised. As the competitor oligonucleotide is raised, it begins to compete with the bound ^{32}P-labeled oligonucleotide for ARDBD and the unbound radiolabeled DNA is observed by EMSA. When 50% of the labeled oligonucleotide is competed to the unbound form, the oligonucleotide competitor has exceeded the amount of active protein (ARDBD) by two-fold. The ARDBD active protein concentration was then calculated to be equivalent to one-half of the molar concentration of the oligonucleotide or ~$4X10^{-7}$ M. The active protein concentration was independently calculated with consensus ARE, PSA AREIII and PSCA-high oligonucleotides and similar results were obtained.

Having calculated the active protein concentration, ARDBD dose response reactions at low concentrations of ARDBD were carried out in EMSAs over consensus ARE, PSA AREIII and PSCA-high oligonucleotides. The gels were scanned by a phosphorimager to calculate the intensity of the bound and unbound complexes and the amount of active protein required for 50% complex formation was determined. This value was equivalent to the K_d.

Generation of Stable Cell Lines

GFP-expressing stable cell lines were generated in LNCaP cells. pEGFP-promoterless was generated from pEGFP-N1 (Clontech) by removing the CMV promoter (AseI-Eco47III). pEGFP-N1 contains a neomycin-resistance cassette (neo^r), which allows stably transfected eukaryotic cells to be selected using G418. PSCA-6.0 GFP clone was

constructed by cloning the 6 kb PSCA promoter as a HindIII/BglII fragment into pEGFP-promoterless clone. pEGFP-promoterless and PSCA-6.0 GFP clones were transfected into LNCaP cells using Tfx-50 reagent (Promega) and stable clones were selected over a 3 week period using 500 μg/ml of G418. To avoid a bias for an integration site, G418-resistant positive populations were employed for the analyses without separating the high expressing populations from the low expressing ones.

Flow Cytometry and Fluorescence Microscopy

Flow cytometric and fluorescent microscopic analysis were performed after the stable cell lines were starved in steroid-depleted RPMI media for a week followed by a 48 h induction with 10nM R1881 or ethanol as a negative control. In brief, cells were resuspended in RPMI at ~10^5 cells/ml and analyzed for GFP fluorescence. In each analysis, 10,000 cells were counted. Analysis was performed on a FACScan (Becton Dickinson) using Cellquest software. GFP-fluorescence microscopy on live LNCaP cells 48 h post R1881 treatment was performed using the Leica DM IRBE microscope attached to the Hamamatsu Digital Camera (both instruments were obtained from McBain Instruments, Chatsworth, CA). GFP-fluorescence was captured using Openlab V3.0 software (Improvision, England).

LEGENDS TO FIGURES

Figure 1. Activity of the PSCA promoter in cell lines

The 6-kb PSCA promoter, PSCA-6.0, was analyzed by transient transfection into various cell lines in the presence or absence of 10 nM R1881. For each cell line tested, the data are represented as a percentage of the CMV-luc activity. The PSCA promoter is active in human prostate (LNCaP, LAPC4 and LAPC9) and bladder (HT1376) cell lines but is relatively inactive in FLAG-tagged AR containing cervical carcinoma cells (fAR-HeLa). The promoter is also active in primary prostate epithelial cell culture (PrEC) but not in primary prostate stromal cell culture (PrSC). The promoter is androgen-inducible in LNCaP and LAPC4 cells. PSCA expression has been observed in LAPC4, LAPC9, PrEC and HT1376 cells while it is absent in fAR-HeLa and PrSC cells.

Figure 2. PSCA promoter is androgen-responsive in a genomic context

The androgen responsiveness of the PSCA promoter was assessed in the human prostate cancer cell line, LNCaP. Stable LNCaP cell lines expressing the GFP reporter were generated using either the PSCA 6-kb promoter (PSCA 6 kb+GFP) or a promoterless construct (Promoterless+GFP) as a negative control. These lines were grown in steroid-depleted medium for one week and androgen (10 nM R1881) was added for 48 h. The GFP expression was assessed by FACS (fluorescence activated cell sorting; *left figure in every panel*) and by fluorescence microscopy (*right figure in every set)* in the presence (*panels b and d*) and absence (*panels a and c*) of 10 nM R1881. The x-axis on the FACS

graph represents the FL1 channel which measures light in the green range of the spectrum (515-545 nm) and the y-axis represents the FL2 channel which measures the orange-red light (564-606 nm). The PSCA promoter was clearly induced in the presence of androgen as is demonstrated by the increase in the number (39 to 73%) and intensity (~10-fold induction) of cells expressing GFP.

Figure 3. Delineating the PSCA enhancer

A, Schematic of PSCA promoter deletion constructs. Progressive 5' deletions of the PSCA promoter between –6 kb and the TATA box at -0.038 ($PSCA_T$) were linked to the luciferase reporter gene and analyzed in transient transfection assays. The *shaded boxes 1-3* represent exons I-III of the PSCA gene. 5' UTL and 3' UTR refer to the 5' untranslated leader and 3' untranslated regions respectively. The PSA promoter-enhancer construct (PSA 2.4), quadruplicated PSA AREI construct (ARE4) and PSA enhancer core construct (EnhE4) were used as a positive controls (30). ARE4 and EnhE4 were cloned upstream to the E4 TATA box in the $E4_T$ construct. *B*, The PSCA promoter exhibits distinct androgen-dependent and-independent modes of regulation. The PSCA promoter deletion series ($PSCA_T$, PSCA-0.5, PSCA-1.0, PSCA-1.5, PSCA-2.0, PSCA-3.0, PSCA-6.0) was analyzed by transient transfection into LNCaP cells in the presence or absence of 10 nM R1881. The pGL3basic (promoterless vector alone) construct was used as a negative control. PSA2.4, ARE4 and EnhE4 were used as positive controls to assess androgen responsiveness. The results are average +/- the standard deviation of triplicate samples and are expressed in relative light units (RLU). Luciferase values were

normalized to the protein content. The table below the graph indicates the fold activation of a construct in the presence (+R1881) of androgen. Fold activation in the presence of androgen was calculated by dividing the average luciferase value obtained in the presence of androgen by that obtained in the absence of androgen. *C*, The PSCA androgen-responsive enhancer lies within a 300-bp sequence between -2.7 kb and -3.0 kb. The PSCA androgen-responsive element was narrowed down to a 300-bp region by transfection of finer deletions between -2.0 kb and -3.0 kb (PSCA-2.2, PSCA-2.5 and PSCA-2.7). The deletion series was analyzed in the presence or absence of 10 nM synthetic androgen analogue, R1881. The luciferase activity is the average of an experiment performed in triplicate and is represented as relative luciferase units (RLU). The numbers in parentheses represent the fold induction in the presence of R1881.

Figure 4. The 300-bp PSCA enhancer can function autonomously

Constructs bearing the 300-bp enhancer (-2.7-kb to -3.0-kb) linked to the PSCA TATA box ($PSCA_T$+2.7-3) or to the E4 TATA box ($E4_T$+2.7-3) were generated. These were tested in transient transfection assays in *A*, LNCaP cells or *B*, HT1376 cells in the presence or absence of 10 nM R1881. The numbers in parentheses indicate the fold induction in the presence of the androgen analogue, R1881.

Figure 5. The PSCA enhancer binds recombinant ARDBD

In vitro DNase I footprinting of the PSA enhancer region with increasing amounts of recombinant ARDBD was used as a positive control (*lanes 1-4*). The positions of ARE III, IIIA, IV, V and VI are shown. DNase I footprinting of the 300-bp PSCA promoter region with recombinant ARDBD revealed two distinct protected sites (*lanes 6-8*; *lane 5* is a DNA alone control)- a high affinity site and a low affinity site. Similar amounts of active ARDBD (0 {*lanes 1 and 5*}, 14.8 nM {*lanes 2 and 6*}, 44.4 nM {*lanes 3 and 7*} and 133.3 nM {*lanes 4 and 8*}; ARDBD active concentration: $4X10^{-7}$ M) were used for both PSA and PSCA enhancers.

Figure 6. PSCA binding site mutations abrogate ARDBD binding

A, An EMSA demonstrating the ARDBD dose response curve on consensus ARE, consensus ARE mutant (*top panel*), PSA AREIII, PSCA high and PSCA high mutant (*bottom panel*) oligonucleotides is shown. See *Table II* for a description of the PSCA ARE mutations. The ARDBD complex (bound) and the free probe (unbound) are marked with arrows. These dose curves were used to calculate the K_d of ARDBD on various ARE sequences (*see Materials and Methods and Table I*). The molar active concentrations of ARDBD used are as follows- *Top panel:*- 0 (*lanes 1 and 6*), 1.6 nM (*lanes 2 and 7*), 4.9 nM (*lanes 3 and 8*), 14.8 nM (*lanes 4 and 9*) and 44.4 nM (*lanes 5 and 10*). *Bottom panel:*- 0 (*lanes 1, 6 and 11*), 14.8 nM (*lanes 2, 7 and 12*), 44.4 nM (*lanes 3, 8 and 13*), 133.3 nM (*lanes 4, 9 and 14*) and 400 nM (*lanes 5, 10 and 15*). *B*, DNaseI footprinting analysis was carried out with the PSCA binding sites and their mutants in presence of recombinant ARDBD. Mutation of either the high affinity binding site (high mut; *lanes*

6-10 in the left panels) or the low affinity binding site (low mut; *lanes 6-10 in the right panels*) abolished ARDBD binding when compared to the unmutated (WT) control (*lanes 1-5 in both left and right panels*). ARDBD active concentrations used are as follows: 0 (*lanes 1 and 6*), 20 nM (*lanes 2 and 7*), 40 nM (*lanes 3 and 8*), 80 nM (*lanes 4 and 9*) and 160 nM (*lanes 5 and 10*).

Figure 7. PSCA AREI responds to androgen *in vivo*

The contribution of PSCA ARDBD binding sites to androgen responsiveness was demonstrated by analyzing the binding site mutations in the context of PSCA-6.0 (PSCA-6.0 AREImut, PSCA-6.0 low-mut; see *Materials and Methods* and *Table II* for mutant details) in transient transfection assays in the presence and absence of R1881. The mutations were tested in AR-responsive prostate cancer cell lines- *A,* LNCaP cells and *B,* LAPC4 cells. *C,* The mutations were also tested in the context of the sufficieny clones ($PSCA_T$+2.7-3 AREImut and $PSCA_T$+2.7-3 low-mut). Relative luciferase activity (RLU) normalized to total protein amount is presented. The values in brackets indicate the fold enhancement in luciferase activity in the presence of R1881.

Figure 8. PSCA AREI is a bonafide androgen response element

PSCA AREI oligonucleotide sequence and the mutated version were quadruplicated ($E4_T$+PSCA ARE4 and $E4_T$+PSCA ARE4mut) and cloned next to a heterologous E4 TATA box. The multimerized clones were analyzed in a transient transfection assay in

LNCaP cells with or without 10nM R1881. pGL3basic (vector alone), $E4_T$, $E4_T$+2.7-3 (300-bp PSCA enhancer cloned next to the $E4_T$) and PSA ARE4 (quadruplicated PSA AREI sequence cloned next to the $E4_T$) were used as controls. The data are presented normalized to the total protein content and the numbers in parentheses indicate the fold induction achieved in the presence of R1881.

Figure 9. The 300-bp PSCA enhancer consists of multiple components which are necessary for androgen-responsiveness

The 300-bp PSCA enhancer was characterized further by generating additional 5' deletions within the enhancer sequence (PSCA-2.8 and PSCA-2.9). These were analyzed by transient transfection into LNCaP cells in the presence and absence of 10 nM R1881. The data are presented as relative luciferase units (RLU) normalized to protein content and the numbers indicate the fold androgen responsiveness.

Figure 10. Sequence comparison of the PSCA enhancer

The 300-bp human PSCA enhancer sequence (hPSCA Enhancer) was aligned to that of the mouse PSCA sequence (mPSCA Enhancer). The bases in *bold* represent the identical bases between the two sequences. The position of AREI and the low affinity binding site (low affinity) in the human enhancer sequence is *underlined* with *arrows*. The –2.8 kb and –2.9 kb positions on the human PSCA enhancer are shown. The *bold line* represents the region of high homology between the two sequences. The box below shows the

sequence comparisons between the human PSCA ARDBD binding sites and the putative mouse sequences.

TABLE I	
Androgen response element	**ARDBD K_d (nM)**
Consensus ARE	9.6±1 nM
PSA AREIII	46.3±2 nM
PSCA AREI or High affinity site	87.5±5 nM
Values from literature:	
PB ARE1 (35)	45±6 nM
PB ARE2 (35)	23±5 nM
C3 (1) ARE (35)	5±1 nM
PSA AREI (35)	26±4 nM
SC ARE1.2 (59)	251 nM
TAT HRE II (64)	152 nM
Slp HRE3 (64)	460 nM
Slp HRE2 (59)	166 nM
C3 IVS (64)	43 nM

Table I. K_d values of androgen response elements.

The dissociation constants of consensus ARE, PSA AREIII and PSCA AREI are compared to some of the known androgen response elements. The dissociation constants were determined in triplicate sets of experiments in an EMSA (see Materials and Methods) and an average of those values ± standard deviations is presented.

TABLE II	
Consensus ARE	GGTACAnnnTGTTCT
PSCA low affinity site (antisense)	ccCGCACAagaCGTTTTct
PSCA low-mut	ccCCGGGAagaCGTTTTct
PSCA high affinity site (antisense)	ctGGAACTttcCGTCCTca
PSCA high-mut	ctGCGGGTttcCGTCCTca

Table II. Sequences of PSCA AR binding site mutations

The table shows the consensus ARE sequence with the critical guanosines in *bold*. PSCA high affinity site and PSCA low affinity site are compared to the consensus ARE sequence (AR binding sequence shown in *upper case*). The critical guanosines conserved in these sequences are shown in *bold*. In each half-site of the AR binding sequence, the crucial contacts are between the first lysine of the ARDBD recognition helix (CGSCKVFFKRAAE), which binds to the second guanine GGTACA of the consensus half-site and the arginine, which binds to a conserved G base paired to cytosine GGTACA. We mutated the PSCA AR binding sequences based on this knowledge. Four bases in one half-site of each PSCA AR binding site were mutated (the mutation is *underlined*).

TABLE III			
Consensus ARE	GGTACA	nnn	TGTTCT
Highest Affnity ARE (33)	G/AGTACA/g	tNG/t	TGTTCT
Receptor specific ARE (33)	G/AGT/AACA/G	C/tg/aG/c	TGTTCT
Consensus Class I ARE (62)	RGAACA	ngn	TGTNCT
Consensus Class II ARE (62)	RGGACA	nna	AGCCAA
Human PSCA low affinity binding site (sense)	AAAACG	tct	TGTGCG
Human PSCA AREI (sense)	AGGACG	gaa	AGTTCC
AR specific ARE (59)	KGNTCW	nnn	AGTWCT
Probasin ARE2 (65)	GGTTCT	tgg	AGTACT
SC ARE1.2 (59)	GGCTCT	ttc	AGTTCT
Slp HRE2 (59)	TGGTCA	gcc	AGTTCT
Probasin ARE1 (65)	ATAGCA	tct	TGTTCT
PSA AREIII (31)	AATACA	ata	TGTTGG
PSA ARR (62)	GAGACT	ccc	TGATCC
PSA ARE (62)	AGCACT	tgc	TGTTCT
Slp3 (44)	GAAACA	gcc	TGTTCT

Table III. Comparison of human PSCA AR binding sites to naturally occurring AREs

The human PSCA AR binding sequences are compared on the antisense strands to the high affinity ARE consensus and receptor-specific ARE determined on the basis of the CAAB assay (33). The class I and class II ARE sequences (62) are also shown. The two binding sequences are also compared to a few naturally occurring AREs in prostate-specific genes. The critical guanosines are shown in *bold.*

ACKNOWLEDGEMENTS

We thank Dr. Owen Witte for the mouse genomic clone containing the mouse PSCA regulatory sequences, Drs. Charles Sawyers, Owen Witte and Purnima Dubey for helpful discussions, Dr. Joann Zhang for careful reading of the manuscript and Kim Le for help with the digital artwork.

Abbreviations- [5]The abbreviations used are: AD, androgen dependent; AI, androgen independent; ARDBD, androgen receptor DNA binding domain; ARE, androgen response element; AR, androgen receptor; ARR, androgen responsive region; PSA, prostate specific antigen; CAAB, competitive amplification and binding; EMSA, electrophoretic mobility shift assay; FACS, fluorescence activated cell sorting; GFP, green fluorescent protein; GPI, glycosylphosphatidyl-inositol; GR, glucocorticoid receptor; GRDBD, glucocorticoid receptor DNA binding domain; HRE, hormone response element; K_d, dissociation constant; mPSCA, murine prostate stem cell antigen; PSCA, prostate stem cell antigen; PrEC, prostate epithelial cell; PrSC, prostate stromal cell; PTEN, phosphatase and tensin homologue; RACE, rapid amplification of cDNA ends; Slp, sex-limited protein; SC, secretory component; TRAMP, transgenic adenocarcinoma of the mouse prostate

REFERENCES

1. Isaacs JT 1999 The biology of hormone refractory prostate cancer. Why does it develop? Urol Clin North Am 26:263-73.
2. Abate-Shen C, Shen MM 2000 Molecular genetics of prostate cancer. Genes Dev 14:2410-34.
3. Elo JP, Visakorpi T 2001 Molecular genetics of prostate cancer. Ann Med 33:130-41.
4. Weigel NL, Zhang Y 1998 Ligand-independent activation of steroid hormone receptors. J Mol Med 76:469-79.
5. Craft N, Sawyers CL 1998 Mechanistic concepts in androgen-dependence of prostate cancer. Cancer Metastasis Rev 17:421-7
6. Jenster G 1999 The role of the androgen receptor in the development and progression of prostate cancer. Semin Oncol 26:407-21.
7. Lamb DJ, Weigel NL, Marcelli M 2001 Androgen receptors and their biology. Vitam Horm 62:199-230
8. Brinkmann AO 2001 Molecular basis of androgen insensitivity. Mol Cell Endocrinol 179:105-9.
9. Avila DM, Zoppi S, McPhaul MJ 2001 The androgen receptor (AR) in syndromes of androgen insensitivity and in prostate cancer. J Steroid Biochem Mol Biol 76:135-42.
10. Cinar B, Koeneman KS, Edlund M, Prins GS, Zhau HE, Chung LW 2001 Androgen receptor mediates the reduced tumor growth, enhanced androgen

responsiveness, and selected target gene transactivation in a human prostate cancer cell line. Cancer Res 61:7310-7.

11. Stamey TA 2001 Preoperative serum prostate-specific antigen (PSA) below 10 microg/l predicts neither the presence of prostate cancer nor the rate of postoperative PSA failure. Clin Chem 47:631-4.

12. Pannek J, Partin AW 1997 Prostate-specific antigen: what's new in 1997. Oncology (Huntingt) 11:1273-8; discussion 1279-82.

13. Lee CT, Oesterling JE 1995 Diagnostic markers of prostate cancer: utility of prostate-specific antigen in diagnosis and staging. Semin Surg Oncol 11:23-35.

14. Reiter RE, Gu Z, Watabe T, et al. 1998 Prostate stem cell antigen: a cell surface marker overexpressed in prostate cancer. Proc Natl Acad Sci U S A 95:1735-40.

15. Gu Z, Thomas G, Yamashiro J, et al. 2000 Prostate stem cell antigen (PSCA) expression increases with high gleason score, advanced stage and bone metastasis in prostate cancer. Oncogene 19:1288-96.

16. Dubey P, Wu H, Reiter RE, Witte ON 2001 Alternative pathways to prostate carcinoma activate prostate stem cell antigen expression. Cancer Res 61:3256-61.

17. Ross S, Spencer SD, Lasky LA, Koeppen H 2001 Selective expression of murine prostate stem cell antigen in fetal and adult tissues and the transgenic adenocarcinoma of the mouse prostate model of prostate carcinogenesis. Am J Pathol 158:809-16.

18. Amara N, Palapattu GS, Schrage M, et al. 2001 Prostate stem cell antigen is overexpressed in human transitional cell carcinoma. Cancer Res 61:4660-5.

19. Argani P, Rosty C, Reiter RE, et al. 2001 Discovery of new markers of cancer through serial analysis of gene expression: prostate stem cell antigen is overexpressed in pancreatic adenocarcinoma. Cancer Res 61:4320-4.

20. Beissert S, He HT, Hueber AO, et al. 1998 Impaired cutaneous immune responses in Thy-1-deficient mice. J Immunol 161:5296-302.

21. Killeen N 1997 T-cell regulation: Thy-1 - hiding in full view. Curr Biol 7:R774-7.

22. Saffran DC, Raitano AB, Hubert RS, Witte ON, Reiter RE, Jakobovits A 2001 Anti-PSCA mAbs inhibit tumor growth and metastasis formation and prolong the survival of mice bearing human prostate cancer xenografts. Proc Natl Acad Sci U S A 98:2658-63.

23. Watabe T, Lin M, Ide H, et al. 2002 Growth, regeneration, and tumorigenesis of the prostate activates the PSCA promoter. Proc Natl Acad Sci U S A 99:401-6.

24. Klein KA, Reiter RE, Redula J, et al. 1997 Progression of metastatic human prostate cancer to androgen independence in immunodeficient SCID mice. Nat Med 3:402-8.

25. Horoszewicz JS, Leong SS, Kawinski E, et al. 1983 LNCaP model of human prostatic carcinoma. Cancer Res 43:1809-18.

26. Rasheed S, Gardner MB, Rongey RW, Nelson-Rees WA, Arnstein P 1977 Human bladder carcinoma: characterization of two new tumor cell lines and search for tumor viruses. J Natl Cancer Inst 58:881-90.

27. Huang W, Shostak Y, Tarr P, Sawyers C, Carey M 1999 Cooperative assembly of androgen receptor into a nucleoprotein complex that regulates the prostate-specific antigen enhancer. J Biol Chem 274:25756-68.

28. Cordingley MG, Riegel AT, Hager GL 1987 Steroid-dependent interaction of transcription factors with the inducible promoter of mouse mammary tumor virus in vivo. Cell 48:261-70.

29. Archer TK, Lefebvre P, Wolford RG, Hager GL 1992 Transcription factor loading on the MMTV promoter: a bimodal mechanism for promoter activation. Science 255:1573-6.

30. Wu L, Matherly J, Smallwood A, et al. 2001 Chimeric PSA enhancers exhibit augmented activity in prostate cancer gene therapy vectors. Gene Ther 8:1416-26.

31. Cleutjens KB, van der Korput HA, van Eekelen CC, van Rooij HC, Faber PW, Trapman J 1997 An androgen response element in a far upstream enhancer region is essential for high, androgen-regulated activity of the prostate- specific antigen promoter. Mol Endocrinol 11:148-61.

32. Roche PJ, Hoare SA, Parker MG 1992 A consensus DNA-binding site for the androgen receptor. Mol Endocrinol 6:2229-35.

33. Nelson CC, Hendy SC, Shukin RJ, et al. 1999 Determinants of DNA sequence specificity of the androgen, progesterone, and glucocorticoid receptors: evidence for differential steroid receptor response elements. Mol Endocrinol 13:2090-107.

34. Massaad C, Garlatti M, Wilson EM, Cadepond F, Barouki R 2000 A natural sequence consisting of overlapping glucocorticoid-responsive elements mediates glucocorticoid, but not androgen, regulation of gene expression. Biochem J 350 Pt 1:123-9.

35. Claessens F, Verrijdt G, Schoenmakers E, et al. 2001 Selective DNA binding by the androgen receptor as a mechanism for hormone-specific gene regulation. J Steroid Biochem Mol Biol 76:23-30.

36. Craft N, Shostak Y, Carey M, Sawyers CL 1999 A mechanism for hormone-independent prostate cancer through modulation of androgen receptor signaling by the HER-2/neu tyrosine kinase. Nat Med 5:280-5.

37. Ray DW, Suen CS, Brass A, Soden J, White A 1999 Structure/function of the human glucocorticoid receptor: tyrosine 735 is important for transactivation. Mol Endocrinol 13:1855-63.

38. Mitchell SH, Murtha PE, Zhang S, Zhu W, Young CY 2000 An androgen response element mediates LNCaP cell dependent androgen induction of the hK2 gene. Mol Cell Endocrinol 168:89-99.

39. Yu DC, Sakamoto GT, Henderson DR 1999 Identification of the transcriptional regulatory sequences of human kallikrein 2 and their use in the construction of calydon virus 764, an attenuated replication competent adenovirus for prostate cancer therapy. Cancer Res 59:1498-504.

40. Xie X, Zhao X, Liu Y, et al. 2001 Robust prostate-specific expression for targeted gene therapy based on the human kallikrein 2 promoter. Hum Gene Ther 12:549-61.

41. Schuur ER, Henderson GA, Kmetec LA, Miller JD, Lamparski HG, Henderson DR 1996 Prostate-specific antigen expression is regulated by an upstream enhancer. J Biol Chem 271:7043-51.

42. Pang S, Dannull J, Kaboo R, et al. 1997 Identification of a positive regulatory element responsible for tissue- specific expression of prostate-specific antigen. Cancer Res 57:495-9.

43. Farmer G, Connolly ES, Jr., Mocco J, Freedman LP 2001 Molecular analysis of the prostate-specific antigen upstream gene enhancer. Prostate 46:76-85.

44. Adler AJ, Scheller A, Robins DM 1993 The stringency and magnitude of androgen-specific gene activation are combinatorial functions of receptor and nonreceptor binding site sequences. Mol Cell Biol 13:6326-35.

45. Adler AJ, Danielsen M, Robins DM 1992 Androgen-specific gene activation via a consensus glucocorticoid response element is determined by interaction with nonreceptor factors. Proc Natl Acad Sci U S A 89:11660-3.

46. Kasper S, Rennie PS, Bruchovsky N, et al. 1994 Cooperative binding of androgen receptors to two DNA sequences is required for androgen induction of the probasin gene. J Biol Chem 269:31763-9.

47. Devos A, Claessens F, Alen P, et al. 1997 Identification of a functional androgen-response element in the exon 1- coding sequence of the cystatin-related protein gene crp2. Mol Endocrinol 11:1033-43.

48. Claessens F, Celis L, De Vos P, et al. 1993 Intronic androgen response elements of prostatic binding protein genes. Biochem Biophys Res Commun 191:688-94.

49. Celis L, Claessens F, Peeters B, Heyns W, Verhoeven G, Rombauts W 1993 Proteins interacting with an androgen-responsive unit in the C3(1) gene intron. Mol Cell Endocrinol 94:165-72.

50. Oettgen P, Finger E, Sun Z, et al. 2000 PDEF, a novel prostate epithelium-specific ets transcription factor, interacts with the androgen receptor and activates prostate-specific antigen gene expression. J Biol Chem 275:1216-25.

51. Ning YM, Robins DM 1999 AML3/CBFalpha1 is required for androgen-specific activation of the enhancer of the mouse sex-limited protein (Slp) gene. J Biol Chem 274:30624-30.

52. Perez-Stable CM, Pozas A, Roos BA 2000 A role for GATA transcription factors in the androgen regulation of the prostate-specific antigen gene enhancer. Mol Cell Endocrinol 167:43-53.

53. Scheller A, Hughes E, Golden KL, Robins DM 1998 Multiple receptor domains interact to permit, or restrict, androgen- specific gene activation. J Biol Chem 273:24216-22.

54. Luisi BF, Xu WX, Otwinowski Z, Freedman LP, Yamamoto KR, Sigler PB 1991 Crystallographic analysis of the interaction of the glucocorticoid receptor with DNA. Nature 352:497-505.

55. Gewirth DT, Sigler PB 1995 The basis for half-site specificity explored through a non-cognate steroid receptor-DNA complex. Nat Struct Biol 2:386-94.

56. Zhou Z, Corden JL, Brown TR 1997 Identification and characterization of a novel androgen response element composed of a direct repeat. J Biol Chem 272:8227-35.

57. Saatcioglu F, Lopez G, West BL, et al. 1997 Mutations in the conserved C-terminal sequence in thyroid hormone receptor dissociate hormone-dependent activation from interference with AP-1 activity. Mol Cell Biol 17:4687-95.

58. Brinkmann AO, Blok LJ, de Ruiter PE, et al. 1999 Mechanisms of androgen receptor activation and function. J Steroid Biochem Mol Biol 69:307-13.

59. Verrijdt G, Schoenmakers E, Haelens A, et al. 2000 Change of specificity mutations in androgen-selective enhancers. Evidence for a role of differential DNA binding by the androgen receptor. J Biol Chem 275:12298-305.

60. Schoenmakers E, Verrijdt G, Peeters B, Verhoeven G, Rombauts W, Claessens F 2000 Differences in DNA binding characteristics of the androgen and glucocorticoid receptors can determine hormone-specific responses. J Biol Chem 275:12290-7.

61. Nordeen SK, Suh BJ, Kuhnel B, Hutchison CD 1990 Structural determinants of a glucocorticoid receptor recognition element. Mol Endocrinol 4:1866-73.

62. Reid KJ, Hendy SC, Saito J, Sorensen P, Nelson CC 2001 Two classes of androgen receptor elements mediate cooperativity through allosteric interactions. J Biol Chem 276:2943-52.

63. Craft N, Chhor C, Tran C, et al. 1999 Evidence for clonal outgrowth of androgen-independent prostate cancer cells from androgen-dependent tumors through a two-step process. Cancer Res 59:5030-6.

64. Rundlett SE, Miesfeld RL 1995 Quantitative differences in androgen and glucocorticoid receptor DNA binding properties contribute to receptor-selective transcriptional regulation. Mol Cell Endocrinol 109:1-10.

65. Rennie PS, Bruchovsky N, Leco KJ, et al. 1993 Characterization of two cis-acting DNA elements involved in the androgen regulation of the probasin gene. Mol Endocrinol 7:23-36.

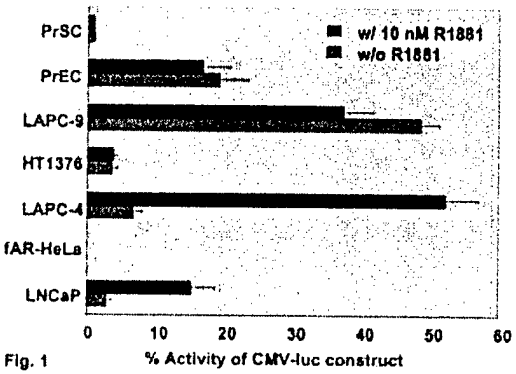
PrSC
PrEC
LAPC-9
HT1376
LAPC-4
fAR-HeLa
LNCaP
w/ 10 nM R1881
w/o R1881
0
10
20
30
40
50
60
% Activity of CMV-luc construct

Fig. 1

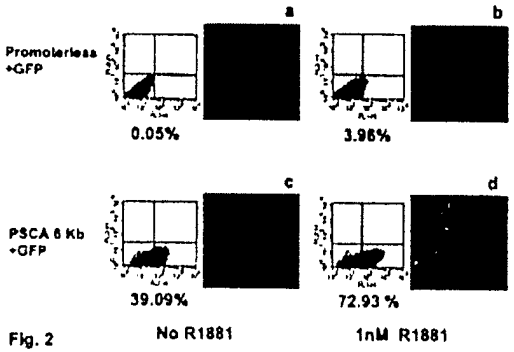
a
b
Promoterless
+GFP
0.05%
3.96%
c
d
PSCA 6 Kb
+GFP
39.09%
72.93 %
No R1881
1nM R1881

Fig. 2

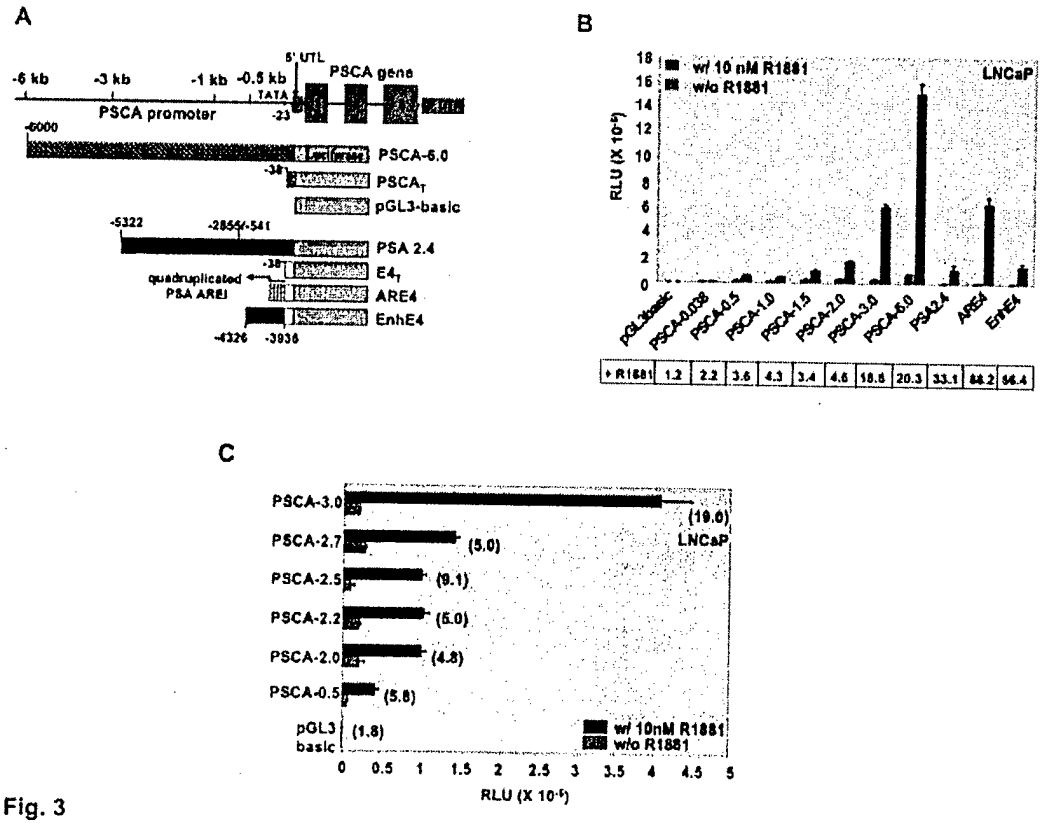
A
5' UTL
-6 kb
-3 kb
-1 kb
-0.5 kb
PSCA gene
TATA
PSCA promoter
-23
-6000
PSCA-6.0
PSCA$_T$
pGL3-basic
-5322
-2856/-541
PSA 2.4
E4$_T$
quadruplicated PSA ARE
ARE4
EnhE4
-4326
-3936
B
w/ 10 nM R1881
w/o R1881
LNCaP
RLU (X 10^{-5})
pGL3basic
PSCA-0.038
PSCA-0.5
PSCA-1.0
PSCA-1.5
PSCA-2.0
PSCA-3.0
PSCA-6.0
PSA2.4
ARE4
EnhE4
+ R1881
1.2
2.2
3.6
4.3
3.4
4.6
18.8
20.3
33.1
88.2
56.4
C
PSCA-3.0
(19.0)
PSCA-2.7
(5.0)
LNCaP
PSCA-2.5
(9.1)
PSCA-2.2
(5.0)
PSCA-2.0
(4.8)
PSCA-0.5
(5.8)
pGL3 basic
(1.8)
w/ 10nM R1881
w/o R1881
RLU (X 10^{-5})

Fig. 3

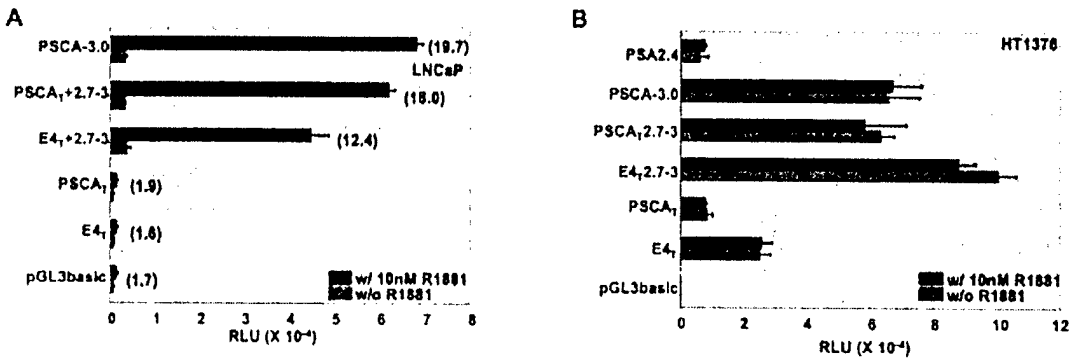
A
PSCA-3.0
(19.7)
LNCaP
PSCA1+2.7-3
(18.0)
E41+2.7-3
(12.4)
PSCA1
(1.9)
E41
(1.6)
pGL3basic
(1.7)
w/ 10nM R1881
w/o R1881
0 1 2 3 4 5 6 7 8
RLU (X 10-4)
B
HT1376
PSA2.4
PSCA-3.0
PSCA12.7-3
E412.7-3
PSCA1
E41
pGL3basic
w/ 10nM R1881
w/o R1881
0 2 4 6 8 10 12
RLU (X 10-4)

Fig. 4

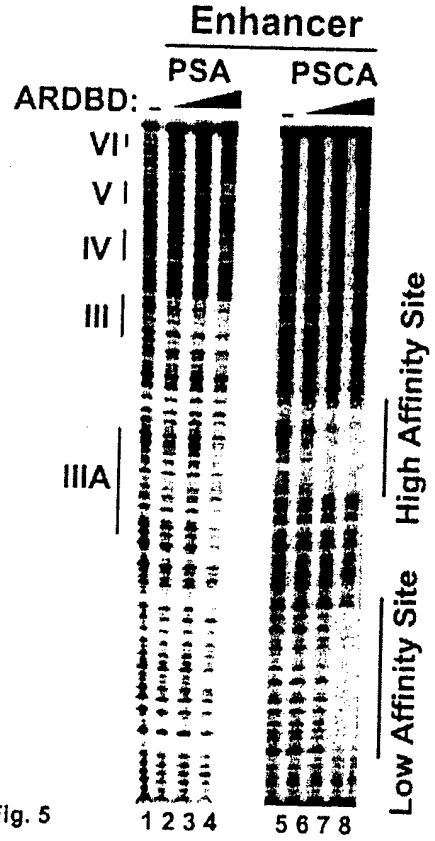
Enhancer
PSA
PSCA
ARDBD:
VI'
V
IV
III
IIIA
High Affinity Site
Low Affinity Site
1 2 3 4
5 6 7 8

Fig. 5

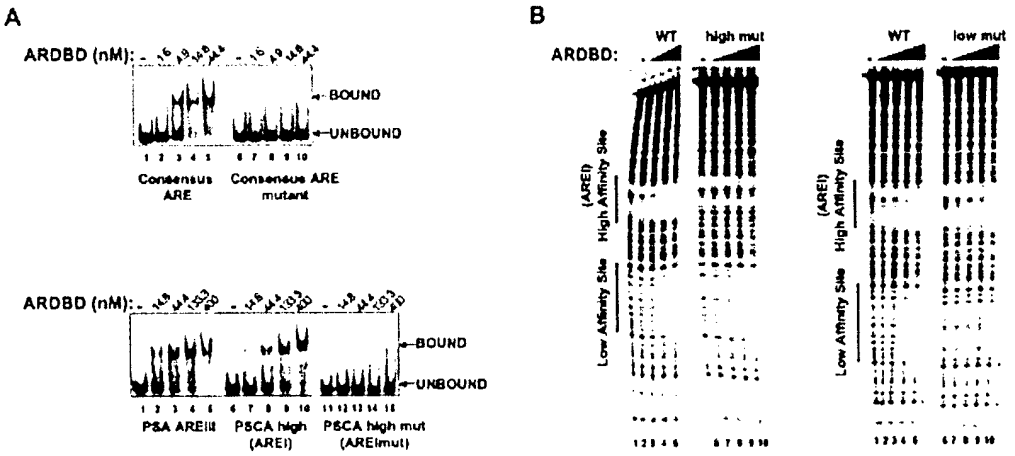
A
ARDBD (nM):
BOUND
UNBOUND
Consensus ARE
Consensus ARE mutant
ARDBD (nM):
BOUND
UNBOUND
P&A AREIII
PSCA high (AREI)
PSCA high mut (AREImut)
B
ARDBD:
WT
high mut
WT
low mut
(AREI)
High Affinity Site
Low Affinity Site

Fig. 6

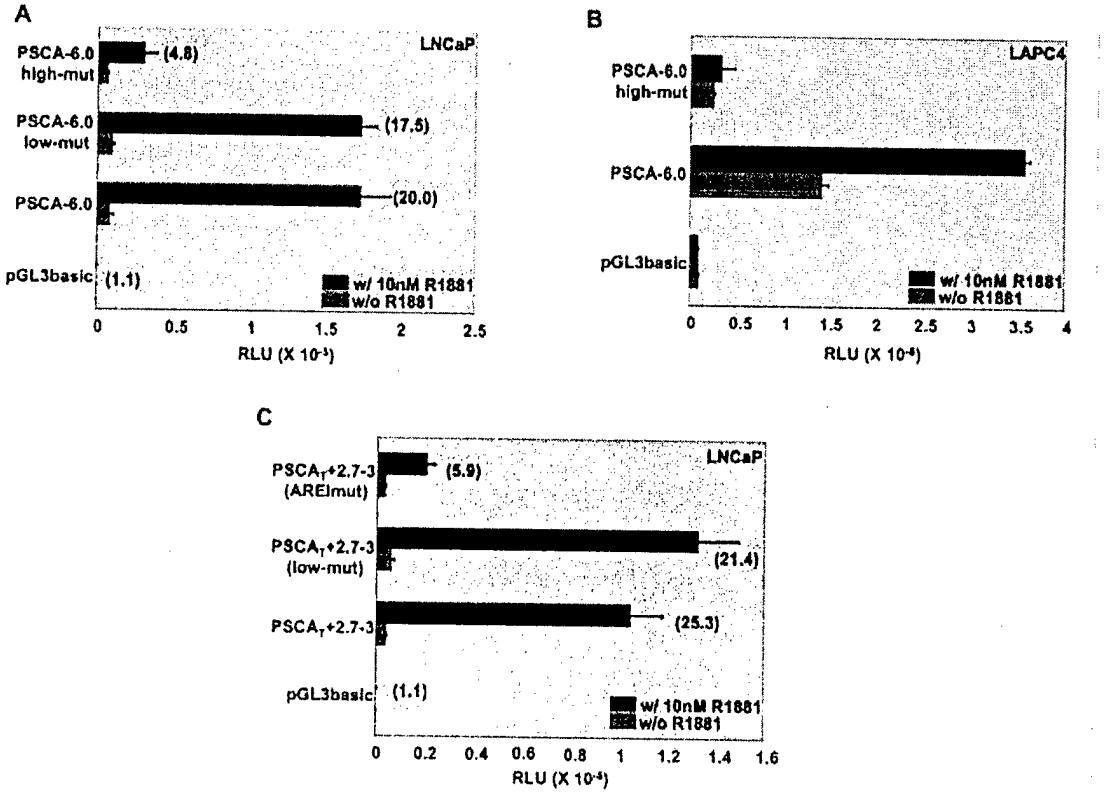
A
LNCaP
PSCA-6.0 high-mut
(4.8)
PSCA-6.0 low-mut
(17.5)
PSCA-6.0
(20.0)
pGL3basic
(1.1)
w/ 10nM R1881
w/o R1881
0
0.5
1
1.5
2
2.5
RLU (X 10-3)
B
LAPC4
PSCA-6.0 high-mut
PSCA-6.0
pGL3basic
w/ 10nM R1881
w/o R1881
0
0.5
1
1.5
2
2.5
3
3.5
4
RLU (X 10-4)
C
LNCaP
PSCAT+2.7-3 (AREmut)
(5.9)
PSCAT+2.7-3 (low-mut)
(21.4)
PSCAT+2.7-3
(25.3)
pGL3basic
(1.1)
w/ 10nM R1881
w/o R1881
0
0.2
0.4
0.6
0.8
1
1.2
1.4
1.6
RLU (X 10-4)

Fig. 7

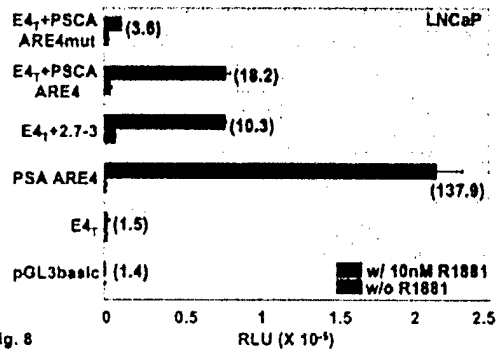
E4T+PSCA ARE4mut
(3.6)
LNCaP
E4T+PSCA ARE4
(18.2)
E4T+2.7-3
(10.3)
PSA ARE4
(137.9)
E4T
(1.5)
pGL3basic
(1.4)
w/ 10nM R1881
w/o R1881
0
0.5
1
1.5
2
2.5
RLU (X 10-4)

Fig. 8

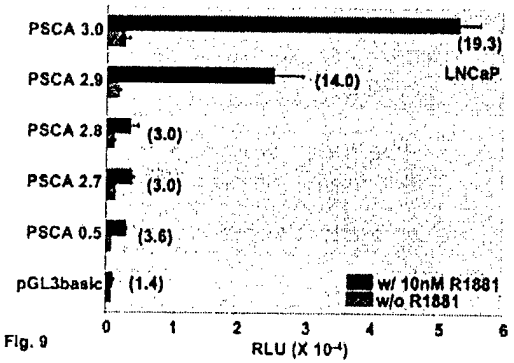
PSCA 3.0
(19.3)
PSCA 2.9
(14.0)
LNCaP
PSCA 2.8
(3.0)
PSCA 2.7
(3.0)
PSCA 0.5
(3.6)
pGL3basic
(1.4)
w/ 10nM R1881
w/o R1881
0
1
2
3
4
5
6
RLU (X 10-4)

Fig. 9

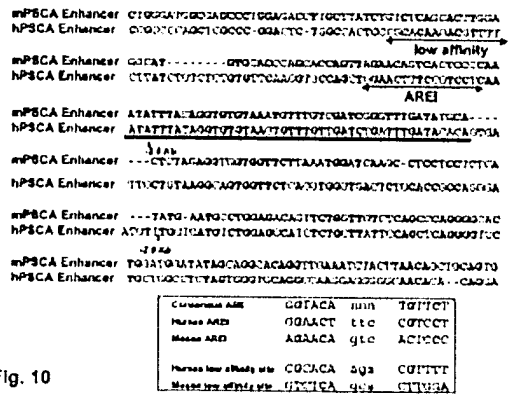

Consensus ARE	GGTACA	nnn	TGTTCT
Human ARE1	GGAACT	ttc	CGTCCT
Mouse ARE1	AGAACA	gtc	ACTCCC
Human low affinity site	CGCACA	agg	CGTTTT
Mouse low affinity site	GTCTCA	gcg	CTTTGA

Fig. 10

Insulin-like Growth Factor Binding Protein-3 Mediates Tumor Necrosis Factor-α-induced Apoptosis: Role of Bcl-2 Phosphorylation[1]

Roopmathy Rajah, Kuk-Wha Lee, and Pinchas Cohen[2]

Department of Pediatrics, Mattel Children's Hospital at UCLA, Los Angeles, California 90095

Abstract

The insulin-like growth factor (IGF)-independent effects of insulin-like growth factor binding protein-3 (IGFBP-3) to effect cellular apoptosis have now been described in various cellular systems. IGFBP-3 mediates transforming growth factor-β-induced apoptosis. Other growth-inhibitory and apoptosis-inducing agents such as tumor necrosis factor-α (TNF-α) and the tumor suppressor gene *p53* also induce IGFBP-3. In this report, we demonstrate the role of IGFBP-3 as a mediator of apoptosis induced by TNF-α and elucidate the process involved in its signaling mechanism. Treatment of PC-3 cells with TNF-α resulted in the induction of IGFBP-3 expression in a dose- and time-dependent fashion and also induced apoptosis. TNF-α-induced apoptosis was prevented by cotreatment with IGFBP-3 neutralizing antibodies or IGFBP-3-specific antisense thiolated oligonucleotides. Both IGFBP-3 and TNF-α treatment increased the levels of the inactive, serine phosphorylated form of the survival protein Bcl-2. The effect of TNF-α on Bcl-2 serine phosphorylation was blocked by IGFBP-3 antisense oligomers. These findings confirm that IGFBP-3 is essential for TNF-α-induced apoptosis in PC-3 cells and that this IGFBP-3 effect includes the inactivation of Bcl-2 through serine phosphorylation.

Introduction

IGFBP[3]-3 belongs to a family of high-affinity IGFBPs that bind to IGFs and modulate their actions. In addition to regulating the availability of free IGFs and therefore their mitogenic activity (1–4), IGFBPs also play an important role in directly regulating cell growth. These independent cell growth-regulatory effects of IGFBPs have been shown to be either growth inducing (5–7) or growth inhibiting (8–17) in prostate cancer cells, breast cancer cells, and fibroblasts. This negative growth regulation by IGFBP-3 has been proposed to involve a separate cellular signaling pathway (15–17). In support of its role as a negative regulator of cell growth and proliferation, *IGFBP-3* gene expression has also been shown to be induced by other growth-inhibitory (and apoptosis-inducing) agents such as TGF-β1 (18–20), retinoic acid (19, 21, 22), TNF-α (21–23), and the tumor suppressor gene *p53* (24).

We demonstrated a novel p53-independent apoptosis induction by IGFBP-3 in the prostate cancer cell line PC-3 (17). Using a mouse fibroblast cell line from an IGF receptor knock out mouse, we confirmed that IGFBP-3 induces apoptosis in an IGF-/IGF-receptor-independent mechanism. Furthermore, we demonstrated that IGFBP-3 mediates the apoptosis induced by TGF-β. In the present study, we demonstrate the role of IGFBP-3 as a mediator of the apoptosis induced by TNF-α and describe a process involved in its signal mechanism through the inactivation of the cell survival protein Bcl-2, implicated previously in the action of TNF-α (25).

Results

Induction IGFBP-3 in PC-3 Cells by TNF-α. At a concentration of 10 ng/ml after 72 h of treatment, TNF-α induced IGFBP-3 levels in PC-3 cells. The increase in IGFBP-3 levels was observed both at the mRNA level as well as the protein level. To determine the level of IGFBP-3 mRNA expression under control (SFM) and TNF-α treatment conditions, total RNA samples from PC3 cells were analyzed by RT-PCR. The levels of the 440-bp IGFBP-3 double-stranded DNA and 157-bp L7 double-stranded DNA RT-PCR products were quantified using densitometry. As seen in Fig. 1*A*, the RT-PCR product derived from IGFBP-3 mRNA in SFM-treated and TNF-α-treated PC-3 cells appears as a single distinct 440-bp band. Three SFM (*Lanes 1–3*)-treated and three TNF-α-treated samples (*Lanes 5–7*) are shown with respect to the molecular weight markers in *Lane 4* (1-kb DNA ladder). Densitometric analysis of these bands was normalized to that of L7 RNA for each sample and then plotted in a graph (Fig. 1*B*). Analysis of the mean of four experiments on 3 SFM- and 3 TNF-α-treated samples are shown. After normalization for L7 RNA, the TNF-α treatment condition demonstrated a 20-fold increase in IGFBP-3 mRNA relative to the SFM treatment condition (*, $P < 0.0001$).

We examined the levels of IGFBPs secreted into the PC-3 conditioned medium in the presence or absence of TNF-α.

Received 10/18/01; revised 2/22/02; accepted 2/25/02.
The costs of publication of this article were defrayed in part by the payment of page charges. This article must therefore be hereby marked *advertisement* in accordance with 18 U.S.C. Section 1734 solely to indicate this fact.
[1] Supported in part by NIH Grants 2R01 DK47591, 1RO1 AI40203, 1R01AG20954, and 1UO1CA 84128; a grant from the American Cancer Society; and a grant from Pharmacia GEM (to P. C.); as well as fellowship awards from the Giannini Foundation and from Eli Lilly (to K. L.).
[2] To whom requests for reprints should be addressed, at Division of Endocrinology, Department of Pediatrics, Mattel Children's Hospital at UCLA, 10833 Le Conte Avenue, MDCC 22-315, Los Angeles, CA 90095. Phone: (310) 206-5844; Fax: (301) 206-5843; E-mail: hassy@mednet.ucla.edu.
[3] The abbreviations used are: IGFBP, insulin-like growth factor binding protein; TGF, transforming growth factor; TNF, tumor necrosis factor; RT-PCR, reverse transcription-PCR; SFM, serum-free FK-12 medium; TUNEL, terminal deoxynucleotidyl transferase-mediated dUTP nick end labeling; ODN, oligodeoxynucleotide.

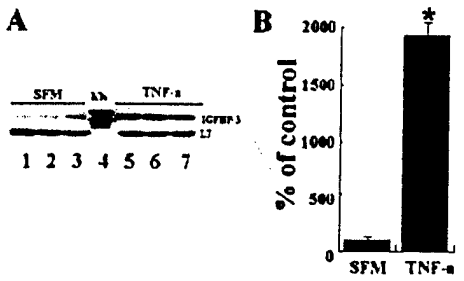

Fig. 1. Induction of IGFBP-3 mRNA by TNF-α. Cells were grown in SFM in the presence or absence of TNF-α (10 ng/ml). Total RNA was isolated from 75-cm^2 flasks of PC-3 cells using the acid guanidinium thiocyanate phenol-chloroform extraction method. *A*, RT-PCR. IGFBP-3 mRNA levels were analyzed by ^{33}P-labeled RT-PCR and compared with L7 mRNA levels. One μg of total RNA was reverse-transcribed, and L7 and IGFBP-3 cDNAs were amplified using 20 and 30 cycles, respectively. Primers amplified 157- and 400-bp fragments, respectively. Three SFM-treated samples (*Lanes 1–3*) and three TNF-α-treated samples (*Lanes 5–7*) are shown in respect to markers (*Lane 4*). *B*, densitometrically analyzed IGFBP-3 mRNA levels normalized for L7 RNA from three SFM-treated and three TNF-α-treated samples are shown. The mean of each is also shown (*, $P < 0.0001$ relative to SFM); *bars*, SE.

Fig. 2*A* is a western ligand blot that shows the expression of IGFBP-2, IGFBP-3, and IGFBP-4 by PC-3 cells. Exposure to 10 ng/ml TNF-α increased the levels of IGFBP-3 protein secreted into conditioned medium at all time points tested between 24 and 96 h. No statistically significant changes in the levels of IGFBP-2, IGFBP-4, or a M_r 19,000 IGFBP-3 fragment were noted (Table 1).

We quantified the levels of IGFBP-3 secreted into the PC-3 conditioned medium in the presence or absence of TNF-α using specific immunoblots. Treatment with TNF-α significantly increased IGFBP-3 secreted into conditioned medium at 48 and 72 h compared with SFM treatment. At 72 h as measured by densitometry, the rise in IGFBP-3 was 10-fold compared with the SFM treatment condition. Fig. 2*B* shows the immunodetection of IGFBP-3 in PC-3 cell conditioned medium in response to a 72-h treatment with SFM (*Lanes 1* and *2*) or increasing concentrations of TNF-α (*Lanes 3–10*). Fig. 2*C* shows the data from densitometric analyses of IGFBP-3 immunoblots from four different experiments demonstrating the time and dose response of IGFBP-3 secretion induced by TNF-α. At 0.1 ng/ml concentration, TNF-α induces a 4-fold increase in IGFBP-3 secretion. Treatment with 1 ng/ml concentration increased IGFBP-3 levels to 1000% of baseline and plateaued at higher concentration.

Effect of IGFBP-3 and TNF-α on PC-3 Cell Growth. Cells in SFM were treated with either IGFBP-3 or TNF-α alone or TNF-α with either IGFBP-3 sense or antisense thiolated IGFBP-3 oligonucleotides for 72 h. Data from 96-well cell-proliferation assay are presented as the percentage of basal (SFM) cell growth in Fig. 3. Treatment with IGFBP-3 (500 ng/ml) and TNF-α (10 ng/ml) resulted in suppression of 40 and 50% of cell growth, respectively (*, $P < 0.001$ relative to SFM). TNF-α treatment in the presence of IGFBP-3 antisense oligomers significantly blocked the TNF-α-induced PC-3 cell growth inhibition (**, $P < 0.001$ relative to TNF-α alone). The oligomers had no significant effect in SFM.

Induction of Apoptosis in PC-3 Cells by IGFBP-3 and TNF-α. We detected IGFBP-3- and TNF-α-induced apoptosis in PC-3 cells using both qualitative (TUNEL) and quantitative (ELISA) methods. To localize the apoptotic cells *in situ*, we detected the fragmented DNA in monolayer cell cultures treated with SFM, IGFBP-3, or TNF-α using TUNEL (Fig. 4). The DNA fragments bound to the peroxidase-diaminobenzidine reaction product in apoptotic cells were visualized as dark brown cells. Cells in SFM displayed an insignificant number of apoptotic cells (Fig. 4, *top panel*); however, both IGFBP-3 and TNF-α treatment revealed numerous apoptotic cells (Fig. 4, *middle* and *bottom panel*, respectively). This method was not used to quantify the number of apoptotic cells in the SFM and IGFBP-3 treatment conditions because many of the apoptotic cells, after 72 h of incubation, were found floating in the conditioned medium. Loss of cells from the culture plate attributable to the increased apoptotic index was seen as empty spaces in IGFBP-3 treatment condition. However, the control condition showed confluent cells.

Demonstration of the Role of IGFBP-3 in TNF-α-induced Apoptosis in PC-3 Cells. Because TNF-α is known to induce apoptosis in some cells and also to up-regulate IGFBP-3 expression in similar cells, we examined its relation to IGFBP-3-induced apoptosis. At a concentration of 10 ng/ml, TNF-α significantly increased the number of apoptotic PC-3 cells. We recorded the changes in the apoptotic index after treatment of PC-3 cells with IGFBP-3 and TNF-α using photometric ELISA (Fig. 5). Quantitative analyses by ELISA revealed a basal level of apoptosis in SFM, the suppression of this basal level by addition of 10% fetal bovine serum, and a significant level of apoptosis induced by IGFBP-3 and TNF-α, which was similar to the effect of Ca^{2+} ionophore. This induction of apoptosis by TNF-α was 95% as potent as the apoptosis induced by the Ca^{2+} ionophore. In addition, when compared with SFM, both IGFBP-3 and TNF-α demonstrated a significant increase in the apoptotic index ($P < 0.001$).

To test whether IGFBP-3 is required for TNF-α-induced apoptosis, we treated PC-3 cells with TNF-α concomitantly with IGFBP-3 sense or antisense oligonucleotides, as well as IGFBP-3 neutralizing antibodies or control IgG (Fig. 6). IGFBP-3 and TNF-α-induced apoptosis as shown above. The IGFBP-3 antisense oligomer effectively blocked the TNF-α induced apoptosis in PC-3 cells (**, $P < 0.001$ compared with TNF-α treatment), suggesting that TNF-α induces apoptosis by increasing IGFBP-3 expression. The sense IGFBP-3 oligomer had no significant effect on TNF-α-induced apoptosis. Also noticeable is the effect of IGFBP-3 antisense on the basal level of apoptosis in PC-3 cells. Similarly, IGFBP-3 neutralizing antibody (but not control IgG) inhibited TNF-α-induced apoptosis.

Role of Bcl-2 in IGFBP-3-induced Apoptosis in PC-3 Cells. The effect of IGFBP-3 on Bcl-2 protein levels was examined in PC-3 cells by the use of specific immunoblot analyses. IGFBP-3 induced enhancement of apoptosis, and suppression of cell viability were associated with the appearance of a M_r 32,000 Bcl-2 band in addition to the M_r 29,000 Bcl-2 protein seen in SFM conditions. Fig. 7*A* (*top panel*) shows the M_r 29,000 band representing unphosphorylated Bcl-2 seen in

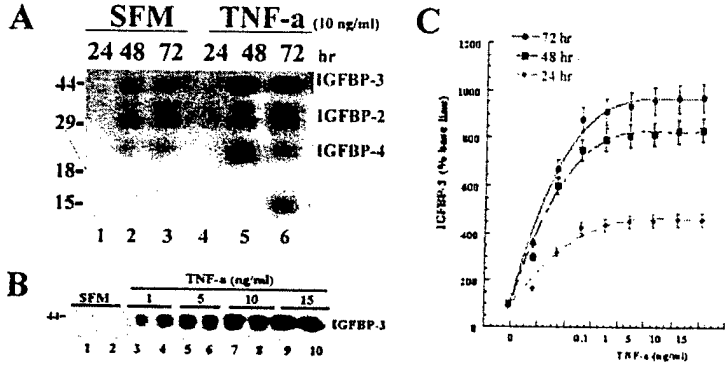

Fig. 2. Regulation of IGFBPs in PC-3 conditioned medium by TNF-α. IGFBP-3 protein levels were measured using conditioned medium from PC-3 cells incubated for 24, 48, and 72 h with SFM plus and minus 10 ng/ml TNF-α. *A*, samples of 50 ml were separated by nonreducing 12.5% SDS-PAGE and electroblotted onto nitrocellulose. The IGFBPs were visualized by incubating the membrane with 10^6 cpm each of ^{125}I-labeled IGF-I and IGF-II, followed by autoradiography. *B*, PC-3 cells were cultured in the medium from SFM and TNF-α treatment, and cells (1×10^5) were separated on a 12.5% SDS-PAGE overnight at constant voltage, electroblotted onto nitrocellulose. IGFBP-3 on the nitrocellulose membrane was detected using affinity-purified IGFBP-3 specific antibodies and ECL detection system (Pierce, Rockford, IL). *C*, densitometric measurements of immunoblots were performed, and protein levels were estimated by comparing the absorbance of each specific protein band from the SFM *versus* TNF-α treatment cell conditioned media. Values are mean for triplicate samples; *bars*, SE.

Table 1 Effects of TNF-α on IGFBPs in PC-3 cell conditioned medium[a]

IGFBP	TNF 48 h	*P vs.* SFM	TNF 72 h	*P vs.* SFM
IGFBP-3	820 ± 60	<0.001	980 ± 80	<0.001
IGFBP-2	130 ± 35	NS[b]	105 ± 40	NS
IGFBP-4	125 ± 45	NS	102 ± 35	NS
M_r 19,000 IGFBP-3 fragment	Not detected	NS	155 ± 85	NS

[a] All values are expressed as a percentage of the levels in SFM. $P < 0.05$ was considered significant.
[b] NS, not significant.

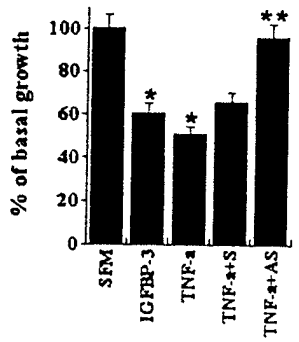

Fig. 3. Detection and quantification of PC-3 cell growth. Cells in SFM were treated with IGFBP-3 and TNF-α alone or TNF-α with either IGFBP-3 sense or antisense thiolated IGFBP-3 oligonucleotides for 72 h. Samples were collected and assayed for cell growth using a 96-well cell proliferation assay. Results are presented as the percentage of basal growth as observed in the SFM treatment conditions. Values are the means for five experiments, each with eight samples (*, $P < 0.001$ relative to SFM; **, $P < 0.001$ relative to TNF-α alone); *bars*, SE.

the presence of SFM (*Lanes 1–3*), IGFBP-3 (*Lanes 4–6*), and TNF-α (*Lanes 7–9*) treatment conditions. However, the M_r 32,000 band representing the phosphorylated form of Bcl-2 appeared only in IGFBP-3 (*Lanes 4–6*) and TNF-α (*Lanes 7–9*) treatment conditions. To determine the type of phosphorylation Bcl-2 underwent with treatment with IGFBP-3 and TNF-α, the immunoprecipitated samples were immunoblotted individually with antibodies to tyrosine, serine, and threonine residues. With appropriate positive controls, immunoblotting for both tyrosine and threonine gave negative results. However, the M_r 32,000 Bcl-2 band was revealed when the Bcl-2 immunoprecipitated samples were immunoblotted with anti-phosphoserine antibodies, indicating that the Bcl-2 was phosphorylated at a serine residue (Fig. 7*A, bottom panel*). Densitometric analyses of the M_r 32,000 serine phosphorylated Bcl-2 band demonstrated a significant increase (*, $P < 0.001$) in IGFBP-3 and TNF-α treatment conditions (Fig. 7*B*). Assessment of Bcl-2 mRNA levels by RT-PCR disclosed no significant changes in the expression of Bcl-2 in response to TNF-α or IGFBP-3 (data not shown).

Role of IGFBP-3 in TNF-α-induced Serine Phosphorylation of Bcl-2 in PC-3 Cells. To demonstrate a role for IGFBP-3 in the phosphorylation of a serine residue of Bcl-2 by TNF-α, PC-3 cells in SFM were treated for 72 h with either TNF-α (10 ng/ml) alone or with 20 μg/ml of either IGFBP-3 sense oligomers or IGFBP-3 antisense oligomers (Fig. 8). Cell lysates immunoprecipitated with Bcl-2 antibodies and probed with Bcl-2-specific antibodies revealed the M_r 29,000 Bcl-2 form in all four conditions (Fig. 8*A, Lanes 1–4*). Along with this M_r 29,000 band, a M_r 32,000 band was also visible in TNF-α and TNF-α with IGFBP-3 sense oligomer treatment conditions (*Lanes 2–4*). However, the M_r 32,000 band in TNF-α treatment in the presence of IGFBP-3 antisense oligomer was very faint (Fig. 8*A, Lane 4*). When these samples were probed with anti-phosphoserine, antibodies revealed only the M_r 32,000 band representing the phosphorylated form of Bcl-2 (Fig. 8*B, Lanes 2–4*), and this M_r 32,000 band was again nearly absent in *Lane 4*, which is the sample treated with TNF-α in presence of IGFBP-3 antisense oligomers. Fig. 8*C* shows the densitometric analyses of the phosphorylated Bcl-2 bands from Fig. 8*B* and similar experiments performed in triplicates, demonstrating the significant blockage in TNF-α-induced serine phosphorylated form of Bcl-2 in the presence of IGFBP-3 antisense oligomers (*, $P < 0.001$).

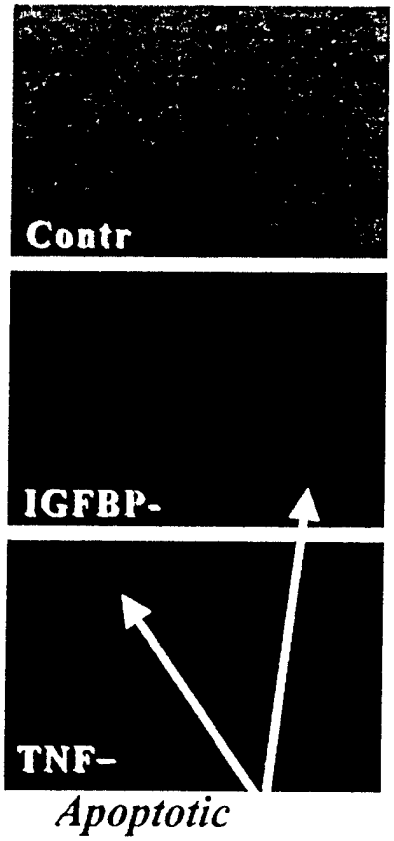

Fig. 4. In situ localization of TNF-α-induced apoptosis prostate cancer cell line, PC-3. PC-3 cells were cultured in serum-free condition with either TNF-α (10 ng/ml) or IGFBP-3 (500 ng/ml) for a duration of 72 h. The cytoplasmic DNA fragments were detected *in situ* in the monolayer cultures using the Apoptag detection system (Oncor, Gaithersburg, MD).

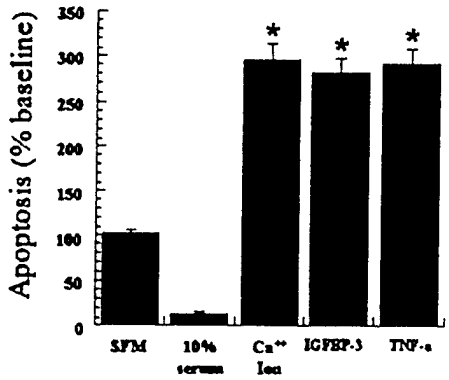

Fig. 5. Detection and quantification of TNF-α-induced apoptosis in PC-3 cells. *A*, a comparative quantitative analysis of the apoptotic index induced by the SFM, 10% serum containing medium, Ca^{2+} ionophore, IGFBP-3 (500 ng/ml), and TNF-α (10 ng/ml) using photometric ELISA. Results are presented as the percentage of baseline apoptosis. Values are the average for triplicate experiments (*, $P < 0.001$ relative to SFM); *bars*, SE.

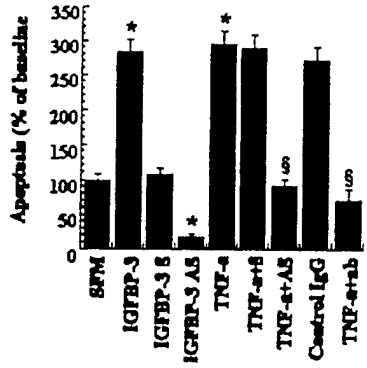

Fig. 6. TNF-α-induced apoptosis is mediated through IGFBP-3 in PC-3 cells. Cells in SFM were treated with TNF-α alone or with either IGFBP-3 sense or antisense thiolated oligonucleotides or IGFBP-3 neutralizing antibodies or control IgG for 72 h. Samples were collected for photometric ELISA and assayed to determine the role of IGFBP-3 in TNF-α-induced apoptosis. Results are presented as the percentage of baseline apoptosis. Values are the means for five experiments, each with triplicate samples (*, $P < 0.001$ relative to SFM; §, $P < 0.001$ relative to TNF-α alone); *bars*, SE.

Discussion

IGFs have been shown to protect cells from undergoing apoptosis through an IGF receptor-mediated cell survival pathway (26–30). The proapoptotic p53 protein, commonly abnormal in malignant states, has been shown to repress IGF receptor expression (29). Both decreases in the number of IGF receptors causing massive apoptosis and overexpression of IGF receptors protecting cells from apoptosis have been demonstrated *in vivo* (30). All of the above-mentioned studies indicate the important role of IGFs and IGF receptors in preventing cells from undergoing apoptosis through a cell survival pathway. In this report, we discuss the ability of IGFBP-3 to directly induce apoptosis as well as mediate the apoptosis-inducing effect of cytokines such as TNF-α.

Initially, the negative cell growth regulatory action of IGFBP-3 was thought to occur through the ability of IGFBP-3 to bind IGFs with high affinity and thereby sequester IGFs from binding to their receptors. Later, IGFBP-3 was shown to also act directly, through an IGF-independent pathway, to mediate cell growth arrest (12, 13). Recently, we and others have demonstrated that IGFBP-3 induces apoptosis in cancer cells in an IGF-independent pathway and that this effect of IGFBP-3 may be mediated by interaction with a putative IGFBP-3 receptor (15–17). We further demonstrated that IGFBP-3 is required for the apoptosis-inducing effects of TGF-β on PC-3 cells (17), and others have shown that IGFBP-3 is required for the growth-inhibitory effects of TGF-β on breast cancer cells (15). IGFBP-3 not only induces and mediates apoptosis in cancer cells but also accentuates apoptosis induced by ceramide in an IGF-independent manner (31).

The growth-inhibitory and apoptotic effects of TNF-α have been demonstrated in several cell lines (25, 32, 33). Although TNF-α has no consistent effects on the levels of IGF-I, IGF-II, or IGF-I receptor expression, it has been shown to stimulate IGFBP activity and particularly IGFBP-3 in human fibroblasts (21), Sertoli cells (22), articular chondrocytes (23), and human salivary cell line (34). In rheumatoid arthritis patients, the synovial fluid concentration of IGFBP-3 has been shown to

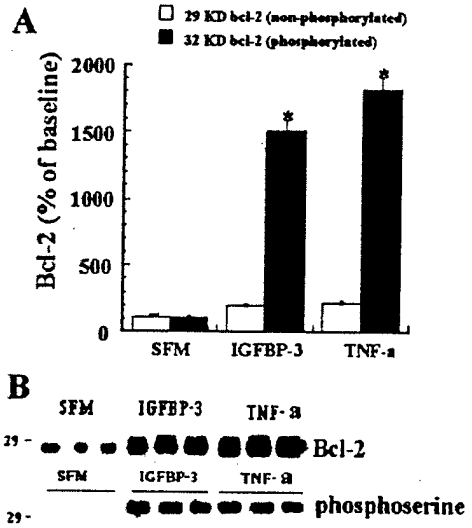

Fig. 7. TNF-α-induced apoptosis is mediated through IGFBP-3: role of Bcl-2 phosphorylation. PC-3 cells in SFM were treated with either IGFBP-3 (500 ng/ml) or TNF-α (10 ng/ml). *A*, cell lysates were immunoprecipitated with Bcl-2 antibodies. The immunoprecipitated samples were separated on a 10% SDS-PAGE over night at a constant voltage, electroblotted onto nitrocellulose, and probed with either Bcl-2-specific antibodies or with anti-phosphoserine antibodies. *B*, densitometric analyses of the phosphorylated band from each condition demonstrated the significant increase in the phosphorylated band (*, $P < 0.001$).

be positively correlated with synovial fluid levels of TNF-α (35). In this report, we demonstrated that treatment of PC-3 prostate cancer cells with TNF-α resulted in a decreased cell number secondary to the induction of apoptosis. We also showed that TNF-α induces IGFBP-3 expression (at both the mRNA and protein levels) in these cells and showed that IGFBP-3 was necessary for the TNF-α-induced apoptosis to occur. Rozen *et al.* (36) have similarly shown that IGFBP-3 is necessary for TNF-α-induced antiproliferative action in breast cancer cells.

PC-3 cells are p53 negative and have the machinery to express low levels of IGFBP-3 under serum-free conditions and undergo apoptosis through a p53-independent pathway (7, 17). The dramatic elevation in IGFBP-3 levels 9 h after TNF-α treatment followed by apoptosis that was observed 12–18 h after treatment suggests that the TNF-α-induced elevation of IGFBP-3 protein in the conditioned medium may be the primary signal that activated apoptosis in this cell line. Blocking TNF-α-induced apoptosis at the IGFBP-3 transcriptional level confirmed the role of IGFBP-3 as the mediator of TNF-α-induced apoptosis in PC-3 cells. Cotreatment with IGFBP-3 antisense (but not sense) thiolated oligonucleotide and TNF-α verified the role of IGFBP-3 in the TNF-α-induced apoptosis. These observations confirm that IGFBP-3 plays a significant role in mediating TNF-α-induced apoptosis.

The family of Bcl-2-related proteins comprises both death-inducing (Bax, Bak, Bcl-xS, Bad, Bid, Bik, and Hrk) and death-inhibiting (Bcl-2, Bcl-xL, Bcl-w, Bfl-1, Mcl-1, and Boo) members, and the mechanisms by which each protein exerts its effects are only partially understood. The ratio of death antagonists to agonists has been proposed to regulate the death-life rheostat within the cell (37). TGF-β1 (38–40), retinoic acid (41), TNF-α (42–44), and p53 (45) are known to induce apoptosis by regulating Bcl-2 expression and altering the Bcl-2:Bax ratio (38–45). TNF-α-induced apoptosis is also readily blocked by Bcl-2 and Bcl-xL overexpression (46). TNF-α independently up-regulated Fas antigen expression on the colorectal carcinoma cell line COLO 201 and induced apoptosis (25). This effect of TNF-α resulted in a decreased Bcl-2:Bax ratio favoring apoptosis (47).

Because the apoptosis-inducing agents p53, TGF-β, retinoic acid, and TNF-α also induce IGFBP-3 expression, we anticipate that IGFBP-3-induced apoptosis may also involve regulation of this death:life ratio. In this study, treatment with TNF-α or IGFBP-3 did not alter the mRNA or protein levels of Bcl-2; however, both these agents increased the levels of the serine-phosphorylated form of inactive Bcl-2, thereby favoring the death pathway, which presumably involves the recently described association of Bcl-2 with Bax and culminates in the formation of the recently described oligomeric Bax/Bak "pores" (48–50), thus releasing cytochrome *c* from mitochondria (51). This is consistent with previous observations indicating that serine phosphorylation of Bcl-2 leads to its inactivation and its inability to form dimers with Bax, and therefore the survival effect of Bcl-2 is lost (52–58). This serine phosphorylation of Bcl-2 has been suggested to occur on serine 70 (52) and to require interaction with raf-1 (53, 54). The apoptotic effects of paclitaxol (55), retinoids (56), and the TNF family member CD95 (55) have also been shown to be mediated by inactivating bcl-2 through serine phosphorylation. Our study is the first to our knowledge to demonstrate that TNF-α and, more interestingly, IGFBP-3, induce serine phosphorylation of Bcl-2 concomitantly with the induction of apoptosis. Furthermore, we have shown here that antisense oligomers that prevent IGFBP-3 expression block the serine phosphorylation of Bcl-2 by TNF-α, and thus we believe that IGFBP-3 is necessary for both TNF-α-induced Bcl-2 inactivation and the ensuing apoptosis.

IGFBP-3-mediated cell death is IGF, p53, and cell cycle independent, making it particularly attractive for application to prostate and other cancer cells that are p53 negative and therefore resistant to induction of apoptosis by irradiation. We present a hypothesis based on the results from this study and other previous reports from this and other groups in the diagrammatic representation shown in Fig. 9. We propose that the independent and interdependent effects of IGFs and IGFBP-3 on the regulation of cell number involve two pathways, which interact at several levels. IGFs mediate survival via the IGF receptor, leading to an increase in Bcl-2 as well as Bcl-xL expression (59–62). TNF-α-induced IGFBP-3 is able to block this pathway by sequestering IGFs away from the IGF receptor and by mediating apoptosis via its own receptors. Thus, IGFBP-3 can mediate cell death by both IGF-dependent and IGF-independent pathways. Moreover, IGFBP-3 can mediate apoptosis induced by several agents, and this involves the inactivation of Bcl-2 via serine phosphorylation. The nature of the serine-threonine kinase, which may be activated to phosphorylate Bcl-2, is unknown, but both TOR and cdc-2 have been proposed to be involved (63,

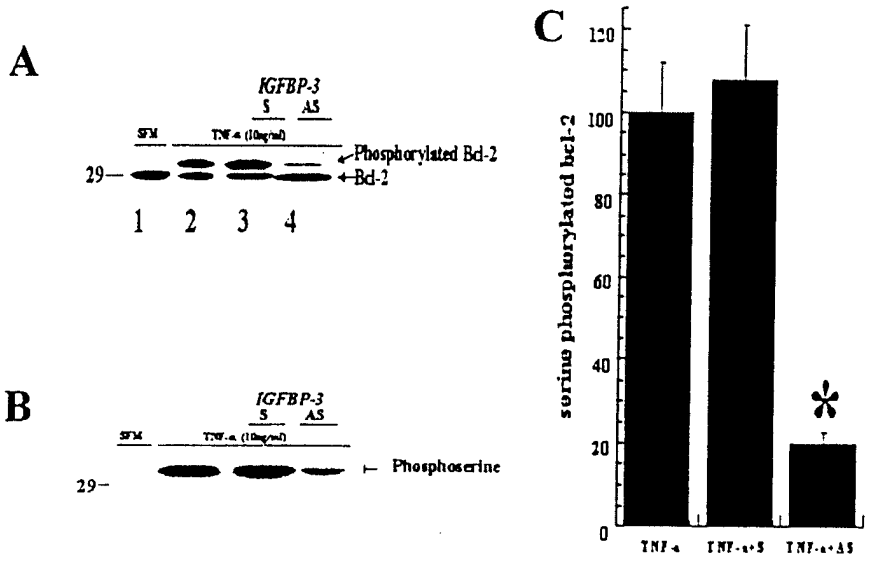

Fig. 8. TNF-α-induced phosphorylation is mediated through IGFBP-3. PC-3 cells in SFM were treated for 72 h with either TNF-α (10 ng/ml) alone or with 20 μg/ml of either IGFBP-3 sense oligomers or IGFBP-3 antisense oligomers. Cell lysates were immunoprecipitated with Bcl-2 antibodies. The immunoprecipitated samples were separated on a 10% SDS-PAGE over night at a constant voltage, electroblotted onto nitrocellulose, and probed with either Bcl-2- specific antibodies (*A*) or with anti-phosphoserine antibodies (*B* and *C*). *C*, densitometric analyses of the phosphorylated band from the IGFBP-3 antisense treatment condition demonstrated a significant decrease in the phosphorylated Bcl-2 bands (*, $P < 0.001$). *Bars*, SE.

64). It is also possible that IGFBP-3 inhibits a phosphatase, which dephosphorylates Bcl-2. Regardless of the exact mechanism, our data propose a new pathway for the apoptotic effects of IGFBP-3.

Materials and Methods

Materials. Tissue culture supplies were purchased from Flow Laboratories (McLean, VA), Corning (Corning, NY), and Hyclone (Logan, UT). Recombinant, glycosylated (Chinese hamster ovary) human IGFBP-3 was the generous gift of Dr. Desmond Mascarenhas (Celtrix, Santa Clara, CA). OLIGOS Etc., Inc. (Guilford, CT) prepared the IGFBP-3 phosphorothioate ODNs used in these experiments (17). The IGFBP-3 antisense ODN was complimentary to the 20 nucleotides that encode the NH_2 terminus of human IGFBP-3 as described previously (17, 18) and had the sequence 5′-CAT GAC GCC TGC AAC CGG GG-3′ (positions 2021–2040). The sequence of the IGFBP-3 sense ODN was 5′-CCC CGG TTG CAG GCG TCA TG-3′. IGFBP-3 neutralizing antibodies were purchased from Diagnostic Systems Laboratories (Webster, TX) and were prepared by affinity purification on an IGFBP-3 column (17, 65). Control IgG (affinity-purified antigoat IgG) was purchased from Vector Laboratories (Burlingame, CA). The apoptosis-inducing Ca^{2+} ionophore Valinomycin was purchased from Sigma Chemical Co. (St. Louis, MO). FITC-conjugated secondary antibodies were purchased from Vector Laboratories. TNF-α was purchased from R&D systems (Abingdon, Oxon, United Kingdom). Bcl-2 antibodies and positive-control peptides were purchased from Santa Cruz Biotechnology, Inc. (Santa Cruz, CA). Anti-phosphoserine antibodies were purchased from Zymed (Camarillo, CA).

PC-3 Cell Culture. The human PC-3 cell line was purchased from American Type Culture Collection (Rockville, MD) and was originally initiated from a grade IV prostatic adenocarcinoma from a 62-year-old male Caucasian. PC-3 cells were grown in 75-cm^2 flasks according to the recommended protocol (FK-12 supplemented with 10% fetal bovine serum and 1% penicillin-streptomycin. For each experiment, cells were dissociated, centrifuged, and resuspended in serum containing FK-12 medium with antibiotics and inoculated at a density of 1×10^5 cells/cm^2 in 24-well or 6-well tissue culture dishes and grown to confluence in a humidified atmosphere of 5% CO_2 at 37°C, before treatment. After a quick wash with SFM, the confluent cells were treated with various concentrations of IGFBP-3, TNF-α, and/or other specified reagents for the specific times indicated. SFM with antibiotics was used as the control treatment.

Cell Growth Assays. For each experimental condition, cells were plated at 1×10^4 cells/cm^2 in 96-well plates. The nonradioactive CellTiter 96 assay (Promega Corp., Madison, WI) was used to measure cell proliferation. Samples were treated in multiples of eight for each condition. This method measures the cellular conversion of the tetrazolium salt, 3-(4,5-dimethylthiazol-2-yl)-5-(3-carboxymethoxy-phenyl)-2-(4-sulfonyl)-2*H*-tetrazolium, into a formazan, which is measured at 490 nm directly in the plate. The absorbance reading is directly proportional to the number of viable cells/well, and means and SDs were determined. Absorbance values were significantly correlated to cell number measurements made with a Coulter counter (data not shown).

RNA Analysis. Total RNA was isolated from 75-cm^2 flasks of ASM cells using the acid guanidinium thiocyanate phenol-chloroform extraction method but modified to include a proteinase K (in 0.5% SDS) digestion of proteins in the initial RNA pellet. One μg of RNA sample was analyzed by quantitative RT-PCR as described previously (28). PCR was performed on a Perkin-Elmer 4800 thermocycler, and all RT-PCR reagents were purchased from Perkin-Elmer/Cetus (Norwalk, CT). After reverse transcription, cDNA was amplified with the following IGFBP-3 primers: sense, 5′-GTG TGT GGA TAA GTA TGG G-3′ and antisense 5′-CTA AGT CAC AAA GTC AGT GG-3′. These primers amplify a 440-bp double-stranded DNA sequence. PCR conditions were 94°C for

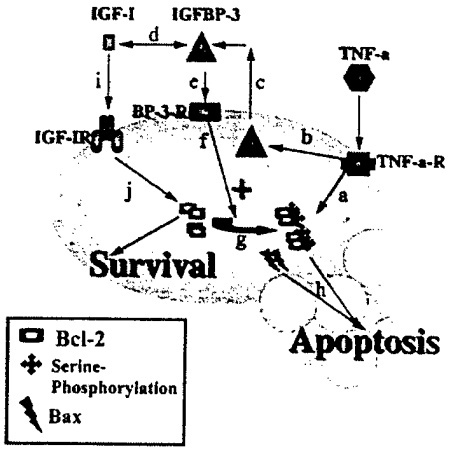

Fig. 9. IGF, IGFBP-3, and cytokine-induced apoptosis: a theoretical model. TNF-α induces apoptosis directly (*a*) by binding to its receptor or by inducing IGFBP-3 (*b–h*). IGFBP-3 induces apoptosis by inducing serine phosphorylation of bcl-2 (*g*) and thereby increasing the inactive bcl-2 form and targeting the bcl-2:bax ratio toward apoptosis induction (*h*). This apoptosis-inducing effect of IGFBP-3 can be blocked when IGFBP-3 binds to IGFs with high affinity (*d*). IGFs mediate survival via the IGF receptor (*i*), leading to an increase in Bcl-2 (*j*) as well as Bcl-xL expression (33, 38, 57–59). TNF-α-induced IGFBP-3 is able to block this pathway by sequestering IGFs away from the IGF receptor (*d*) and by mediating apoptosis via its own receptors (*e*). Thus, IGFBP-3 can mediate cell death by both IGF-dependent and IGF-independent pathways. Moreover, IGFBP-3 can mediate apoptosis induced by several agents, and this involves the inactivation of Bcl-2 via serine phosphorylation.

1 min, 56°C for 45 s, and 72°C for 1 min for 33 cycles. RNA quantity was normalized for L7 RNase with the primers sense, 5′-AAG GGC TCT CAT TTT CCT GGC TG-3′ and antisense, 5′-TCC GTT CCT CCC CAT AAT GTT CC-3′ that was amplified using the same protocol for 20 cycles. These primers amplify a 157-bp double-stranded DNA sequence. The PCR products were electrophoresed on an ethidium bromide-stained 2% agarose gel (Life Technologies, Inc.; Ultra Pure) in TAE buffer. Gels were photographed and analyzed densitometrically on a Bio-Rad 670GS scanning densitometer (Hercules, CA).

TUNEL. *In situ* detection of apoptosis in cultured cells was performed with the use of direct immunoperoxidase detection of biotin-labeled genomic DNA in monolayer cells. In brief, after treatment with different conditions, the monolayer cultures were fixed in 3.7% paraformaldehyde solution for 10 min at room temperature, followed by dehydration in 70% ethanol for 5 min at room temperature. After this step, the endogenous peroxidase was quenched by treatment with 2% hydrogen peroxide in methanol for 5 min. The cells were incubated in the labeling mixture (Biotin dNTP mix, 50× $MgCl_2$, TdT, and labeling buffer) for 60 min at 37°C. The free 3′-OH DNA in the apoptotic cells were visualized using the streptavidin-horseradish peroxidase-DAB detection system. The apoptotic cells appeared as dark brown cells.

Apoptosis ELISA Assay. Photometric cell death detection ELISA (Boehringer Mannheim, Indianapolis, IN) was performed to quantitate the apoptotic index by detecting the histone-associated DNA fragments (mono- and oligonucleosomes) generated by the apoptotic cells. The assay is based on the quantitative sandwich enzyme immunoassay principle using mouse monoclonal antibodies directed against DNA and histones, respectively, for the specific determination of these nucleosomes in the cytoplasmic fraction of cell lysates. In brief, an equal number of cells were plated in 24-well culture plates ($1 \times 10^4/cm^2$) in SFM and grown to confluency for 72 h. At the time of sample collection, the confluent cells were washed with PBS and treated with various concentrations of IGFBP-3, TNF-α, or other required agents for the designated time period. The cells were dissociated gently (PBS with 0.1 M EDTA) and pelleted along with the floating cells (mostly apoptotic cells) collected from the conditioned medium. The cell pellets were used to prepare the cytosol fractions, which contained the smaller fragments of DNA. Equal volumes of these cytosolic fractions were incubated in anti-histone antibody-coated wells (96-well plates), and the histones of the DNA fragments were allowed to bind to the anti-histone antibodies. The peroxidase-labeled mouse monoclonal DNA antibodies were used to localize and detect the bound fragmented DNA using photometric detection with 2,2′-azino-di-(3-ethylbenzathiazoline sulfonate) as the substrate. Ca^{2+} ionophore treatment conditions were used as positive controls. SFM treatment conditions were used as negative controls. Each experimental condition was performed with at least three samples and was repeated at least three times. The reaction products in each 96-well plate were read using a Bio-Rad microplate reader (Model 3550-UV). Averages of the values ± SE from double absorbance measurements of the samples were plotted.

Western Ligand Blots. IGFBP protein levels were assessed using conditioned medium from PC-3 cells incubated for various periods of time with SFM with or without 10 ng/ml TNF-α. Samples of 50 μl were separated by nonreducing 10% SDS-PAGE overnight at constant voltage and electroblotted onto nitrocellulose. The membranes were then sequentially washed with NP40, 1% BSA, and Tween 20, incubated with 10^6 cpm each of ^{125}I-labeled IGF-I and IGF-II for 12 h, dried, and exposed to film for 5 days.

Western Immunoblots for IGFBP-3. IGFBP-3 protein levels using conditioned medium from PC-3 cells incubated for various periods of time with SFM with or without 10 ng/ml TNF-α were assessed. Samples of 50 μl were separated by nonreducing 10% SDS-PAGE overnight at constant voltage and electroblotted onto nitrocellulose. The membranes were then sequentially washed with NP40, 1% BSA, and Tween 20, blocked with 5% nonfat dry milk in Tris-buffered saline, probed with specific IGFBP-3 antibodies, and detected using a peroxidase-linked enhanced chemiluminescence detection system (Pierce, Rockford, IL).

Bcl-2 Immunoprecipitation. Bcl-2 levels were measured in the cell lysates. PC-3 cells treated with either SFM, or IGFBP-3 (500 ng/ml), or TNF-α (10 ng/ml), or TNF-α in the presence of IGFBP-3 sense and antisense oligomers, or TNF-α in presence of control IgG and IGFBP-3 antibodies for 72 h were collected and disrupted in buffer (1× PBS, 1% NP40, 0.5% sodium deoxycholate, and SDS) in the presence of inhibitors. After removing the debris, the cell

lysates were incubated at 4°C with protein G-agarose-conjugated Bcl-2 polyclonal antibodies. The immunoprecipitates were washed, boiled, and stored in aliquots at −20°C until further use.

Bcl-2 and Phosphoserine Western Immunoblots. Bcl-2 immunoprecipitated cell lysates (15 μl equal to 10^6 cells) PC-3 cultures treated with the agents mentioned above for 72 h were used to detect Bcl-2 and phosphorylated Bcl-2 levels. Samples were electrophoresed through 10% nonreducing SDS-PAGE overnight at constant voltage, electroblotted onto nitrocellulose, blocked with 5% nonfat dry milk in Tris-buffered saline, probed with specific Bcl-2 and phosphoserine antibodies, and detected using a peroxidase-linked enhanced chemiluminescence detection system (Pierce).

Densitometric and Statistical Analysis. Densitometric measurement of immunoblots was performed using a Bio-Rad GS-670 Imaging Densitometer (Bio-Rad, Melville, NY). Protein levels were estimated by comparing the absorbance of each specific protein band from control (SFM) conditions to that of the TNF-α treatment conditions. All experiments were repeated at least three times. When applicable, mean ± SE are shown. Student *t* tests were used for statistical analysis.

References

1. Cohen, P., Fielder, P. J., Hasegawa, Y., Frisch, H., Giudice, L. C., and Rosenfeld, R. G. Clinical aspects of insulin-like growth factor binding proteins. Acta. Endocrinol., *124:* 74–85, 1991.

2. Giudice, L. C., Irwin, J. C., Dsupin, B. A., Pannier, E. M., Jin, I. H., Vu, T. H., and Hoffman, A. R. Insulin-like growth factor (IGF). IGF binding protein (IGFBP), and IGF receptor gene expression and IGFBP synthesis in human uterine leiomyomata. Hum. Reprod., *8:* 1796–1806, 1993.

3. Rosenfeld, R. G., Pham, H., Cohen, P., Fielder, P., Gargosky, S. E., Muller, H., Nonoshita, L., and Oh, Y. Insulin-like growth factor binding proteins and their regulation. Acta. Paediatr. Suppl., *399:* 154–158, 1994.

4. Jones, J. I., and Clemmons, D. R. Insulin-like growth factors and their binding proteins: biological actions. Endocr. Rev., *16:* 3–34, 1995.

5. Conover, C. A. Potentiation of insulin-like growth factor (IGF) action by IGF-binding protein-3: studies of underlying mechanism. Endocrinology, *130:* 3191–3199, 1992.

6. Conover, C. A., Clarkson, J. T., and Bale, L. K. Factors regulating insulin-like growth factor-binding protein-3 binding, processing, and potentiation of insulin-like growth factor action. Endocrinology, *137:* 2286–2292, 1996.

7. Angelloz-Nicoud, P., and Binoux, M. Autocrine regulation of cell proliferation by the insulin-like growth factor (IGF) and IGF binding protein-3 protease system in a human prostate carcinoma cell line (PC-3). Endocrinology, *136:* 5485–5492, 1995.

8. Figueroa, J. A., Lee, A. V., Jackson, J. G., and Yee, D. Proliferation of cultured human prostate cancer cells is inhibited by insulin-like growth factor (IGF) binding protein-1: evidence for an IGF-II autocrine growth loop. J. Clin. Endocrinol. Metab., *80:* 3476–3482, 1995.

9. Cohen, P., Peehl, D. M., Graves, H. C., and Rosenfeld, R. G. Biological effects of prostate specific antigen as an insulin-like growth factor binding protein-3 protease. J. Endocrinol., *142:* 407–415, 1994.

10. Perkel, V. S., Mohan, S., Baylink, D. J., and Linkhart, T. A. An inhibitory insulin-like growth factor binding protein (In-IGFBP) from human prostatic cell conditioned medium reveals N-terminal sequence identity with bone derived In-IGFBP. J. Clin. Endocrinol. Metab., *71:* 533–535, 1990.

11. Cohen, P., Lamson, G., Okajima, T., and Rosenfeld, R. G. Transfection of the human *insulin-like growth factor binding protein-3* gene into Balb/c fibroblasts inhibits cellular growth. Mol. Endocrinol., *7:* 380–386, 1993.

12. Velez-Yanguas, M. C., Kalebic, T., Maggi, M., Kappel, C. C., Letterio, J., Uskokovic, M., and Helman, L. J. 1α,25-Dihydroxy-16-ene-23-yne-26,27-hexafluorocholecalciferol (Ro24-5531) modulation of insulin-like growth factor-binding protein-3 and induction of differentiation and growth arrest in a human osteosarcoma cell line. J. Clin. Endocrinol. Metab., *81:* 93–99, 1996.

13. Moerman, E. J., Thweatt, R., Moerman, A. M., Jones, R. A., and Goldstein, S. Insulin-like growth factor binding protein-3 is overexpressed in senescent and quiescent human fibroblasts. Exp. Gerontol., *28:* 361–370, 1993.

14. Goldstein, S., Moerman, E. J., Jones, R. A., and Baxter, R. C. Insulin-like growth factor binding protein 3 accumulates to high levels in culture medium of senescent and quiescent human fibroblasts. Proc. Natl. Acad. Sci. USA, *88:* 9680–9684, 1991.

15. Oh, Y., Muller, H. L., Lamson, G., and Rosenfeld, R. G. Insulin-like growth factor (IGF)-independent action of IGF-binding protein-3 in Hs578T human breast cancer cells. Cell surface binding and growth inhibition. J. Biol. Chem., *268:* 14964–14971, 1993.

16. Valentinis, B., Bhala, A., DeAngelis, T., Baserga, R., and Cohen, P. The human insulin-like growth factor (IGF) binding protein-3 inhibits the growth of fibroblasts with a targeted disruption of the IGF-I receptor gene. Mol. Endocrinol., *9:* 361–367, 1995.

17. Rajah, R., Valentinis, B., and Cohen, P. Insulin-like growth factor (IGF)-binding protein-3 induces apoptosis and mediates the effects of transforming growth factor-β1 on programmed cell death through a p53- and IGF-independent mechanism. J. Biol. Chem., *272:* 12181–12188, 1997.

18. Oh, Y., Muller, H. L., Ng, L., and Rosenfeld, R. G. Transforming growth factor-β-induced cell growth inhibition in human breast cancer cells is mediated through insulin-like growth factor-binding protein-3 action. J. Biol. Chem., *270:* 13589–13592, 1995.

19. Gucev, Z. S., Oh, Y., Kelley, K. M., and Rosenfeld, R. G. Insulin-like growth factor binding protein 3 mediates retinoic acid- and transforming growth factor β2-induced growth inhibition in human breast cancer cells. Cancer Res., *56:* 1545–1550, 1996.

20. Martin, J. L., Ballesteros, M., and Baxter, R. C. Insulin-like growth factor-I (IGF-I) and transforming growth factor-β1 release IGF-binding protein-3 from human fibroblasts by different mechanisms. Endocrinology, *131:* 1703–1710, 1992.

21. Yateman, M. E., Claffey, D. C., Cwyfan Hughes, S. C., Frost, V. J., Wass, J. A., and Holly, J. M. Cytokines modulate the sensitivity of human fibroblasts to stimulation with insulin-like growth factor-I (IGF-I) by altering endogenous IGF-binding protein production. J. Endocrinol., *137:* 151–159, 1993.

22. Besset, V., Le Magueresse-Battistoni, B., Collette, J., and Benahmed, M. Tumor necrosis factor α stimulates insulin-like growth factor binding protein 3 expression in cultured porcine Sertoli cells. Endocrinology, *137:* 296–303, 1996.

23. Olney, R. C., Wilson, D. M., Mohtai, M., Fielder, P. J., and Smith, R. L. Interleukin-1 and tumor necrosis factor-α increase insulin-like growth factor-binding protein-3 (IGFBP-3) production and IGFBP-3 protease activity in human articular chondrocytes. J. Endocrinol., *146:* 279–286, 1995.

24. Buckbinder, L., Talbott, R., Velasco-Miguel, S., Takenaka, I., Faha, B., Seizinger, B. R., and Kley, N. Induction of the growth inhibitor IGF-binding protein 3 by p53. Nature (Lond.)., *377:* 646–649, 1995.

25. Koshiji, M., Adachi, Y., Sogo, S., Taketani, S., Oyaizu, N., Than, S., Inaba, M., Phawa, S., Hioki, K., and Ikehara, S. Apoptosis of colorectal adenocarcinoma (COLO 201) by tumour necrosis factor-α (TNF-α) and/or interferon-γ (IFN-γ), resulting from down-modulation of Bcl-2 expression. Clin. Exp. Immunol., *111:* 211–218, 1998.

26. Singleton, J. R., Dixit, V. M., and Feldman, E. L. Type I insulin-like growth factor receptor activation regulates apoptotic proteins. J. Biol. Chem., *271:* 31791–31794, 1996.

27. Dews, M., Nishimoto, I., and Baserga, R. IGF-I receptor protection from apoptosis in cells lacking the IRS proteins. Receptor Signal Transduct., *7:* 231–240, 1997.

28. Esposito, D. L., Blakesley, V. A., Koval, A. P., Scrimgeour, A. G., and LeRoith, D. Tyrosine residues in the C-terminal domain of the insulin-like growth factor-I receptor mediate mitogenic and tumorigenic signals. Endocrinology, *138:* 2979–2988, 1997.

29. Webster, N. J., Resnik, J. L., Reichart, D. B., Strauss, B., Haas, M., and Seely, B. L. Repression of the insulin receptor promoter by the tumor

suppressor gene product p53: a possible mechanism for receptor overexpression in breast cancer. Cancer Res., *56:* 2781–2788, 1996.

30. Resnicoff, M., Abraham, D., Yutanawiboonchai, W., Rotman, H. L., Kajstura, J., Rubin, R., Zoltick, P., and Baserga, R. The insulin-like growth factor I receptor protects tumor cells from apoptosis *in vivo*. Cancer Res. *55:* 2463–2469, 1995.

31. Gill, Z. P., Perks, C. M., Newcomb, P. V., and Holly, J. M. Insulin-like growth factor-binding protein (IGFBP-3) predisposes breast cancer cells to programmed cell death in a non-IGF-dependent manner. J. Biol. Chem., *272:* 25602–25607, 1997.

32. Slowik, M. R., Min, W., Ardito, T., Karsan, A., Kashgarian, M., and Pober, J. S. Evidence that tumor necrosis factor triggers apoptosis in human endothelial cells by interleukin-1-converting enzyme-like protease- dependent and -independent pathways. Lab. Investig., *77:* 257–267, 1997.

33. Monney, L., Olivier, R., Otter, I., Jansen, B., Poirier, G. G., and Borner, C. Role of an acidic compartment in tumor-necrosis-factor-α-induced production of ceramide, activation of caspase-3 and apoptosis. Eur. J. Biochem., *251:* 295–303, 1998.

34. Katz, J., Weiss, H., Goldman, B., Kanety, H., Stannard, B., LeRoith, D., and Shemer, J. Cytokines and growth factors modulate cell growth and insulin-like growth factor binding protein secretion by the human salivary cell line (HSG). J. Cell. Physiol., *165:* 223–227, 1995.

35. Neidel, J., Blum, W. F., Schaeffer, H. J., Schulze, M., Schonau, E., Lindschau, J., and Foll, J. Elevated levels of insulin-like growth factor (IGF) binding protein-3 in rheumatoid arthritis synovial fluid inhibit stimulation by IGF-I of articular chondrocyte proteoglycan synthesis. Rheumatol. Int., *17:* 29–37, 1997.

36. Rozen, F., Zhang, J., and Pollak, M. Antiproliferative action of tumor necrosis factor-α on MCF-7 breast cancer cells is associated with increased insulin-like growth factor binding protein-3 accumulation. Int. J. Oncol., *13:* 865–869, 1998.

37. Kroemer, G. The proto-oncogene *Bcl-2* and its role in regulating apoptosis. Nat. Med., *3:* 614–620, 1997.

38. Tsukada, T., Eguchi, K., Migita, K., Kawabe, Y., Kawakami, A., Matsuoka, N., Takashima, H., Mizokami, A., and Nagataki, S. Transforming growth factor β1 induces apoptotic cell death in cultured human umbilical vein endothelial cells with down-regulated expression of bcl-2. Biochem. Biophys. Res. Commun., *210:* 1076–1082, 1995.

39. Rorke, E. A., and Jacobberger, J. W. Transforming growth factor-β1 (TGF-β1) enhances apoptosis in human papillomavirus type 16-immortalized human ectocervical epithelial cells. Exp. Cell Res., *216:* 65–72, 1995.

40. Selvakumaran, M., Lin, H. K., Miyashita, T., Wang, H. G., Krajewski, S., Reed, J. C., Hoffman, B., and Liebermann, D. Immediate early up-regulation of bax expression by p53 but not TGF β1: a paradigm for distinct apoptotic pathways. Oncogene, *9:* 1791–1798, 1994.

41. Aebi, S., Kroning, R., Cenni, B., Sharma, A., Fink, D., Los, G., Weisman, R., Howell, S. B., and Christen, R. D. all-*trans* retinoic acid enhances cisplatin-induced apoptosis in human ovarian adenocarcinoma and in squamous head and neck cancer cells. Clin. Cancer Res., *3:* 2033–2038, 1997.

42. Tewari, M., Beidler, D. R., and Dixit, V. M. CrmA-inhibitable cleavage of the 70-kDa protein component of the U1 small nuclear ribonucleoprotein during Fas- and tumor necrosis factor-induced apoptosis. J. Biol. Chem., *270:* 18738–18741, 1995.

43. Tewari, M., and Dixit, V. M. Fas- and tumor necrosis factor-induced apoptosis is inhibited by the poxvirus crmA gene product. J. Biol. Chem., *270:* 3255–3260, 1995.

44. Klefstrom, J., Vastrik, I., Saksela, E., Valle, J., Eilers, M., and Alitalo, K. c-Myc induces cellular susceptibility to the cytotoxic action of TNF-α. EMBO J., *13:* 5442–5450, 1994.

45. Koseki, T., Yamato, K., Krajewski, S., Reed, J. C., Tsujimoto, Y., and Nishihara, T. Activin A-induced apoptosis is suppressed by BCL-2. FEBS Lett., *376:* 247–250, 1995.

46. Vanhaesebroeck, B., Reed, J. C., De Valck, D., Grooten, J., Miyashita, T., Tanaka, S., Beyaert, R., Van Roy, F., and Fiers, W. Effect of *bcl-2* proto-oncogene expression on cellular sensitivity to tumor necrosis factor-mediated cytotoxicity. Oncogene, *8:* 1075–1081, 1993.

47. Burow, M. E., Weldon, C. B., Tang, Y., Navar, G. L., Krajewski, S., Reed, J. C., Hammond, T. G., Clejan, S., and Beckman, B. S. Differences in susceptibility to tumor necrosis factor α-induced apoptosis among MCF-7 breast cancer cell variants. Cancer Res., *58:* 4940–4946, 1998.

48. Perez, D., and White, E. TNF-α signals apoptosis through a bid-dependent conformational change in Bax that is inhibited by E1B 19K. Mol. Cell, *6:* 53–63, 2000.

49. Wei, M. C., Lindsten, T., Mootha, V. K., Weiler, S., Gross, A., Ashiya, M., Thompson, C. B., and Korsmeyer, S. J. tBID, a membrane-targeted death ligand, oligomerizes BAK to release cytochrome c. Genes Dev., *14:* 2060–2071, 2000.

50. Antonsson, B., Montessuit, S., Lauper, S., Eskes, R., and Martinou, J. C. Bax oligomerization is required for channel-forming activity in liposomes and to trigger cytochrome c release from mitochondria. Biochem. J., *345* (Pt. 2): 271–278, 2000.

51. Sundararajan, R., Cuconati, A., Nelson, D., and White, E. TNF-α induces Bax-Bak interaction and apoptosis which is inhibited by adenovirus E1B 19K. J. Biol. Chem., *24:* 45120–45127, 2001.

52. Haldar, S., Basu, A., and Croce, C. M. Serine-70 is one of the critical sites for drug-induced Bcl2 phosphorylation in cancer cells. Cancer Res., *58:* 1609–1615, 1998.

53. Blagosklonny, M. V., Giannakakou, P., el-Deiry, W. S., Kingston, D. G., Higgs, P. I., Neckers, L., and Fojo, T. Raf-1/bcl-2 phosphorylation: a step from microtubule damage to cell death. Cancer Res., *57:* 130–135, 1997.

54. Blagosklonny, M. V., Schulte, T., Nguyen, P., Trepel, J., and Neckers, L. M. Taxol-induced apoptosis and phosphorylation of Bcl-2 protein involves c- Raf-1 and represents a novel c-Raf-1 signal transduction pathway. Cancer Res., *56:* 1851–1854, 1996.

55. Roth, W., Wagenknecht, B., Grimmel, C., Dichgans, J., and Weller, M. Taxol-mediated augmentation of CD95 ligand-induced apoptosis of human malignant glioma cells: association with bcl-2 phosphorylation but neither activation of p53 nor G2/M cell cycle arrest. Br. J. Cancer, *77:* 404–411, 1998.

56. Hu, Z. B., Minden, M. D., and McCulloch, E. A. Phosphorylation of BCL-2 after exposure of human leukemic cells to retinoic acid. Blood, *92:* 1768–1775, 1998.

57. Haldar, S., Jena, N., and Croce, C. M. Inactivation of Bcl-2 by phosphorylation. Proc. Natl. Acad. Sci. USA, *92:* 4507–4511, 1995.

58. Haldar, S., Chintapalli, J., and Croce, C. M. Taxol induces bcl-2 phosphorylation and death of prostate cancer cells. Cancer Res., *56:* 1253–1255, 1996.

59. Jasty, R., van Golen, C., Lin, H. J., Solomon, G., Heidelberger, K., Polverini, P., Opipari, A., Feldman, E., and Castle, V. P. Bcl-2 and N-myc coexpression increases IGF-IR and features of malignant growth in neuroblastoma cell lines. Neoplasia, *3:* 304–313, 2001.

60. Nakao, Y., Otani, H., Yamamura, T., Hattori, R., Osako, M., and Imamura, H. Insulin-like growth factor 1 prevents neuronal cell death and paraplegia in the rabbit model of spinal cord ischemia. J. Thorac. Cardiovasc. Surg., *122:* 136–143, 2001.

61. Yamamura, T., Otani, H., Nakao, Y., Hattori, R., Osako, M., and Imamura, H. IGF-I differentially regulates Bcl-xL and Bax and confers myocardial protection in the rat heart. Am. J. Physiol. Heart Circ. Physiol., *280:* H1191–H1200, 2001.

62. Chrysis, D., Calikoglu, A. S., Ye, P., and D'Ercole. A. J. Insulin-like growth factor-I overexpression attenuates cerebellar apoptosis by altering the expression of Bcl family proteins in a developmentally specific manner. J. Neurosci., *21:* 1481–1489, 2001.

63. Pathan, N., Aime-Sempe, C., Kitada, S., Basu, A., Haldar, S., and Reed, J. C. Microtubule-targeting drugs induce bcl-2 phosphorylation and association with pin1. Neoplasia, *3:* 550–559, 2001.

64. Calastretti, A., Bevilacqua, A., Ceriani, C., Vigano, S., Zancai, P., Capaccioli, S., and Nicolin, A. Damaged microtubules can inactivate BCL-2 by means of the mTOR kinase. Oncogene, *20:* 6172–6180, 2001.

65. Dong, G., Rajah, R., Vu, T., Hoffman, A. R., Rosenfeld, R. G., Roberts, C. T., Jr., Peehl, D. M., and Cohen, P. Decreased expression of Wilms' tumor gene *WT-1* and elevated expression of insulin growth factor-II (IGF-II) and type 1 IGF receptor genes in prostatic stromal cells from patients with benign prostatic hyperplasia. J. Clin. Endocrinol. Metab., *82:* 2198–2203, 1997.

0021-972X/01/$03.00/0
The Journal of Clinical Endocrinology & Metabolism

Vol. 86, No. 4
Printed in U.S.A.

Transferrin Is an Insulin-Like Growth Factor-Binding Protein-3 Binding Protein*

STUART A. WEINZIMER, TARA BEERS GIBSON, PAULO F. COLLETT-SOLBERG, ARUNA KHARE, BINGRONG LIU, AND PINCHAS COHEN

Children's Hospital of Philadelphia (S.A.W.), University of Pennsylvania, Philadelphia, Pennsylvania 19104; Department of Pharmacology (T.B.G.), University of Texas, Southwestern Medical Center, Dallas, Texas 75235; Department of Pediatrics (P.F.C.-S.), Duke University, Durham, North Carolina 27710; Diagnostic Systems Laboratories, Inc. (A.K.), Webster, Texas 77598; and Mattel Children's Hospital at UCLA (B.L., P.C.), University of California at Los Angeles, Los Angeles, California 90095-1752

ABSTRACT

Insulin-like growth factor (IGF)-binding protein-3 (IGFBP-3) possesses both growth-inhibitory and -potentiating effects on cells that are independent of IGF action and are mediated through specific IGFBP-3 binding proteins/receptors located at the cell membrane, cytosol, or nuclear compartments and in the extracellular matrix. We have here characterized transferrin (Tf) as one of these IGFBP-3 binding proteins. Human serum was fractionated over an IGFBP-3 affinity column, and a 70-kDa protein was eluted, sequenced, and identified (through database searching and Western immunoblot) as human Tf. Tf bound IGFBP-3 but had negligible affinity to the other five IGFBPs, and iron-saturated holo-Tf bound IGFBP-3 more avidly than unsaturated Tf. Biosensor interaction analysis confirmed that this interaction is specific and sensitive, with a high association rate similar to IGF-I, and suggested that binding occurs in the vicinity of the IGFBP-3 nuclear localization site. As an independent confirmation of this interaction, using a yeast two-hybrid system, we cloned Tf from a human liver complementary DNA library as an IGFBP-3 protein partner. Tf treatment blocked IGFBP-3-induced cell proliferation in bladder smooth muscle cells, and IGFBP-3-induced apoptosis in prostate cancer cells. In summary, we have employed a combination of techniques to demonstrate that Tf specifically binds IGFBP-3, and we showed that this interaction has important physiological effects on cellular events. (*J Clin Endocrinol Metab* **86:** 1806–1813, 2001)

THE INSULIN-LIKE GROWTH factor (IGF)-binding proteins (IGFBPs) are a family of proteins that bind IGFs with high affinity and specificity. They modulate IGF action by increasing IGF half-life and inhibiting or potentiating IGF binding to the IGF receptor (IGF-R). There are six high-affinity IGFBPs, of which IGFBP-3 is the most abundant in serum. IGFBP-3 binds to IGFs and the acid labile subunit in the serum to form the 150-kDa ternary complex (1). The ternary complex stabilizes and increases the half-lives of IGFs and IGFBP-3 in the circulation and decreases the passage of IGFs and IGFBP-3 from the intravascular into the extravascular space (2). Circulating IGFBP-3 is derived primarily from hepatic Kupffer cells, primarily under regulation by GH; but IGFBP-3 is also produced locally in many tissues, where it serves important paracrine and autocrine roles in modulating cellular growth and apoptosis (3). IGFBP-3 activity in the circulation and at the cellular level is regulated not only by its rate of synthesis but also by post-translational modification and proteolysis (4).

The ability of IGFBP-3 to bind other molecules in addition to the IGFs, acid labile subunit, and IGFBP-3 proteases has been previously demonstrated. IGFBP-3 is noted to have a heparin-binding domain (heparin-BD) in its midregion and is known to interact with heparin-containing molecules in the extracellular matrix (5). IGFBP-3 has been observed in the nucleus of certain cells and contains a nuclear localization sequence that may allow it to interact with nuclear transcription factors (6, 7). Several groups, including our own, have demonstrated specific binding of IGFBP-3 to other proteins in cell lysates (8, 9) and cell membrane preparations (10–13), and it has been proposed that IGFBP-3 may share a common receptor with transforming growth factor-β (14).

We have previously demonstrated serum proteins of 70, 100, and 150 kDa that specifically bind IGFBP-3 and that may function as IGFBP-3 carriers in human serum (15). We report here the identification of the 70-kDa protein as transferrin (Tf), confirm the validity of Tf/IGFBP-3 binding through multiple independent *in vitro* methods, and demonstrate physiologically significant consequences of Tf/IGFBP-3 binding on cell proliferation and apoptosis.

Materials and Methods

Materials

Serum samples were collected from healthy young adult volunteers (with informed consent). Samples were collected in serum separator tubes, centrifuged, and frozen at −70 C.

Received March 4, 2000. Revision received August 14, 2000. Rerevision received January 3, 2001. Accepted January 4, 2001.

Address all correspondence and requests for reprints to: Pinchas Cohen, M.D., Professor and Director of Research and Training, Division of Endocrinology, Department of Pediatrics, Mattel Children's Hospital at UCLA, 10833 Le Conte Avenue, MDCC 22-315, Los Angeles, California 90095-1752. E-mail: hassy@mednet.ucla.edu.

* Supported in part by Grants 2R01-DK-47591 and 1RO1-AI-40203 (to P.C.) and a Molecular Approaches to Pediatric Science-Child Health Research Center grant (to S.W.) from the NIH and by awards from the Department of Defense, the American Cancer Society, the Juvenile Diabetes Foundations (to P.C.), and the McCabe Foundation (to S.W.).

Recombinant human IGF-I was provided by Pharmacia (Stockholm, Sweden). Recombinant human IGFBP-3 and IGFBP-3 mutants were provided by Protigen Inc. (Mountain View, CA). IGFBP-1 was the gift of Genentech, Inc. (San Francisco, CA). IGFBP-2 was the gift of Sandoz Pharmaceuticals Corp. (Basel, Switzerland). IGFBP-4, -5, and -6 was purchased from Austral (San Francisco, CA). Recombinant human ^{125}I-IGFBP-3 and affinity-purified antihuman IGFBP-3 antibody were purchased from Diagnostic Systems Laboratories, Inc.. Human Tf was purchased from Life Technologies, Inc. (Gaithersburg, MD). Holo-Tf, partially-saturated Tf, dimethylsulfoxide, and Igepal CA-630 were purchased from Sigma (St. Louis, MO). Tris (crystallized free base) was purchased from Fisher (Fair Lawn, NJ). Antihuman Tf antibody was purchased from Chemicon (Temecula, CA). SDS-PAGE reagents, Tween, and fat-free milk were purchased from Bio-Rad Laboratories, Inc. (Richmond, CA). Yeast strain *Saccharomyces cerevisiae* HF7c and yeast two-hybrid screening kit, including liver complementary DNA (cDNA) library, were purchased from CLONTECH Laboratories, Inc. (Palo Alto, CA).

Reverse ligand blot

Reverse Western ligand blots (WLB) were used to assess the presence of serum IGFBP-3 binding proteins/association proteins. Two microliters of normal serum were electrophoresed on SDS-PAGE (8%), at constant voltage, overnight, then transferred to nitrocellulose for 4 h at 170 mA. The nitrocellulose was buffered in Tris-buffered saline (TBS)/3% Igepal CA-630 for 30 min. The membranes were blocked for 3 h with TBS/1% BSA, and then incubated overnight with ^{125}I-IGFBP-3 (10^6 cpm) in TBS/0.1% Tween/1% BSA. The nitrocellulose was washed four times with TBS/0.1% Tween and TBS. The resulting bands were visualized by autoradiography or phosphorimaging.

Reverse ligand dot blot

Increasing concentrations of Tf were carefully dot-blotted directly onto nitrocellulose (2 μL at a time) and allowed to dry completely. The nitrocellulose was then treated as described above for a reverse ligand blot.

Western immunoblot

Two microliters of serum were separated by SDS-PAGE (8%) at constant voltage overnight, then transferred to nitrocellulose for 4 h at 170 mA. The nitrocellulose was immersed in blocking solution (5% nonfat milk/TBS) for 45 min, washed with TBS/0.1% Tween, and incubated with primary antihuman Tf or antihuman IGFBP-3 antibody (1:4,000) for 2 h. After washing off any unbound antibodies, the nitrocellulose was incubated with a general secondary antibody (1:10,000) for 1 h. The membrane was washed four times with TBS/0.1% Tween and TBS. Bands were visualized using the peroxidase-linked enhanced chemiluminescence detection system (ECL, Amersham Pharmacia Biotech, Uppsala, Sweden).

Western immunodot blot

Five-microgram samples of IGFBP-1 through -6 were carefully dot-blotted directly onto nitrocellulose (2 μL at a time) and allowed to dry completely. The membranes were then incubated overnight with holo-Tf (4 μg/mL) followed with a series of washes in TBS. The nitrocellulose was then treated, as described above, for a Western immunoblot, using an antihuman Tf antibody (1:4,000) as the primary antibody.

Affinity chromatography

One milliliter of human plasma was diluted (1:3) with 0.05 mol/L sodium phosphate buffer, pH 7.4, and then filtered through a 0.4-μm filter and loaded onto an IGFBP-3 antigen affinity column. Bound proteins were first eluted with 0.05 mol/L sodium phosphate buffer, pH 7.4 containing 0.6 mol/L NaCl, followed by 0.1 mol/L glycine (pH 2.75) containing 0.15 mol/L NaCl (no. 1) or 0.1 mol/L citrate buffer, pH 4.5 and pH 2.5 (no. 2). Five milliliter fractions were collected. Fractions with optical density more than 0.03 were pooled and concentrated. Two fractions were collected for elution condition no. 1, and three fractions were collected for elution condition no. 2. The fractions were combined and dialyzed overnight at 4 C in dH_2O to remove excess salt and to neutralize the buffer. Two microliters were loaded onto SDS-PAGE (8%) and then processed for amido black staining, immunoblotted, or reverse ligand blotted as described above.

Amino acid sequencing

Amino acid sequencing was provided by the Protein Chemistry Laboratory of the University of Pennsylvania Medical School, supported by core grants of the Diabetes and Cancer Centers (DK-19525 and CA-16520). Twenty microliters of samples eluted of the IGFBP-3 column were separated by 10% SDS-PAGE under nonreducing conditions, then transferred to a polyvinylidene difluoride membrane for 1.5 h. Bands were stained with 2% amido black. Bands were excised and subjected to Edmon degradation for sequencing in x machine. The first 10 amino acids of each indicated band were determined.

Sensor chip immobilization

The BIAcore 2000, Sensorchip CM5 (certified grade), amine coupling reagents (*N'*-ethyl-*N'*-(dimethylaminopropyl)-carbodiimide, *N*-hydroxysuccinimide, and ethanolamine hydrochloride) were purchased from Pharmacia Biosensor (Sweden). Biosensor chips were made by immobilizing wild-type IGFBP-3 (IGFBP-3_{WT}) and NLS-IGFBP3 mutant via primary amine groups. *N'*-ethyl-*N'*-(dimethylaminopropyl)-carbodiimide coupling chemistry was used to activate the carboxymethylated dextran surface for protein immobilization. Approximately 20 μg/mL of each IGFBP-3 solution (10 mmol/L sodium acetate, pH 5.5) were injected over the chip surface, at 5 μL/min at 25 C, to a level of approximately1000 response units (~1 ng/mm^2). Ethanolamine solution (1 mol/L) was added to inactivate unbound carboxyl groups. The surface was then exposed to 5 mmol/L HCl solution for washing excess bound protein after each injection. Association and dissociation phases were 180 sec.

BIAcore kinetic assays

The sensor chip was used to screen human serum Tf binding to IGFBP-3. All experiments were conducted at 25 C, with a constant flow rate of 30 μL/min PBS/0.005% Tween buffer. Holo-Tf or IGF-I were automatically injected over the chip surface using the kinject command in the BIAlogue control software. The association phase lasted 3 min. PBS buffer alone was then flowed over the chip to commence the dissociation phase for an additional 3 min. The sensor chip surface was regenerated, after each cycle, by injecting PBS buffer, at 10 μL/min twice, followed by 5 mM HCl at 100 μL/min for 30 sec three times, and a final wash of PBS buffer at 100 μL/min.

Biosensor interaction analysis (BIA)

BIAevaluation 3.0 software was used to perform global analysis of the resulting sensorgrams. The bulk refractive index effect of PBS buffer alone on the sensor chip was subtracted from each kinetic curve. The association and dissociation curves of each interaction between Tf and IGFBP-3 were fitted using standard kinetic equations as previously described in detail (16, 17). The program calculated the kinetic rates and the binding affinities for these reactions.

Yeast two-hybrid screening

The yeast strain *Saccharomyces cerevisiae* HF7c [MATa, ura3–52, his3–200, lys2–801, ade2–101, trp1–901, leu2–3, 112, gal4–542, gal80–538, LYS2::GAL1—HIS3, URA3::(GAL4 17 mers)$_3$—CYC1—lacZ] was purchased from CLONTECH Laboratories, Inc. The fusion gene IGFBP-3/BD was constructed by splicing cDNA encoding the human IGFBP-3 gene into the plasmid pGBT9 directly 5' to and in phase with the gene encoding the BD of the yeast transcriptional activator GAL4 (CLONTECH Laboratories, Inc.). A human liver cDNA library with the activation domain (AD) of the GAL4 gene was purchased (CLONTECH Laboratories, Inc.) and screened by cotransforming yeast with both plasmids. Yeast colonies were made competent for transformations according to the manufacturer's instructions (CLONTECH Laboratories,

Inc. Matchmaker protocol handbook). Positive cotransformants were selected by growth on histidine-deficient agar media and assayed for β-galactosidase activity according to the manufacturer's instructions (CLONTECH Laboratories, Inc. Matchmaker protocol handbook). Genes encoding IGFBP-3-binding proteins identified through this method were isolated by plasmid recovery, amplified using PCR, sequenced, and compared with known sequences in GenBank using the MacVector software program (Oxford Molecular Ltd., Williamstown, MA).

Cell proliferation assay

Cell proliferation assays were performed using the CellTiter 96 aqueous nonradioactive proliferation assay kits (Promega Corp., Madison, WI). Sheep bladder smooth muscle (sBLSM) cells in primary culture were obtained from Dr. Ed Macarak at the University of Pennsylvania School of Dentistry. An equal number of cells were plated in 96-well plates in serum-free medium treated with various concentrations of IGFBP-3, Tf, and a combination thereof, and grown for 72 h. The quantity of formazan product was measured spectrophotometrically by the amount of absorbance at 490 nM (Bio-Rad Laboratories, Inc.). Sample size for each condition in the experiment was eight. Samples were pipetted with a multistep multidispenser using fine pipettes to eliminate any operator errors. Each experiment was repeated three times for reproducibility.

Apoptosis enzyme-linked immunosorbent assay (ELISA) assay

Photometric cell death detection ELISA (Roche Molecular Biochemicals, Indianapolis, IN) was performed to quantitate the apoptotic index by detecting the histone-associated DNA fragments (mono- and oligonucleosomes) generated by the apoptotic cells. The assay is based on the quantitative sandwich-ELISA principle using mouse monoclonal antibodies directed against DNA and histones, respectively, for the specific determination of these nucleosomes in the cytoplasmic fraction of cell lysates. In brief, an equal number of prostate cancer PC-3 cells (from ATCC, Manassas, VA) were plated in 24-well culture plates (1×10^4/cm^2) in serum supplemented FK-12 medium, and grown to confluency for 72 h. At the time of sample collection, the confluent cells were washed with PBS and treated with various concentrations of IGFBP-3, Tf, and a combination thereof. The cells were dissociated gently (PBS with 0.1 M EDTA) and pelleted along with the floating cells (mostly apoptotic cells) collected from the conditioned media. The cell pellets were used to prepare the cytosol fractions, which contained the smaller fragments of DNA. Equal volumes of these cytosolic fractions were incubated in antihistone antibody-coated wells (96-well plates), and the histones of the DNA fragments were allowed to bind to the antihistone antibodies. The peroxidase-labeled mouse monoclonal DNA antibodies were used to localize and detect the bound fragmented DNA using photometric detection with 2,2′-azino-di-[3-ethylbenzathiazoline sulfonate] as the substrate. Calcium ionophore treated conditions were used as positive controls (see Ref. 20). Serum-free-medium-treated conditions were used as negative controls. Each experimental condition was performed with at least three samples and was repeated at least three times. The reaction products in each 96-well plate were read using a Bio-Rad Laboratories, Inc. microplate reader (Model 3550-UV). Averages of the values ± SEM from double absorbance measurements of the samples were plotted.

Immunofluorescence confocal microscopy

PC-3 cells (1×10^4) were plated on coverglasses in F12K medium containing 10% FBS for 2 days. The cells were then incubated in serum-free media, with or without IGFBP-3 (500 ng/mL) or Tf (1000 ng/mL), for 3 h before staining for immunofluorescence. After three washes in PBS, fixation and permeabilization of the cells were performed with 1% paraformaldehyde in PBS for 15 min at room temperature and 0.2% Triton X-100 in PBS for 15 min on ice, and cells were washed twice with PBS. IGFBP-3 protein localization was detected using the DSL hIGFBP-3 goat polyclonal antibody (which was previously purified in an IGFBP-3 column), diluted 1:200, followed by Fluorescein anti-Goat antibody from Vector Laboratories, Inc. (Burlingame, CA). Tf protein localization was detected using a human Tf chicken polyclonal antibody, from Chemicon, diluted 1:150, followed by fluorescein isothiocyanate antichicken IgG from Sigma. Specimens were incubated with primary antibodies in PBS for 1 h at room temperature, with secondary antibodies in PBS for 40 min at room temperature, and then incubated with HOECHST from Electron Microscopy Sciences (Ft. Washington, PA) for 2 min. Samples were analyzed using the Inverted Confocal Microscope (Leica Corp., Heidelberg, Germany), and operated by TCS-nt software (Leica Corp.).

Results

Identification of Tf as an IGFBP-3 binding protein in human serum

Using rWLBs with ^{125}I-IGFBP-3, we demonstrated that IGFBP-3 binds to two specific proteins in normal serum, which are separated by gel electrophoresis (Fig. 1A and Ref. 15). Similarly, normal serum that has been passed over an IGFBP-3 affinity column also demonstrates these same specific proteins that bind to ^{125}I-IGFBP-3 in an rWLB (data not shown) and were uniquely separated from other serum proteins as shown in Fig. 1B, demonstrating amido black protein staining. These proteins, at 70 and 100 kDa, were subjected to N-terminal amino acid sequencing, and the 70-kDa protein was identified through the Swiss Protein database, searching as human serum Tf (N-terminal sequence: PDKTVRWCA).

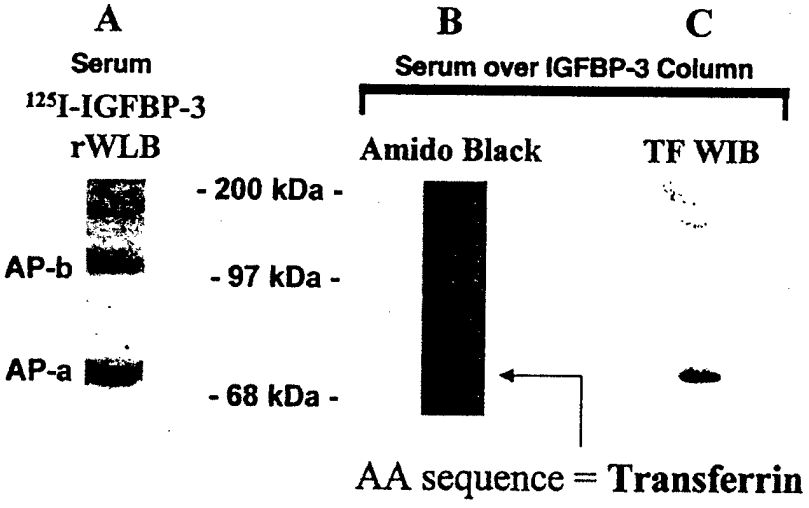

FIG. 1. Demonstration of Tf as an IGFBP-3 binding protein in human serum. A, Reverse Western ligand blot (rWLB) of electrophoresed human serum with yields bands at 70 and 100 kDa. B, Amido black staining of the eluted fractions of human serum, after passage over an IGFBP-3 purification column, enhances the bands shown in A. The 70-kDa band was extracted from membrane, sequenced, and determined to be human Tf, by amino acid sequence analysis. C, Western immunoblot (WIB) of identical membrane from B, using specific anti-Tf antibody, confirms sequence analysis data showing that the 70-kDa band is human Tf (TF). AP, Associated protein; AA, amino acid.

Once this initial identification was performed, we further confirmed the identity of this protein as Tf by performing a Western immunoblot on the IGFBP-3 affinity-purified serum fraction. Antibodies to human Tf specifically bound to the 70-kDa band separated by the IGFBP-3 column (Fig. 1C). Using specific antihuman IGFBP-3 and antihuman Tf, we coimmunoprecipitated IGFBP-3 and Tf from human serum (data not shown).

Comparison of Tf binding among IGFBPs

We tested the degree of specificity of Tf binding to IGFBP-3 by comparing binding to all six human IGFBPs. A nitrocellulose membrane was dot-blotted with 5 μg each of IGFBP-1 (0.2 nmol), IGFBP-2 (0.16 nmol), IGFBP-3 (0.11 nmol), IGFBP-4 (0.21 nmol), IGFBP-5 (0.17 nmol), and IGFBP-6 (0.15 nmol), incubated with a Tf solution, washed, and probed with anti-Tf antibodies in manner similar to that of a Western immunoblot (Fig. 2). The results indicate that Tf preferentially binds to IGFBP-3 at several orders of magnitude greater than the other IGFBPs, indicating a strong specificity of Tf for IGFBP-3.

Effect of iron saturation

We then investigated the effect of iron saturation on Tf-IGFBP-3 binding. Increasing amounts [10 μg (0.14 nmol) to 80 μg (1.14 nmol)] of unsaturated and iron-saturated (holo-) Tf were carefully dot-blotted onto a nitrocellulose membrane, allowed to dry, probed with ^{125}I-IGFBP-3, and visualized by autoradiography (Fig. 3). The results demonstrate that holo-Tf binds to IGFBP-3 with approximately twice the affinity as unsaturated Tf.

Dose response of Tf binding to IGFBP-3

We also compared the affinity of IGFBP-3 for Tf *vs.* IGF-I with a reverse ligand dot blot. IGF-I and Tf, in equimolar amounts ranging from 25–1000 nmol, were dot-blotted to a nitrocellulose membrane, allowed to dry, probed with ^{125}I-IGFBP-3, and visualized by autoradiography. Tf-IGFBP-3 binding was dose-responsive and of a magnitude similar to that of IGF-I (Fig. 4). Insulin and albumin, at the same molar quantities, had no appreciable binding to IGFBP-3.

Quantification of binding kinetics

We employed BIAcore technology (Pharmacia) to directly measure protein-protein interactions between IGFBP-3 and Tf. Using surface plasmon resonance, the system detects and displays a signal from resultant evanescent waves that is proportional to the change in mass as one protein molecule binds to the immobilized ligand on the sensorchip. In this manner, we observed changes in the association and dissociation phases of Tf/IGFBP-3 interactions and compared them with those of IGF-I/IGFBP-3 interactions. We performed kinetic analyses using both IGFBP-3_{WT} and a IGFBP-3 protein mutated in the nuclear localization sequence (IGFBP-$3_{NLS(-)}$ generously provided by Protigen Inc.)

Qualitative inspection of the IGF-I/IGFBP-3 curve (Fig. 5A) reveals a rapid initial association followed by a gradual dissociation, corresponding to a specific, high-affinity binding event. IGF-I bound to IGFBP-$3_{NLS(-)}$ with a similar affinity as IGFBP-3_{WT}, suggesting that the NLS domain is not involved in IGF-I/IGFBP-3 binding. Inspection of the Tf–IGFBP-3_{WT} curve (Fig. 5B, *black line*) reveals a rapid association phase, equal in magnitude to that of the IGF-I -IGFBP-3 association, followed by a relatively rapid dissociation phase. The Tf–IGFBP-$3_{NLS(-)}$ curve (Fig. 5B, *gray line*) is characterized by a significantly slower (by two orders of magnitude) association phase and rapid dissociation phase. Taken together, these data suggest that Tf/IGFBP-3 binding occurs rapidly at high affinity but with rapid dissociation, such that functional interactions are probably short-lived. Furthermore, comparison of the Tf–IGFBP-3_{WT} and Tf–IGFBP-$3_{NLS(-)}$ curves suggests that the Tf binding site on IGFBP-3 involves the NLS region.

Yeast two-hybrid screening

The ability of Tf to bind IGFBP-3 in an *in vivo* situation was tested using a yeast two-hybrid system. We used the yeast strain Hf7c (which is unable to grow in histidine-, leucine-, or tryptophan-deficient media) with a histidine-selection marker and β-galactosidase marker under control by the GAL1 promoter. The transcriptional activator GAL4 consists of two separable domains: a DNA-BD that binds to an upstream activating sequence, and a transcriptional AD necessary for RNA synthesis. We performed cotransformations

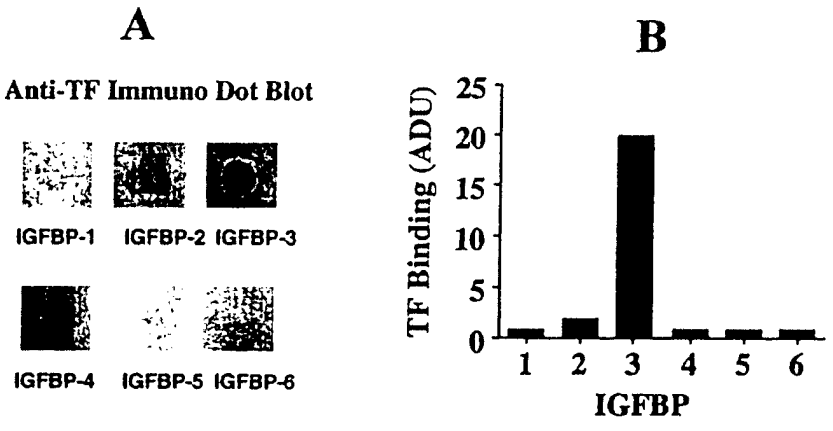

FIG. 2. Specificity of Tf for IGFBP-3 over other IGFBPs. A, Nitrocellulose membrane was dot-blotted with IGFBP-1 through -6, bathed in Tf solution, washed, and then probed with antihuman Tf to visualize bound Tf. Densitometry (B) reveals Tf bound IGFBP-3 with a 10- to 30-fold greater affinity than IGFBP-1, -2, -4, -5, and -6. ADU, Arbitrary data units.

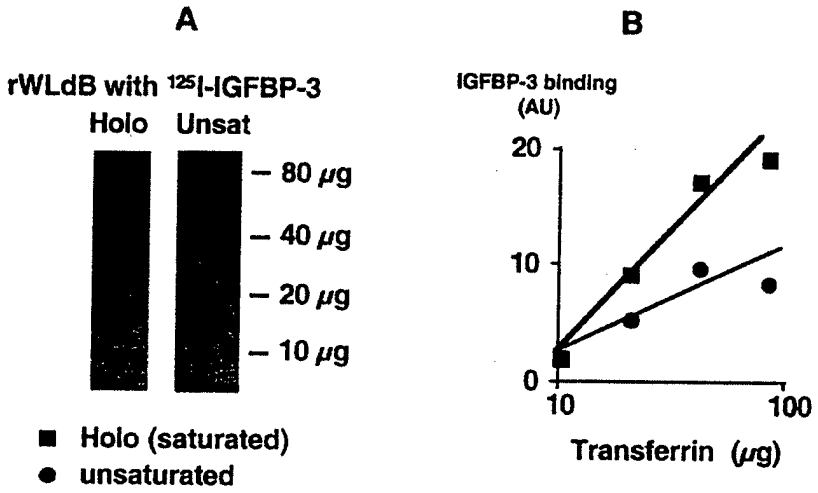

FIG. 3. Effect of saturation of Tf with iron on binding to IGFBP-3. A, Increasing amounts [10 μg (0.14 nmol) to 80 μg (1.14 nmol)] of holo-Tf (saturated) and unsaturated Tf were dot-blotted onto a nitrocellulose membrane and probed with ^{125}I-IGFBP-3. B, Densitometric analysis of visualized blots demonstrates dose-responsive binding of Tf to IGFBP-3, with greater binding to holo-Tf at all concentrations tested. rWLdB, Reverse Western ligand dot blot; AU, arbitrary units.

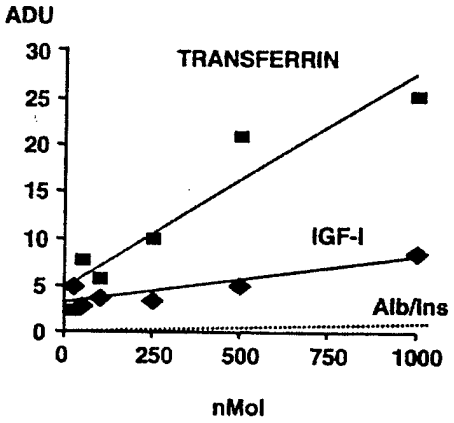

FIG. 4. Dose-responsiveness of Tf-IGFBP-3 binding. Increasing amounts of Tf and IGF-I were dot-blotted to a nitrocellulose membrane, probed with ^{125}I-IGFBP-3, and visualized with autoradiography. Densitometric analysis revealed affinity of IGFBP-3 for Tf, of a magnitude similar to that of IGF-I at given equimolar amounts, but no affinity of IGFBP-3 to insulin or albumin. Alb/Ins, Albumin/insulin.

with: 1) pGBT9 plasmid containing the fusion gene IGFBP-3/GAL4 BD and a histidine-selection marker; plus 2) pGAD424 plasmid containing a liver cDNA library/GAL4 AD fusion gene and a tryptophan-selection marker. Positive cotransformants were isolated by growth on tryptophan-, leucine-, and histidine-deficient media; and colonies with β-galactosidase activity were harvested to recover library plasmid. Library fragments were amplified using PCR and were sequenced. We isolated a 830-base pair cDNA fragment encoding 160 amino acids of the C-terminal portion of the human Tf gene followed by 350 base pairs of the 3′ untranslated region of the human Tf cDNA (GenBank sequence 339452; M12530.1).

In vivo effects of Tf-IGFBP-3 interactions

Tf, IGF-I, and IGFBP-3 were added to sBLSM and a human prostate cancer cell line (PC-3) to determine the physiological consequences of Tf-IGFBP-3 interactions. We have previously demonstrated the stimulatory role of IGFBP-3 on growth in sBLSM (9). As demonstrated in Fig 6, incubation of sBLSM with IGF-I [100 ng/mL (13.3 pmol/L)], IGFBP-3 [0.5 μg/mL (11.4 pmol/L)] or Tf [4 μg/mL (57.4 pmol/L)] alone increased cell proliferation by 35 ± 3%, 38 ± 4%, and 51 ± 2%, respectively. The coincubation of sBLSM with both Tf and IGFBP-3, however, resulted in a 33 ± 11% inhibition of growth, as compared with baseline conditions.

Physiologically significant effects of Tf-IGFBP-3 binding on apoptosis were also demonstrated, as illustrated in Fig. 7. The addition of Tf alone [4 μg/mL (57.4 pmol/L)] to PC-3 cells inhibited apoptosis, consistent with the well-known viability-enhancing effects of Tf in cell culture systems. IGFBP-3 [0.5 μg/mL (11.4 pmol/L)] alone induced apoptosis in PC-3 cells, to 200% of baseline, but this effect was blocked by the coincubation of IGFBP-3-treated PC-3 cells with Tf [4 μg/mL (57.4 pmol/L)].

IGFBP-3 and Tf modulate each other's cellular localization, as detected by immunofluorescence confocal microscopy

PC-3 cells were plated on coverglasses and treated with either IGFBP-3 [0.5 μg/mL (11.4 pmol/L)] or Tf [1 μg/mL (14.3 pmol/L)] for 3 h. As Fig. 8 shows, both IGFBP-3 and Tf are localized intracellularly and demonstrate some nuclear and perinuclear localization. However, the addition of either molecule results in the enhancement of the intracellular distribution of the other. In Fig. 8A, IGFBP-3 protein was localized to the cytoplasm and to the nucleus under serum-free conditions; the addition of Tf increased both. In Fig. 8B, Tf protein was localized to the inner plasma membrane, the cytoplasm, and to the perinuclear areas under serum-free conditions; the addition of IGFBP-3 resulted in cytoplasmic enhancement of Tf and to some nuclear staining.

Discussion

In addition to its role as an IGF-carrying protein in serum, IGFBP-3 prolongs the half-life of IGFs by preventing IGF clearance from serum. IGFBP-3 also modulates the interaction between IGFs and the type I IGF-R. In this capacity, IGFBP-3 may be inhibitory to growth (by preventing IGF binding to the IGF-R) or growth-potentiating (by presenting

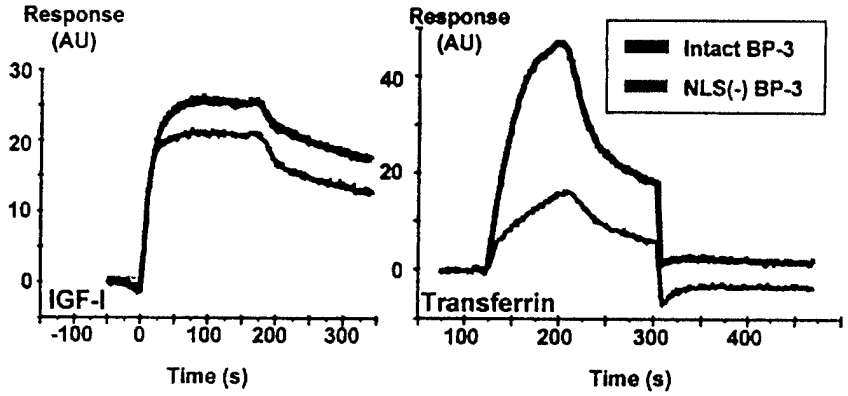

FIG. 5. BIA. Wild-type (WT) and mutated IGFBP-3 protein (at the nuclear localization sequence, NLS) were immobilized to the sensor chip, and IGF-I (A) and Tf (B) solutions were injected over the chip surface. Association and dissociation curves were obtained from sensorgrams as described. A, Steep association curve of IGF-I with little effect of NLS mutant is contrasted with more rapid dissociation curve of Tf with diminished binding to NLS mutant.

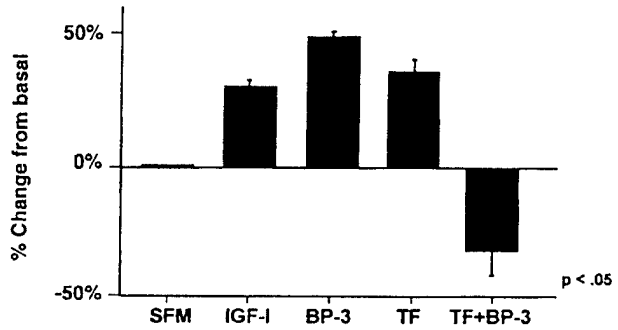

FIG. 6. Effect of Tf-IGFBP-3 binding on BLSM cell growth. Cell growth was assessed by ELISA, $P < 0.005$. Addition of Tf or IGFBP-3 individually to BLSM increased cell number after 72 h of treatment of conditioned media; but coincubation of cells with Tf plus IGFBP-3 inhibited growth, relative to control conditions.

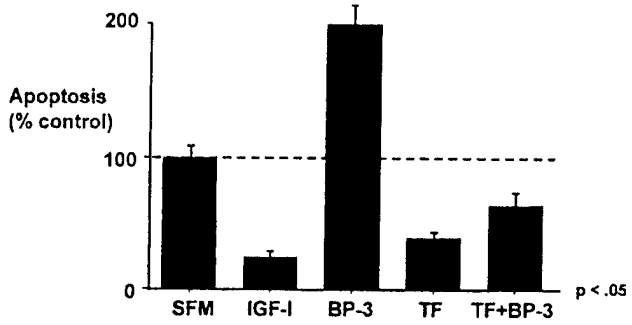

FIG. 7. Effect of Tf-IGFBP-3 binding on PC-3 cell apoptosis. Apoptosis was assessed by ELISA, $P < 0.005$. Tf protects cells from apoptosis, whereas IGFBP-3 induces apoptosis, after treatment of cells for 72 h. Coincubation of cells with Tf plus IGFBP-3, however, blocked IGFBP-3 induction of apoptosis.

IGFs to the IGF-R) in a controlled fashion and preventing down-regulation of the IGF-R (18, 19).

The discovery of IGF-independent modulation of growth by IGFBP-3 provides indirect evidence for the presence of specific IGFBP-3 binding proteins, which may be cell-surface associated, cytosolic, or nuclear in location. Oh *et al.* have demonstrated specific binding of IGFBP-3 to cell surface proteins of 20, 26, and 50 kDa in the estrogen receptor negative breast cancer cell line Hs578T, by affinity cross-linking and immunoprecipitation (10–12). We have similarly identified proteins with IGFBP-3 binding ability in prostate (8) and BLSM whole-cell lysates (9). Evidence for specific IGFBP-3 receptors also comes from experiments characterizing IGFBP-3 as a growth-inhibitory factor in murine knockout cells lacking the IGF-R (20) and as the mediator of apoptosis induced by retinoic acid and TGF-β (12, 13).

In this report, we describe, for the first time, the identification of Tf as another IGFBP-3 binding protein. We have demonstrated specific high-affinity Tf/IGFBP-3 binding through several *in vitro* methods, including column chromatography, coimmunoprecipitation, Western ligand blot, and Western immunoblot techniques. These studies demonstrate not only that Tf binds IGFBP-3 in human serum but that binding is dose-responsive, specific for IGFBP-3, and dependent on the degree of iron saturation. Biosensor BIA kinetic data suggests that the binding of Tf to IGFBP-3 occurs with short duration, perhaps involving the IGFBP-3 nuclear localization sequence. We have also independently cloned Tf as an IGFBP-3 binding protein, through the screening of a liver cDNA library with a yeast two-hybrid system. This method has been demonstrated to be a powerful tool in characterizing protein-protein interactions, even those that involved cell membrane-associated receptors (21, 22).

We have further demonstrated physiologically significant ramifications of Tf/IGFBP-3 interactions on the modulation of cell proliferation and apoptosis in several mammalian cellular systems. Tf and IGFBP-3 are both growth-potentiating in BLSM, but the coincubation of these proteins in BLSM-conditioned media resulted in a dramatic reduction in growth. This phenomenon is consistent with Tf/IGFBP-3 binding with such affinity as to prevent either ligand from interacting with its own natural cell surface receptor, or alternately, affecting access of IGFBP-3 to transcriptional modulators in the nucleus.

Tf is a 70-kDa glycoprotein that functions as the primary iron-carrying protein in serum (23). It is synthesized predominantly in the liver, but smaller amounts are produced in other organs, such as brain and testis (24). Tf normally binds two iron molecules after absorption of iron from the gastric and duodenal mucosa; Tf-iron binding at physiological conditions is nearly complete, so that essentially no free unbound iron exists in the blood (25). The Tf-iron complex circulates in serum and binds to cell surface Tf receptors (Tf-R), undergoes receptor-mediated endocytosis, and is recycled after dissociation of iron and exocytosis (26). Elevated intracellular iron levels are associated with

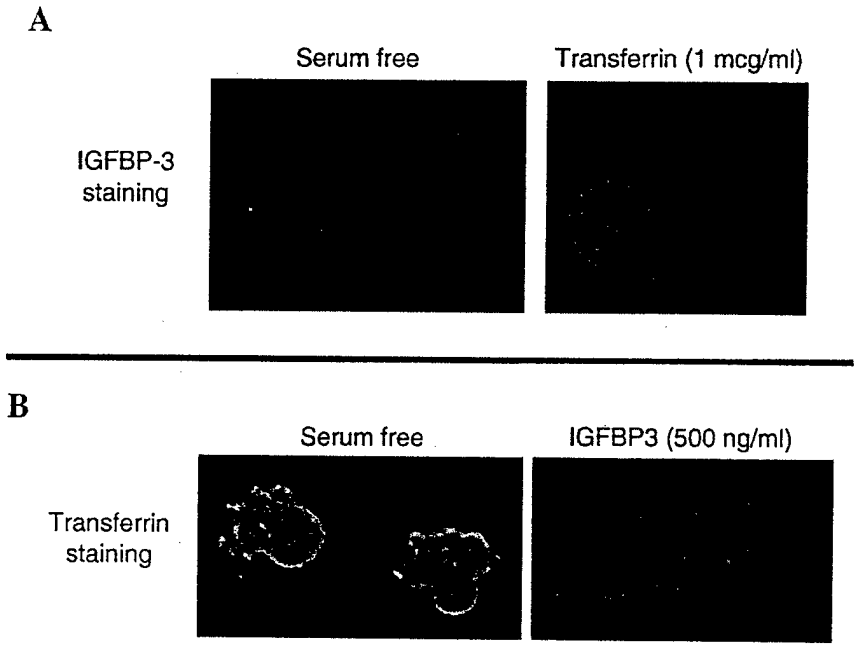

FIG. 8. Comodulation of the cellular localization of IGFBP-3 and Tf. IGFBP-3 and Tf were localized in PC-3 cells by immunofluorescent confocal microscopy using specific antibodies. A, IGFBP-3 protein was localized to the cytoplasm and to the nucleus under serum-free conditions; the addition of Tf increased both. B, Tf protein was localized to the inner plasma membrane, the cytoplasm, and to the perinuclear areas, under serum-free conditions; the addition of IGFBP-3 resulted in cytoplasmic enhancement of Tf and some nuclear staining.

destabilization of Tf-R messenger RNA (mRNA), whereas intracellular iron depletion increases Tf-R mRNA half-life (27).

The growth-enhancing effects of Tf at the cellular level are well-recognized. Tf is required for cell viability or proliferation in many cell culture systems, including cortical neuron (28), lymphocyte (29, 30), renal cortex (31), liver (32, 33), and bladder (34). Tf also seems to be required for differentiation of fetal metanephric mesenchyme during embryogenesis (35). Tf deprivation from cells is associated with elevated indices of apoptosis (36). Growth and aggressiveness of malignancies are also Tf-dependent; Tf-R number is positively correlated with tumor growth rate (37) and metastasis (38). In prostate cancer cells, Tf stimulates both proliferation and invasiveness (39, 40); and suramin, a compound employed in metastatic prostate cancer therapy, has recently been demonstrated to exert its effects by antagonizing the binding of Tf to the Tf-R (41).

The relationship between Tf and the IGF-IGFBP-3 axis is poorly understood. Serum concentrations of Tf are significantly correlated with IGF-I in pubertal girls (42) and boys (43) and with IGFBP-3 in pubertal girls (44). Tf levels are low in growth-hormone deficient children (45, 46) and increase after chronic GH administration (47, 48). At the molecular level, IGF-I seems to increase the expression of cell-surface Tf-Rs by redistributing Tf-Rs from an intracellular compartment to the cell surface (49–51). Tf has been shown to be localized intracellularly and has specifically been shown to be perinuclear (52). Our observations that IGFBP-3 nuclear localization is enhanced by Tf and that Tf is localized perinuclearly in an IGFBP-3-dependent manner suggest that IGFBP-3-Tf interactions may involve cotransport into cellular compartments and possibly additional molecule(s), which facilitate these events.

The nature of the IGFBP-3 to Tf interaction seems to involve an association, which is short-lived, and indeed suggests that a third molecule may be involved, or that this interaction may facilitate presentation of one or the other molecule to a receptor or a transporter. Physically, the interaction seems to occur between the NLS domain region of the IGFBP-3 molecule (as the IGFBP-3 mutant studies suggest) and the C-terminal portion of the Tf molecule (as evident from the two-hybrid screen). The observation that both IGFBP-3 and Tf stimulate smooth-muscle cell growth, but that their combination inhibits growth, suggests that the IGFBP-3-Tf complex may still be able to inhibit endogenously produced IGF-II, which we have shown to be made in these cells (7).

It is exciting to speculate that some of the previously recognized survival effects of Tf, which where, until now, completely unexplained, may be mediated through the inactivation of IGFBP-3 effects, as we have shown in PC-3 cells. There is substantial production of IGFBP-3 by epithelial cells, which may is responsible for the baseline apoptosis observed in such cells, as apoptosis is reduced in the presence of an IGFBP-3 neutralizing antibody (8).

The discovery of Tf as an IGFBP-3 binding protein adds a further level of complexity to the modulation of growth at the cellular level. In addition to the modulation of IGF activity at the cell membrane and direct interactions with its own specific receptors, IGFBP-3 may also affect cell growth through several Tf- and Tf-R-dependent mechanisms. Sequestration or presentation of IGF-I to the cell surface by IGFBP-3 may indirectly influence growth by regulating Tf-R density at the cell surface, and Tf/IGFBP-3 binding may directly interfere with each ligand from binding its own natural receptor, depending on the iron status of the tissue or organism. Whether these Tf/IGFBP-3 interactions occur predominantly at the cell surface or in the cytosolic or nuclear compartments is unknown, although it is intriguing to speculate that Tf may also modulate IGFBP-3 activity by binding IGFBP-3 and preventing its nuclear entry. These findings

suggest that IGFBP-3 may serve an important role in coordinating growth to the nutritional state of the tissue or organism and that further IGFBP-3 binding proteins remain to be discovered.

References

1. **Cohen P, Rosenfeld RG.** 1994 Physiologic and clinical relevance of the insulin-like growth factor binding proteins. Curr Opin Pediatr. 6:462–467.
2. **Baxter RC.** 1994 Insulin-like growth factor binding proteins in the human circulation: a review. Horm Res. 42:140–144.
3. **Ferry Jr RJ, Katz LEL, Grimberg A, Cohen P, Weinzimer SA.** 1999 Cellular actions of insulin-like growth factor binding proteins. Horm Metab Res. 31:192–202.
4. **Collett-Solberg PF, Cohen P.** 1996 The role of the insulin-like growth factor binding proteins and the IGFBP proteases in modulating IGF action. Endocrinol Metab Clin North Am. 25:591–614.
5. **Fowlkes JL, Thrailkill KM, George-Nascimento C, Rosenberg CK, Serra DM.** 1997 Heparin-binding, highly basic regions within the thyroglobulin type-1 repeat of insulin-like growth factor (IGF)-binding proteins (IGFBPs) -3, -5, and -6 inhibit IGFBP-4 degradation. Endocrinology. 138:2280–2285.
6. **Jaques G, Noll K, Wegmann B, et al.** 1997 Nuclear localization of insulin-like growth factor binding protein 3 in a lung cancer cell line. Endocrinology. 138:1767–1770.
7. **Schedlich LJ, Young TF, Firth SM, Baxter RC.** 1998 Insulin-like growth factor binding protein (IGFBP)-3 and IGFBP-5 share a common nuclear transport pathway in T47D human breast carcinoma cells. J Biol Chem. 29:18347–18352.
8. **Rajah R, Valentinis B, Cohen P.** 1997 Insulin-like growth factor (IGF)-binding protein-3 induces apoptosis and mediates the effects of transforming growth factor-β1 on programmed cell death through a p53- and IGF-independent mechanism. J Biol Chem. 272:12181–12188.
9. **Weinzimer SA, Zhao H, Macarak E, Cohen P,** Proc of the 80th Meeting of The Endocrine Society, New Orleans, LA, 1998; pp 316–317.
10. **Oh Y, Muller HL, Lamson G, Rosenfeld RG.** 1993 Insulin-like growth factor (IGF)-independent action of IGF-binding protein-3 in Hs578T human breast cancer cells. Cell surface binding and growth inhibition. J Biol Chem. 268:14964–14971.
11. **Oh Y, Muller HL, Pham H, Rosenfeld RG.** 1993 Demonstration of receptors for insulin-like growth factor binding protein-3 on Hs578T human breast cancer cells. J Biol Chem. 268:26045–26048.
12. **Oh Y, Muller HL, Ng L, Rosenfeld RG.** 1995 Transforming growth factor-beta-induced cell growth inhibition in human breast cancer cells is mediated through insulin-like growth factor-binding protein-3 action. J Biol Chem. 270:13589–13592.
13. **Gucev ZS, Oh Y, Kelley KM, Rosenfeld RG.** 1996 Insulin-like growth factor binding protein 3 mediates retinoic acid- and transforming growth factor beta2-induced growth inhibition in human breast cancer cells. Cancer Res. 56:1545–1550.
14. **Leal SM, Liu Q, Huang SS, Huang JS.** 1997 The type V transforming growth factor beta receptor is the putative insulin-like growth factor binding protein 3 receptor. J Biol Chem. 272:20572–20576.
15. **Collett-Solberg PF, Nunn SE, Gibson TB, Cohen P.** 1998 Identification of novel high molecular weight insulin-like growth factor-binding protein-3 association proteins in human serum. J Clin Endocrinol Metab. 83:2843–2848.
16. **Karlsson R, Roos H, Fägerstam L, Persson B.** 1994 Methods Companion Methods Enzymol. 6:99–110.
17. **Karlsson R, Fält A.** 1997 Experimental design for kinetic analysis of protein-protein interactions with surface plasmon resonance biosensors. J Immunol Methods. 200:121–133.
18. **Conover CA, Powell DR.** 1991 Insulin-like growth factor (IGF)-binding protein-3 blocks IGF-I-induced receptor down-regulation and cell desensitization in cultured bovine fibroblasts. Endocrinology. 129:710–716.
19. **Conover CA.** 1992 Potentiation of insulin-like growth factor (IGF) action by IGF-binding protein-3: studies of underlying mechanism. Endocrinology. 131:3191–3199.
20. **Valentinis B, Bhala A, de Angelis T, Baserga R, Cohen P.** 1995 The human insulin-like growth factor (IGF) binding protein-3 inhibits the growth of fibroblasts with a targeted disruption of the IGF-I receptor gene. Mol Endocrinol. 9:361–367.
21. **Fields S, Song O.** 1989 A novel genetic system to detect protein-protein interactions. Nature. 340:245–246.
22. **Zhu J, Kahn CR.** 1997 Analysis of a peptide hormone-receptor interaction in the yeast two-hybrid system. Proc Natl Acad Sci USA. 94:13063–13068.
23. **Aisen P, Brown EB.** 1977 The iron-binding function of transferrin in iron metabolism. Semin Hematol. 14:31–53.
24. **Zakin MM.** 1992 Regulation of transferrin gene expression. FASEB J. 6:3253–3258.
25. **van Eijk HG, de Jong G.** 1992 The physiology of iron, transferrin, and ferritin. Biol Trace Elem Res. 35:13–24.
26. **Morgan EH, Baker E.** 1988 Role of transferrin receptors and endocytosis in iron uptake by hepatic and erythroid cells. Ann NY Acad Sci. 526:65–82.
27. **Mullner EW, Kuhn LC.** 1988 A stem-loop in the 3' untranslated region mediates iron-dependent regulation of transferrin receptor mRNA stability in the cytoplasm. Cell. 53:815–825.
28. **Aizenman Y, de Vellis J.** 1987 Brain neurons develop in a serum and glial free environment: effects of transferrin, insulin, insulin-like growth factor-I and thyroid hormone on neuronal survival, growth and differentiation. Brain Res. 406:32–42.
29. **Soyano A, Pons H, Romano E.** 1985 Synergistic effect of albumin and transferrin on the mitogen stimulation of human mononuclear leukocytes in serum-free medium. Immunol Lett. 9:57–62.
30. **Okamoto T, Tani R, Yabumoto M, et al.** 1996 Effects of insulin and transferrin on the generation of lymphokine-activated killer cells in serum-free medium. J Immunol Methods. 195:7–14.
31. **Briere N, Ferrari J, Chailler P.** 1991 Insulin and transferrin restore important cellular functions of human fetal kidney in serum-free organ culture. Biochem Cell Biol. 69:256–262.
32. **Tsao MS, Sanders GH, Grisham JW.** 1987 Regulation of growth of cultured hepatic epithelial cells by transferrin. Exp Cell Res. 171:52–62.
33. **Shapiro LE, Wagner N.** 1988 Growth of H-35 rat hepatoma cells in unsupplemented serum-free media: effect of transferrin, insulin, and cell density. In Vitro Cell Dev Biol. 24:299–303.
34. **Tanoguchi H, Tachibana M, Murai M.** 1997 Autocrine growth induced by transferrin-like substance in bladder carcinoma cells. Br J Cancer. 76:1262–1270.
35. **Ekblom P, Thesleff I, Saxen L, Miettinen A, Timpl R.** 1983 Transferrin as a fetal growth factor: acquisition of responsiveness related to embryonic induction. Proc Natl Acad Sci USA. 80:2651–2655.
36. **Muta K, Krantz SB.** 1995 Inhibition of heme synthesis induces apoptosis in human erythroid progenitor cells. J Cell Physiol. 163:38–50.
37. **Tampanaru-Sarmesiu A, Stefaneanu L, Kontogeorgos G, Sumi T, Kovacs K.** 1998 Transferrin and transferrin receptor in human hypophysis and pituitary adenomas. Am J Pathol. 152:413–422.
38. **Nicolson GL.** 1993 Paracrine and autocrine growth mechanisms in tumor metastasis to specific sites with particular emphasis on brain and lung metasis. Cancer Metastasis Rev. 12:325–343.
39. **Rossi MC, Zetter BR.** 1992 Selective stimulation of prostatic carcinoma cell proliferation by transferrin. Proc Natl Acad Sci USA. 89:6197–6201.
40. **Bhatti RA, Gadarowski JJ, Ray PS.** 1997 Metastatic behavior of prostatic tumor as influenced by the hematopoietic and hematogenous factors. Tumour Biol. 18:1–5.
41. **Donat SM, Powell CT, Israeli RS, Fair WR, Heston WD.** 1995 Reversal by transferrin of growth-inhibitory effect of suramin on hormone-refractory human prostate cancer cells. J Natl Cancer Inst. 87:41–46.
42. **Wilson DM, Killen JD, Hammer LD, et al.** 1991 Insulin-like growth factor-I as a reflection of body composition, nutrition, and puberty in sixth and seventh grade girls. J Clin Endocrinol Metab. 73:907–912.
43. **Misaki M, Shima T, Yano Y, Okazaki T.** 1991 Serum transferrin as a marker of bone growth in boys: correlation with serum alkaline phosphatase activity, plasma insulin-like growth factor I and rate of growth in height. Horm Metab Res. 23:230–232.
44. **Wilson DM, Stene MA, Killen JD, et al.** 1992 Insulin-like growth factor binding protein-3 in normal pubertal girls. Acta Endocrinol (Copenh). 126:381–386.
45. **Donnadieu M, Schimpff RM, Garnier P, Chaussain JL, Job JC.** 1980 A possible relationship between serum transferrin, growth hormone secretion, and height velocity in children. Acta Endocrinol (Copenh). 93:134–138.
46. **Repellin AM, Schimpff RM, Georges P, Job JC.** 1984 Somatomedin, transferrin and amino-acids in serum following injection of human growth hormone in children with growth disease. Horm Metab Res. 16:539–543.
47. **Kemp SF, Canfield ME.** 1983 Acute effects of growth hormone administration: vitamin A and visceral protein concentrations. Acta Endocrinol (Copenh). 104:390–396.
48. **Vihervuori E, Cook JD, Siimes MA.** 1997 Iron status of children with short stature during accelerated growth due to growth hormone treatment. Acta Paediatr. 86:588–593.
49. **Davis RJ, Czech MP.** 1986 Regulation of transferrin receptor expression at the cell surface by insulin-like growth factors, epidermal growth factor and platelet-derived growth factor. EMBO J. 5:653–658.
50. **Davis RJ, Faucher M, Racaniello LK, Carruthers A, Czech MP.** 1987 Insulin-like growth factor I and epidermal growth factor regulate the expression of transferrin receptors at the cell surface by distinct mechanisms. J Biol Chem. 262:13126–13134.
51. **Lombardi A, Tramontano D, Braverman LE, Ingbar SH.** 1989 Transferrin in FRTL5 cells: regulation of its receptor by mitogenic agents and its role in growth. Endocrinology. 125:652–658.
52. **Sakaguchi M, Kondo T, Pu H, Namba M.** 1998 Differential localization of two types of transferrin: produced by human fibroblasts or incorporated from culture medium. Cell Struct Funct. 2:69–72.

Growth Hormone & IGF Research 2001, **11**, 336–338
doi:10.1054/ghir.2001.0255, available online at http://www.idealibrary.com on IDEAL®

COMMENTARY

Clinical implications of the IGF-cancer connection

Pinchas Cohen

Pediatric Endocrinology, UCLA, MDCC 22-315, Los Angeles, CA 90095-1752, USA

In this issue of Growth Hormone & IGF Research, Dr. Yee summarizes data in support of a role for the insulin-like growth factors-insulin-like growth factor receptor (IGF-IGF1R) system in the development and progression of human malignancy.[1] This exciting area of science has been the subject of a number of additional recent reviews in other journals,[2–6] which together with the current review argue an epidemiological and functional connection between IGFs and cancer. The vast majority of the experimental studies involving animals or cell culture systems are demonstrative for the role of the IGF system in stimulating the growth of established tumour models rather than initiating the carcinogenic process. Furthermore, there are many explanations for the epidemiological data linking serum IGF-I and cancer other than a direct causative relation. This includes an ascertainment bias in patient selection, tumour-related source of IGF-I, or a non-causative confounding relationship, all of which have been extensively reviewed.[7,8] Nevertheless, the data needs to be interpreted conservatively by clinicians involved in trophic factor therapies. There are at least five major implications for this relationship that are important in the context of clinical practice, drug development, and cancer prevention.

First, it is well known that serum IGF-I levels are regulated by growth hormone (GH) and concerns have been raised regarding the possible pro-cancerous effects of GH in GH recipients. This topic has been recently reviewed in this Journal,[9] and has also been addressed by a consensus workshop sponsored by the GH Research Society.[10] Based on recent evidence from extensive surveillance studies, GH therapy does not increase the risk of de novo neoplasms (including leukemia) or of cancer recurrence in GH recipients.[11] The role of GH in cancer initiation is further negated by the observation that the incidence of cancer, other than possibly colonic neoplasia, does not appear to be significantly increased in acromegaly.[12] Furthermore, GH transgenic mice, with high IGF-I levels, do not develop common malignancies.[13] It is known that IGF binding protein-3 (IGFBP-3) can inhibit IGF action on cancer cells *in vitro* and also can induce apoptosis via an IGF-independent mechanism.[14] In addition to increasing IGF-I levels, GH also increases the serum levels of IGFBP-3 and serum IGFBP-3 levels have been shown to be negatively correlated with the risk of cancer in epidemiological studies.[15] In subjects treated with GH, IGF-I and IGFBP-3 levels both rise together so that the ratio is not within the elevated cancer-risk range. Nonetheless, long-term studies are needed to assess the potential cancer risk associated with GH therapy. These should take into account several factors, including the duration of exposure, the risk magnitude associated with the degree of serum IGF-I elevation, and the adjusted risk based on a concomitant increase in IGFBP-3 levels. Since GH treated patients often have subnormal IGF-I serum levels, which normalise on therapy, one might predict that their cancer risk on GH therapy should not increase above the normal population. Until further research in the area dictates otherwise, on-going cancer surveillance and routine monitoring of serum IGF-I and IGFBP-3 levels in GH-recipients

Correspondence to: Pinchas Cohen, M.D., Professor and Chief, Division of Endocrinology, Department of Pediatrics, Mattel Children's Hospital at UCLA, 10833 Le Conte Ave., MDCC 22-315, Los Angeles, CA 90095-1752. Tel: 310 206 5844; Fax: 310 206 5843; E-mail: hassy@mednet.ucla.edu

Supported in part by grants from the National Institutes of Health and the Department of Defense.

1096–6374/01/060336+03 $35.00/0

should be the standard of care. At present, the data that are available do not to warrant a change in our current management of approved indications for GH therapy.

Second, over the last decade, IGF-I itself has been developed as a therapeutic agent.[16,17] Should the evidence discussed in Dr. Yee's review preclude its use? It is the opinion of this author that in selected circumstances, IGF-I therapy may be appropriate. The short-term use of IGF-I is not of particular relevance to long-term cancer risk. Furthermore, the use of IGF-I in conditions associated with substantially reduced life expectancy is completely rational as long as clear efficacy can be demonstrated for this therapy. One such condition is amyotrophic lateral sclerosis (ALS), where the benefit of IGF-I therapy has been investigated.[18,19] Unfortunately, the response to IGF-I in ALS was not sufficiently dramatic at the doses used. Nevertheless, whether ALS and similar terminal conditions may benefit from the neuro-survival inducing effects of IGF-I deserve further evaluation. Finally, in conditions where serum IGF-I levels are very reduced and are associated with significant morbidity unresponsive to other therapies (such as Laron Syndrome) judicious use of IGF-I is indicated (and is in fact approved by the regulatory agencies in Japan and Israel).

Third, it is well recognized that nutritional factors can affect serum IGF-I levels independently of GH[20] without affecting IGFBP-3 levels. Nutrition and exercise can modulate the bioavailability of IGF-I by regulating insulin levels and insulin sensitivity, thereby controlling IGFBP-1 levels.[21] The role of diet in cancer prevention is highly publicized, but the possibility that IGF-I serves as an intermediary in this equation needs further exploration. Indeed new studies on dietary interventions suggest such a link.[22]

Fourth, it has been proposed that serum IGF screening may have a role in identifying individuals with a high risk of developing cancer. While it is clearly not an approach that can be currently recommended, if future non-invasive dietary interventions that prevent cancer and reduce serum IGF-I prove effective, a role for routine IGF-I and IGFBP-3 monitoring could be envisioned.[23]

Finally, Yee discusses various strategies for inhibiting IGF signalling as a possible new approach to cancer therapy.[1] Indeed, such interventions are being explored by a number of drug companies with multiple agents being evaluated at various pre-clinical and phase I studies including: GH antagonists[24] and IGFBP-3,[25] which act by limiting IGF availability, IGF1R antagonists and IGF1R blocking antibodies,[26] which interfere with IGF-IGF1R interactions as well as tyrosine kinase antagonists[27] and PI3K/AkT inhibitors,[28] which act distal to the IGF receptor. The successes of these therapies in animal models are further indications for the role of the IGF system in established tumours.

Thus, it is clear that the IGF-cancer connection is not merely of academic interest. It drives, and will continue to stimulate new approaches to clinical practice in endocrinology, public health, and oncology. It is the responsibility of clinicians to integrate the rapidly emerging information in this field into safe and effective clinical practice.

REFERENCES

1. Yee D. Are the IGFs relevant to Cancer? GH & IGF Res; Current issue; 2002.
2. Werner H, Le Roith D. New concepts in regulation and function of the insulin-like growth factors: implications for understanding normal growth and neoplasia. Cell Mol Life Sci 2000; 57: 932–942.
3. Valentinis B, Baserga R. IGF-I receptor signalling in transformation and differentiation. Mol Pathol 2001; 54: 133–137.
4. Yu H, Rohan T. Role of the insulin-like growth factor family in cancer development and progression. J Natl Cancer Inst 2000; 92: 1472–1489.
5. Khandwala HM, McCutcheon IE, Flyvbjerg A, Friend KE. The effects of insulin-like growth factors on tumourigenesis and neoplastic growth. Endocr Rev 2000; 21; 215–244.
6. Holly JM, Gunnell DJ, Davey Smith G. Growth hormone, IGF-I and cancer. Less intervention to avoid cancer? More intervention to prevent cancer? J Endocrinol 1999; 162: 321–330.
7. Grimberg A, Cohen P: Growth hormone and prostate cancer: Guilty by association? J Enocrinol Invest 1999; 22: 64–73.
8. Shim M, Cohen P. IGFs and human cancer: implications regarding the risk of growth hormone therapy. Horm Res 1999; 51 Suppl 3: 42–51.
9. Cohen P, DR Clemmons RG Rosenfeld. Does the GH–IGF axis play a role in cancer pathogenesis? Growth Hormone & IGF Research 2000; 10: 1–9.
10. Officers of the GH Research Society. Critical evaluation of the safety of recombinant human growth hormone administration: statement from the Growth Hormone Research Society. J Clin Endocrinol Metab 2001; 86: 1868–1870.
11. Nishi Y, Tanaka T, Takano K, Fujieda K, Igarashi Y, Hanew K, Hirano T, Yokoya S, Tachibana K, Saito T, Watanabe S and the GH Treatment Study Committee of the Foundation for Growth Science, Japan. Recent status in the occurrence of leukemia in growth hormone-treated patients in Japan. J Clin Endocrinol Metab 84: 1961–1965; 1999.
12. Orme SM, McNally RJ, Cartwright RA, Belchetz PE. Mortality and cancer incidence in acromegaly: a retrospective cohort study. United Kingdom Acromegaly Study Group. J Clin Endocrinol Metab 1998; 83: 2730–2734.
13. Wennbo H, Gebre-Medhin M, Gritli-Linde A, Ohlsson C, Isaksson OG, Tornell J Activation of the prolactin receptor but not the growth hormone receptor is important for induction of mammary tumours in transgenic mice. J Clin Invest 1997; 100: 2744–2751.
14. Liu B, Lee HY, Weinzimer SA, Powell DR, Clifford JL, Kurie JM, Cohen P. Direct Functional Interactions between Insulin-like Growth Factor-binding Protein-3 and Retinoid X Receptor-alpha

Regulate Transcriptional Signaling and Apoptosis. J Biol Chem 2000; 275: 33607–33613.
15. Ma J, Pollak MN, Giovannucci E, Chan JM, Tao Y, Hennekens CH, Stampfer MJ. Prospective study of colorectal cancer risk in men and plasma levels of insulin-like growth factor (IGF)-I and IGF-binding protein-3. J Natl Cancer Inst 1999; 91: 620–625.
16. Camacho-Hubner C, Savage M. Insulin-like growth factor-I deficiency. Horm Res 2001; 55 S1: 17–20.
17. Savage MO, Camacho-Hubner C, Dunger DB, Ranke MB, Ross RJ, Rosenfeld RG. Is there a medical need to explore the clinical use of insulin-like growth factor I? Growth Horm IGF Res 2001; 11: S65–S69.
18. Ackerman SJ, Sullivan EM, Beusterien KM, Natter HM, Gelinas DF, Patrick DL. Cost effectiveness of recombinant human insulin-like growth factor I therapy in patients with ALS. Pharmacoeconomics 1999; 15: 179–195.
19. Borsaio GD, Robberecht W, Leigh PN, Emile J, Guiloff RJ, Jerusalem F, Silani V, Vos PE, Wokke JH, Dobbins T. A placebo-controlled trial of insulin-like growth factor-I in amyotrophic lateral sclerosis. European ALS/IGF-I Study Group. Neurology 1998; 51: 583–586.
20. Kari FW, Dunn SE, French JE, Barrett JC. Roles for insulin-like growth factor-I in mediating the anti-carcinogenic effects of caloric restriction. J Nutr Health Aging 1999; 3: 92–101.
21. McCarty MF. Up-regulation of IGF binding protein-1 as an anticarcinogenic strategy: relevance to caloric restriction, exercise, and insulin sensitivity. Med Hypotheses 1997; 48: 297–308.
22. Mucci LA, Tamimi R, Lagiou P, Trichopoulou A, Benetou V, Spanos E, Trichopoulos D. Are dietary influences on the risk of prostate cancer mediated through the insulin-like growth factor system? BJU Int 2001; 87: 814–820.
23. Pollak M. Insulin-like growth factor physiology and cancer risk. Eur J Cancer 2000; 36: 1224–1228.
24. Friend KE. Targeting the growth hormone axis as a therapeutic strategy in oncology. Growth Horm IGF Res 2000; 10 Suppl A: S45–S46.
25. Portera CA, Shinohara H, Mima T, Miller A, Tsan R, Mascarenhas D, Radinsky R. Targeting the IGF axis in the therapy of colorectal carcinoma liver metastasis. Growth Hormone and IGF Research 10: S47–S48; 2000.
26. Scotlandi K, Benini S, Nanni P, Lollini PL, Nicoletti G, Landuzzi L, Serra M, Manara MC, Picci P, Baldini N. Blockage of insulin-like growth factor-I receptor inhibits the growth of Ewing's sarcoma in athymic mice. Cancer Res 1988; 58; 4127–4131.
27. Hermanto U, Zong CS, Wang LH. Inhibition of mitogen-activated protein kinase kinase selectively inhibits cell proliferation in human breast cancer cells displaying enhanced insulin-like growth factor I-mediated mitogen-activated protein kinase activation. Cell Growth Differ 2000; 11: 655–664.
28. Podsypanina K, Lee RT, Politis C, Hennessy I, Crane A, Puc J, Neshat M, Wang H, Yang L, Gibbons J, Frost P, Dreisbach V, Blenis J, Gaciong Z, Fisher P, Sawyers C, Hedrick-Ellenson L, Parsons R. An inhibitor of mTOR reduces neoplasia and normalizes p70/S6 kinase activity in Pten+/- mice. Proc Natl Acad Sci USA 2001; 98: 10320–10325.

Best Practice & Research Clinical Endocrinology and Metabolism
Vol. 16, No. 3, pp. 000–000, 2002
doi:10.1053/beem.2002.0212, available online at http://www.idealibrary.com on IDEAL®

BEST PRACTICE & RESEARCH

9

IGFs and IGFBPs: role in health and disease

Roshanak Monzavi
????

Pinchas Cohen* MD
Professor and Chief
Division of Endocrinology, Department of Pediatrics, Mattel Children's Hospital at UCLA, 10833 Le Conte Ave. MDCC 22-315, Los Angeles, CA 90095-1752, USA

AQ1

The insulin-like growth factors (IGFs), IGF-binding proteins (IGFBPs), and IGFBP proteases are the main regulators of somatic growth and cellular proliferation. IGFs are involved in growth pre-natally and post-natally. Dysregulation of the IGF axis can lead to growth disorders such as growth hormone deficiency and acromegaly. Pre-natally, this dysregulation can lead to IUGR or macrosomia. IGFs also have an important mitogenic action and play a role in tumorigenesis and cancer. These actions are regulated by co-interactions with IGFBPs, especially IGFBP-3. In addition to somatic growth and mitogenic activity, IGFs have hypoglycaemic and insulin sensitizing actions, and their dysregulation is involved in diabetes and its complications.

In this chapter, we examine the role of IGFs and IGFBPs in growth, tumorigenesis and diabetes, and discuss treatment modalities for each disease involving the GH–IGF–IGFBP axis, including discussion of current in vitro and in vivo investigations in this field.

Key words: insulin-like growth factor; insulin-like growth factor binding protein; insulin-like growth factor receptor; insulin-like growth factor binding protein protease; growth; growth hormone deficiency; growth hormone therapy.

IGFs AND IGFBPs

The insulin-like growth factors (IGF-I and IGF-II) are important factors in the regulation of somatic growth and cellular proliferation. This regulation is modulated further by insulin-like growth factor binding proteins (IGFBPs) and IGFBP proteases. The interaction between free IGFs and IGF receptors are the main determinant of IGF action. The level of free IGFs is affected by rate of IGF production, clearance, and binding to IGFBPs. IGFBPs also have IGF-independent actions, which include inhibition of cell growth and induction of apoptosis. There are six proteins from the IGFBP super protein (IGFBP-1 to -6) that bind with high affinity to IGFs, as well as a group of IGFBP-related proteins (IGFBP-rP 1–9) that bind with low affinity to IGFs.[1] Proteases

*To whom correspondence should be addressed

1521–690X/02/$ - see front matter

(BP-Pr) that cleave IGFBPs also play an important role in modulating levels of IGFs and IGFBPs and their action (Figure 1).

Some roles of IGFs include a positive effect on somatic growth and a synergistic role with insulin on post-prandial hypoglycaemia. IGFBPs are involved in several functions, including prolongation of IGF half-life in circulation, prevention of IGF-induced hypoglycaemia, regulation of the transport of IGFs between intra- and extravascular space, limitation of IGF bioavailability via limiting free IGFs, enhancement of IGF action through a slow-releasing pool of IGF, and modulation of cellular proliferation and death via IGFBP receptors independent of IGFs.[2]

IGFs and IGFBPs in vivo

IGF-I, or somatomedin-C, with a gene located on chromosome 12[3], is a 70 amino acid peptide. Growth hormone (GH), and to a lesser extent estrogen, PTH and glucocorticoids, have a role in IGF-I production.[2] IGF-I levels are age-dependent, with a peak at puberty.[2,4] IGF-II is a 67 amino acid peptide, with its gene on the short arm of chromosome 11.[5] Its production is not as dependent on GH, although it can be affected by IGFBP levels.[2] IGF-II levels are low at birth and increase in the first week of life and then stay stable. Most of IGF-I and IGF-II in the serum forms a ternary complex with IGFBP-3 and the glycoprotein known as the acid labile sub-unit (ALS). To a lesser amount with, IGF-I and IGF-II forms a ternary complex with IGFBP-5.). Small amounts of IGFs bind to IGFBPs as a binary complex, and less than 1% circulate in free form.[6] ALS plays an important role in modulating IGFs and IGFBPs. It occurs exclusively in intravascular space and does not cross the capillary bed.[7] The half-life of the ternary complex is 12 hours – long compared with that of the free IGF, which is only 10 minutes; unbound IGFBP-3 has a half-life of 30–90 minutes.[8] The binary complex of IGF-I and IGFBP-3 plays a role in the movement of IGF to the extravascular space and its effect on peripheral tissue. IGFBPs are produced in almost all tissues, in varying degrees of each, depending on the producing tissue.

Although there are other tissues that are also involved in the physiologically important production of IGFs, most of the circulating IGFs derive from the hepatic

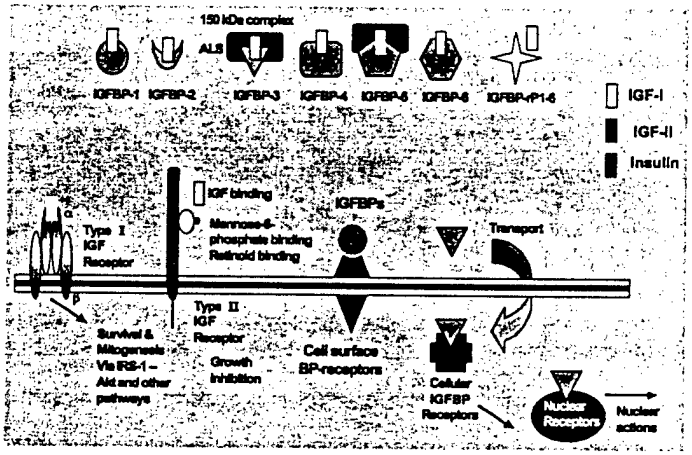

Figure 1. The IGF-IGFBP axis.

system. The liver is also the major producer of IGFBP-3, the most abundant IGF binding protein, and ALS.[9] IGFBP-3 is produced mainly by hepatic endothelia and Kupffer cells, while ALS and IGF-I are made by hepatocytes.[2] The production of all three components is directly affected by GH; they are produced less in growth-hormone-deficient states, and more in conditions of growth hormone excess.[2,10,11]

IGFBP-1 and IGFBP-2 levels have diurnal variation, and IGFBP-4 to -6 have age-dependent variation. IGFBP-3 is the most abundant IGF binding protein. Its level does not change acutely and does not represent a diurnal variation but it is also age-dependent; it is affected by factors such as nutritional state and level of growth hormone (GH).[2]

Insulin-like growth factors: growth, glycaemic control and tumorigenesis

IGF-I has been found to be important in cell growth in all systems, both pre-natally and post-natally. Studies of knock-out mice have shown poor prenatal growth and neurological development.[12,13] A report of a child with complete IGF-I deficiency due to a gene deletion showed that the child had a low birth weight, failure to thrive and mental retardation.[14] However, growth hormone deficiency (GHD) does not severely affect birth weight and prenatal neurological development, suggesting that IGF-I is important for prenatal growth and brain development, independently of GH.[2]

IGF-I also has a hypoglycaemic role by working synergistically with insulin in the fed state. Free IGF levels are acutely determined by IGFBP-1, which itself is regulated by insulin. IGFs also play a role in tumorigenesis. An association has been found between dysregulation of cell growth in malignancies and increased levels of IGF-I.[15] IGF-II is also over-expressed in several malignancies, such as adrenocortical and renal tumours.[16]

In this chapter, we review three major pathophysiological situations in which IGFs, as well as IGFBPs by their action on IGFs, play an important role, as described in this section: growth abnormalities, diabetes and tumorigenesis.

GROWTH DISORDERS AND THE GH–IGF–IGFBP AXIS

GH is the main regulator of IGF-1; it acts by inducing hepatic and local tissue production of IGF-I and also increases IGFBP-3. IGFBP-3, by binding to IGF-I, prolongs its half-life and also plays a crucial role in human growth. It has been shown that, in GH-deficient children, about 80% show IGF-I levels below −2 SD for age-related mean values.[17] IGFBP-3 is also usually low in children with GHD.[18] In adults, studies have shown an increase in IGFBP-3 and ALS in acromegaly and a reduction in both in GHD.[19,20] More recently, IGF-I and IGFBP-3 have played a more important role in the diagnosis of growth disorders and for continuous monitoring to assess efficacy and safety of GH treatment. Table I summarizes the common abnormalities seen in these conditions.

Growth hormone deficiency and treatment

Today, in the United States, the Food and Drug Administration has approved growth hormone therapy for short stature in children with any the following: (1) GHD, (2) Turner syndrome, (3) Prader–Willi syndrome, (4) chronic renal insufficiency, (5) history of intrauterine growth retardation (IUGR) with no catch-up growth in the first 24 months of life.[21–23] Classically, the diagnosis of GHD is made through GH provocation tests such as insulin, clonidine, arginine, or L-dopa stimulation. These

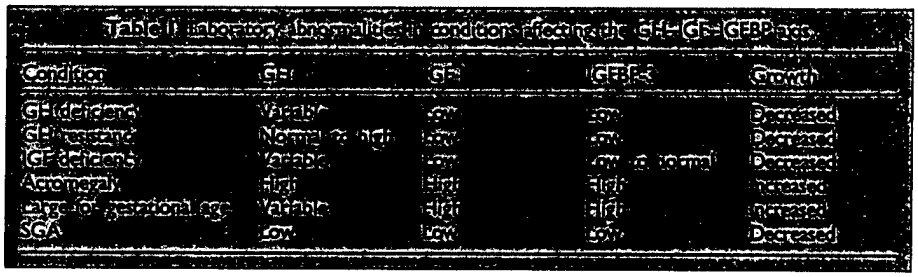

tests, however, are neither specific nor completely sensitive for GHD.[21] IGF-I and IGFBP-3 are believed to be valuable diagnostic tools in growth hormone deficiency.[21] In addition, IGF-I and OIGFBP-3 are becoming recognized as markers of GH response and treatment efficiency regardless of the aetiology.[24]

IGF-I/IGFBP-3 monitoring in GH treatment

It is evident that IGF-I and IGFBP-3 are below the mean and, in most cases, below normal in GH-deficient children and increase with GH therapy.[18] A recent small prospective European study showed a positive relationship between the dose of GH and serum IGF-I but not IGFBP-3.[25] A large randomized American study showed that height response to GH therapy correlated with both IGF-I z-score and IGFBP-3 z-score, supporting the notion that both IGF-I and IGFBP-3 are good markers for GH response and efficiency.[24] In this study, using both parameters was found to be a better predictor for growth than either one alone. About one-third of children in the study showed IGF-I levels above the age-adjusted normal range when treated with GH at 0.05 mg/kg daily. Also, patients with subnormal IGF-I levels on therapy showed slower growth, suggesting that they could benefit from higher than 0.05 mg/kg daily dose of GH to achieve a more normal IGF-I. Indeed, it seems that in pre-pubertal children, an IGF-I level close to +2 SD for 2 years will help them with catch-up growth and will not influence cancer risk later in life.[26]

IGF-I and IGFBP-3 measurement have been found to be useful in adults with adult GHD as well. IGF-I and IGFBP-3 are low in most patients with adult GHD and decrease with age.[19] Also, IGF-I levels have been used to assess the safety of GH therapy. Thus, IGFs are useful markers to follow up during adult as well as paediatric GH treatment; it is suggested that a safe and effective IGF-I level in adults treated with GH would be between −1 and +1 standard deviations for the age-related normal range.[27]

Acromegaly

Acromegaly is characterized by chronic hypersecretion of GH, which can be secondary to a pituitary somatotroph tumour.[28] As GH secretion is pulsatile, many investigators have looked at growth factors as a tool for diagnosing and monitoring acromegaly. Recent studies have shown that plasma levels of factors, including IGF-I, ALS and IGFBP-3, are higher in acromegalic patients than in normal subjects.[19,29] In both studies, IGF-I was elevated more than +2 SD in 100% of acromegalic patients. They also showed elevated ALS and IGFBP-3, but to a slightly lesser degree of sensitivity. In one study, post-surgical patients showed a decrease of ALS levels to normal, suggesting that this is a good way of assessing the success of surgical treatment.[29] Another recent study has

shown that, in acromegaly, GH continues its diurnal pattern but its suppression by IGF-I is attenuated.[30] Interestingly, both in GHD and acromegaly, the relationship of GH and IGF-I level are gender-specific.[31] Healthy females secrete more GH than do males, yet they have similar levels of IGF-I. Also in adults with GHD, females need higher doses of GH than do males to attain the same levels of IGF-I in serum. The elevated levels of IGF-I found in acromegalic patients are higher in men than in women. This makes IGF-I more complex as a diagnostic and monitoring tool in acromegaly.

Growth factors in fetal period

Animal models have shown that growth factors play an important role in fetal growth. Expression of IGFs and IGFBPs occurs very early in embryogenesis in animal models.[32] IGF regulation in fetal life is not GH-dependent but is closely regulated within each tissue, depending on the developmental stage in fetal life.[32]

The role of IGF-I in the fetus, and its relation to GH, has been studied through transgenic animal models. GH-deficient mice have been mated with IGF-I transgenic mice, and their offspring have had normal body weight and linear growth – as well as signs of non-GH-dependent effects of IGF-I, including a larger brain, suggesting that IGF-I plays a larger role than GH in fetal growth.[33] Mice whose IGF-II gene has been eliminated are severely growth retarded in utero (60% of normal birth weight) and have small placentas, but they survived and grew normally post-nataly.[34,35] This suggests that IGF-II affects placental growth, and thus fetal size, but is not essential for postnatal growth. Mice with a deleted IGF-I gene are also very small at birth (60% of normal) but have a normal placenta, and they had severe postnatal growth arrest and neonatal death.[34,36] This implies that IGF-I plays a large role in prenatal as well as postnatal growth. The roles of IGF-I and IGF-II in fetal life may be additive as mice missing both genes have severe intrauterine growth retardation, with birth weight 30% of normal. The actions of IGF-I and -II are most likely through type I IGF receptor as mice with deletion in this gene also have severe IUGR.[36] AQ7

Growth factors and human fetal growth

Studies on animal models have shown that IGF-II expression precedes that of IGF-I, suggesting its importance in early embryogenesis. Indeed, IGF-II mRNA is detected in human trophoblasts as early as day 12–18 of gestation.[32] In the second trimester, however, both IGFs are expressed in all human tissues.[37] This is mostly GH-independent and is probably influenced by other hormones, growth factors and IGFBPs. In the third trimester, IGF-I continues to rise as fetal growth increases in velocity. Both IGF-I (maternal and fetal cord serum) and fetal IGF-II have been found to correlate with birth weight. However, this is not a consistent finding. Also, while fetal growth through IGFs in animals seems completely independent from GH, this is not the case in all human studies. For example, humans with congenital hypopituitarism often have birth lengths 0.8–1.7 SD below mean.[38] Also neonates with GH insensitivity have lower IGF-I and IGF-II at birth and are small at birth.[39] These data' suggest that IGF-I and IGF-II have some dependence on GH pre-nataly.

Small-for-gestational-age versus large-for-gestational-age-Infants

Intrauterine growth retardation (IUGR) has occurred in all infants with birth-weight below the 3rd percentile for gestational age; this can have many different causes, such

as genetic, environmental, maternal nutrition or infectious; it can be symmetric or asymmetric, where the size of head is spared. Multiple studies have shown that IUGR infants have decreased IGF expression and decreased levels of placental GH and maternal IGF-I.[40–42] However, this is not a consistent finding in all investigations. Other studies have also shown that IUGR infants have increased IGFBP-1, decreased IGF-II and decreased IGFBP-3.[43,44] The increase in IGFBP-1 is most probably due to poor nutrition leading to hypoinsulinaemia. IGFBP-1 has been postulated to bind IGFs and make them less bio-available. Recently, GH therapy has been approved for children who have been born IUGR/SGA and have failed to catch up by the age of 2 years. These children have low levels of IGF and IGFBP-3 as described in Table 2, and these levels of growth factors respond to GH therapy.[45] Similarly, infants large for gestational age (LGA) are also found to have altered growth factors. IGF-I, insulin and IGFBP-3 are elevated in LGA infants, and IGFBP-1 is decreased.[41]

Infants with Beckwith–Wiedemann syndrome have a doubling in the IGF-II gene due to alterations in chromosome 11p15.5. Interestingly, they do not have an increased level of IGF-II in cord serum but they do have placental hypertrophy[46], through which they most likely have an increase in fetal growth. They also have hyperinsulinaemia. They have a higher risk of developing Wilm's tumour and other neoplasms that are IGF-II-dependent. It has been found that other infants, who eventually develop these tumours, also have a higher birth-weight – as in infants with Beckwith–Wiedemann syndrome.[47]

DIABETES

Type I diabetes mellitus (TIDM) is an autoimmune mediated disease in which destruction of beta cells in the liver leads to permanent insulin deficiency and chronic insulin dependence. Patients with TIDM also show abnormalities in the GH–IGF axis, which further contributes to the hyperglycaemia, and plays a role in the pathogenesis of certain complications related to diabetes.[48]

GH–IGF–IGFBP dysregulation and hyperglycaemia

Patients with TIDM have an increased level of circulating GH and less growth-hormone-binding protein (GHBP).[49] This leads to a state of GH resistance, and thus a decrease in the levels of IGF-I and IGFBP-3.[50–52] Insulin plays an inhibitory role in IGFBP-1 gene expression. While in states of hyperinsulinaemia, such as congenital

Table 2 IGF and IGFBP-3 concentrations, expressed in SDS, in children born SGA who completed 2 years of GH treatment

	IGF-I SDS: Baseline	IGF-I SDS: After 1 year Rx	IGF-I SDS: After 2 years Rx	IGFBP-3 SDS: Baseline	IGFBP-3 SDS: After 1 year Rx	IGFBP-3 SDS: After 2 years Rx
Untreated	−0.73 (0.53)	−0.58 (1.02)	−0.85 (1.07)	−0.78 (0.60)	−0.52 (0.76)	−0.16 (0.95)
GH-0.1 IU/kg/day	−0.70 (0.98)	−0.02 (0.97)	−0.48 (0.99)	−0.38 (0.89)	−0.24 (0.69)	−0.27 (1.05)
GH-0.2 IU/kg/day	−0.82 (1.59)	−0.07 (1.23)	−0.07 (1.14)	−0.55 (1.12)	−0.38 (1.03)	−0.27 (0.97)

hyperinsulinism, the level of IGFBP-1 decreases, in states of insulinopenia, such as TIDM, its level increases. An increased level of IGFBP-1 leads to a decrease in IGF-I bioavailability. Through these two mechanisms IGF-I is less available and cannot play its role in maintaining euglycaemia.[48] Studies in animals have shown an improved euglycaemic state in diabetic rats[43] injected with IGF-I, leading to the idea of IGF-I as a therapy for diabetes. This is discussed later.

GH–IGF–IGFBP dysregulation in diabetic complications

IGF-I is a trophic factor for the growth of many tissues and its dysregulation may pose problems in tissue growth and survival.

IGF-I is a neurotrophic growth factor which stimulates motor neuron proliferation, neuronal sprouting and myelination and inhibits neuronal apoptosis.[48] Animal models have shown a decrease of IGF-I and IGF-II at several levels of the nervous system in diabetic animals, including the peripheral nerves, CNS neurons, cerebellar tissue and spinal cord.[44,53] IGF-I treatment in diabetic animal models, on the other hand, has shown a block in progression and partial reversal of nerve regeneration impairment.[54] In parallel, human studies looking at patients with type II diabetes and peripheral neuropathy have found lower serum IGF-I and RBC IGF-I receptors in these patients in comparison to controls.[55]

The kidney produces IGF-I and is a target for its actions, undergoing increased renal blood flow and hypertrophy in the presence of IGF-I. In diabetic rats, an increase in IGFBP-1 in the renal cortex increases IGF-I in the local tissue, causing renal hypertrophy and eventual increase in urinary albumin excretion.[56] Human studies showed that diabetic patients with microalbuminuria have higher 24-hour urinary IGF-I and GH concentrations.[57]

While rapid improvement of glycaemic control improves neuropathy and nephropathy, it may actually worsen retinal disease. While some early studies in animals show that injection of IGF-I into vitreous fluid leads to retinopathy very similar to that in diabetic patients, other studies show a decrease in IGF-I in the retinal tissue of the diabetic rat.[48] Clinical studies have been inconsistent. Serum IGF-I from vitrectomy samples has been shown to be higher in diabetic patients with retinopathy than in those with diabetes but not retinopathy.[58,59] Other studies, however, did not find an association between IGF-I level and incidence and progression of retinopathy in diabetes patients, including a large population-based study by Wang et al over a 6-year period.[60] IGF-I treatment, however, has become more controversial owing to the possible risk of damage to the retina. In a study by Thrailkill et al treatment with IGF-I increased the risk of optic swelling and retinal damage if glycaemic improvement was too rapid.[61] This suggests that the rapid improvement of glycaemic control, rather than IGF-I itself, could contribute to the development of retinopathy.

IGF-I therapy in diabetes

There are several mechanisms which suggest that IGF-I might serve as a therapy in diabetes. IGF-I can inhibit beta cell apoptosis and restore the GH–IGF–IGFBP axis and improve glycaemic control.[48] Studies in NOD mice have shown a delay in development of diabetes and a decrease in severity of insulinitis when treated with IGF-I.[62] Studies have also found direct insulin-sensitizing effects of IGF-I, by normalization of GLUT-1, GLUT-2 and GLUT-5 in kidney[63], as well as through enhancement of insulin-stimulated oxidative and non-oxidative glucose disposal.

In type I diabetes, multiple clinical studies have shown improved glycaemic control and decreased insulin requirement through IGF-I therapy. Both Cheetham et al[64] and Bach et al[65] looked at pubertal children and found that IGF-I treatment, either as a single subcutaneous injection, or a continuous infusion, decreased overnight GH secretion and reduced insulin requirement. In another study IGF-I administration for 28 days to 6 adolescents with type I diabetes showed increased IGF-I levels and reduced AQ10 HbA1C and insulin requirement.[66] Thrailkill et al showed a decrease in mean blood sugar and haemoglobin A1C in patients treated with daily IGF-I versus placebo in a 4 week, randomized, placebo-controlled, double-blind study of 43 children with type I diabetes.[67] A further study by the same group looked at 223 patients treated for 12 weeks, either with intensive insulin therapy or twice-daily IGF-I in addition to insulin AQ10 therapy.[61] They found a decrease in Hgb A1c and insulin requirement. However, 8–12% of patients treated with IGF-I, especially the group treated with the highest dose, had early worsening of diabetic retinopathy and optic disc swelling.

Similar studies, on a short-term basis, have been performed in patients with type 2 diabetes; these studies have shown improved glycaemic control, haemoglobin A1c, insulin and C-peptide levels, and clinical signs of improved insulin sensitivity.[68] At this point, further studies are needed, on a more long-term basis, to evaluate the benefits as well as the safety of IGF-I treatment in diabetes glucose management and the prevention of complications.

TUMORIGENESIS

The role of the IGF axis in tumorigenesis has been increasingly studied in the past few years as higher levels of IGF-I have been found in three important cancers in the United States: prostate, lung, and breast cancer. In addition, IGFBPs, especially IGFBP-3, are believed to modulate the role of IGFs in cell growth and cancer and to independently affect cell growth, primarily by inducing apoptosis.

IGF-I, IGFBPs and cancer: in vitro models

IGFs exert their activity by binding to IGF receptors, especially type I IGF receptor (IGF-1R), which is involved in the growth-promoting actions of both IGF-I and IGF-II. IGF-1R stimulates mitogenesis in many types of cell, protects cells from apoptosis, and is involved in cellular transformation, a role that seems necessary for transformation by other agents as well.[69]

IGFBPs modulate IGF actions, positively or negatively, by binding to them and controlling their bioavailability. In addition, they can also inhibit growth, independently of IGF-I. In IGF-1R knock-out mice, fibroblasts transfected with IGFBP-3 showed growth inhibition correlated with degree of IGFBP-3 expression through induction of apoptosis.[70] Recently, IGFBP-3 and IGFBP-5 have been shown to be translocated into the nucleus and to possess a nuclear localization sequence (NLS) in their C-terminus.[71] It has recently been found that the retinoid X-receptor is a binding protein for IGFBP-3 and that it forms a complex with IGFBP-3 which is taken into the nucleus after treatment with retinoic acid.[72] Thus, it is possible that many IGF-independent actions of IGFBP-3, including apoptosis, are mediated through direct effects on gene expression.

Many cell cycle regulators, such as retinoic acid, TGF-beta, and tumour suppresser p53, control IGFBP-3-mediated apoptosis. IGFBP proteases also modulate IGFBP

actions. Prostate specific antigen (PSA), in seminal plasma, is the first IGFBP protease to be identified[73]; PSA fragmented IGFBP-3s have lower affinity for IGFs, and less inhibitory affects on cell growth.[74]

IGF, IGFBPs and human malignancy

Many in vitro and animal studies, especially looking at breast, prostate and lung cancer models, have found a positive correlation between IGF-I and tumorigenesis and an inverse effect of IGFBP-3 on this process. Human studies have not been fully consistent.[75]

Recent case–control studies show a 7–8% increase in serum IGF-I in patients with prostate cancer versus controls, an association found especially in younger men.[76] Chan et al found a 2.4 higher risk of developing prostate cancer in men in the highest quartile of serum IGF-I versus men with the lowest quartile, 7 years before the cancer was clinically evident.[77] An inverse association was found with IGFBP-3. However, some other studies have not found this association with prostate cancer.[78,79] In parallel, studies on breast cancer have been inconclusive. In a recent prospective case–control study, Hankinson et al showed a positive relationship between circulating IGF-I and risk for breast cancer.[80] Another prospective cohort analysis did not show this relationship.[81] Also, interestingly, recent clinical studies have shown high levels of IGFBP-3 to be associated with poor prognostic indicators for breast cancer, further complicating the role of IGFBP-3 in breast cancer.[82] A recent retrospective case–control study by Yu et al found higher IGF-I levels and lower IGFBP-3 levels in patients with lung cancer.[83] Ma et al showed that IGF-I was not found to be statistically associated with colorectal cancer risk; however, the combination of high IGF-I and low IGFBP-3 was shown to be related to an increased risk in cancer.[84]

Changes in the IGF axis, mainly an increase in the balance of IGF/IGF-1R activity versus IGFBP function, can contribute to carcinogenesis.[69] An increased amount of IGF or increased IGF-1R function, as well as a decrease in IGFBP activity, may be associated with carcinogenesis. However, this could be a mere association rather than a cause for carcinogenesis. Further investigation is necessary to confirm or refute this possible cause and effect relationship.

GH and cancer: implications for acromegaly and growth hormone therapy

While studies are in process to assess IGF-I role in tumorigenesis, the role of GH in cancer development is not clear. Early studies have not shown a relationship between physiological doses of GH and cancer. Cancer risk is suggested to be directly related to IGF-I and inversely related to IGFBP-3. But as GH increases both IGF-I and IGFBP-3, its role in cancer development, if any, is unclear.[85]

Cancer in acromegaly, a state of GH excess, has been much discussed. In recent studies, states of GH excess such as acromegaly, were implicated in benign conditions such as benign prostate hyperplasia (BPH)[86]; however, no clear association has been found between excess GH and cancer. The strongest association between acromegaly and different neoplasms is that of an increase in incidence of colonic polyps and adenocarcinoma.[87,88] However, findings of gastric and colonic cancer are inconsistent in different studies looking at people with acromegaly.[89,90] Also, despite an increase in BPH, no association is found to date between acromegaly and prostate cancer.

A possible role of IGF-I on tumorigenesis raises questions regarding potential risks of GH therapy and carcinogenesis. A study in Japan from 1987 suggested a relationship

between GH therapy and leukaemia, raising concerns regarding GH therapy.[91] Future studies, however, have not reproduced similar data. Also, re-evaluation of the original study suggested possible confounding variables involved in risk of leukaemia, such as previous neoplasms, radiotherapy or chemotherapy. Nor has there been found to be an association between GH therapy and relapse of leukaemia or brain tumour. An example is a study by Tuffli et al which looked at 12 209 GH recipients where no significant correlation was found.[92] A recent review of the National Cooperative Growth Study data on adverse events of GH from 1985 to 1999 showed no increase in rates for leukaemia, brain tumours and extra-cranial non-leukaemic malignancy in GH-treated children with no other risk factors.[93] Another recent study showed no increase in recurrence of brain tumour in children with a history of brain tumour treated with growth hormone.[94] Meanwhile, as current studies suggest an association between IGF-I and cancer, it is important to investigate this relationship and to see whether it suggests a cause and effect relationship. If so, it is imperative to explore further the risks of GH therapy, especially in non-deficient states. Also, if such a relationship exists, IGF-I and IGFBP-3 will not only be useful as tumour risk markers during GH therapy but also as mediators and mechanisms through which further cancer treatment research can be undertaken.

FUTURE DIRECTION

As discussed in the last few pages, growth factors and their binding proteins play an important role in human physiology and many human disease states. Current investigations in the clinical role of IGFs and IGFBPs have opened new horizons in our understanding of growth disorders, diabetes and cancer. Future research is necessary to characterize further the roles of IGFs and IGFBPs in these conditions, through which we can gain new perspectives to their pathophysiology, implement improved ways of diagnosis, and create new treatment modalities involving the GH–IGF–IGFBP axis.

Practice points

- serum levels of IGF-I and IGFBP-3 are invaluable for the diagnosis of growth hormone deficiency and excess and are excellent tools for monitoring growth hormone treatment
- in children, safe and effective GH therapy should include regular monitoring of IGF-I and maintaining its levels close to +2 SDS
- in adults treated with GH, a safe and effective IGF-I level should be between −1 and +1 standard deviations for the age-matched normal range
- disturbances in the IGF axis play an important role in glycaemic control and diabetic complications
- IGF-I therapy may improve glycaemic control and reduce insulin requirements in patients with diabetes
- IGFBP-1 is an excellent diagnostic tool in diabetes and hypoglycaemic disorders
- growth hormone treatment is contraindicated in patients who already have tumours but it does not seem to increase cancer risk in otherwise healthy patients
- monitoring of IGF-I and IGFBP-3 levels is useful to prevent an increase in the risk of malignancy in patients with acromegaly or in those treated with GH

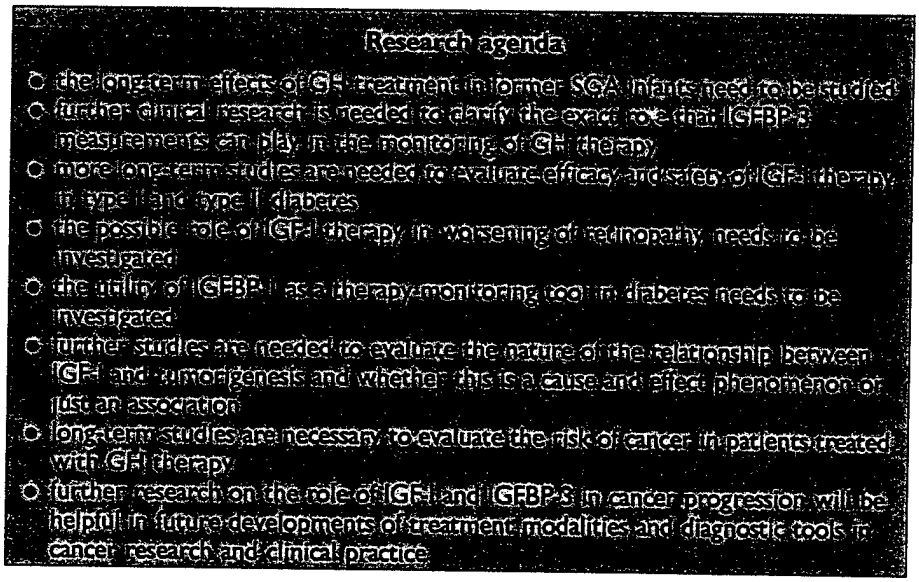

Acknowledgements

Supported in part, by grants 2RO1 DK47591, 1R01AG20954, 1RO1 AI40203 (from the NIH and grants from the ACS, JDRF, DOD, CaP CURE, CP Foundation, Pharmacia GEM Growth Research Center and a Lilly Fellowship Award.

REFERENCES

AQ11

1. Wetterau LA, Moore MG, Lee K et al. Novel aspects of the insulin-like growth factor binding proteins. *Molecular Genetics and Metabolism* 1999; **68:** 161–181.
2. Collett-Solberg PF & Cohen P. Genetics, Chemistry, and function of the IGF/IGFBP System. *Endocrine* 2000; **12:** 1–16. AQ12
3. Tricoli JV, Rall LB, Scott J et al. Localization of insulin-like growth factor genes to human chromosomes 11 and 12. *Nature* 1984; **310:** 784–786.
4. Cohen P & Rosenfeld RG. Physiologic and clinical relevance of the insulin-like growth factor binding proteins. *Current Opinion in Pediatrics* 1994; **6:** 462–467.
5. Daughaday WH & Rotwin P. Insulin-like growth factors I and II. Peptide, messenger ribonucleic acid and gene structures, serum, and tissue concentrations. *Endocrinology Reviews* 1989; **10:** 68–91.
6. Baxter RC. Insulin-like growth factor binding proteins in the human circulation: a review. *Hormone Research* 1994; **42:** 140–144.
7. Khosravi MG, Diamandi A, Mistry J et al. Acid-labile subunit of human insulin-like growth factor-binding protein complex: measurement, molecular, and clinical evaluation. *Journal of Clinical Endocrinology Metabolism* 1997; **82:** 3944–3951.
8. Hasegawa T, Cohen P & Rosenfeld RG. Characterization of the insulin-like growth factors (IGF) axis in a cultured mouse Leydig cell line (TM-3). *Growth Regulation* 1995; **5:** 151–159.
9. Cohen P & Rosenfeld RG. The IGF axis. In Rosenbloom AL (ed.) *Human Growth Hormone, Basic and Scientific Aspects*, pp 43–58. Boca Raton: CRC Press, 1995.
10. Rosenfeld RG, Pham H, Cohen P et al. Insulin-like growth factor binding proteins and their regulation. *Acta Paediatrica* 1994; **399(supplement):** 154–158.
11. Cohen P, Fielder PJ, Hasegawa Y et al. Clinical aspects of insulin-like growth factor binding proteins. *Acta Endocrinologica* (Copenhagen) 1991; **124 (supplement 2):** 74–85.

12. Liu JP, Baker J, Perkins A et al *Mice carrying null mutations of the genes encoding insulin-like growth factor I (Igf-1) and type 1 IGF receptor (Igf1r). Cell* 1993; **75:** 59–72.
13. Baker J, Liu JP, Robertson EJ et al. Role of insulin-like growth factors in embryonic and postnatal growth. *Cell* 1993; **75:** 73–82.
14. Woods KA, Camacho-Hubner C, Savage MO et al. Intrauterine growth retardation and postnatal growth failure associated with deletion of the insulin-like growth factor I gene. *New England Journal of Medicine* 1996; **335:** 1363–1367.
15. Werner H & LeRoith D. The role of the insulin-like growth factor system in human cancer. *Advances in Cancer Research* 1996; **68:** 183–223.
16. Boulle N, Logie A, Gicquel C et al. Increased levels of insulin-like growth factor II (IGF-II) and IGF-binding protein-2 are associated with malignancy in sporadic adrenocortical tumors. *Journal of Clinical Endocrinology Metabolism* 1998; **83:** 1713–1720.
17. Rosenfeld RG, Wilson DM, Lee PD et al. Insulin-like growth factors I and II in evaluation of growth retardation. *Journal of Pediatrics* 1986; **109:** 428–433.
18. Blum WF. Insulin-like growth factors and IGF-binding proteins: their use for diagnosis of growth hormone deficiency. In Juul A & Jorgensen LOL (eds) *Growth Hormone in Adults: Physiological and Clinical Aspects*, pp 48–74. Cambridge: Cambridge University Press, 1996.
19. Marzullo P, Di Somma C, Pratt KL et al. Usefulness of different biochemical markers of the insulin-like growth factor (IGF) family in diagnosing growth hormone excess and deficiency in adults. *Journal of Clinical Endocrinology and Metabolism* 2001; **86:** 3001–3008.
20. Arosio M, Garrone S, Bruzzi P et al. Diagnostic value of the acid-labile subunit in acromegaly: evaluation in comparison with insulin-like growth factor (IGF) I, and IGF-binding protein-1, -2, and -3. *Journal of Clinical Endocrinology and Metabolism* 2001; **86:** 1091–1098.
21. Lee KW & Cohen P. Individualizing growth hormone dosing in children. *Hormone Research* 2001; **56 (supplement 1):** 29–34.
22. de Zhegher F, Ong K, van Helvoirt M et al. High-dose growth hormone (GH) treatment in non-GH-deficient children born small for gestational age induces growth responses related to pretreatment GH secretion and associated with a reversible decrease in insulin sensitivity. *Journal of Clinical Endocrinology and Metabolism* 2002; **87:** 148.
23. de Zegher F, Albertsson-Wikland K, Wollmann HA et al. Growth hormone treatment of short children born small for gestational age: growth responses with continuous and discontinuous regimens over 6 years. *Journal of Clinical Endocrinology and Metabolism* 2000; **85:** 2816–2821.
24. Cohen P, Bright GM, Rogol AD et al. Effects of Dose and Gender on the Growth and Growth Factor Response to GH in GH-Deficient Children: Implications for Efficacy and Safety. *Journal of Clinical Endocrinology and Metabolism* 2002; **87:** 90–98.
25. Tillmann V, Patel L, Gill MS et al. Monitoring serum insulin-like growth factor-I (IGF-I), IGF binding protein-3 (IGFBP-3), IGF-I/IGFBP-3 molar ratio and leptin during growth hormone treatment for disordered growth. *Clinical Endocrinology (Oxford* 2000; **53:** 329–336.
26. Cohen P, Clemmons DR & Rosenfeld RG. Does the GH-IGF axis play a role in cancer pathogenesis? *Growth Horm IGF Res* 2000; **10:** 297–305.
27. Murray RD, Skillicorn CJ, Howell SJ et al. Dose titration and patient selection increases the efficacy of GH replacement in severely GH deficient adults. *Clinical Endocrinology (Oxford)* 1999; **50:** 749–757.
28. Melmed S. Acromegaly. *New England Journal of Medicine* 1990; **322:** 966–977.
29. Arosio M, Garrone S, Bruzzi G et al. Diagnostic value of the acid-labile subunit in acromegaly: evaluation in comparison with insulin-like growth factor (IGF) I, and IGF-binding protein-1, -2, and -3. *Journal of Clinical Endocrinology and Metabolism* 2001; **86:** 1091–1098.
30. Jaffe CA, Pan W, Brown MB et al. Regulation of GH secretion in acromegaly: reproducibility of daily GH profiles and attenuated negative feedback by IGF-I. *Journal of Clinical Endocrinology and Metabolism* 2001; **86:** 4364–4370.
31. Parkinson C, Ryder WDJ, Trainer PJ et al. The relationship between serum GH and serum IGF-I in acromegaly is gender-specific. *Journal of Clinical Endocrinology and Metabolism* 2001; **86:** 5240–5244.
32. Katz LEL & Cohen P. *Growth Factor Regulation of Fetal Growth. FETAL AND NEONATAL PHYSIOLOGY*, 2nd edn. pp 2401–2409. W. B. SAUNDERS, 1998.
33. Behringer R, Lewin T, Quaife CJ et al. Expression of insulin-like growth factor I stimulates normal somatic growth in growth hormone-deficient transgenic mice. *Endocrinology* 1990; **127:** 1033–1040.
34. Baker J, Liu JP, Robertson EJ et al. Role of insulin-like growth factors in embryonic and postnatal growth. *Cell* 1993; **75:** 73–82.
35. DiChiara T, Efstratiadis A & Robertson E. A growth deficiency phenotype in heterozygous mice carrying an insulin-like growth factor-II gene disrupted by targeting. *Nature* 1990; **345:** 78–80.
36. Liu JP, Baker J, Perkins AS et al. Mice carrying null mutations of the genes encoding insulin-like growth factor I (Igf-1) and type 1 IGF receptor (Igf1r). *Cell* 1993; **75:** 59–72.

AQ13

37. Han VKM, D'Ercole AJ & Lund PK. Cellular localization of IVF messenger RNA in the human fetus. *Science* 1987; **236:** 193–197.
38. Gluckman PD, Gunn AJ, Cutfield WS et al. Congenital idiopathic growth hormone deficiency associated with prenatal and early postnatal growth failure. The International Board of the Kabi Pharmacia International Growth Study. *Journal of Pediatrics* 1992; **121:** 920–923.
39. Savage MO, Blum WF, Ranke MB et al. Clinical features and endocrine status in patients with growth hormone insensitivity (Laron syndrome). *Journal of Clinical Endocrinology and Metabolism* 1993; **77:** 1465–1471.
40. Mirlesse V, Frankenne F, Alsat E et al. Placental growth hormone levels in normal pregnancy and in pregnancies with intrauterine growth retardation. *Pediatrics Research* 1993; **34:** 439–442.
41. Guidice LC, de Zegher F, Gargosky SE et al. Insulin-like growth factors and their binding proteins in the term and preterm human fetus and neonate with normal and extremes of intrauterine growth. *Journal of Clinical Endocrinology and Metabolism* 1995; **80:** 1548–1555. AQ18
42. Verhaege J, Van Bree R, Van Herck E et al. C-peptide, the insulin-like growth factors I and II and IGF binding protein 1 in umbilical cord serum: correlations with birthweight. *American Journal of Obstetrics and Gynecology* **169:** 89–97. AQ18
43. Jacob RJ, Sherwin RS, Bowen L et al. Metabolic effects of IGF-I and insulin in spontaneously diabetic BB/w rats. *American Journal of Physiology* 1991; **260:** 262–268. AQ18
44. Wuarin L, Guertin DM & Ishii DN. Early reduction in insulin-like growth factor gene expression in diabetic nerve. *Experimental Neurology* 1994; **130:** 106–114. AQ18
45. Boguszewski M, Albertsson-Wikland K, Aronsson S et al. *Acta Pediatrica* 1998; **87:** 257–263.
46. Takayama M, Soma H, Yagahi S et al. Abnormally large placenta associated with Beckwith–Wiedemann syndrome. *Gynecologic and Obstetrics Investigation* 1986; **22:** 165–168. AQ18
47. Leiseenring WM, Breslow NE, Beckwith JB et al. Increased birthweight of national Wilm's tumor study patients suggests growth factor excess. *Cancer Research* 1994; **4680–4683.** AQ18
48. Thrailkill KM. Insulin-like growth factor-I in diabetes mellitus: its physiology, metabolic effects, and potential clinical utility. *Diabetes Technology and Therapeurics* 2000; **2:** 69–80. AQ18
49. Menon RK, Arslanian S, May B et al. Diminished growth hormone-binding protein in children with insulin-dependent diabetes mellitus. *Journal of Clinical Endocrinology and Metabolism* 1992; **74:** 934–938.
50. Amiel SA, Sherwin RS, Hintz RL et al. Effect of diabetes and its control on insulin-like growth factors in the young subject with type I diabetes. *Diabetes* 1984; **33:** 1175–1179. AQ14
51. Batch JA, Baxter RC & Werther G. Abnormal regulation of insulin-like growth factor binding proteins in adolescents with insulin-dependent diabetes. *Journal of Clinical Endocrinology and Metabolism* 1991; **73:** 964–968. AQ18
52. Hanaire-Broutin H, Sallerin-Caute B, Poncet MF et al. Insulin therapy and GH-IGF-I axis disorders in diabetes: impact of glycaemic control and hepatic insulinization. *Diabetes and Metabolism* 1996; **22:** 245–250. AQ18
53. Wuarin L, Namdev R, Burns JG et al. Brain insulin-like growth factor-II mRNA content is reduced in insulin-dependent and non-insulin-dependent diabetes mellitus. *Journal of Neurochemistry* 1996; **67:** 742–751. AQ18
54. Zhuang HX, Snyder CK, Pu SF et al. Insulin-like growth factors reverse or arrest diabetic neuropathy: effects on hyperalgesia and impaired nerve regeneration in rats. *Experimental Neurology* 1996; **140:** 198–205. AQ18
55. Migdalis IN, Kalgeropoulou K, Kalantzis L et al. Insulin-like growth factor-I and IGF-I receptors in diabetic patients with neuropathy. *Diabetes Medicine* 1995; **12:** 823–827. AQ18
56. Fervenza FC, Tsao T, Hoffman AR et al. Regional changes in the intrarenal insulin-like growth factor-I axis in diabetes. *Kidney International* 1997; **51:** 811–818.
57. Cummings EA, Sochett EB, Dekker MG et al. Contribution of growth hormone and IGF-I to early diabetic nephropathy in type I diabetes. *Diabetes* 1998; **47:** 1341–1346. AQ18
58. Janssen JA, Jacobs ML, Derkx FH et al. Free and total insulin-like growth factor I (IGF-I), IGF-binding protein-1 (IGFBP-1), and IGFBP-3 and their relationships to the presence of diabetic retinopathy and glomerular hyperfiltration in insulin-dependent diabetes mellitus. *Journal of Clinical Endocrinology and Metabolism* 1997; **82:** 2809–2815. AQ15
59. Boulton M, Gregor Z, McLeod D et al. Intravitreal growth factors in proliferative diabetic retinopathy: correlation with neovascular activity and glycaemic management. *British Journal of Ophthalmology* 1997; **81:** 228–233.
60. Wang Q, Dills DG, Klein R et al. Does insulin-like growth factor I predict incidence and progression of diabetic retinopathy? *Diabetes* 1995; **44:** 161–164.
61. Thrailkill KM, Quattrin T, Baker L et al. Cotherapy with recombinant human insulin-like growth factor I and insulin improves glycemic control in type I diabetes. RhIGF-I in IDDM Study Group. *Diabetes Care* 1999; **22:** 585–592.

62. Kaino Y, Hirai H, Ito T et al. Insulin-like growth factor I (IGF-I) delays the onset of diabetes in non-obese diabetic (NOD) mice. *Diabetes Research and Clinical Practice* 1996; **34:** 7–11.
63. Asada T, Ogawa T, Iwai M et al. Recombinant insulin-like growth factor I normalizes expression of renal glucose transporters in diabetic rats. *American Journal of Physiology* 1997; **273:** F27–F37.
64. Cheetham TD, Jones J, Taylor AM et al. The effects of recombinant insulin-like growth factor I administration on growth hormone levels and insulin requirements in adolescents with type I (insulin-dependent) diabetes mellitus. *Diabetologia* 1993; **36:** 678–681.
65. Bach MA, Chin E & Bondy CA. The effects of subcutaneous insulin-like growth factor-I infusion in insulin-dependent diabetes mellitus. *Journal of Clinical Endocrinology and Metabolism* 1994; **79:** 1040–1045.
66. Cheetham TD, Holly JM, Clayton K et al. The effects of repeated daily recombinant human insulin-like growth factor I administration in adolescents with type I diabetes. *Diabetes Medicine* 1995; **12:** 885–892.
67. Thrailkill K, Quattrin T, Baker L et al. Dual hormonal replacement therapy with insulin and recombinant human insulin-like growth factor (IGF)-I in insulin-dependent diabetes mellitus: effects on the growth hormone/IGF/IGF-binding protein system. *Journal of Clinical Endocrinology and Metabolism* 1997; **82:** 1181–1187.
68. Moses AC, Young SC, Morrow LA et al. Recombinant human insulin-like growth factor I increases insulin sensitivity and improves glycemic control in type II diabetes. *Diabetes* 1996; **45:** 91–100.
69. Grimberg A & Cohen P. Role of insulin-like growth factors and their binding proteins in growth control and carcinogenesis. *Journal of Cell Physiology* 2000; **183:** 1–9.
70. Valentinis B, Bhala A, DeAngelis T et al. The human insulin-like growth factor (IGF) binding protein-3 inhibits the growth of fibroblasts with a targeted disruption of the IGF-I receptor gene. *Molecular Endocrinology* 1995; **9:** 361–367.
71. Schedlich LJ, Young TF, Firth SM et al. Insulin-like growth factor-binding protein (IGFBP)-3 and IGFBP-5 share a common nuclear transport pathway in T47D human breast carcinoma cells. *Journal of Biological Chemistry* 1998; **273:** 18 347–18 352.
72. Liu B, Lee HY, Weinzimer SA et al. Direct functional interactions between insulin-like growth factor-binding protein-3 and retinoid X receptor-alpha regulate transcriptional signaling and apoptosis. *Journal of Biological Chemistry* 2000; **275:** 33 607–33 613.
73. Cohen P, Graves HC, Peehl DM et al. Prostate-specific antigen (PSA) is an insulin-like growth factor binding protein-3 protease found in seminal plasma. *Journal of Clinical Endocrinology and Metabolism* 1992; **75:** 1046–1053.
74. Cohen P, Peehl DM, Graves HC et al. Biological effects of prostate specific antigen as an insulin-like growth factor binding protein-3 protease. *Journal of Endocrinology* 1994; **142:** 407–415.
75. Cohen P, Clemmons DR & Rosenfeld RG. Does the GH-IGF axis play a role in cancer pathogenesis? *Growth Horm & IGF Res* 2000; **10:** 297–305.
76. Wolk A, Mantzoros CS, Andersson SO et al. Insulin-like growth factor I and prostate cancer risk: a population-based, case-control study. *Journal of the National Cancer Institute* 1998; **90:** 911–915.
77. Chan JM, Stampfer MJ, Giovannucci E et al. Plasma insulin-like growth factor-I and prostate cancer risk: a prospective study. *Science* 1998; **279:** 563–566.
78. Serel TA & Kecelioglu M. Serum insulin-like growth factor is not a useful marker of prostate cancer. *BJU Int* 2000; **85:** 559–560.
79. Kurek R, Tunn UW, Eckart O et al. The significance of werum levels of insulin-like growth factor-lin patients with prostate cancer. *BJU Int* 2000; **85:** 125–129.
80. Hankinson SE, Willett WC, Colditz GA et al. Circulating concentrations of insulin-like growth factor-I and risk of breast cancer. *Lancet* 1998; **351:** 1393–1396.
81. Jernstrom H & Barrett-Connor E. Obesity, weight change, fasting insulin, proinsulin, c-peptide, and insulin-like growth factor-I levels in women with and without breast cancer: the Rancho Bernardo Study. *Journal of Women's Health and Gender-Based Medicine* 1999; **8:** 1267–1272.
82. Yu H, Levesque MA, Khosravi MJ et al. Insulin-like growth factor-binding protein-3 and breast cancer survival. *International Journal of Cancer* 1998; **79:** 624–628.
83. Yu H, spitz MR, Mirtry J et al. Plasma levels of insulin-like growth factor-I and lung cancer risk: a case-control analysis. *Journal of National Cancer Institute* 1999; **91:** 151–156.
84. Ma J, Pollak MN, Giovannucci E et al. Prospective study of colorectal cancer risk in men and plasma levels of insulin-like growth factor and IGF-binding protein-3. *Journal of National Cancer Institute* 1999; **91:** 620–625.
85. Shim M & Cohen P. IGFsand Human Cancer: Implications regarding the risk of growth hormone therapy. *Homone Research* 1999; **51 (supplement 3):** 42–51.
86. Colao A, marzullo P, Ferone D et al. Prostatic hyperplasia: an unknown feature of acromegaly. *Journal of Clinical Endocrinology and Metabolism* 1998; **83:** 775–779.

87. Colao A, Balzano A, Ferone D et al. Increased prevalence of colonic polyps and altered lymphocyte subset pattern in the colonic lamina propria in acromegaly. *Clinical Endocrinology* (Oxford) 1997; **47:** 23–28.
88. Ezzat S, Strom C & Melmed S. Colon polyps in acromegaly. *Annals of Internal Medicine* 1991; **114:** 754–755.
89. Jenkins PJ. Acromegaly and colon cancer. *Growth Horm IGF Res* 2000; **10 (supplement A):** S35–S36.
90. Ladas SK, Thalassinos NC, Toannides G et al. Does acromegaly really predispose to an increased prevalence of gastrointestinal tumors? *Clinical Endocinology* (Oxford) 1994; **41:** 597–601.
91. Watanabe S, Tsunematus Y & Fujimoto J. Leukaemia in patients treated with growth hormone. *Lancet* 1988; **21:** 1159–1162.
92. Tuffli GA, Johanson A, Rundle AC et al. Lack of increased risk for extracranial, nonleukemic neoplasms in recipients of recombinant deoxyribonucleic acid growth hormone. *Journal of Clinical Endocrinology and Metabolism* 1995; **80:** 1416–1422.
93. Maneatis T, Baptista J, Connelly K et al. Growth hormone safety update from the National Cooperatvie Growth Study. *Journal of Pediatric Endocrinology and Metabolism* 2000; **13 (supplement 2):** 1035–1044.
94. Swerdlow AJ, Reddinguis RE, Higgins CD et al. Growth hormone treatment of children with brain tumors and risk of tumor recurrence. *Journal of Clinical Endocrinology and Metabolism* 2000; **85:** 4444–4449.

Author Queries for Chapter 9 of beem.2002.0212

AQ	Orig. m/s page nos: Page	Line	Brief expanation of author query
(1)	1		Degrees + position of first author?
(2)	3	+1	Please confirm that the legend for Fig. 1 is 'The IGF-IGFBP axis."
(3)	4	+3,4	"To a lesser " English? Sense?
(4)	4	+14	Kuppfer *or* Kupffer? (Selling?)
(5)	4	+15	Please note that "GHD" cannot have two different meanings: growth hormone deficient and growth hormone deficiency We have edited the text so that GHD now means **only**" growth hormone deficiency". Please note at proof.
(6)	6	+	'OIGFBP-3" ?
(7)	8	+12	"with deletion in" - does this mean "with a deletion in" *OR* "with a deletion *of*"?
(8)	9	+	10 Please spell out SGA.
(9)	9	+9	In Table 2: meaning of "R_x"?
(10)	12		In line 8: HbA1C.
(10)	12		In line 13: Hgb A1C. Are these meant to be two different designations?
(11)	16		*References*. Please indicate the 10 most important refs for the chapter (to be asterisked when printed).
(12)	16		Ref 2: name of journal "Endocrine"
(13)	12		Ref 26: name of journal in full.
(14)	18		Ref 45: (re-numbered 47) - volume number.
(15)	21		Ref 58: check names.
(16)	22		Ref 75: name of journal in full?.
(17)	23		Refs 78 and 79: name of journal in full?.
(18)	9		On page 9 of the manuscript, the references run in the following order: 40, 41, 42, 51, 52, 43 To keep the references in numerical order,we have re-numbered references in the text and list as follows: